

# Annual Report 2007

**Association  
EURATOM / IPP.CR**

**INSTITUTE OF PLASMA PHYSICS, v.v.i.**  
ACADEMY OF SCIENCES OF THE CZECH REPUBLIC

## TABLE OF CONTENTS

PREFACE.....	5
<b>I. RESEARCH UNIT.....</b>	<b>6</b>
1 ASSOCIATION EURATOM/IPP.CR .....	6
2 MANPOWER AND BUDGET .....	8
3 INTERNATIONAL COLLABORATION.....	9
<b>II. PHYSICS .....</b>	<b>13</b>
OVERVIEW OF ACTIVITIES - PHYSICS .....	13
LIST OF PUBLICATIONS (PHYSICS) .....	20
1 PROVISION OF SUPPORT TO THE ADVANCEMENTS OF THE ITER PHYSICS BASIS .....	33
<i>Carbon transport in the TCV L-modes.....</i>	<i>33</i>
<i>Ball-pen probes on ASDEX Upgrade tokamak.....</i>	<i>35</i>
<i>ELM pace making by biasing.....</i>	<i>37</i>
<i>Determination of reflection characteristics of small hydrocarbon ions of low incident energies         in collisions with with room-temperature and heated carbon and tungsten surfaces .....</i>	<i>38</i>
<i>Experiments and modeling of fast particle generation at LH and ICRF heating .....</i>	<i>40</i>
<i>Modeling of LH wave ionization, development of EDGE2D code to 3D.....</i>	<i>44</i>
<i>Cherenkov detectors for fast electron measurements .....</i>	<i>48</i>
<i>JET neutron data analyses via inversion algorithms         based on Minimum Fisher Regularisation.....</i>	<i>50</i>
2 DEVELOPMENT OF PLASMA AUXILIARY SYSTEMS .....	52
<i>Neutral beam injection system for COMPASS.....</i>	<i>52</i>
<i>Spectroscopic diagnostics for COMPASS.....</i>	<i>54</i>
<i>Performance analysis of ITER candidate Hall sensors in tokamak environment.....</i>	<i>56</i>
<i>Development of advanced probe for edge tokamak plasmas - Emissive probes.....</i>	<i>59</i>
<i>Development of millimeter-wave reflectometry system for the measurement of edge pedestal         plasma in tokamak COMPASS.....</i>	<i>61</i>
<i>Neutral particle analyzer for tokamak COMPASS .....</i>	<i>63</i>
<i>HRTS diagnostic development .....</i>	<i>65</i>
<i>Magnetic diagnostics and development of the feedback system for the COMPASS tokamak.....</i>	<i>67</i>
<i>COMPASS Control, Data Acquisition, and Communication system .....</i>	<i>69</i>
<i>Development and tests of Hall probe based magnetic diagnostics for fusion devices.....</i>	<i>71</i>

3	DEVELOPMENT OF CONCEPT IMPROVEMENTS AND ADVANCES IN FUNDAMENTAL UNDERSTANDING OF FUSION PLASMAS .....	72
	<i>EEDF Measurements in the CASTOR Tokamak Using the First Derivative Langmuir Probe</i>	
	<i>Modelling of ITER Plasma Facing Component Damage and Consequences for Plasma Evolution Following ELMs and Disruptions .....</i>	75
	<i>Measurement of plasma flows into tile gaps .....</i>	77
	<i>Electron Bernstein waves simulations for WEGA.....</i>	79
	<i>EFIT2006 Parallelization .....</i>	81
	<i>QPIC study of secondary electron emission in response to fast electron flow to tokamak edge target plates, including the effect of electron emission on sheath potentials.....</i>	82
	<i>Simulation of processes in high-temperature plasma toward better interpretation of experimental data.....</i>	88
	<i>Results of PIC modeling of the ball-pen probe .....</i>	90
	<i>Adaptation of ASTRA and CRONOS for COMPASS simulations .....</i>	92
	<b>III. TECHNOLOGY.....</b>	<b>94</b>
	OVERVIEW .....	94
	<i>Measurement of Activation Cross Sections at Neutron Energies below 35 MeV, Data for Nickel.....</i>	97
	<i>Development of new numerical macro elements method for distortion prediction of the big welded construction .....</i>	99
	<i>Establishing of a specialized laboratory for handling, manipulations and analysis of beryllium coated PFW mock-ups .....</i>	101
	<i>Structure and phase composition of surfaces of Eurofer 97-2 modified by plasma treatment ..</i>	103
	<i>The Eurofer steel: microstructural degradation and embrittlement.....</i>	105
	<i>Assessment of PSM welding distortions and field welding .....</i>	107
	<i>Mechanical testing of a primary first wall panel attachment system (ITER).....</i>	109
	<i>Thermal fatigue test of beryllium coated primary first wall mock-ups .....</i>	111
	<i>Static and dynamic fracture toughness of plates and weldments at the transition irradiated up to 2.5 dpa at 200°C – 250°C.....</i>	113
	<i>Development and testing cold traps, high temperature flanges and circulation pump for the liquid metal Pb-Li loop .....</i>	115
	<i>Evaluation Pb-Li compatibility of EUROFER samples coated by Al and Er<sub>2</sub>O<sub>3</sub> layers under higher temperature conditions.....</i>	117
	<i>EUROFER and Pb-Li melts testing under higher temperature irradiation conditions .....</i>	118
	<i>Experiments for the Validation of Bi Cross-Sections up to 35 MeV in a Quasi-monoenergetic Neutron Spectrum .....</i>	120
	<b>IV. KEEP-IN-TOUCH ACTIVITY ON INERTIAL CONFINEMENT FUSION.....</b>	<b>122</b>
	<i>Interaction of Laser-produced Plasma Jets with Ambient Gas.....</i>	122

**V. TRAINING, EDUCATION, OUTREACH AND PUBLIC INFORMATION  
ACTIVITES..... 125**

*Training and Education .....125*  
*Outreach and Public Information Activities .....127*  
*List of Public Activities .....128*

**APPENDIX :**

**OVERVIEW OF THE TOKAMAKCOMPASS REINSTALLATION  
IN THE INSTITUTE OF PLASMA PHYSICS AS CR, V.V.I., ASSOCIATION  
EURATOM-IPP.CR IN 2007 ..... 132**

EXECUTIVE SUMMARY OF THE APPENDIX..... 133  
1. COMPASS-D TOKAMAK DISMANTLING AND TRANSPORT..... 134  
2. TOKAMAK BUILDING..... 136  
3. TOKAMAK ENERGETICS ..... 138  
4. VACUUM SYSTEM ..... 142  
5. DIAGNOSTICS ..... 143  
6. CODAC, INTERLOCK AND IT INFRASTRUCTURE..... 149  
7. FEEDBACK CONTROL ..... 151  
8. MODELLING ..... 152  
9. NEUTRON BEAM INJECTION ..... 154  
10. HUMAN RESOURCES FOR THE REINSTALLATION OF THE COMPASS TOKAMAK..... 156  
11. FINANCIAL REPORT ..... 159  
12. TIMETABLE..... 162

## PREFACE

This report summarizes the main activities and achieved results of the Association EURATOM/IPP.CR in the year 2007. The Association participates in the joint European effort in mastering controlled fusion by carrying out relevant plasma physics and technology R&D, including participation in JET and other European devices and activities related to the international fusion experiment ITER.

The Association was founded on December 22, 1999 through a contract between the European Atomic Energy Community (EURATOM) represented by the European Commission and the Institute of Plasma Physics, Academy of Sciences of the Czech Republic (IPP). Several other institutions have been included in the Research Unit to contribute to the work programme in physics and technology research:

- Faculty of Mathematics and Physics, Charles University in Prague
- Institute of Physical Chemistry, v.v.i., Academy of Sciences of the Czech Republic
- Faculty of Nuclear Science and Physical Engineering, Czech Technical University
- Nuclear Physics Institute, v.v.i., Academy of Sciences of the Czech Republic
- Nuclear Research Institute, Rez, Plc
- Institute of Applied Mechanics, Brno, Ltd

The overall manpower involved in the Association's fusion research at the end of 2007 was 110, of which 85 (77%) were professionals (i.e. those with a University degree). The total effort expended is about 52 person years of which roughly 61% was devoted to physics tasks and the remaining 39% to underlying technology and technology tasks. The overall 2007 expenditure was about 4.87 M€ (the major part of which, 2.87M€, was spent on the COMPASS project).

Our activities in physics were based on the approved Work Programme 2007 both in experiment and theory. With the tokamak CASTOR decommissioned at the end of 2006, and its successor, the COMPASS tokamak under reinstallation, the fusion-relevant plasma physics was oriented namely to the preparation for scientific exploitation of COMPASS and on research in the framework of international collaborations. The research was focused on the study of phenomena at the plasma edge, part of our activities was devoted to studies of wave-plasma interaction and analyses of plasma – fast particles interaction. Some selected atomic processes relevant to fusion plasmas, such as the interaction of molecular ions with first wall elements, were studied in test-bed experiments. The research was performed in collaboration with 17 other Associations (*CEA, CIEMAT, Confédération Suisse, ENEA, Etat Belge, FZK, HAS, IPP, IPPLM, IST, MEdC, ŌAW, TEKES, UKAEA, VR, INRNE.BG, FOM*) and *JET EFDA*.

In the technology area, the R&D was substantially enhanced and focused on the fields Vessel/In Vessel, Tritium Breeding and Materials and Physics Integration. In total 19 Technology / Underlying Technology Tasks were worked upon, mostly exploiting the cyclotron, the fission reactor and computational capabilities of our Association.

In 2007, a significant part of our manpower concentrated on preparation of the IPP site for the arrival of the COMPASS tokamak, its dismantling in Culham Science Centre and the first steps of its reinstallation in Prague. Tokamak COMPASS arrived to Prague on 20<sup>th</sup> October 2007 and was fixed in its final position on 18<sup>th</sup> December 2007. For more details see the Appendix to this Annual report.

Pavol Pavlo  
Head of Research Unit  
Association EURATOM/IPP.CR

# I RESEARCH UNIT

---

## 1 Association EURATOM/IPP.CR

---

### Composition of the Research Unit

**IPP** Institute of Plasma Physics, v.v.i.,  
Academy of Sciences of the CR  
Address: Za Slovankou 3,  
182 00 Praha 8, Czech Republic  
Tel: +420 286 890 450  
Fax: +420 286 586 389  
Contact Person: Jan Stöckel  
e-mail: stockel@ipp.cas.cz

**FMP** Faculty of Mathematics and Physics,  
Charles University  
Address: V Holešovičkách 2,  
182 00 Praha 8, Czech Republic  
Tel: +420 221 912 305  
Fax: +420 221 912 332  
Contact person: Milan Tichý  
tichy@mbox.troja.mff.cuni.cz

**JHIPC** J Heyrovský Institute of Physical  
Chemistry, v.v.i., Academy of  
Sciences of the CR  
Address: Dolejškova 3,  
182 23 Praha 8, Czech Republic  
Tel: +420 266 053 514  
Fax: +420 286 582 307  
Contact person: Zdeněk Herman  
zdenek.herman@jh-inst.cas.cz

**FNSPE** Faculty of Nuclear Science and  
Physical Engineering,  
Czech Technical University  
Address: Břehová 7,  
115 19 Praha 1, Czech Republic  
Tel: +420 224 358 296  
Fax: +420 222 320 862  
Contact person: Vojtěch Svoboda  
svoboda@br.fjfi.cvut.cz

**NPI** Institute of Nuclear Physics, v.v.i.,  
Academy of Sciences of the CR  
Address: 250 68 Řež, Czech Republic  
Tel: +420 266 172 105 (3506)  
Fax: +420 220 941 130  
Contact person: Pavel Bém  
e-mail: bem@ujf.cas.cz

**NRI** Nuclear Research Institute Plc., Řež  
Address: 250 68 Řež, Czech Republic  
Tel: +420 266 172 453  
Fax: +420 266 172 045  
Contact person: Karel Šplíchal  
e-mail: spl@ujv.cz

**IAM** Institute of Applied Mechanics Brno,  
Ltd.  
Address: Veveří 85,  
611 00 Brno, CR  
Phone: +420 541 321 291  
Fax: +420 541 211 189  
Contact person: Lubomír Junek  
e-mail: junekl@uam.cz

## Steering Committee

### EURATOM

Yvan Capouet, Head of Unit RTD J4  
Steven Booth, Scientific Officer RTD J4  
C. Dedeu Fontcuberta, Administrator RTD J5

### IPP.CR

Ivan Wilhelm (Charles University)  
Petr Křenek (Ministry of Education, Youth and Sports)  
Pavel Chráska (Institute of Plasma Physics)

### Head of Research Unit

Pavol Pavlo

### Secretary of the SC

Jan Mlynář

## International Board of Advisors of the Association EURATOM-IPP.CR

Prof. Hardo Bruhns	Chair
Dr. Carlos Hidalgo	CIEMAT, Madrid, Spain
Dr. Jochen Linke	Forschungszentrum Jülich GmbH, Jülich, Germany
Dr. Bernard Saoutic	CEA Cadarache, France
Prof. Fernando Serra	Centro de Fusao Nuclear, Lisboa, Portugal
Dr. Wolfgang Suttrop	Max-Planck-Institut für Plasmaphysik (IPP), Garching, Germany
Dr. Martin Valovič	UKAEA, Culham laboratory, United Kingdom
Prof. Guido Van Oost	Ghent University, Gent, Belgium
Dr. Henri Weisen	EPFL, Lausanne, Switzerland
Dr. Sandor Zoletnik	RMKI KFKI, Budapest, Hungary

The Board was established to help with the formulation of scientific program, and to assess the scientific achievements of the Association EURATOM-IPP.CR.

## Representatives of the Association in European Committees

### *Consultative Committee for the EURATOM Specific Programme on Nuclear Energy Research – Fusion (CCE-FU)*

Pavel Chráska      Institute of Plasma Physics, Academy of Sciences of the Czech Republic  
Milan Tichý      Faculty of Mathematics and Physics, Charles University, Prague

### *Scientific and Technical Advisory Committee*

Jan Stöckel      Institute of Plasma Physics, Academy of Sciences of the Czech Republic

### *EFDA Steering Committee*

Jan Kysela      Nuclear Research Institute pls., Řež  
Pavol Pavlo      Institute of Plasma Physics, Academy of Sciences of the Czech Republic

### *Governing Board of the European Joint Undertaking for ITER and the Development of Fusion Energy (“Fusion for Energy”)*

Pavol Pavlo      Institute of Plasma Physics, Academy of Sciences of the Czech Republic  
Milan Zmítko      Nuclear Research Institute pls., Řež

## 2 Manpower and Budget

### Manpower Analysis of the Association EURATOM/IPP.CR in 2007

Institution	STAFF, PY			STAFF, Person					
	Physics	Technology	TOTAL	Female	Male	Prof.	Non-Prof.	TOTAL	Total, %
IPP	30.13	2.59	32.72	10	49	43	16	59	53.7
FMP	1.00	0	1.00	1	5	5	1	6	5.5
IAM	0	5.60	5.60	0	13	12	1	13	11.8
JHIPC	0	1.79	1.79	0	3	3	0	3	2.7
FNSPE	0.50	0.53	1.03	0	4	4	0	4	3.6
NRI	0	6.80	6.80	2	12	9	5	14	12.7
NPI	0	2.90	2.90	1	10	9	2	11	10.0
<b>TOTAL</b>	<b>31.63</b>	<b>20.21</b>	<b>51.84</b>	<b>14</b>	<b>96</b>	<b>85</b>	<b>25</b>	<b>110</b>	<b>100.0</b>
<b>Total, %</b>	<b>61.0</b>	<b>39.0</b>	<b>100.0</b>	<b>12.7</b>	<b>87.3</b>	<b>77.3</b>	<b>22.7</b>	<b>100.0</b>	

### Expenditures in 2007

	Euro
Physics	807 473
Underlying Technologies	329 042
Inertial Fusion Energy	7 169
EFDA Basic Support Technology	11 684
<b>Sub-total</b>	<b>1 155 368</b>
Large Devices	<b>2 875 185</b>
Technology tasks Art 5.1a	335 057
Technology tasks Art 5.1b	374 041
EFDA Article 6.3 Contracts	7 922
EFDA Article 9 - secondment to Garching	35 247
EFDA Article 9 - secondment to Culham	3 392
<b>Sub-total</b>	<b>755 659</b>
<b>Mobility Actions</b>	<b>84 373</b>
<b>TOTAL</b>	<b>4 870 585</b>

## Collaborative Projects in 2007

### PROJECT NO. 1: Edge turbulence - JET

**Objective:** Edge turbulence studies - Characterisation of the link between edge plasma flows and turbulence at JET. Characterisation of JET SOL and edge plasma turbulence, comparison with ESEL model.

*Collaborating Associations :*

- CIEMAT
- *RISØ*
- *Confédération Suisse*

### PROJECT NO. 2: Carbon Transport on TCV

**Objective:** Active charge exchange spectroscopy experimental study of carbon transport phenomena Evaluation of the radial density profile of C6+ in presence of additional core heating on TCV tokamak. Assessment of the C5+ and C4+ radial density profiles predominantly in L-mode. Establishment of the radial profile of  $Z_{\text{eff}}$  with the help of numerical simulation.

*Collaborating Associations:*

- *Confédération Suisse*

### PROJECT NO. 3: Katsumata probe

**Objective:** Measurements of the ion and electron temperature and of the plasma potential and diffusion coefficient in the edge plasma on RFX and on ASDEX-U using the Katsumata type probe.

*Collaborating Associations:*

- ENEA
- *MedC*
- IPP
- *Etat Belge*
- ÖAW

### PROJECT NO. 4: ELM pace making

**Objective:** Test the possibilities of ELM pace making by edge plasma biasing or by pellet injection on the tokamak ASDEX-U.

*Collaborating Associations:*

- IPP

### PROJECT NO. 5: Small hydrocarbons – reflection characteristics

**Objective:** Determination of reflection characteristics of small hydrocarbon ions of low incident energies in collisions with room-temperature and heated carbon and tungsten.

*Collaborating Associations:*

- ÖAW

### PROJECT NO. 6: Small hydrocarbons – surface retention

**Objective:** Determination of surface retention of impinging ion constituents - small hydrocarbon ions of low incident energies in collisions with room-temperature and heated carbon and tungsten.

*Collaborating Associations:*

- IPP

### PROJECT NO. 7: Modelling of power load on Plasma Facing Components

**Objective:** Study of the power deposition on the plasma facing components (PFCs). 2D particle-in-cell code modelling of the power load in ITER PFCs. Joint development of a multi-probe diagnostics for its possible implementation on the Magnum-PSI.

*Collaborating Associations:*

- CEA Cadarache
- *MEdC*
- *Confédération Suisse*

### PROJECT No. 8: Fast particles at RF heating

**Objective:** Experiments and modelling of fast particle generation at LH and ICRF heating. Determination of the energy distribution of accelerated particles on Tore-Supra. Getting more knowledge about parasitic wave absorption and consequent unwanted heat loads. Modelling of ICRF impurity production mechanisms.

*Collaborating Associations:*

- CEA
- IPP

### PROJECT NO. 9: Direct ionisation by Lower Hybrid Wave

**Objective:** Modelling of direct Lower Hybrid (LH) wave ionisation, development of EDGE2D code to 3D. Getting more knowledge about LH wave coupling in ITER like JET discharges.

*Collaborating Associations:*

- UKAEA
- *TEKES*
- CEA



**PROJECT NO. 21: Simulation of Electron Bernstein Waves (EBW) for WEGA stellarator**

**Objective:** Simulation of EC waves from overdense plasma in order to simulate EBW for the WEGA stellarator.

*Collaborating Associations:*       ▪ *IPP*

**PROJECT NO. 22: Particle-in-cell (PIC) simulations of the Scrape-Off Layer (SOL)**

**Objective:** PIC simulations of the SOL in the presence of non-Maxwellian and/or supra-thermal particles. Interpretation of Langmuir, tunnel and RFA probe diagnostics by using complex simulations with 1-D quasi-neutral PIC (presheath) and 2-D PIC (sheath) for modeling of tunnel probe.

*Collaborating Associations:*       ▪ *CEA*

**PROJECT NO. 23: PIC simulations of the ball-pen probe**

**Objective:** To provide the current-voltage characteristics of the ball-pen probe with respect to the probe collector.

*Collaborating Associations:*       ▪ *MEdC*

**PROJECT NO. 24: CRONOS for COMPASS**

**Objective:** To adapt the CRONOS code for COMPASS simulations. CRONOS simulations of COMPASS operation with lower hybrid (LH) and neutral beam (NB) heating and current drive.

*Collaborating Associations:*       ▪ *CEA*

**PROJECT NO. 25: Core-edge code for COMPASS**

**Objective:** To develop a new modelling tool, a version of a self-consistent core-edge code for the COMPASS tokamak, 0D in the core and 1D in the SOL.

*Collaborating Associations:*       ▪ *IPPLM*

**PROJECT NO. 27: Nuclear data for IFMIF**

**Objective:** Measurements of activation cross sections at neutron energies below 35 MeV for nickel. Neutron irradiation and cooling measurement of Ni samples, evaluation of data for activation cross-section. Comparison with IFMIF activation data file.

*Collaborating Associations:*       ▪ *FZK*

**PROJECT NO. 28: Laser induced removal**

**Objective:** Laser-induced removal of fuel and co-deposits from plasma facing components in tokamaks and characterisation of laser-irradiated surfaces. Study of samples influenced by laser ablation by various methods.

*Collaborating Associations:*       ▪ *IPPLM*

**PROJECT NO. 29: Transport and reinstallation of the COMPASS tokamak**

**Objective:** Transport of the COMPASS subsystems and parts. Design and test of the magnetic diagnostics and the feedback system for the COMPASS tokamak.

*Collaborating Associations:*       ▪ *UKAEA*

**PROJECT NO. 30: Turbulence studies**

**Objective:** Full Hamiltonian description of the interaction of particles with magnetic islands and edge plasma electrostatic turbulence. Anomalous diffusion of ions in the regimes of interchange instability and of the drift wave turbulence.

*Collaborating Associations:*       ▪ *ÖAW*



*In the end of 2007 tokamak COMPASS was moved from Culham Science Centre to its new location in the Institute of Plasma Physics, Prague*

*For more details, see the Appendix of this report*

# II PHYSICS

The main areas of the research undertaken in the Association EURATOM/IPP.CR in 2007 were as follows:

1. Provision of Support to the Advancements of the ITER Physics Basis
2. Development of Plasma Auxiliary Systems
3. Development of Concept Improvements and Advances in Fundamental Understanding of Fusion Plasmas

Here, the most important results, activities and achievements are briefly summarized; details are given after the list of publications. Notice that the major part of the Association activities in Physics relies on broad collaboration with other EURATOM Associations.

## 1. Provision of Support to the Advancements of the ITER Physics Basis

**Measurements of the ion and electron temperature and of the plasma potential and diffusion coefficient in the edge plasma using the Katsumata type probe.** The direct measurements of the plasma potential have been performed on ASDEX-U tokamak in June 2007. It has been used the design of the Ball-pen probe instead of the Katsumata-type probe due the better comparison with achieved results on CASTOR tokamak (2006, 2005). The Ball-pen probe head has been mounted on the reciprocating manipulator located at the midplane. The probe has been exposed in the edge plasma, a few millimeters outside the limiter shadow, for several times during the discharge. The measurements have been performed in the L-mode and H-mode. The data are analyzed to estimate also the electron temperature and the diffusion coefficient. It is not possible to obtain the values of the ion temperature from the I-V characteristics because this method is very sensitive to presence of the supra-thermal electrons, which modifies the shape of the measured I-V characteristics. The Ball-pen probes has been also used for the direct measurements of the plasma potential and the electron temperature on toroidal device RFX in Padova (first test was in 2006). The Ball-pen probes measured the plasma potential in a low magnetic field  $B_t = 0.1$  T, which is much lower than on ASDEX Upgrade ( $B_t = 2.5$  T). The above mentioned experiments have shown that the Ball-pen probe is suitable for the direct measurements of the plasma potential and consequently of the electron temperature in different fusion facilities with wide range of the magnetic field.

**ELM pace making.** The ELM pacing experiments were realized on the ASDEX-Upgrade tokamak in several shots. As a biasing electrode, the midplane manipulator (MEM) with several carbon tips inserted into the massive carbon envelope was used. The first analysis of measured data shows a change of natural ELM frequency during a period of the biased MEM insertion and an occurrence of new smaller satellite ELMs. The data evaluation is in progress.

**Determination of reflection characteristics of small hydrocarbon ions of low incident energies in collisions with room-temperature and heated carbon and tungsten surfaces.** Collisions of simple hydrocarbon ions  $CD_3^+$ ,  $CD_4^+$ , and  $CD_5^+$  with room-temperature carbon (HOPG) surfaces were investigated at low incident energies of 3–10 eV. Mass spectra, angular and translational energy distributions of the product ions were determined. From

these data, information on processes at surfaces, absolute ion survival probabilities, scattering diagrams, and effective mass of the surface involved in the collisions was determined. Incident ions  $CD_3^+$  and  $CD_5^+$  showed inelastic non-dissociative ( $CD_3^+$ ) or non-dissociative and dissociative ( $CD_5^+$ ) scattering, the radical cation  $CD_4^+$  exhibited both inelastic, dissociative, and reactive scattering, namely occurrence of H-atom transfer and C-chain build-up in reactions with hydrocarbons present on the room-temperature carbon surface. The absolute survival probability, at 10 eV and the incident angle of 300 (with respect to the surface), was about 12 % for  $CD_5^+$ , and 0.3-0.4 % for  $CD_3^+$  and  $CD_4^+$ . It decreased towards zero at lower incident energies. Estimation of the effective surface mass involved in the collisional process led to  $m(S)_{eff}$  corresponding roughly to the mass of one or several  $CH_3^-$  (or  $C_2H_5^-$ ) terminal units of surface hydrocarbons (accepted for publication). Fragmentation of polyatomic cations and dications ( $C_7H_n^{+/2+}$ ,  $n=6,7,8$ ) with hydrocarbon-covered surface was investigated over the incident energy range 5-50 eV to estimate the role of the projectile charge on energy partitioning in surface collisions (see the reference). Surfaces relevant to fusion devices (plasma-sprayed tungsten, carbon fiber composite, Be) were bombarded by deuterated hydrocarbon ions of energies up to 100 eV. Sticking coefficients to the surface of one of the collision products, deuterium molecules, were determined using the nuclear reaction analysis combined with the Rutherford back-scattering method. Upon bombardment with  $CD_3^+$  ions, the sticking coefficient of  $D_2$  to plasma-sprayed tungsten (PSW) was found to be about 0.2, and 0.2-0.3 on carbon fiber composite (CFC), in both cases little dependent on the incident energy between a few and 100 eV.

**Experiments and modeling of fast particle generation at LH and ICRF heating.** A retarding field analyzer (RFA) was used during lower hybrid (LH) and ion cyclotron resonance frequency (ICRF) experiments in the Tore Supra tokamak to measure the flux of supra-thermal particles emanating from the near field region in front of the antennas. The fast electron energy distribution of accelerated particles in the fast electron beam was determined. The fast electron beam generated by the parasitic LH wave absorption extends for high PLH up to the LCFS and is up to 5 cm or even more radially wide, with possible corresponding radially broader heat loads in case that the beam impacts on the wall. The observed existence of the wide beam needs to be explained by theory, as the current theory predicts the radial width of the beam of several mm. The fast electron beam intensity very near to the LCFS decreases more quickly with decreasing PLH than the fast beam intensity near the LH grill mouth. As the comparison of the 1st and 2nd beam shows, the mean collector current (and therefore similar unwanted heat loads) in the two beams is comparable at higher PLH.

**Modeling of direct LH wave ionization, development of EDGE2D code to 3D.** We performed numerical modeling of near Lower Hybrid (LH) grill Scrape-off-Layer (SOL) plasma density variations as a function of gas puff and LH power with the fluid code EDGE2D. The gas puff ionization is difficult to model because it is a 3D problem, the antenna, first wall components and gas pipe have finite dimensions in the toroidal direction, but an amended 2D poloidal – radial model can provide useful insights. The code includes direct SOL ionization by the LH wave. The modeling shows that both puff and heating/ionization are important in raising the density in the far SOL, what is important for LH wave coupling in ITER like discharges. Although OMP (Outer midplane) seems to be the best location for gas puffing, the other two puff locations (near RCP – reciprocating probe, and at the top) also give an increase in far SOL density with heating. This is again an important information for ITER, where top and not OMP gas puffing is assumed. The modeling shows the flattening of the far SOL density profile, which is observed in experiments.

**Cherenkov detectors for fast electron measurements.** Measurements indicate that

introduced modifications of the Cherenkov detection system enabled an electromagnetic interference to be reduced and a direct hard radiation to be eliminated completely. It was confirmed that the recorded Cherenkov signals were induced just by fast electrons ( $> 50$  keV). On the CASTOR tokamak, the dependences of the fast electron signals on the radial position of the Cherenkov detector, as well as on the plasma density, plasma current and toroidal magnetic field value were investigated and explained. A connection between the Cherenkov emission and the hard X-rays, which were measured at a close vicinity of the Cherenkov detector, was found and discussed. The results of the statistical approach using a single-count analysis of the time-resolved Cherenkov data indicates possible transport mechanisms of fast electrons – the fast burst losses in combination with a slow diffusion. A question on an unclear origin of the hard radiation of energy approximately 3.9 MeV reaching the shielded detection system only during the tokamak discharges stays still unanswered.

**Neutron data analysis on JET.** The Minimum Fisher Regularisation (MFR) algorithm, adapted for tomography analyses of the JET neutron profile monitor, was further extended by the Abel inversion where neutron emissivities are constrained to constants on flux surfaces. The upgraded algorithm was applied to studies of both fuel transport in TTE and recent data from JET campaigns C15-C19, see [65]. These studies confirmed that the Abel inversion constraint is not relevant for typical JET neutron emissivities with stronger radiation from the low field side. However, the Abel inversion can be used as a sensitive indicator of asymmetries. Following these results, the 2D MFR algorithm with unisotropic smoothing constrained by magnetic flux surfaces was implemented, tested on JET Neutron profile monitor data and optimised to the expected use in the fuel transport studies. This upgrade was used in quantitative analyses of Tritium transport, with results that have been submitted for publication. Concerning the MFR unfolding of the NE213 neutron detector data, the algorithm was slightly upgraded, in particular the dependence of the photomultiplier gain factor on the neutron intensity was taken into account.

## 2. Development of Plasma Auxiliary Systems

**NBI for COMPASS-D.** Predictive simulations of the beam performance were in 2007 focussed on the finalisation of the technical specifications for the system. Code Astra has been setup to use its internal NBI package. Besides that, it can use external outputs from the ACCOME code. Based on the extensive modelling, technical specifications were agreed upon at the end of the year and implemented into detailed Call for tender for two neutral beam injectors for the COMPASS tokamak.

**Spectroscopic diagnostics for COMPASS.** Spectroscopic diagnostics on the COMPASS tokamak will cover a wide spectral range of the core and edge plasma emission aiming to realize a fast tomography at microsecond time scales (fast bolometry, soft X-rays, visible range). Additionally, the fast visible camera will be implemented on COMPASS in a cooperation with the HAS Association.

**Performance analysis of ITER candidate Hall sensors in tokamak environment.** Use of various configurations of flux loops for measurement of magnetic field in fusion devices is inherently limited by the pulsed operation of these machines. A principally new diagnostic method must be developed to complement the magnetic measurements in true steady state regime of operation of fusion reactor. One of the options is the use of diagnostics based on Hall sensors. Several experiments dedicated to testing of various types of Hall probes were done or they are being prepared on CASTOR, JET, and Tore Supra. On CASTOR, the

measurements with a ring of integrated Hall sensors were further analyzed including the modeling of CASTOR vacuum field configuration [4, 13, 92]. Previous, in-vessel measurements with 3D Hall probe on CASTOR were published in [93]. Collaboration on preparation of a set of ex-vessel Hall probes for JET continued leading to delivery of the full set of probes to JET in the end of 2007 by MSL Lviv Ukraine [73,76,91]. A new high temperature resistant (up to 200 degC) Hall probe with measurement bandwidth DC-250 kHz was installed in in-vessel environment of Tore Supra in the end of 2007.

**Development of advanced probe for edge tokamak plasmas - Emissive and tunnel probes.** We have found that applicability of the strongly emitting probe technique for the estimation of the space potential depends on ratio  $T_e/T_{eW}$  and  $n$ , where  $T_e$  is temperature of plasma electrons,  $T_{eW}$  is temperature of emitted electrons and  $n$  is plasma density. If the  $T_e$  and  $T_{eW}$  are comparable the plasma potential determined by the strongly emitting probe can be overestimated. If  $T_{eW}$  can be neglected with respect to  $T_e$  (hot plasma), the plasma potential determined by the strongly emitting probe is underestimated by approximately one  $kT_e/e$ . In addition, a relatively thorough study of the electron saturation current variations at varying probe heating was performed in the cylindrical magnetron (Prague) and DP-machine (Innsbruck) plasma. Magnitude of electron saturation current variations were characterized – variations were more pronounced in case of shorter probes. In the reference various possible processes leading to electron saturation current variations were discussed. New experimental data were recently obtained that give better understanding of studied phenomena. We concluded that strongly emitting probe technique is applicable in low temperature plasma with  $T_e \sim 2-3$  eV and plasma density  $n \sim 10^{16} \text{ m}^{-3}$ . Observed variations of the electron saturation current at varying probe heating can be ascribed from the most part to the probe surface cleaning and contamination in laboratory argon discharge plasma.

**Development of millimeter-wave reflectometry methods for the measurement of edge pedestal plasma in tokamak COMPASS.** IST/CFN Lisbon was agreed in 2006 to be the main supplier of the reflectometry system with the technical support of IPP Prague. Five individual reflectometers are supposed to measure the density profile. The advanced reflectometers allow an arbitrary frequency sweeping modes and therefore the reflectometers can be used as well as an experimental diagnostics for studies of plasma turbulence. The realization of the reflectometry system was supposed in a close collaboration with IST/CFN during 2006 – 2009. Unfortunately soon it was realized that IST/CFN has problem with the manpower for the construction, manufacturing and installation of the system. The workplan agreed in 2006 was delayed and consequently cancelled. Therefore, because of no contribution of IST/CFN in 2006/2007, it was decided to construct the Ka-band (26.5 – 40 GHz) reflectometer in IPP. The design of the reflectometer was made in a similar way to the reflectometers developed in IST/CFN. In 2007 most of microwave electronics was constructed and tested in parts. Development of control unit and control SW is in progress. This reflectometer will be able to work with a quasioptical band-combiners and antennas. The control unit and control SW has to be develop by our own way.

**High Resolution Thomson Scattering for COMPASS.** For the TS system, several different systems are considered and relevant parameters were calculated for both edge as well as core plasma. A large trade survey looking for new technologies was carried out in order to find some new possibilities for the edge detection system realization. With regards to the required measured range of electron temperature and density and requirements for the temporal and spatial resolution, two possibilities were chosen as the most suitable: a use of the Nd:YAG laser at the second harmonic frequency and the Littrow spectrometer with the ICCD camera, or a use of this laser at the first harmonic frequency and the Littrow spectrometer with the CMOS camera for the core, and the spectral filters with avalanche photodiodes for the edge.

A multi-pass system can be taken into account in order to increase the laser power effectively. The use of the Nd:YAG laser at the second harmonic frequency was investigated in details and corresponding calculations of the scattered and detected photons were performed for this particular case. An implementation of a multi pass system as a future upgrade was discussed.

**Development of magnetic diagnostics and the feedback system for the COMPASS tokamak.** Magnetic diagnostics: The dismantling of magnetic diagnostics on COMPASS was carried out during two missions of IPP staff in the Culham Science Centre. The existing documentation of magnetic diagnostics was checked and completed. The magnetic sensors position was identified and documented. Cables from magnetic sensors to corresponding cubicles were disconnected. All equipment was transported to IPP Prague. Feed-back system: Test of the integrators and the other electronic equipment (Waveform Generators, PID controllers) were done. The existing documentation was checked and completed. As the result, the existing analogue feedback system was found to be obsolete and not appropriate for our tasks. Therefore, it was decided not to restore it. Digital system under contract collaboration with the IST Lisbon, which is experienced in building similar systems for other Associations, was selected. Algorithms for feedback control will be generated by the MAXFEA code, developed by P.Barabaschi. Geometry, mesh, material, and circuits files were done for COMPASS. Hardware and control of the the digital system will be based on the ATCA technology standard; MIMO controllers, developed in IST, will be used. Three identical fast amplifiers are being built in the IPP for the feedback stabilization of the horizontal and vertical plasma positions. The circuit safety is designed for overcurrent, overvoltage and optical isolation protection inside the energizer that determines the amplifiers inputs.

**COMPASS Control and data acquisition system design.** An efficient operation of COMPASS in Prague requires a new CODAC (Control, Data Acquisition, and Communication) system, which is being developed jointly by the Associations IPP.CR and IST. The tokamak control involves several areas, each of different levels: 24 hours a day control of building infrastructure, interlock, central experiment control, and real time control during the experiment run. Each of the systems has different purposes and diverse features.

### **3. Development of Concept Improvements and Advances in Fundamental Understanding of Fusion Plasmas**

**EEDF Measurements in the CASTOR Tokamak Using the First Derivative Langmuir Probe Method.** Langmuir probes (LP) are widely used to provide local measurements of important plasma parameters like the plasma potential, the density of the charged particles or the electron energy distribution function (EEDF). The accuracy of LPs under adverse conditions, such as the presence of magnetic fields or high plasma temperature, is still being questioned. We report here the application of a new technique, the first-derivative method, for processing the electron part of the I-V characteristics measured in the CASTOR tokamak. EEDFs at different radial positions in the edge plasma are presented and the values of the plasma potential, electron temperature and electron densities are estimated. In the confined plasma we find the EEDF to be bi-Maxwellian. The results obtained are in good agreement with classical method (second derivative) usually used for LP data processing. Results from different methods of differentiating the I-V characteristics are also discussed.

**Modelling of ITER Plasma Facing Component Damage and Consequences for Plasma Evolution Following ELMs and Disruptions.** We have developed a unique tool to measure the plasma deposition into a gap between tiles. The experimental data confirm the

numerical predictions we made with our 2D self-consistent numerical code. In the case of toroidal gaps, we have a quantitative and qualitative agreement. However, in the case of poloidal gaps, it is only qualitatively acceptable. The 2-sided deposition is confirmed, with the good order of magnitude. This set of experiments confirms nevertheless the understanding of the plasma deposition in tile gaps presented in [26].

**Measurement of plasma flows into tile gaps.** A two-dimensional cylindrical, self-consistent kinetic code for the tunnel probe calibration has been developed. For this purpose, we used an existing code in Cartesian coordinates. After benchmarking, we used the code to perform a set of simulations that cover the range of expected density and temperature in tokamak edge plasmas for characterizing the plasma deposition inside the tunnel probe. The electron temperature depends on the ratio of the current collected by the tunnel over the back plate and calibration curves has been performed.

**Edge turbulence studies.** Robustness of the combined magnetic probe for TJ-II, containing set of Hall probes and coils was enhanced preparing for its installation on a new TJ-II reciprocating probe drive.

**Simulation of EC waves from overdense plasma.** We have adapted our EBW code to obtain a crude estimate of the profile of the current driven by 2.45 GHz wave in the WEGA stellarator. We investigated the dependence of the current profile on the central magnetic field and the temperature of the suprathermal component present in the WEGA plasma. Significant effects of the suprathermal electron population on EBW propagation have been demonstrated. Even a modes fraction of suprathermal electrons enables very efficient absorption. The parallel wave vector direction of the EBWs can be reversed during the propagation through the plasma. The driven current direction has to be reversed analogously. Such behaviour has been observed experimentally. The current density profile was, for the first time, measured by a small Rogowski coil. EFIT2006, a modern EFIT implementation in C++ and Fortran 95, has been successfully parallelized. Boost MPI libraries have been applied to enable convenient transmission of the complex C++ objects used in EFIT2006. Linear scaling of the computational power has been demonstrated. EFIT2006 has been installed to IPP Prague computers and benchmarked using MAST data, which were read remotely from UKAEA server through IDAM interface. Equilibrium reconstructions have been performed for COMPASS, applying experimental data from UKAEA database and predicted equilibria with ACCOME.

**PIC simulations of the SOL in the presence of non-Maxwellian and/or supra-thermal particles.** In collaboration with J. P. Gunn at CEA Cadarache, a quasineutral particle-in-cell code (QPIC) was developed for simulating ion and electron transport along magnetic field lines in the Scrape off Layer (SOL) of the tokamak plasma edge. The code has been recently validated by comparison of its results with a known solution of a kinetic problem, namely that of the Mach probe in a strongly magnetized plasma. [67]. Last year's effort on QPIC included an extension of the code to a SOL configuration with non-floating walls allowing a non-zero SOL current. First results were reported at the 2007 EPS conference [68].

**Simulation of processes in high-temperature plasma toward better interpretation of experimental data.** The work in 2007 covered two main areas: (i) Numerical investigations of plasma parameters in COMPASS tokamak and (ii) Preparation of 3D particle code of magnetized plasmas. In frame of the first part numerical investigation of plasma parameters in COMPASS tokamak was performed and presented in the 34th EPS Plasma Conference on Plasma Physics in Warsaw, Poland. The plasma parameters in the device were analyzed in the

frame of the self-consistent model of central plasma and edge region. The possibility of achieving high recycling and detached regimes in COMPASS divertor was discussed. In frame of the task preparation of 3D particle code of magnetized plasmas there was developed during 2007 the self-consistent fully 3D Particle-In Cell code for modeling of plasma-solid interaction with new Poisson solver based on direct LU decomposition combined with multigrid approach. The model was tested on a cylindrical cavity geometry, i.e. on a hollow cylindrical chamber opened to the plasma, in both collisionless and collisional plasmas (see Fig. 2). The basic studied feature was the influence of non-axial orientation of magnetic field – this parameter is important for the analysis of experimental data from the Katsumata probe. Earlier version has been accepted for publication in the Vacuum journal.

**PIC simulations of the ball-pen probe.** The first systematic PIC modeling (using the XOOPIE code) of the Ball-pen probe has shown that the floating potential of the probe is varying with respect to the ration  $R$  of the electron and ion saturation currents. This is in agreement with the Langmuir probe theory and the systematic measurements on CASTOR tokamak (2005, 2006). Moreover, the simulation also confirmed that the Ball-pen probe can reach  $R$  to be equal to one. Then, the corresponding probe potential is assumed as the plasma potential, which is expected from the theory. However, that probe potential was not equal to the value obtained directly in 3D potential profile in PIC simulation. This discrepancy might be caused by wrong determination of the unperturbed plasma potential in PIC simulation. The PIC modeling did not provide any explanation why the strongly magnetized ( $B = 1$  T) electrons are detected inside the ceramic shielding tube in the measurements with Ball-pen probe.

**Adaptation of CRONOS for COMPASS simulations.** Currently, transport modeling of the tokamak COMPASS is performed using the ASTRA and CRONOS codes. The ASTRA and CRONOS codes solve coupled diffusion equations for heat, matter, and magnetic field (current). These partial differential equations are coupled to a magnetic field equilibrium code and modules for LH and NB injection. Such codes thus allow fully self-consistent calculations of tokamak operation, and are highly desirable for the study of COMPASS operation with the planned LH and NB systems. During the mobility stay of M. Stránský at CEA Cadarache in April 2007, the CRONOS transport code was acquired and adapted for the COMPASS tokamak, and installed in Prague by the CEA staff in November 2007. In addition, during the visit of Irina Voitsekhovitch in September 2007 a robust transport model for COMPASS was developed for the ASTRA code, including the possibility of external heating, so now transport simulations and comparisons are possible on two transport codes. In December 2007, Y. Peysson of the CEA staff has also made available to us the “Starwars” suite of lower hybrid (LH) toroidal ray-tracing (C3PO) and 3-D Fokker-Planck (LUKE) codes, which can simulate LH heating and current drive in a stationary state.

## LIST OF PUBLICATIONS

[1]	<b>Stöckel J., Adamek J., Balan P., Bilyk O., Brotankova J., Dejarnac R., P Devynck P., Duran I., Gunn J.P., Hron M., Horacek J., Ionita C., Kocan M., Martines E., Panek R., Peleman P., Schrittwieser R., Van Oost G., Zacek F</b> : Advanced probes for edge plasma diagnostics on the CASTOR tokamak. <i>Journal of Physics, Conference Series</i> 63 (2007), 012001
[2]	<b>Van Oost G., Bulanin V.V., Donne A.J.H., Gusakov E.Z., Kraemer-Flecken A., Krupnik L.I., Melnikov A., Nanobashvili S., Peleman P., Razumova K.A., Stockel J., Vershkov V., Adamek J., Altukov A.B., Andreev V.F., Askinazi L.G., Bondarenk I.S., Brotankova J., Dnestrovskij A.Yu., Duran I., Eliseev L.G., Esipov L.A., Grashin S.A., Gurchenko D., Hogewej G.M.D., Hron M., Ionita C., Jachmich S., Khrebtov S.M., Kouprienko D.V., Lysenko S.E., Martines E., Perfilov S.V., Petrov A.V., Popov A.Yu., Reiser D., Schrittwieser R., Soldatov S., Spolaore M., Stepanov A.Yu., Telesca G., Urazbaev A.O., Verdoolaege G., Zacek F. and Zimmermann O</b> : Multi-machine studies of the role of turbulence and electric fields in the establishment of improved confinement in tokamak plasma. <i>Plasma Phys. Control. Fusion</i> 49 (2007) A29–A44
[3]	<b>Van Rompuy T., Gunn J.P., Dejarnack R., Stöckel J., Van Oost G.</b> : Sensitivity of electron temperature measurements with the tunnel probe to a fast electron component. <i>Plasma Phys. Control. Fusion</i> 49 (2007) 619–629
[4]	<b>Van Oost G., Berta M., Brotankova J., Dejarnac R., Del Bosco E., Dufkova E., Duran I., Gryaznevich M.P., Hron M., Malaquias A., Mank G., Peleman P., Sentkerestiova J., Stöckel J., Weinzettl V., Zoletnik S., Ferrera J., Fonseca A., Hegazy H., Kuznetsov Y., Ossyanniko A., Sing A., Sokholov M., Talebitaher A.</b> : Joint Experiments on Small Tokamaks. <i>Nucl. Fusion</i> 47 (2007) 378–386
[5]	<b>Popov Tsv., Stockel J., Dejarnac R., Dimitrova M., Ivanova P., Naydenova Tsv.</b> : Advanced Probe Measurements of Electron Energy Distribution Functions in CASTOR Tokamak Plasma. <i>Journal of Physics, Conference Series</i> 63 (2007), 012002
[6]	<b>Peleman P., Xu Y., Spolaore M., Brotankova J., Devynck P., Stöckel J., Van Oost G., Boucher C.</b> : Highly resolved measurements of periodic radial electric field and associated relaxations in edge biasing experiments. <i>Journal of Nuclear Materials</i> Vol. 363-365, 2007, 638-642
[7]	<b>Kočan M., Pánek R., Stöckel J., Hron M., Gunn J.P. and Dejarnac R.</b> : Ion temperature measurements in the tokamak scrape-off layer. <i>Journal of Nuclear Materials</i> Vol. 363-365, 2007, p. 1436-1440
[8]	<b>Gunn J., Boucher C., Dionne M., Duran I., Fuchs V., Loarer T., Nanobashvili I., Pánek R., Pascal J.-Y., Saint-Laurent F., Stockel J., Van Rompuy T., Zagorski R., Adámek J., Bucalossi J., Dejarnac R., Devynck P., Hertout P., Hron M., Lebrun G., Moreau P., Rimini F., Sarkissian A., Van Oost G.</b> : Evidence for a poloidally localized enhancement of radial

	transport in the scrape-off layer of the Tore Supra tokamak. <i>Journal of Nuclear Materials</i> Vol. 363-365, 2007, p. 484-490
[9]	<b>Stockel J., Adamek J., Brotánková J., Dejarnac R., Devynck P., Duran I., Gunn J.P., Horacek J., Hron M., Kocan M., Martines E., Panek R., Spolaore M., Van Oost G.:</b> Survey of results on plasma biasing in the CASTOR tokamak. <i>34th EPS Conference on Plasma Physics, Warsaw, Poland, June 2-6, 2007</i> Book of Abstracts, P2-031
[10]	<b>Pedrosa M.A. Carreras., B.A, Silva, C., Hron M., Hidalgo C., Alonso J.A., García L., Calvo I., de Pablos J.L., Stöckel J.:</b> Sheared flows and turbulence in fusion plasmas. <i>34th EPS Conference on Plasma Physics, Warsaw, Poland, June 2-6, 2007</i> Book of Abstracts I-2.021, invited lecture
[11]	<b>Gryaznevich M., Van Oost G., Del Bosco E, Berta M, Brotankova J, Dejarnac R, Dufkova E., Duran I., Hron M., Zajac J., Malaquias A., Mank G., Peleman P., Sentkerestiova J., Stöckel J, Weinzettl V., Zoletnik S, Tál B., Ferreira J., Fonseca A., Hegazy H., Kuznetsov Y., Ruchko L., Vorobjev G.M., Ovsyannikov A., Sukhov E., Singh A., Kuteev B., Melnikov A., Vershkov V, Kirneva N., Kirnev G., Budaev V., Sokolov M., Talebitaher A., Khorshid P., Gonzales R., El Chama Neto I., Kraemer-Flecken A,W., Soldatov V., Marques Fonseca A.M., Gutierrez Tapia C.R. Krupnik L.I. :</b> Progress on Joint Experiments on Small Tokamaks. <i>34th EPS Conference on Plasma Physics, Warsaw, Poland, June 2-6, 2007</i> Book of Abstracts, P-1.070
[12]	<b>Brotankova J., Orozco O., Pedrosa M.A., Hidalgo C., Sanchez E., Stockel J.:</b> Study of the statistical properties of fluctuations in the plasma boundary region of the TJ-II stellarator. <i>34th EPS Conference on Plasma Physics, Warsaw, Poland, June 2-6, 2007</i> Book of Abstracts, P-1.086
[13]	<b>Duran I., Sentkerestiova J., Bilykova O., Havlicek J., Stockel J. :</b> Measurement of magnetic field using array of integrated Hall detectors on the CASTOR tokamak. <i>34th EPS Conference on Plasma Physics, Warsaw, Poland, June 2-6, 2007</i> Book of Abstracts, P-2.152
[14]	<b>Jakubowski L., Sadowski M.J., Stanislowski J., Malinowski K., Zebrowski J., Jakubowski M., Weinzettl V., Stockel J., Vacha M., Peterka M. :</b> Application of Cerenkov detectors for fast electron measurements in CASTOR tokamak. <i>34th EPS Conference on Plasma Physics, Warsaw, Poland, June 2-6, 2007</i> Book of Abstracts, P-5.097
[15]	<b>K. Popov Tsv., Ivanova P., Dias F.M., Stöckel J., Dejarnac R. :</b> Langmuir Probe Measurements of Electron Energy Distribution Functions in CASTOR Tokamak Plasma. <i>34th EPS Conference on Plasma Physics, Warsaw, Poland, June 2-6, 2007</i> Book of Abstracts,P-5.104
[16]	<b>Adámek J., Pánek R., Komm M., Stöckel J. :</b> Simulation of Ball-pen probe using XOOPIE code. <i>10th Workshop on Electric Fields, Structures, and Relaxation in Plasmas, Warsaw, Poland, June 8-9, 2007</i> Book of Abstracts, p. 17
[17]	<b>Nanobashvili I., Devynck P., Nanobashvili S., Peleman P., Stöckel J., Van Oost G :</b> Characterization of Intermittent Bursts at the Edge of the CASTOR Tokamak. <i>10th Workshop on Electric Fields, Structures, and Relaxation in</i>

	<i>Plasmas, Warsaw, Poland, June 8-9, 2007 Book of Abstracts, p. 8</i>
[18]	<b>J. Ongena, A. Ekedahl, L.-G. Eriksson, J.P. Graves, M.-L. Mayoral, J. Mailloux, V. Petržilka, S.D. Pinches, K. Rantamäki, Yu. Baranov, L. Bertalot, C.D. Challis, G. Corrigan, K. Erents, M. Goniche, T. Hellsten, I. Jenkins, T. Johnson, D.L. Keeling, V. Kiptily, P.U. Lamalle, M. Laxåback, E. Lerche, M.J. Mantinen, J.-M. Noterdaeme, V. Parail, S. Popovichev, A. Salmi, M. Santala, J. Spence, S. Sharapov, A.A. Tuccillo, D. Van Eester and JET EFDA contributors:</b> Recent Progress in JET on Heating and Current Drive Studies in View of ITER. <i>JET Research Report EFD-P(06)19</i>
[19]	<b>V. Petržilka, G. Corrigan, V. Parail, K. Erents, M. Goniche, Y. Baranov, P. Belo, A. Ekedahl, G. Granucci, J. Mailloux, J. Ongena, C. Silva, J. Spence, F. Zacek and JET EFDA contributors:</b> SOL ionization by the lower hybrid wave during gas puffing. <i>submitted to Nuclear Fusion (on JET pinboard)</i> preprint EFD-P(06)25
[20]	<b>K.K.Kirov, Yu. Baranov, L. Colas, A. Ekedahl, K. Erents, M. Goniche, J. Mailloux, M.L. Mayoral, V. Petržilka, M. Stamp and JET EFDA Contributors :</b> LHCD Coupling And ICRF Sheaths At JET. <i>17th USA RF Topical Conference, Florida, 7-9 May 2007, preprint EFDA-JET-CP(07)01-08</i>
[21]	<b>M.Goniche, A.Ekedahl, J.Mailloux, V.Petržilka, K.Rantamäki, L.Delpech, K.Erents, M.Stamp, K.-D.Zastrow, and JET EFDA contributors:</b> SOL characterization and LH coupling measurements in different plasma configurations and gas puffing on JET. <i>34th EPS07 Conference, Warszawa, July 2-6th, 2007</i> paper P1. 152 (on JET pinboard), preprint EFDA-JET-CP(07)03/40.
[22]	<b>K.Rantamäki, A.Ekedahl, M.Goniche, J.Mailloux, V.Petržilka, G.Granucci, B.Alper, G.Arnoux, Y. Baranov, L.Delpech, K.Erents, N.Hawkes, J. Hobirk, E.Joffrin, K.Kirov, T.Loarer, F. Nave, I.Nunes, J.Ongena, V.Parail, F.Piccolo, E.Rachlew, C.Silva, M.Stamp, K.-D.Zastrow and JET EFDA contributors:</b> LH Wave Coupling over ITER-Like Distances at JET. <i>17th USA RF Topical Conference, Florida, 7-9 May 2007. preprint EFDA-JET-CP(07)01-09</i>
[23]	<b>V. Petržilka, J. Mailloux, M. Goniche, K. Rantamäki, G. Corrigan, V. Parail, P. Belo, L. Colas, A. Ekedahl, K. Erents, P. Jacquet, K. Kirov, M. Mayoral, J. Ongena, J. Spence:</b> Near LH Grill Density Variations as a Function of Gas Puff and LH power. <i>34th EPS07 Conference, Warszawa, July 2-6th, 2007</i> paper P4.100, preprint EFDA-JET-CP(07)03/60
[24]	<b>L. Colas, J.P. Gunn, I. Nanobashvili, V. Petržilka, M. Goniche, A. Ekedahl, S. Heurax, E. Joffrin, F. Saint-Laurent, C. Balorin, C. Lowry, V. Basiuk:</b> 2-D Mapping of ICRF-Induced SOL Perturbations in Tore Supra tokamak. <i>J. Nucl. Materials</i> 363-365 (2007) 555-559
[25]	<b>A. Ekedahl, M. Goniche, C. Balorin, V. Basiuk, Ph. Bibet, M. Chantant, L. Colas, L. Delpech, C. Desgranges, L.-G. Eriksson, E. Joffrin, F. Kazarian, C. Lowry, Ph. Moreau, V. Petržilka, C. Portafaix, M. Prou, H. Roche:</b> Thermal and non-thermal particle interaction with the LHCD launchers in Tore Supra. <i>Journal of Nuclear Materials</i> 363-365 (2007) 1329-1333

[26]	<b>R. Dejarnac and J. P. Gunn:</b> Kinetic calculation of plasma deposition in castellated tile gaps. <i>Journal of Nuclear Materials</i> 363-365 (2007) 560-564
[27]	<b>Havlíčková E., Zagórski R., Pánek R. :</b> Numerical Investigations of Plasma Parameters in COMPASS Tokamak. <i>10th Workshop on Electric Fields, Structures, and Relaxation in Plasmas, Warsaw, Poland, June 8-9, 2007</i> Book of Abstracts, p. 20
[28]	<b>Cahyna P., Becoulet M., Panek R., Fuchs V., Nardon E., Krlin L.:</b> Resonant magnetic perturbations and edge ergodization on the COMPASS tokamak. <i>10th Workshop on Electric Fields, Structures, and Relaxation in Plasmas, Warsaw, Poland, June 8-9, 2007</i> Book of Abstracts, p. 19
[29]	<b>Adamek J., Kocan M., Panek R., Gunn J.P., Stockel J., Martines E., Schrittwieser R., Ionita C., Popa G., Costin C., Brotankova J., Oost G. Van, Peppel L. van de:</b> Comparison of ion temperature measurements by Katsumata and Segmented Tunnel probes. <i>7th International Workshop on Electrical Probes in Magnetized Plasmas, Prague, July 22-25, 2007</i> Book of abstracts, p. 36
[30]	<b>Brotánková J., Martines E., Adámek J., Stöckel J., Popa G., Costin C., Schrittwieser R., Ionita C., Oost G. Van:</b> Novel technique for direct measurement of the plasma diffusion coefficient in magnetised plasma. <i>7th International Workshop on Electrical Probes in Magnetized Plasmas, Prague, July 22-25, 2007</i> Book of abstracts, p. 40
[31]	<b>Brotankova J., Belsky P., Weinzettl V., Bohm P., Barth R., Meiden H. Van:</b> New High Resolution Thomson Scattering system for the COMPASS tokamak. <i>Week of Doctoral Students 2007, June 5 - 8, 2007</i> to be published in proceedings
[32]	<b>Aftanas M., Belsky P., Bohm P., Weinzettl V., Brotankova J., Barth R., Meiden H. Van:</b> Exploitation of Avalanche Photodiodes for Thomson Scattering Diagnostics in tokamaks. <i>Week of Doctoral Students 2007, June 5 - 8, 2007</i> to be published in proceedings
[33]	<b>A.V. Chankin, D.P.Coster, N.Asakura, G.D.Conway, Corrigan, S.K.Erents, W.Fundamenski, Günter, J.Horacek, A.Kallengach, M.Kaufmann, C.Konz, K.Lackner, H W Müller, J.Neuhauser, R.A.Pitts, M.Wischmeier:</b> Discrepancy between modelled and measured radial electric fields in the scrape-off layer of divertor tokamaks: a challenge for 2D fluid codes?. <i>Nuclear Fusion</i> 47 (2007) 479–489.
[34]	<b>O E Garcia, J Horacek, V Naulin, A H Nielsen, R A Pitts and J J Rasmussen:</b> Fluctuations, transport and flows in TCV scrape-off layer plasmas. <i>Nuclear Fusion</i> 47 (2007) 667-676.
[35]	<b>O. E. Garcia, J. Horacek, J. S. Larsen, J. Madsen, V. Naulin, A. H. Nielsen, R. A. Pitts, J. J Rasmussen:</b> Convective transport by filamentary structures in scrape-off layer plasmas. <i>Book of Abstracts, Invited talk I-1.004</i> 34th EPS Conference on Plasma Physics, Warsaw, Poland, June 2-6, 2007
[36]	<b>R. A. Pitts, J. Horacek:</b> Neoclassical and transport driven parallel SOL flows [n TCV. <i>Book of Abstracts, Oral O-4.007</i> 34th EPS Conference on Plasma

	Physics, Warsaw, Poland, June 2-6, 2007
[37]	<b>B. Gulejová, R.A. Pitts, X. Bonnin, D. Coster, R. Behn, J. Horacek, J. Marki:</b> Time-dependent modelling of ELMing H-mode at TCV with SOLPS5. <i>Book of Abstracts, P-1.044</i> 34th EPS Conference on Plasma Physics, Warsaw, Poland, June 2-6, 2007
[38]	<b>Cahyna P., Krlín L., Pánek R., Kurian M.:</b> Interaction of particles with systems of magnetic islands and edge turbulence in tokamaks in fully Hamiltonian approach. <i>34th EPS Conference on Plasma Physics, Warsaw, Poland, June 2-6, 2007</i> Book of Abstracts, P-4.044
[39]	<b>Cahyna P., Pánek R., Fuchs V., Krlín L., Bécoulet M., Nardon E.:</b> Field Ergodization by External Coils on the COMPASS Tokamak. <i>WDS'07 Proceedings of Contributed Papers: Part II - Physics of Plasmas and Ionized Media, ed. Safrankova, J. and Pavlu, J. Prague, CR: Matfyzpress (2007)</i> p. 240-245
[40]	<b>J. Havlicek, J. Urban:</b> A Magnetic Equilibrium Reconstruction in Tokamak. <i>WDS'07 Proceedings of Contributed Papers: Part II - Physics of Plasmas and Ionized Media, ed. Safrankova, J. and Pavlu, J. Prague, CR: Matfyzpress (2007)</i> p. 234-239
[41]	<b>Cahyna P., Bécoulet M., Pánek R., Fuchs V., Nardon E., Krlín L.:</b> Resonant magnetic perturbations and edge ergodization on the COMPASS tokamak. <i>submitted to Plasma Physics Reports</i>
[42]	<b>B.P. LeBlanc, R.E. Bell, S. Bernabei, J.B. Caughman, L. Delgado-Aparicio, S.J. Diem, P.C. Efthimion, R.W. Harvey, J.C. Hosea, C.K. Phillips, J. Preinhaelter, P.M. Ryan, S. Sabbagh, G. Taylor, K. Tritz, J. Urban, J.B. Wilgen, J.R. Wilson:</b> HHFW and EBW Research on NSTX. 34th Annual European Physical Society Conference on Controlled Fusion and Plasma Physics. <i>34th Annual European Physical Society Conference on Controlled Fusion and Plasma Physics (2007)</i> P4.160
[43]	<b>H.P. Laqua, D. Andruczyk, E. Holzhauer, S. Marsen, M. Otte, Y.Y. Podoba, J. Preinhaelter, J. Urban, G.B. Warr:</b> Electron Cyclotron Wave Experiments at the WEGA Stellarator. <i>34th Annual European Physical Society Conference on Controlled Fusion and Plasma Physics (2007)</i> P1.154
[44]	<b>J. Preinhaelter, J. Urban, H.P. Laqua, Y.Y. Podoba, L. Vahala, G. Vahala:</b> Simulation of EBW Heating in WEGA. <i>Topical Conferences on Radio Frequency Power in Plasmas, ed. Ryan, P.M. and Rasmussen, D. 933 (2007)</i> p. 343-346
[45]	<b>Naydenkova D., Bilyk O., Stockel J.:</b> Magnetic diagnostic application for COMPASS tokamak. <i>Week of Doctoral Student 2007, June 5 - 8, 2007</i> oral presentation, article will be published in proceedings
[46]	<b>S.J. Diem, G. Taylor, J.B. Caughman, T. Bigelow, G.D. Garstka, R.W. Harvey, B.P. LeBlanc, J. Preinhaelter, S.A. Sabbagh, J. Urban, and J.B. Wilgen:</b> Electron Bernstein Wave Research on NSTX and PEGASUS. <i>17th Topical Conference on RF Power in Plasmas, Clearwater, Florida, May 7-9</i>
[47]	<b>G. Taylor, T.S. Bigelow, J.B. Caughman, S.J. Diem, R.A. Ellis, N.M. Ershov, E.H. Fredd, N.L. Greenough, R.W. Harvey, J.C. Hosea, J.</b>

	<b>Preinhaelter, A.K. Ram, D.A. Rasmussen, P.M. Ryan, A.P. Smirnov, J. Urban, J.B. Wilgen:</b> Plans for Electron Bernstein Wave and Electron Cyclotron Heating in NSTX. <i>17th Topical Conference on RF Power in Plasmas, Clearwater, Florida, May 7-9</i>
[48]	<b>Y. Y. Podoba, H. P. Laqua, G. B. Warr, M. Schubert, M. Otte, S. Marsen, and F. Wagner, D. Andruczyk, E. Holzhauer, J. Preinhaelter, J. Urban:</b> Electron Bernstein Wave Heating by OXB-Mode Conversion at Low Magnetic Field in the WEGA Stellarator. <i>Stellarator News, Issue 109, June 2009, p. 4</i> <a href="http://www.ornl.gov/sci/fed/stelnews/">http://www.ornl.gov/sci/fed/stelnews/</a>
[49]	<b>Kasperczuk A., Borodziuk S., Pisarczyk T., Gus'kov S.Yu., Ullschmied J., Krouský E., Mašek K., M. Pfeifer, Rohlena K., Skála J., Kálal M., Limpouch J., Pisarczyk P.:</b> Laser driven acceleration and collision of thin metal discs with massive targets: Effective energy transfer condition studies. <i>Proc. XXIX ECLIM, Madrid 11.-16.6. 2006 p. 584-589</i>
[50]	<b>Pisarczyk, T., Kasperczuk A., Borodziuk S., Nicolai Ph., Tikhonchuk V., Ullschmied J., Krouský E., Mašek K., Pfeifer M., Rohlena K., Skála J., Hora H., Pisarczyk P.:</b> Investigation of plasma jets produced by a defocused laser beam on planar metallic targets (oral lecture). <i>Proc. XXIX ECLIM, Madrid, 11.-16.6. 2006 p. 441-446.</i>
[51]	<b>Kasperczuk A., Pisarczyk T., Borodziuk S., Krousky E., Masek K., Pfeifer M., Rohlena K., Skala J., Ullschmied J., Hora H.:</b> Plasma jets generation by means of interaction of defocused laser beam with metallic targets of different mass density. <i>33rd EPS conf. on Plasma Phys. and Contr. Fus., Roma, Italy, June 19-23, 2006, Contribution No. P1.009</i>
[52]	<b>Nicolai Ph., Tikhonchuk V.T., Kasperczuk A., Pisarczyk T., Borodziuk S., Rohlena K., Ullschmied J.:</b> Plasma jets produced in a single laser beam interaction with a planar target. <i>33rd EPS conf. on Plasma Phys. and Contr. Fus., Roma, Italy, June 19-23, 2006, Contribution No. P2.033</i>
[53]	<b>Kasperczuk A., Pisarczyk T., Borodziuk S., Ullschmied J., Krousky E., Masek K., Rohlena K., Skala J., Hora H.:</b> Stable dense plasma jets produced at laser power densities around $10^{14}$ W/cm <sup>2</sup> ; <i>Physics of Plasmas</i> , 13(6): Art. No. 062704 Jun 2006
[54]	<b>Nicolai Ph., Tikhonchuk V.T., Kasperczuk A., Pisarczyk T., Borodziuk S., Rohlena K., Ullschmied J.:</b> Plasma jets produced in a single laser beam interaction with a planar target. <i>Physics of Plasmas</i> , 13 (6): Art. No. 062701 Jun 2006
[55]	<b>Nicolai Ph., Tikhonchuk V.T., Kasperczuk A., Pisarczyk T., Borodziuk S., Rohlena K., Ullschmied J.:</b> How produce a plasma jet using a single and low energy laser beam. <i>HEDLA - 6th International Conference on High Energy Density Laboratory Astrophysics, March 11-14, 2006, Rice University, Houston, Texas</i>
[56]	<b>Borodziuk S., Kasperczuk A., Pisarczyk T., Gus'kov S. Yu., Ullschmied J., Krousky E., Masek K., Pfeifer M., Rohlena K., Skala J., Kalal M., Limpouch J., Pisarczyk P.:</b> Study of the conditions for the effective energy transfer in a process of acceleration and collision of thin metal disks with the

	massive target. . <i>Eur. Phys. Jour. D</i> , 41 (2007), 311-317
[57]	<b>Kasperczuk A., Pisarczyk T., Borodziuk S., Ullschmied J., Krousky E. Masek K., Pfeifer M., Rohlena K., Skala J., Pisarczyk P.</b> : The influence of target irradiation conditions on the parameters of laser-produced plasma jets . <i>Physics of Plasmas</i> , 14 (3): Art. No. 032701 MAR 2007 (also US Virtual Journal of Ultrafast Science)
[58]	<b>Nicolai Ph., Tikhonchuk V.T., Kasperczuk A., Pisarczyk T., Borodziuk S., Rohlena K., Ullschmied J.</b> : How produce a plasma jet using a single and low energy laser beam . <i>Astrophysics and Space Science</i> 307 (1-3): 87-91 JAN 2007
[59]	<b>Kasperczuk A., Pisarczyk T., Borodziuk S., Guskov S.Yu., Ullschmied J., Krousky E. Masek K., Pfeifer M., Rohlena K., Skala J., Kalal M., Limpouch J., Pisarczyk P.</b> : Plasma jet generation by flyer disk collision with massive target . <i>Optica Applicata</i> , Vol. XXXVII, No. 1–2, 2007
[60]	<b>Interferometric investigations of influence of target irradiation on the parameters of laser-produced plasma jets</b> : Kasperczuk A., Pisarczyk T., Borodziuk S., Ullschmied J., Krousky E. Masek K., Pfeifer M., Rohlena K., Skala J., Pisarczyk P. . <i>Laser and Particle Beams</i> 25 (2007), 425–433.
[61]	<b>Kasperczuk A., Pisarczyk T., Gus'kov S. Yu., Ullschmied J., Krousky E., Masek K., Pfeifer M., Rohlena K., Skala J., Kalal M., Tikhonchuk V., Pisarczyk P.</b> : Laser Energy Transformation to Shock Waves in Multi-Layer Flyers . <i>PPLA 2007, Scilla, Italy, June 14-16 2007</i> , oral contribution Friday 2-2.
[62]	<b>Pisarczyk T., Kasperczuk A., Borodziuk S., Ullschmied J., Krousky E. Masek K., Pfeifer M., Rohlena K., Skala J., Pisarczyk P.</b> : Laser-driven jets . <i>EPS Conference on Plasma Physics, July 2-6, 2007, Warsaw</i> , paper I5007
[63]	<b>Nicolai Ph., Stenz C., Tikhonchuk V., Ribeyre X., Kasperczuk A., Pisarczyk T., Juha L., Krousk E. y, Masek K., Pfeifer M., Rohlena K., Skala J., Ullschmied J., Kalal M., Klir D., Kravarik J., Kubes P., Pisarczyk P.</b> : Supersonic plasma jet interaction with gases and plasmas at the PALS laser facility . <i>Phys. Rev. Letters</i> (submitted)
[64]	<b>Hron M., J. Pisacka J., Fernandes H., Sousa J., Neto A.:</b> COMPASS Control, Data Acquisition, and Communication system. <i>Sixth IAEA Technical Meeting on Control, Data Acquisition, and Remote Participation for Fusion Research, 4 - 8 June 2007 , Inuyama, Japan</i> P1-27
[65]	<b>Mlynar J., Bonheure G., Murari A., Popovichev S., Svoboda V.</b> : Abelisation of the Neutron Profile Data at JET using Minimum Fisher Regularisation. <i>34th EPS Conference on Plasma Physics, Warsaw, Poland, June 2-6, 2007</i> Book of Abstracts, P-2.129
[66]	<b>Mlynar J.:</b> Focus on: JET, The European Centre of Fusion Research. <i>EFDA JET Report EFD-R(07)01</i>
[67]	<b>J. P. Gunn and V. Fuchs:</b> Mach Probe interpretation in the presence of suprathreshold electrons. <i>Physics of Plasmas</i> 14 (2007) 1
[68]	<b>V. Fuchs and J. P. Gunn:</b> Quasi-neutral simulations of tokamak scrape-off

	layer currents. <i>34th EPS Conference on Plasma Physics and Controlled Fusion, Warsaw, Poland, 2-6 July, 2007.</i>
[69]	<b>Melnikov A.V., Eliseev L.G., Perfilov S.V., Lysenko S.E., Mavrin V.A., Shurygin R.V., Shelukhin D.A., Vershkov V.A., Tilinin G.N., Grashin S.A., Budaev V.P., Ufimtsev M.V., Kharchev N.K., Sarkisian K.A., Skvortsova N.N., Krupnik L.I., Komarov A.D., Kozachek A.S., Kraemer-Flecken A., Soldatov S.V., Ramos G., C.R. Gutierrez-Tapia, Hegazy H., Singh A., Zajac J., Van Oost G., Gryaznevich M.:</b> The study of GAM properties in the T-10 tokamak. <i>34th EPS Conference on Plasma Physics, Warsaw, Poland, June 2-6, 2007 Book of Abstracts, P-1.096</i>
[70]	<b>Perfilov S.V., Melnikov A.V., Eliseev L.G., Lysenko S.E., Mavrin V.A., Shurygin R.V., Shelukhin D.A., Vershkov V.A., Tilinin G.N., Grashin S.A., Krupnik L.I., Komarov A.D., Kozachek A.S., Kraemer-Flecken A., Soldatov S.V., Ramos G., C.R. Gutierrez-Tapia, Hegazy H., Singh A., Zajac J., Van Oost G., Gryaznevich M.:</b> Absolute plasma potential, radial electric field and turbulence rotation velocity measurements in low-density discharges on the T-10 tokamak. <i>34th EPS Conference on Plasma Physics, Warsaw, Poland, June 2-6, 2007 Book of Abstracts, P-2.058</i>
[71]	<b>Zajac J., Zacek F., Lejsek V., Brettschneider Z.:</b> Short-term power sources for tokamaks and other physical experiments. <i>Fusion Engineering and Design</i> Vol. 82 (2007), June, 369-379
[72]	<b>Piffl V., Dufková E.:</b> Plasma relaxations induced by gas-puffing and plasma biasing in the CASTOR tokamak. <i>34th EPS Conference on Plasma Physics and Controlled Fusion, Warsaw, Poland, 2-6 July, 2007 Book of Abstracts, P-1.093</i>
[73]	<b>I.Bolshakova, V. Coccoresse, A.J.H. Donné, I.Duran, S.Gerasimov, J.Gunn, R. Holyaka, O.Horbach, P.Moreau, A.Murari, A.Quercia, F. Saint-Laurent, J.Stockel, G. Vayakis, V. Yerashok :</b> ITER-relevant devices for steady state magnetic field measurement. <i>10th Workshop on Electric Fields, Structures, and Relaxation in Plasmas, Warsaw, Poland, June 8-9, 2007 Book of Abstracts, p. 20, submitted to Plasma Physics Reports</i>
[74]	<b>Brotankova J., Belsky P., Barth R., Meiden H. van der, Weinzettl V., Bohm P.:</b> Development of New High Resolution Thomson Scattering system for the COMPASS tokamak. <i>13th International Symposium on Laser-Aided Plasma Diagnostics</i> to be published in NIFS Proc Series
[75]	<b>Sentkerestiova J., Duran I., Viererbl L., Bolshakova I., Holyaka R.:</b> Impact of neutron irradiation on ITER candidate Hall sensors. <i>Europhysics Conference Abstracts</i> 31F (2007) P2.125
[76]	<b>Duran I, Sentkerestiova J., Viererbl L., I. Bolshakova:</b> Neutron irradiation tests of ITER candidate Hall sensors. <i>materials of Int. workshop on ITER-LMJ-NIF components in harsh environments, Aix-en-Provence, June 27-29, 2007</i> No. 029
[77]	<b>Bolshakova I., Coccoresse V., Donne A.J.H., Duran I., Gerasimov S., Gunn J., Holyaka R., Horbach O., Moreau P., Murari A., Quercia A., Saint-Laurent F., Stockel J., Vayakis G., Yerashok V.:</b> Progress in designing and

	testing ITER-relevant devices for steady state magnetic field measurements, contribution to proceedings. <i>proceedings of Int. workshop on ITER-LMJ-NIF components in harsh environments, Aix-en-Provence, June 27-29, 2007</i> No. 004
[78]	<b>Splichal K., Berka J., Burda J., Lahodova L., Masarik V., Vierebl L.:</b> Evaluation of corrosion and radiation behaviour TBM materials in Pb-Li melts (in Czech). <i>NRI –DRS report 1326</i> (2007)
[79]	<b>Honusek M., Bém P., Burjan V., Götz M., Fischer U., Kroha V., Novák J., Simakov S.P., Simeckova E. :</b> Neutron activation experiments on chromium and tantalum in the NPI p-7Li quasi-monoenergetic neutron field. <i>Proc. of International Conference on Nuclear Data for Science and Technology Nice 2007</i> (to be published)
[80]	<b>Bem P., Burjan V., Götz M., Fischer U., Honusek M., Kroha V., Novák J., Simakov S.P., Simeckova E. :</b> The NPI Cyclotron-based Fast neutron facility . <i>Proc. of International Conference on Nuclear Data for Science and Technology Nice 2007</i> (to be published)
[81]	<b>B. Lloyd, R.J. Akers, F. Alladio, Y. Andrew, L.C. Appel, D. Applegate, K.B. Axon, N. Ben Ayed, C. Bunting, R.J. Buttery, P.G. Carolan, I. Chapman, D. Ciric, J.W. Connor, N.J. Conway, M. Cox, G.F. Counsell, G. Cunningham, A. Darke, E. Delchambre, R.O. Dendy, J. Dowling, B. Dudson, M. Dunstan, A.R. Field, A. Foster, S. Gee, L. Garzotti, M.P. Gryaznevich, A. Gurchenko, E. Gusakov, N.C. Hawkes, P. Helander, T.C. Hender, B. Hnat, D.F. Howell, N. Joiner, D. Keeling, A. Kirk, B. Koch, M. Kuldkepp, S. Lisgo, F. Lott, G.P. Maddison, R. Maingi, A. Mancuso, S.J. Manhood, R. Martin, G.J. McArdle, J. McCone, H. Meyer, P. Micozzi, A.W. Morris, D.G. Muir, M. Nelson, M.R. O'Brien, A. Patel, S. Pinches, J. Preinhaelter, M.N. Price, E. Rachlew, C.M. Roach, V. Rozhansky, S. Saarelma, A. Saveliev, R. Scannell, S.E. Sharapov, V. Shevchenko, S. Shibaev, K. Stammers, J. Storrs, A. Surkov, A. Sykes, S. Tallents, D. Taylor, N. Thomas-Davies, M.R. Turnyanskiy, J. Urban, M. Valovic, R.G.L. Vann, F. Volpe, G. Voss, M.J. Walsh, S.E.V. Warder, R. Watkins, H.R. Wilson, M. Wisse and the MAST and NBI teams :</b> Overview of physics results from MAST . <i>Nuclear Fusion</i> 47 (2007) S658–S667
[82]	<b>R. Dejarnac, J.P. Gunn, J. Stöckel, J. Adámek, J. Brotánková, C. Ioniță:</b> Study of ion sheath expansion and anisotropy of the electron parallel energy distribution in the CASTOR tokamak. <i>Plasma Physics and Controlled Fusion</i> vol.49 (2007) 1791-1808
[83]	<b>G. Taylor , S.J. Diem , R.A. Ellis , E. Fredd , N. Greenough , J.C. Hosea, T.S. Bigelow, J.B. Caughman, D.A. Rasmussen , P. Ryan, J.B. Wilgen, R.W. Harvey ), A.P. Smirnov, N.M. Ershov, Josef Preinhaelter, Jakub Urban, A.K. Ram:</b> Recent EBW Emission Results and Plans for a 350 kW 28 GHz EC/EBW Heating System on NSTX. <i>49th Annual Meeting of the Division of Plasma Physics</i> DDP07 Web Bulletin of the American Physical Society
[84]	<b>H. Laqua, S. Marsen, M. Otte, Y. Podoba, Josef Preinhaelter, Jakub Urban:</b> Direct Measurement of the Electron Bernstein Wave Absorption and Current Drive at the WEGA Stellarator. <i>49th Annual Meeting of the Division of Plasma Physics</i> DDP07 Web Bulletin of the American Physical Society

[85]	<b>J. Urban, J. Preinhaelter, S.J. Diem, G. Taylor, L. Vahala, G. Vahala:</b> Investigation of collisional EBW damping and its importance to EBW emission from NSTX. <i>49th Annual Meeting of the Division of Plasma Physics DDP07</i> Web Bulletin of the American Physical Society
[86]	<b>S.J. Diem, G. Taylor, P.C. Efthimion, B.P. LeBlanc, J.B. Caughman, T.S. Bigelow, J.B. Wilgen, R.W. Harvey, J. Preinhaelter, J. Urban, S.A. Sabbagh :</b> Recent EBW Emission Results on NSTX. <i>49th Annual Meeting of the Division of Plasma Physics DDP07</i> Web Bulletin of the American Physical Society
[87]	<b>Josef Preinhaelter, Jakub Urban, H.P. Laqua, L. Vahala, G. Vahala:</b> O-X-B Mode Conversion Simulations for EBW Heating in the WEGA Stellarator. <i>2007 International Sherwood Fusion Theory Conference, Annapolis, MD, April 23-25, 2007</i> Poster Session 1E, 1E09
[88]	<b>J. Horacek, A. H. Nielsen, O. E. Garcia, R. A. Pitts:</b> Spatio-temporal correlations in edge tokamak plasma fluctuations in both experiment and modelling. <i>Bulletin of the APS, DPP07 APS Meeting, Florida, November 2007</i> NO3.00008
[89]	<b>B. Labit, A. Diallo, A. Fasoli, I. Furno, D. Iraj, S.H. Muller, G. Plyushchev, M. Podesta, F.M. Poli, P. Ricci, C. Theiler and J. Horacek:</b> Statistical properties of electrostatic turbulence in toroidal magnetized plasmas. <i>Plasma Phys. Contr. Fusion</i> 49 (2007) 12B 281
[90]	<b>W Fundamenski, O E Garcia, V Naulin, R A Pitts, A H Nielsen, J J Rasmussen, J Horacek, J P Graves and JET EFDA contributors:</b> Dissipative processes in interchange driven scrape-off layer turbulence. <i>Nuclear Fusion</i> 47 (2007) 417-433
[91]	<b>Bolshakova I., Ďuran I., Holyaka R., Hristoforou E., Marusenkov A.:</b> Performance of Hall Sensor-Based Devices for Magnetic Field Diagnosis at Fusion Reactors. <i>Sensor Letters</i> 5 (2007) 283-288
[92]	<b>Ďuran I., Sentkerestiová J., Bilykova O., Stockel J.:</b> Measurement of magnetic field using array of integrated Hall detectors on the CASTOR tokamak.. <i>Europhysics Conference Abstracts</i> 31F (2007) P2.152
[93]	<b>Kovařík K.:</b> Měření faktoru zásoby stability pomocí Hallových senzorů na tokamaku CASTOR. <i>bachelor thesis on KJR FJFI CVUT Praha 2007</i>
[94]	<b>Kasperczuk A., Pisarczyk T., Badziak J., Miklaszewski R., Parys P., Rosinski M., Wolowski J., Stenz C., Ullschmied J., Krousky E., Masek K., Pfeifer M., Rohlena K., Skala J., Pisarczyk P. :</b> Influence of the focal point position on the properties of a laser-produced plasma. <i>Physics of Plasmas</i> Vol.14, No.10 (2007)Art. No. 102706
[95]	<b>Badziak J., Kasperczuk A., Parys P., Pisarczyk T., Rosinski M., Ryc L., Wolowski J., Jablonski S., Suchanska R., Krousky E., Laska L., Masek K., Pfeifer M., Ullschmied J., Dareshwar L.J., Foldes I., Torrisi L., Pisarczyk P.</b> Production of high-current heavy ion jets at the short-wavelength subnanosecond laser-solid interaction. <i>Applied Physics Letters</i> Vol.91, No.8 (2007) Art. No. 081502

[96]	<b>Pisarczyk T., Kasperczuk A., Krousky E., Masek K., Miklaszewski R., Nicolai Ph., Pfeifer M., Pisarczyk P., Rohlena K., Stenz Ch., Skala J., Tikhonchuk V., Ullschmied J.:</b> The PALS iodine laser-driven jets . <i>Plasma Phys. Control. Fusion</i> 49(2007)B611-B619
[97]	<b>Kasperczuk A., Pisarczyk T., Nicolai Ph., Stenz Ch., Tikhonchuk V., Ullschmied J., Krousky E., Masek K., Pfeifer M., Rohlena K., Skala J., Kalal M., Pisarczyk P. :</b> Plasma jet interaction with ambient media.. <i>Physics of Plasmas</i> Submitted 12.12.2007.
[98]	<b>Velarde, P., Gonzalez M., Garcia-Fernandez C., Oliva E., Kasperczuk A., Pisarczyk T., Ullschmied J., Colombier J-P., Ciardi A., Stehle Ch., Busquet M., Rus, B., Garcia-Senz D., Bravo E., Relano A. :</b> Simulations of radiative shocks and jet formation in laboratory plasmas . <i>IFSA2007, Kobe Japan, September 9-14, 2007</i> paper ThO2.4
[99]	<b>Pisarczyk T., Kasperczuk A., Nicolai Ph., Ribeyre X., Stenz Ch., Krousky E., Masek K., Pfeifer M., Rohlena K., Skala J., Ullschmied J., Kalal M., Pisarczyk P. :</b> PALS laser-driven radiative jets for astrophysical and ICF applications . <i>PLASMA 2007, October 16-19, 2007 Greifswald, Germany</i> poster paper WeP44
[100]	<b>J. P. Gunn, L. Colas, A. Ekedahl, E. Faudot, V. Fuchs, S. Heuraux, M. Goniche, M. Kočan, A. Ngadjeu, V. Petržilka, F. Saint-Laurent, K. Vulliez:</b> Extreme Scrape-off Layer Phenomena during RF Heating in Tore Supra. <i>Proposed for 22nd IAEA Fusion Energy Conference, Geneva 2008, Switzerland.</i>
[101]	<b>M. Goniche, A. Ekedahl, K. Rantamäki, J. Mailloux, V. Petržilka, G. Arnoux, Y. Baranov, L. Delpech, K. Erements, P. Jacquet, K. Kirov, M-L. Mayoral, J. Ongena, F. Piccolo, A. Sirinelli, M. Stamp, K-D. Zastrow and JET EFDA contributors:</b> Lower Hybrid Current Drive Experiments on JET in ITER-Relevant Coupling Conditions. <i>Proposed for 22nd IAEA Fusion Energy Conference, Geneva 2008, Switzerland, on JET pinboard</i>
[102]	<b>J. Gunn, V. Petržilka, A. Ekedahl, V. Fuchs, E. Gauthier, M. Goniche, M. Kocan, F. Saint-Laurent:</b> Measurement of LH hot spots using a retarding field analyzer in Tore Supra. <i>Accepted oral paper for PSI-18 Plasma Surface Interactions in Controlled Fusion Devices, Toledo 2008, Spain</i>
[103]	<b>J. Ongena, Yu. Baranov, V. Bobkov, C.D. Challis, L. Colas, S. Conroy, F. Durodié, A. Ekedahl, G. Ericsson, L.-G. Eriksson, Ph. Jacquet, I. Jenkins, T. Johnson, L. Giacomelli, M. Goniche, G. Granucci, C. Hellesen, T. Hellsten, A. Hjalmarsson, K. Holmström, S. Huygen, J. Källne, V. Kiptily, K. Kirov, A. Krasilnikov, M. Laxåback, E. Lerche, J. Mailloux, M.L. Mayoral, I. Monakhov, M. Nave, M. Nightingale, J.M. Noterdaeme, M. Lennholm, V. Petržilka, K. Rantamäki, A. Salmi, M. Santala, E. Solano, D. Van Eester, M. Vervier, M. Vrancken, A. Walden :</b> ITER-relevant Heating and Current Drive Studies on JET . <i>Propose 22nd IAEA Fusion Energy Conference, Geneva 2008, Switzerland</i>
[104]	<b>K. Rantamäki, A. Ekedahl, M. Goniche, J. Mailloux, V. Petržilka, G. Granucci, B. Alper, G. Arnoux, Y. Baranov, V. Basiuk, P. Beaumont, G. Calabrò, V. Cocilovo, G. Corrigan, L. Delpech, K. Erements, D. Frigione, N.</b>

	<b>Hawkes, J. Hobirk, F. Imbeaux, E. Joffrin, K. Kirov, T. Loarer, D. McDonald, F. Nave, I. Nunes, J. Ongena, V. Parail, F. Piccolo, E. Rachlew, C. Silva, A. Sirinelli, M. Stamp, K-D. Zastrow and JET EFDA contributors:</b> LH power coupling over ITER-like plasma-wall distances at JET. <i>to be submitted to Plasma Physics and Controlled Fusion</i>
[105]	<b>M.Goniche, A.Ekedahl, J.Mailloux, V.Petržilka, K.Rantamäki, P.Belo, G.Corrigan, L.Delpech, K.Erents, P.Jacquet, K.Kirov, M.-L.Mayoral, J.Ongena, C.Portafaix, M.Stamp, K.-D.Zastrow and JET EFDA contributors:</b> SOL characterisation and LH coupling measurements on JET in ITER relevant conditions. <i>to be submitted to Nuclear Fusion</i>
[106]	<b>V. Petrzilka, M. Goniche, F. Clairet, G. Corrigan, P. Belo, J. Ongena and JET EFDA contributors:</b> On SOL Variations as a Function of LH Power <i>35th EPS Conf on Plasma Physics , Hersonissos 2008, Crete, Greece</i>
[107]	<b>Borisenko N.G., Khalenkov A.M., Kmetik V., Limpouch J., Merkuliev Yu.A., Pimenov V.G.:</b> Plastic Aerogel Targets and Optical Transparency of Undercritical Microheterogeneous Plasma, . <i>Fusion Science and Technology</i> 51 (2007) 655-664.
[108]	<b>Borisenko N.G., Akunets A.A., Khalenkov A.M., Klir D., Kmetik V., Krousky E., Limpouch J., Masek K., Merkuliev Yu.A., Pfeifer M., Pimenov V.G., Ullschmied J.:</b> Particular features of the transmission of laser radiation with wavelength 0.438 $\mu\text{m}$ and intensity $(3-7)\times 10^{14}$ W/cm <sup>2</sup> through an undercritical plasma from polymer aerogels, . <i>Journal of Russian Laser Research</i> 28 (2007) 548-566
[109]	<b>Kasperczuk A., Pisarczyk T., Gus'kov S.Yu., Ullschmied J., Krousky E., Masek K., Pfeifer M., Rohlena K., Skala J., Kalal M., Tikhonchuk V., Pisarczyk P.:</b> Laser Energy Transformation to Shock Waves in Multi-Layer Flyers. <i>PPLA-2007 (Plasma Production by Laser Ablation) June, 14th-16th 2007, Scilla, Italy, oral paper Friday 2-2</i>
[110]	<b>Rozanov V., Barishpoltsev D., Vergunova G., Gus'kov S., Demchenko N., Doshach I., Ivanov E., Aristova E., Zmitrenko N., Limpouch J., Klir D., Krousky E., Masek K., Kmetik V., Ullschmied J.:</b> Energy transfer in low-density porous targets doped by heavy elements, . <i>Inertial Fusion Science and Applications, Kobe, Japan, 9.-14.9.2007, paper TuPo26, Book of Abstracts, p. 173 (Proceedings in print).</i>
[111]	<b>Limpouch J., Renner O., Krousky E., Nazarov W., Borisenko N.G., Demchenko N.N., Gus'kov S.Yu., Klir D., Kmetik V., Liska R., Masek K., Merkul'ev Yu.A., Pfeifer M., Sinor M., Ullschmied J.:</b> Laser Interactions with Low-Density Foams for Laser Beam Smoothing and X-ray Source Studies, . <i>34th EPS Conference on Plasma Physics, Warsaw, 2-6 July 2007, ECA, Vol. 31F, O4.006 (2007).</i>
[112]	<b>Limpouch J., Renner O., Borisenko N.G., Klir D., Kmetik V., Krouský E., Liska R., Mašek K., Nazarov W., Ullschmied J.:</b> Applications of low-density foams for X-ray source studies and laser beam smoothing, . <i>Inertial Fusion Science and Applications, Kobe, Japan, 9.-14 September 2007, paper TuPo75, Book of Abstracts, p. 197</i>

[113]	<b>Renner O., Limpouch J., Krousky E., Klimo O., Klir D., Liska R., Nazarov W., Borisenko N.G., Ullschmied J.:</b> Spectroscopic investigation of laser energy deposition in low-density foams. . <i>3rd Moscow Workshop on Targets and Applications, Moscow, October 15 - 19, 2007.</i>
[114]	<b>Limpouch J.:</b> Laser interactions with underdense foams for laser beam and ablation pressure smoothing, (invited paper). . <i>5th Workshop on Direct-Drive and Fast Ignitron Physics, Madrid, 2-4 April 2007</i>
[115]	<b>Zebrowski J., Jakubowski L., Sadowski M.J., Malinowski K., Jakubowski M., Weinzettl V., Stockel J., Vacha M., Peterka M.:</b> Diagnostics of Fast Electrons within Castor Tokamak by Means of a Modified Cherenkov-Type Probe. <i>PLASMA 2007 – International Conference on Research and Applications of Plasmas, Greifswald, Germany, October 16-19, 2007 WeP3</i>
[116]	<b>Jakubowski L., Sadowski M.J., Stanislawski J., Malinowski K., Zebrowski J., Jakubowski M., Weinzettl V., Stockel J., Vacha M., Peterka M.:</b> Cherenkov Detectors For Measurements Of Fast Electrons In CASTOR-Tokamak. <i>17th IAEA Technical Meeting on Research Using Small Fusion Devices, Lisbon, Portugal, October 22-24, 2007 P17</i>
[117]	<b>Bohm P., Brotankova J., Weinzettl V., Aftanas M., Belsky P., Barth R., van der Meiden H.:</b> Design of new Thomson scattering diagnostics for COMPASS-D tokamak. <i>8th Carolus Magnus Summer School on Plasma and Fusion Energy Physics, Bad Honnef, Germany, September 3 – 14, 2007</i>
[118]	<b>Feketeova L., Tepnual T., Grill V., Scheier P., Roithová J., Herman Z., Märk T.D.:</b> Surface-induced dissociation and reactions of cations and dications C <sub>7</sub> H <sub>8</sub> <sup>+2+</sup> , C <sub>7</sub> H <sub>7</sub> <sup>+2+</sup> and C <sub>7</sub> H <sub>6</sub> <sup>2+</sup> : Dependence of mass spectra of product ions on incident energy of the projectiles . <i>International Journal of Mass Spectrometry</i> 265 (2007) 337-346
[119]	<b>Marek A. :</b> Low temperature plasma at intermediate pressures and in the magnetic field experiment and model. <i>Ph.D. Thesis</i> Charles University in Prague (2007)
[120]	<b>Neto A., Fernandes H., Duarte A., Carvalho B.B., Sousa J., Valcárcel D.F., Hron M., Varandas C.A.F.:</b> FireSignal—Data acquisition and control system software. <i>Fusion Engineering and Design</i> 82 (2007) 1359–1364
[121]	<b>Neto A., Fernandes H., Alves D., Valcárcel D.F., Carvalho B.B., Ferreira J., Vega J., Sánchez E., Pena A., Hron M., Varandas C.A.F.:</b> A standard data access layer for fusion devices R&D programs. <i>Fusion Engineering and Design</i> 82 (2007) 1315–1320

# 1 Provision of Support to the Advancements of the ITER Physics Basis

## Carbon transport in the TCV L-modes

V.Piffel

In collaboration with:

A. Zabolotsky, M. Bernard, E. Fable, H. Weisen, A. Bortolon, B.P. Duval, A. Karpushov  
Association Euratom-Confédération Suisse, Lausanne, Switzerland, EPFL, CRPP

The radial profiles of fully ionised carbon  $C^{6+}$  (transition  $n=8-7$ , 529.1 nm) released from TCV ( $R = 0.88$  m,  $a < 0.25$  m,  $B_T < 1.5$  T) wall tiles were measured using active Charge eXchange Recombination Spectroscopy (CXRS). A 1D impurity transport model was used to infer carbon transport parameters from the steady state profiles of fully ionised carbon. In Ohmically heated plasmas at values of  $q_{95} > 4$  a phenomenon of core impurity enrichment. A modest addition of EC Heating in L-mode leads to the flattening of electron density profile and is accompanied by peaked-hollow carbon density profile with clear anomalous origin.

### Experimental observations

The TCV vessel wall is entirely covered by polycrystalline carbon tiles, making carbon the dominant impurity in TCV. TCV is equipped with a diagnostic neutral beam operating at 50keV, delivering approximately  $1.6 \times 10^{19}$  H neutrals per second to the plasma. Ion temperature, toroidal rotation and carbon density profiles are obtained using a multiple chord visible spectrometer tuned to the  $n=8-7$  charge exchange transition of  $C^{+5}$ . The instrument is absolutely calibrated using an integrating sphere. The density of the  $C^{6+}$  along the line of sight was obtained by integrating the fitted active component of the signal corrected for the neutral beam attenuation and the changes of CX rate coefficient along the beam.

### Analyse of the spectroscopic data from the last experimental campaign in February 2007

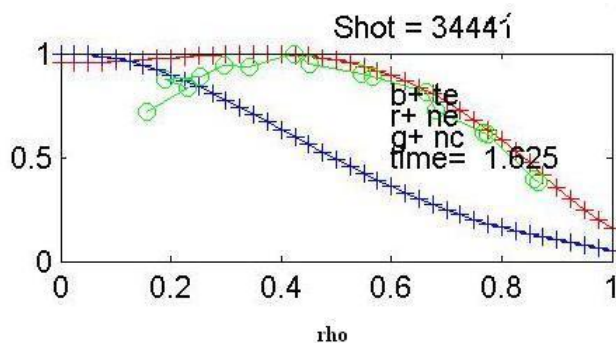


Fig.1 Normalized  $C^{+6}$ ,  $n_e$  and  $T_e$  radial profiles during the off-axis EC Heating (140 kW) in L-mode by  $I_p=140$  kA.

The operation of TCV was stopped in the first half of March for technical improvements of the machine. In February 2007 during the last sessions with ECH power scan the data were complemented also in  $z=0$  plasma position.

An analyse of steady-state fully-ionised carbon profiles from CXRS with off-axis ECH in L-mode indicate that the flattening of electron density profile is

accompanied by peaked-hollow carbon profile with clear anomalous origin.

Electron density profiles in TCV in the Ohmic phase are peaked. The Ware pinch and anomalous convective process like turbulent equipartition (TEP) and turbulent thermodiffusion (TTD) mechanisms may contribute to the shaping of the electron density profiles.

Which of the mechanism plays an important role in carbon density profile forming is unknown yet. An example of carbon density profile behaviour L-mode we demonstrate in **Fig.1**. At the beginning of discharge (shot 34441,  $I_p=140$  kA, without EC Heating), during the OH plasma phase a core impurity enrichment is observed, and more, the normalized  $n_c$  profile is almost the same as normalized  $n_e$  profile!

The presence of EC Heating leads to a flattening of the electron density profile. The dependence of the profile width in Ohmic target plasma is modified in ECH discharges by an additional dependence on deposition localisation – central heating results in profile broadening.

The modest addition of EC Heating in L-mode causes the broadening of electron density profile and consequently a peaked-hollow carbon density profile is observed. Evidently, such examples provide an experimental elements for validating comprehensive turbulent light-impurity transport models. In **Fig.2**, experimental electron density ( $n_e$ ) lines) profiles during the off-axis heating (400kW) in L-mode by  $I_p=140$ kA in shot=34441.and fully-ionized carbon density ( $n_c$ ) together with electron temperature ( $T_e$ ) profiles versus ( $\rho$ ) are shown during the off-axis EC Heating (400kW) in L-mode by  $I_p=140$ kA in shot = 34441. Profiles are normalized to the values at the centre.

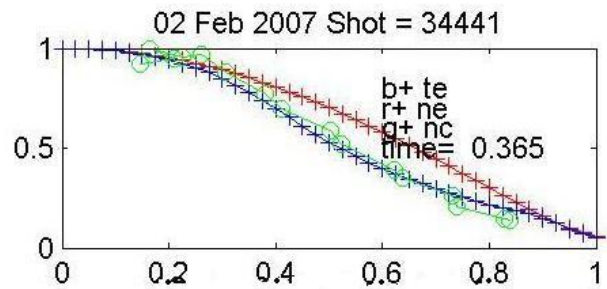


Fig.2 Normalized C+6,  $n_e$  and  $T_e$  radial profiles in L-mode by  $I_p=140$ kA

In **Fig.2**, experimental electron density ( $n_e$ ) lines) profiles during the off-axis heating (400kW) in L-mode by  $I_p=140$ kA in shot=34441.and fully-ionized carbon density ( $n_c$ ) together with electron temperature ( $T_e$ ) profiles versus ( $\rho$ ) are shown during the off-axis EC Heating (400kW) in L-mode by  $I_p=140$ kA in shot = 34441. Profiles are normalized to the values at the centre.

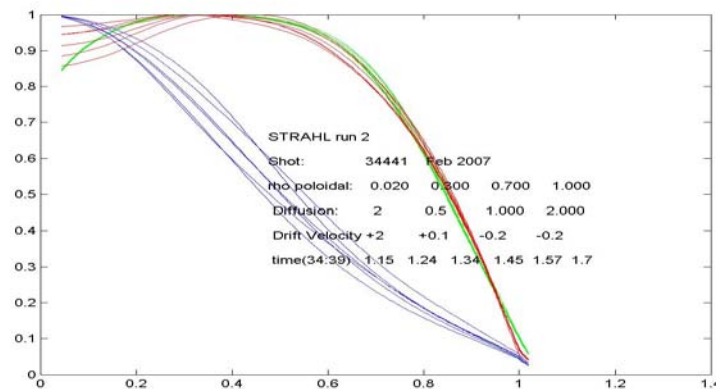


Fig.3 A demonstration example of possible creation of the  $C^{6+}$  hollow profile by simple modelling (five iterative steps) in L-modes with off-axis heating. Calculated radial  $C^{6+}$  density profile by STRAHL (green line). Fitted are experimental measured  $n_e$  (red lines) and  $T_e$  (blue lines)

The experimental and theoretical investigation will be continued with the goals:

- Provides an experimental element for validating comprehensive turbulent transport models.
- Characterise carbon density profiles from CXRS with off-axis ECH in L-mode to complete study undertaken in 2007.
- Characterise transport of Carbon species in same conditions.

## Ball-pen probes on ASDEX Upgrade tokamak

*J. Adámek, J. Stöckel, J. Brotánková*

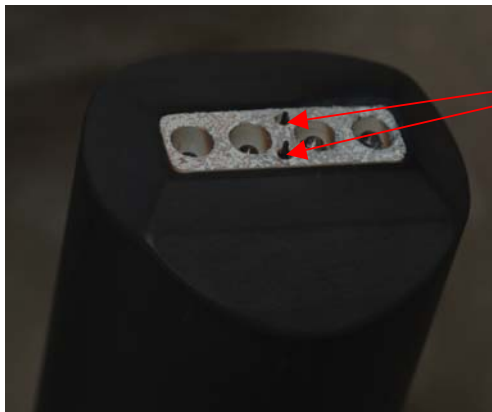
*In collaboration with:*

V. Rohde, W. Müller, A. Herrmann, EURATOM-IPP, Garching, Germany;

R. Schrittwieser, C. Ionita, F. Mehlmann, EURATOM-ÖAW, Innsbruck, Austria;

*The direct measurements of the plasma potential have been performed on ASDEX Upgrade tokamak in June 2007. It has been used a novel design of the ball-pen probe combined with the carbon shield. The ball-pen probe head has been mounted on the reciprocating manipulator located at the midplane. The probe has been exposed in the edge plasma a few millimeters outside the limiter shadow on the low field side. The measurements have been performed in the H-mode and Ohmic regime.*

The so-called ball-pen probe (BPP) was used for a direct determination of the plasma potential (see Fig. 1, probe head after measurements). Such measurements, combined with the results of other probes, would allow the reliable and fast determination of transport parameters and would support and further facilitate the development of a more comprehensive picture of edge plasma phenomena, in particular with respect to the profile of the plasma potential and thence the electric field in this region.



Langmuir probes

*Fig. 1: Photo of the quadruple ball-pen probe used in AUG in the campaign in June 2007 after use. The probe has four stainless steel collectors with conical tips which are retracted into the boron nitride screen with various depths  $h$ : from left to right  $h = -3$  mm,  $-2$  mm,  $-1$  mm and  $-0.5$  mm. In addition there are two graphite Langmuir probe pins.*

The principle of the BPP is to take use of the strongly different gyroradii of electrons and ions in any magnetized plasma. The collector of a BPP is retracted by a certain depth inside a screening channel of ceramic (usually boron nitride – BN). Thereby a certain part of the electron current density is shielded from it, whereas the ions, due to their much larger gyroradii are less impeded from reaching the collector. In this way the current-voltage characteristic of the retracted collector can be made almost symmetric and in a Maxwellian plasma it can be shown that in this case the floating potential of the collector  $V_{fl}$  becomes equal to the plasma potential.

In the AUG campaign of June 2007 a combination of four ball-pen probes was already used. Fig. 1 shows the probe head after several shots during each of which the probe head was inserted three to four times by the midplane manipulator into the AUG-SOL. The depths  $h$  of the four collectors was  $h = -3$  mm,  $-2$  mm,  $-1$  mm and  $-0.5$  mm ( $h = 0$  means the collector tip is exactly in the plane of the screening BN plate).

As we can see (Fig. 1), the surface of the BN screen around and in between the probes was damaged probably due to high energy radiation. For the next campaign a small modification of the carbon shield is suggested to protect the front part of the boron nitride of the BPP probe from radiation and plasma flux. In the campaign, during several shots the floating potential and its fluctuations (with sampling frequency  $f = 0.5$  MHz) of the four collectors was determined and compared, see Fig. 2.

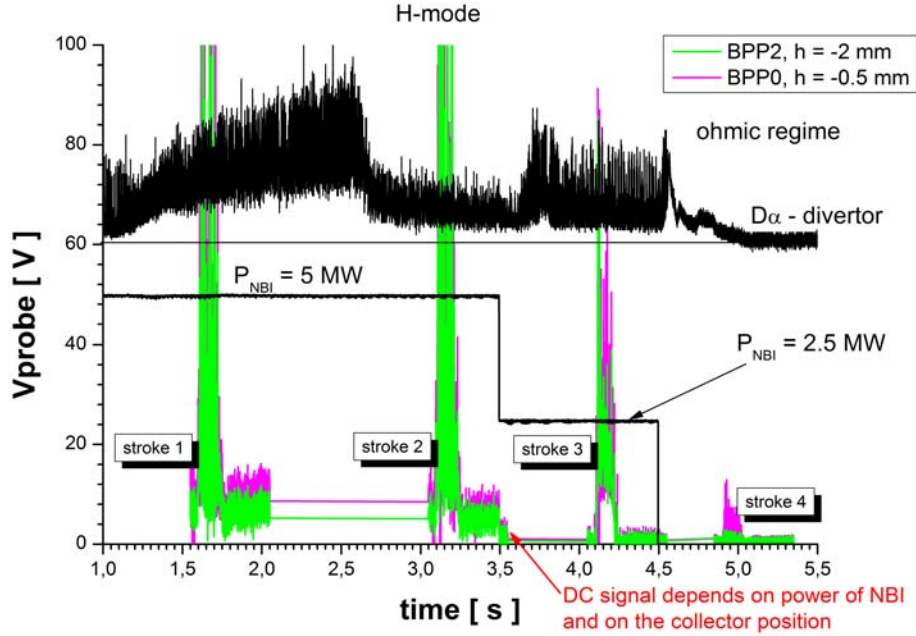


Fig. 2: The temporal evolution of the potential of two ball-pen probes ( $h = -0.5, -2$  mm). All ball-pen probes ( $h = -3, -2, -1, -0.5$  mm) have been inserted four times to the deuterium edge plasma under different conditions. The probes have measured potential in H-mode and ohmic regime as seen from  $D_\alpha$  signal. The reduction of the fluctuations of  $D_\alpha$  signal around 2.7s is caused by change of the gas puffing.

It was found that the four values of the floating potential are almost equal, which is a strong indication that the floating potential of all four collectors is indeed practically equal to the plasma potential, while the retraction depth of the collector did not matter much for the determination of this important parameter. However, all probes have provided different positive signals when the probe head has been located deep in the limiter shadow. These signals can be caused by the presence of high energetic ions due to ion losses during the application of NBI (5 MW).

Unfortunately, the two Langmuir pins which were also mounted on the probe head (see Fig. 1) did not deliver any results. The first Langmuir probe should record the current-voltage characteristic to determine the electron temperature  $T_e$ . The other Langmuir pin should have been negatively biased to record the ion saturation current from which the density fluctuations could have been derived. Another possibility envisaged was to record the cold floating potential  $V_{fl}$ , so that for comparison  $T_e$  could have been determined also by turning around the above mentioned relation  $T_e = (\Phi_{pl} - V_{fl}) / \ln(I_{es}/I_{is})$ , where  $\Phi_{pl}$  would have been taken from one of the BPPs.

## ELM pace making by biasing

V. Weinzettl

In collaboration with:

V. Rohde, P. Lang, Association EURATOM IPP, IPP Garching, Germany

*Experiments in many fusion devices like have shown an ability of the edge plasma biasing to influence plasma turbulences and edge density profile via mechanism of the  $E \times B$  velocity shear. A reduction in poloidal electric field, temperature, and density fluctuations across the shear layer leads to a reduction of the anomalous conducting and convection heat fluxes resulting in an energy transport barrier. On the other hand, such temporarily and spatially well-defined induced effect would be used for an edge plasma perturbation as a potential candidate for the ELM triggering. Some experimental indications have been found for a potential of the edge plasma biasing impacting on the ELM behaviour [1]. The intention of this explorative approach is to establish a well-defined "perturbation" by the pulsed edge plasma biasing and to search for correlations with the ELM behaviour.*

The ELM pacing experiments were realized on the ASDEX-Upgrade tokamak in several shots at  $B_T \sim 2.1\text{-}2.5$  T,  $I_p \sim 0.6\text{-}0.8$  MA,  $n_e \sim 4\text{-}8 \cdot 10^{19}$  m<sup>-3</sup> and with a different auxiliary heating. As a biasing electrode, the midplane manipulator (MEM) with several carbon tips inserted into the massive carbon envelope, usually serving for the probe measurements, was used, see Fig.1.

The tips were biased using four KEPCO sources triggered by a single signal generator. Biasing voltage was set to -100 V and applied as short rectangular pulses (millisecond time scale) at different frequencies close to an ELM natural frequency. A depth of the MEM insertion was chosen to be acceptable for the MEM according to an expected heat load, and set stepwise to be from the limiter position up to 5 mm far from the separatrix. In the realized shots, only a later part of each shot was used for a single MEM insertion, lasting typically 200 ms. There an ELM activity was monitored using the  $H_\alpha$  signals from the inner and outer divertor legs and using magnetic coil signals. At the same time, changes of the stored energy in plasma were measured.



*Fig. 1. Biasing carbon tips of the midplane manipulator head (without a carbon envelope) on the ASDEX-Upgrade tokamak.*

The first analysis of measured data shows a change of natural ELM frequency during a period of the biased MEM insertion and an occurrence of new smaller satellite ELMs. The data evaluation is in progress.

### References:

- [1] M. Tsalas, et al., *J. Nuc. Mater.* 337-339 (2005) 751-755

## Determination of reflection characteristics of small hydrocarbon ions of low incident energies in collisions with with room-temperature and heated carbon and tungsten surfaces

Z. Herman, J. Žabka, A. Pysanenko

J. Heyrovsky Institute of Physical Chemistry, Academy of Sciences of the CR

In collaboration with:

T. D. Märk and his research group (Institute for Ion and Applied Physics, University of Innsbruck, Innsbruck), Association EURATOM-ÖAW, Austria

W. Schustereder, MPI Garching, Association EURATOM, Germany

The aim of this research is investigation of interactions between slow ions and surfaces of materials relevant to plasma-wall interactions in fusion devices. The objective is - on the one hand - to obtain data on the survival of slow ions in surface collisions, product ion energy losses in ion-surface interactions, dissociative and chemical processes at surfaces, and information on collision kinematics, using the special ion-surface scattering apparatus available in Prague, and - on the other hand - to determine reflection characteristics of hydrocarbon ions, namely the sticking coefficient of hydrogen (deuterium) on various surfaces.

### 1. Collisions of small hydrocarbon ions of very low energies with carbon surfaces at room temperature [1].

Using the previously developed scattering method, interaction of hydrocarbon ions  $CD_3^+$ ,  $CD_4^+$ , and  $CD_5^+$  of very low energies (below 10 eV) with carbon (highly oriented pyrolytic graphite, HOPG) surfaces was studied. The ion survival probability,  $S_A(\%)$  at energies below 10 eV (for incident angle  $30^\circ$  with respect to the surface) was measured for the above mentioned incident ions. The  $S_A$  values were found to decrease from about 12% for  $CD_5^+$ , and 0.3 – 0.4 % for  $CD_3^+$  and  $CD_4^+$  at 10 eV towards zero at lower incident energies.

The data are summarized in Fig. 1. The new data for energies below 10 eV fit well data for incident energies 15 – 45 eV (see Fig. 1) obtained earlier [2].

Angular and translational energy distributions of product ions were measured for all three incident ions and several energies between 10 and 3 eV.

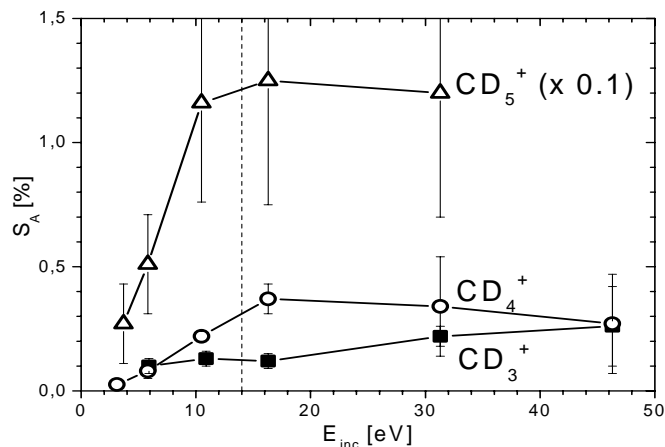


Fig. 1: Survival probability of hydrocarbon ions

The simplest data were for the closed-shell non-reactive incident ion  $CD_5^+$  of a fairly high survival probability, showing single angular peaking and translational energy distributions of the product ions  $CD_3^+$  and its fragment  $CD_3^+$  with about 30% of the incident energy in the translational energy of the product ions (in the angular maximum). The fragmentation to  $CD_3^+$

occurred at these low incident energies partly because of initial internal energy of the projectile ion and it took place after the interaction with the surface, as manifested in similar velocity distributions of both  $CD_5^+$  and  $CD_3^+$ . Analogous data were obtained for the incident ions  $CD_3^+$ . Because of a low survival probability of the incident ion, the angular data had to be corrected for a contribution from background gas-phase scattering of the projectile ion and for a fraction of fast ions deflected in front of the surface by local surface micro-charges (this effect was visible on HOPG only at very low incident energies). The scattering data for the reactive radical cation  $CD_4^+$  showed contributions of inelastic and dissociative scattering of the incident projectile ion and also of reactive scattering from interaction of  $CD_4^+$  with the surface material. The main reaction was H-atom transfer to  $CD_4^+$  from hydrocarbons, adsorbed on room-temperature carbon surface, and at 10 eV formation of  $C_2$  hydrocarbon ions in reactions of  $CD_4^+$  with terminal  $CH_3$ -groups of surface hydrocarbons. The scattering results were used to estimate the effective surface mass involved in the inelastic collisions. The values of it correspond to the mass of one or several terminal hydrocarbon groups of the hydrocarbons adsorbed on the room-temperature carbon surface [1,3].

Analogous data for  $C_2D_4^+$  interaction with room-temperature HOPG are being analyzed and will be published soon.

Fragmentation of polyatomic cations and dications ( $C_7H_n^{+/2+}$ ,  $n=6,7,8$ ) with hydrocarbon-covered surface was investigated over the incident energy range 5-50 eV to estimate the role of the projectile charge on energy partitioning in surface collisions [4].

## 2. Reflection properties of deuterated hydrocarbon ions

Surfaces relevant to fusion devices (plasma-sprayed tungsten, carbon fiber composite, beryllium) were bombarded by deuterated hydrocarbon ions of energies up to 100 eV. Sticking coefficients to the surface of one of the collision products, deuterium molecules, were determined using the nuclear reaction analysis combined with the Rutherford back-scattering method (MPI Plasma Physics, Garching). Upon bombardment with  $CD_3^+$  ions, the sticking coefficient of  $D_2$  to plasma-sprayed tungsten (PSW) was found to be about 0.2, and 0.2-0.3 on carbon fiber composite (CFC), in both cases little dependent on the incident energy between a few and 100 eV [5].

### References:

- [1] A. Pysanenko, J. Žabka, F. Zappa, T.D. Märk, Z. Herman, *Int. J. Mass Spectrom.* (accepted)
- [2] J. Roithová, J. Žabka, Z. Dolejšek, Z. Herman, *J. Phys. Chem. B*, 106 (2002) 8293).
- [3] A. Pysanenko, J. Žabka, Z. Herman: XVI Symposium on Atomic, Cluster, and Surface Physics (SASP 2008), Les Diablerets, (CH), January 2008 (Extended abstract)
- [4] L. Feketeová, T. Tepnual, V. Grill, P. Scheier, J. Roithová, Z. Herman, T.D. Märk, *Int. J. Mass Spectrom.* **265**, 337-346 (2007)
- [5] B. Rasul, F. Zappa, N. Endstrasser, W. Schustereder, J. D. Skalny, Z. Herman, P. Scheier, T.D. Märk, 18th International Conference on Plasma-Surface Interactions, Toledo (E), 2008 (Book of Abstracts).

## Experiments and modeling of fast particle generation at LH and ICRF heating

*V. Petržilka, V. Fuchs*

In collaboration with:

*J. P. Gunn, L. Colas, A. Ekedahl, M. Goniche, M. Kočan, F. Saint-Laurent, Assoc. EURATOM-CEA Cadarache*

*A retarding field analyzer (RFA) was used during lower hybrid (LH) and ion cyclotron resonance frequency (ICRF) experiments in the Tore Supra tokamak to measure the flux of supra-thermal particles emanating from the near field region in front of the antennas.*

As it is well known, fast electrons can be generated in front of the LH grills, and they cause high thermal loads (hot spots) in the locations at which they impact. When these fast electrons escape from the space in front of the grill mouth, they leave the ions behind, and a region of a positive charge is created. This positive charge then possibly can accelerate also ions to energy of several hundreds eV, which might cause sputtering in locations magnetically connected to the grill mouth. According to a novel electron acceleration process recently proposed [1], fast electrons might be possibly generated also near the ICRF antennas: The electrons can gain energy in passing the near ICRF antenna rf field inhomogeneity, because of the temporal phase changes of the field, which do not average out on the electron quiver motion time scale. This mechanism can enhance the RF sheath potential, and consequently also the energy of ions, which are accelerated by this sheath potential.

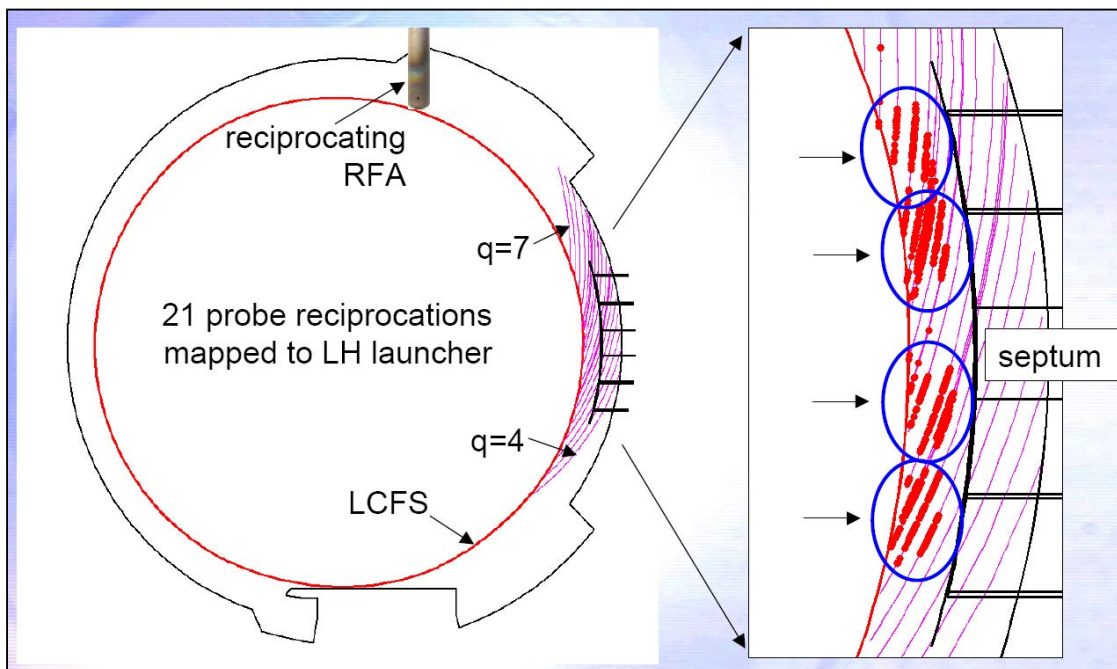


*Fig. 1. Scheme of the RFA fast particle measurements in front of the LH grill.*

To find the fast ions, we considered as beneficial to measure in locations, where the fast electron beam is not too strong. Therefore, during the measurements, the detection and energy distribution measurements of the locally generated fast electrons and ions in front of LH and possibly also in front of the ICRF antennas was attempted to carry out.

For this, we estimated the fast ion drift in the above mentioned electrostatic field in front of the LH antenna, to find such possible locations, where the fast ions can be present, and in the same time, the fast electron energy is as low as possible. No fast ions were found, and we will not describe these measurements in detail. We concluded that, if the fast ions are really generated, they are masked by the fast electrons, and it is necessary to screen these electrons more strongly than it is now possible by the biasing of the RFA grids – the available voltage is too low.

By varying  $q$  from about 4 to about 7, a detailed poloidal – radial mapping of the fast electron beam were done, Fig. 1. The first RFA grid was biased to  $UG1=+200$  V to repel thermal ions, 2<sup>nd</sup> grid voltage was  $UG2=-200$  V to repel thermal electrons,  $P_{C2}=1.5$  MW (maximum available power). Similar mapping was also done for 0.8 MW. It can be seen that fast electrons extend up to the LCFS (“2<sup>nd</sup> beam”), what can have important consequences for the thermal loads and for computations of the LH SOL dissipated power. The next Fig. 2 shows growth of the radial beam intensity distribution with power. As the comparison of the 1st and 2nd beam (more near to the LCFS) shows, the mean collector current in the two beams is comparable at higher PLH.

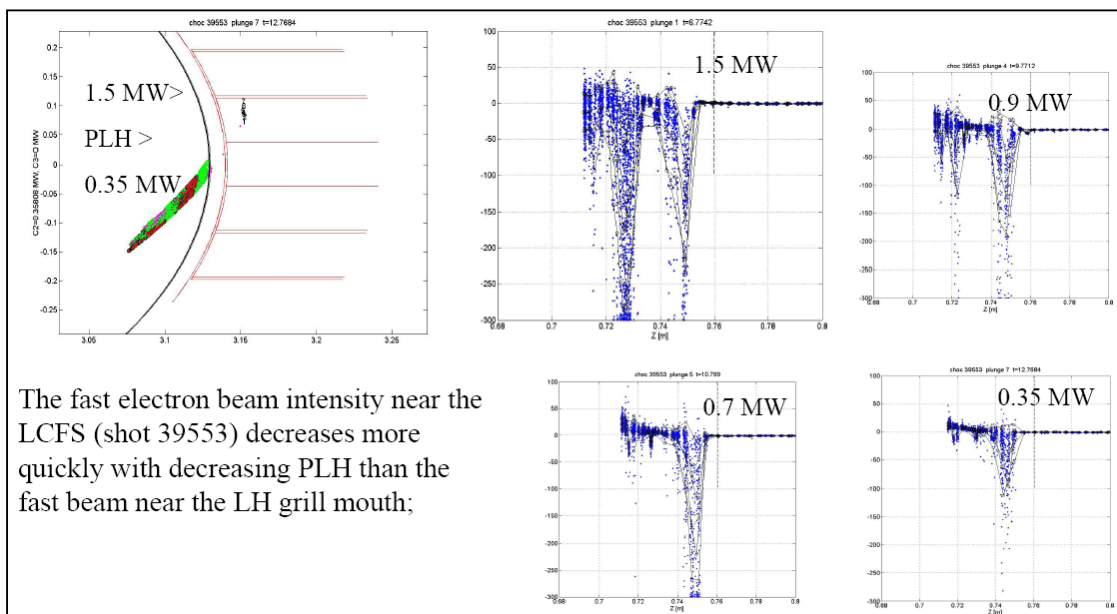


Fig. 2. Variations of the beam intensity (collector current) as a function of LH power.

The 2nd beam (i.e., the unexpected part of the beam radially more distant from the grill mouth) amplitude varies much more strongly with power. The 2nd beam generation might perhaps be connected with the nonlinear production of higher spatial harmonics, studied in exploration of the so called spectral gap problem [2].

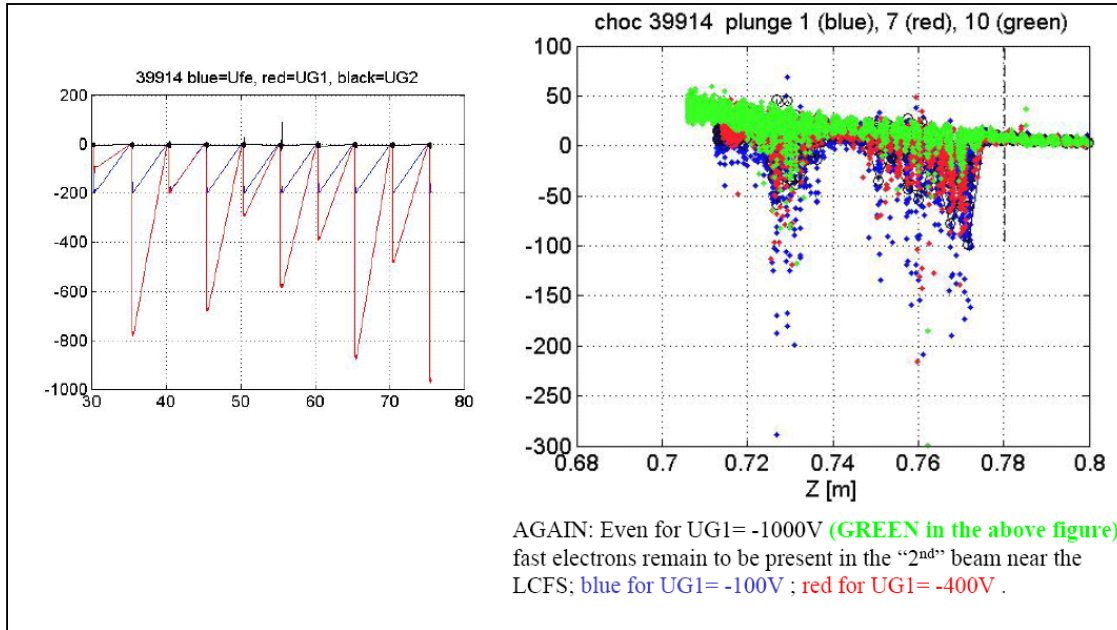


Fig. 3. Variations of the collector current with  $UG1$  up to  $-1000$  V.

Fig. 3 shows that the fast electrons with energy larger than  $1\text{keV}$  remain to be present up to the LCFS for medium LH powers.

Further, new RFA experiments were also performed devoted to exploration of the flux tubes connected to ICRH Q5 antenna to determine sheath potential in presence of ICRF as a function of SOL density, and to determine whether there are any suprathermal electrons or ions using retarding field analyzer (RFA). Strong variations of the RFA slit and collector current were found in locations magnetically connected to the vicinity of the Q5 antenna, in correspondence with the variations of the plasma density and temperature near the antenna. Detailed mapping of the floating potential in the flux tubes connected to an ICRH antenna was done.

To evaluate the transmission factor of the RFA slit, information about the transverse electron energy was needed. To this purpose, a modeling of fast electron generation including the electron transverse energy development was performed. It was found that the gain of the transverse energy of the electrons in the fast particle beam obtained from the LH field or from the transformation of the longitudinal velocity of the fast particles to the transverse velocity by collisions is negligible in the RFA transmission factor calculations.

### Main results:

The fast electron energy distribution of accelerated particles in the fast electron beam was determined: Also for as low LH power as  $0.35$  MW, fast electrons with energy larger than  $400$  eV are generated. Even for  $UG1 = -1000\text{V}$ , fast electrons with energy higher than  $1$  keV remain to be present in the “2nd” beam near the LCFS. The fast electron beam generated by the parasitic wave

absorption extends for high PLH up to the LCFS and is up to 5 cm or even more radially wide, with possible corresponding radially broader heat loads in case that the beam impacts on the wall. The observed existence of the wide beam needs to be explained by theory, as the current theory predicts the radial width of the beam of several mm. The fast electron beam intensity very near to the LCFS decreases more quickly with decreasing PLH than the fast beam intensity near the LH grill mouth. As the comparison of the 1st and 2nd beam shows, the mean collector current (and therefore similar unwanted heat loads) in the two beams is comparable at higher PLH. The 2nd beam generation might perhaps be connected with the nonlinear production of higher spatial harmonics, studied in exploration of the so called spectral gap problem. No locally produced fast ions by the LH wave were found.

A more sophisticated modeling of fast particle generation shows that the locally LH produced gain of the transverse energy of the fast particles can be neglected in the calculations of the transmission factor of the RFA slit. The knowledge of the transmission factor is needed in parasitic absorption heat load calculations from RFA measurements. No clear indications of fast particles emanating from the region of ICRF antenna were found by the RFA. The flux tubes connected to ICRH Q5 antenna were explored by the RFA to determine sheath potential in presence of RF as a function of SOL density.

All results mentioned above were obtained in a team effort.

#### **References:**

- [1] V. Petrzilka et al., presented at the Tarragona EPS05 Conference, paper P-2.095.
- [2] V. Petrzilka, Plasma Physics Contr. Fusion 33 (no 4) (1991) 365.

## Modeling of LH wave ionization, development of EDGE2D code to 3D

*V. Petržílka*

In collaboration with:

*J. Mailloux, G. Corrigan, V. Parail, K. Erents, P. Jacquet, K. Kirov, J. Spence, Assoc. EURATOM-UKAEA;*

*M. Goniche, A. Ekedahl, Assoc. EURATOM-CEA-Cadarache;*

*K. Rantamäki, Association Euratom – Tekes;*

*P. Belo, Association Euratom-IST, Lisboa;*

*J. Ongena, Ass. EURATOM – Belgian State*

*We performed numerical modeling of near Lower Hybrid (LH) grill Scrape-off-Layer (SOL) plasma density variations  $n_{e,SOL}$  as a function of gas puff and LH power ionization with the fluid code EDGE2D. Novel 3D limiter-like features in the EDGE2D are introduced. The modeling shows that both puff and heating/ionization are important in raising the density in the far SOL, what is important for LH wave coupling in ITER like discharges.*

The modeling of gas puff ionization is a 3D problem, but an amended 2D poloidal – radial model can provide useful insights. The code includes direct SOL ionization by the LH wave [1]. It is assumed that the ionization by the LH wave is produced due to the local SOL electron heating by the wave. A fraction of power lost in SOL increases the SOL  $T_e$ , which in turn increases ionisation in the SOL. Locally generated fast particles can also participate in the heating process. EDGE2D [1] is modified so that it can model a SOL up to 10 cm or more. Modelling of the private space in front of the grill needs to introduce 3D limiter-like features into EDGE2D. This is attempted in the present contribution. The poloidal limiters are modeled as spatially localized sinks, where the recombination is artificially strongly enhanced. This quasi 3D modeling with poloidal limiters acting as sinks allows to distinguish the private space of the grill between the poloidal limiters in the modeling.

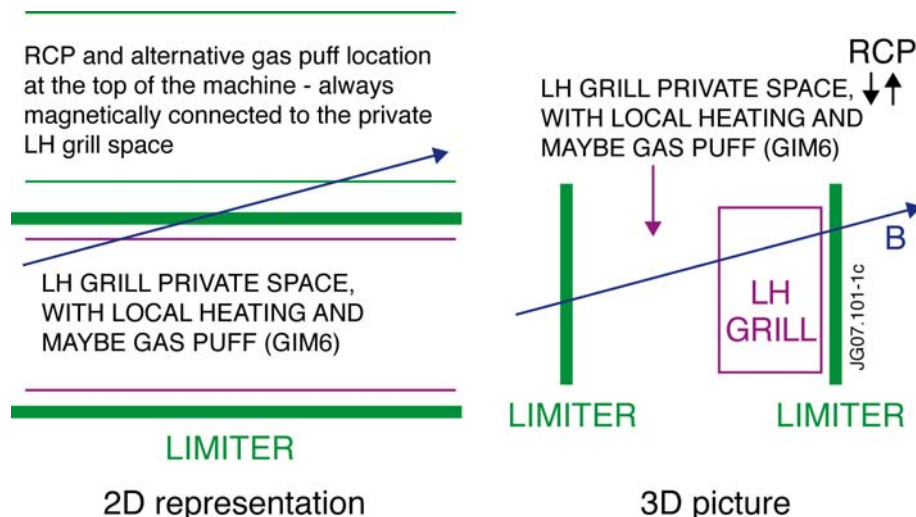


Fig. 1. Schematic representation of the 2D and 3D configuration of the LH grill and RCP.

In this way, it is possible to investigate the impact of parameters such as gas puffing rate, gas puffing poloidal location, LH power dissipated in the SOL and radial location of the LH dissipated power (e.g., radially near the grill mouth, or further away from the grill mouth), separately on the  $n_{e,SOL}$  in the private launcher SOL and in the private RCP (Reciprocating Probe) SOL space. However, the gas puff location in the 2d modeling is always magnetically connected to the LH grill private space, Fig. 1. It is therefore impossible to distinguish between magnetically connected and not-connected gas puff. Similarly, the RCP location is also always connected to the LH grill private space. Obviously, there is a need for a fully 3D modeling code, to obtain a more quantitative description of the trends obtained now by the quasi-3D model.

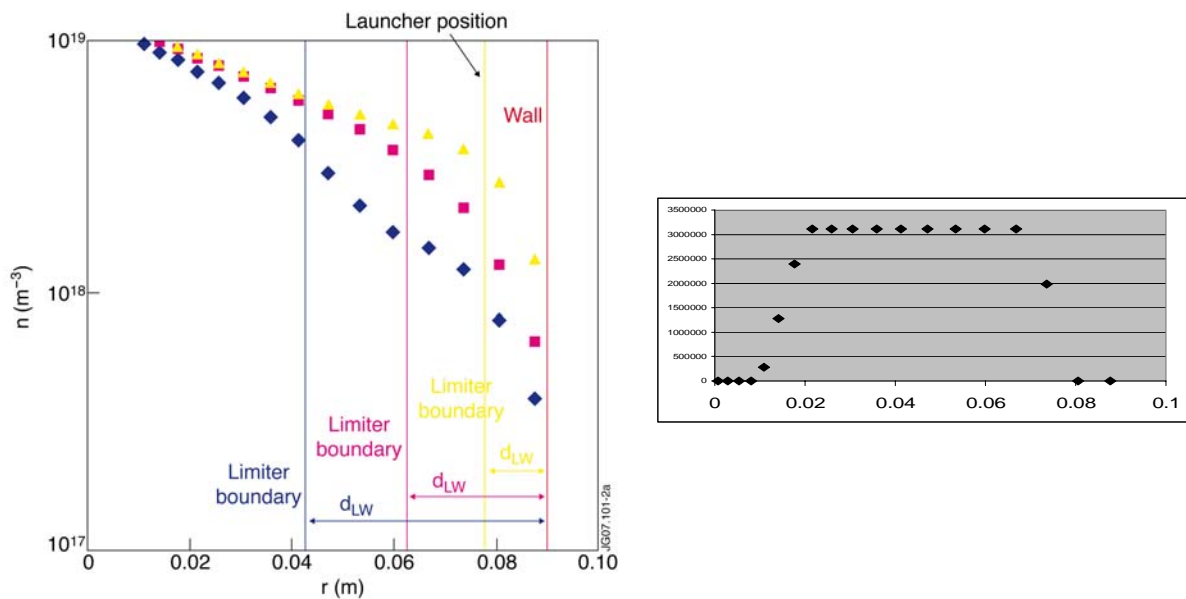


Fig. 2. Left figure: Effects of the limiter boundary location.  $x$ - axis: distance from separatrix in  $m$ . Right figure: Profile “D” of the LH field dissipation [a.u.]. Series 1 (blue diamonds):  $d_{LW} = 4.75$  cm (grill  $\sim 3$  cm behind the limiter), series 2 (magenta rectangles):  $d_{LW} = 2.75$  cm (grill  $\sim 1$  cm behind the limiter), and series 3 (yellow triangles):  $d_{LW} = 1.25$  cm (grill is  $\sim$  flush with the limiter).

Figure 2 then shows  $n_{e,SOL}$  in LH private SOL as a function of the limiter boundary location (changing the distance limiter – wall  $d_{LW}$  is similar to changing the distance launcher-limiter) Gas puff is  $1e22$  el/s near the outer mid-plane (OMP), i.e., by “GIM6”. Heating in front of the grill is 150 kW. The assumed profile of the LH SOL dissipation used in this contribution is shown as profile “D” on the bottom figure. The upper figure shows the  $n_{e,SOL}$  in the OMP (between limiters acting as a sink) in the launcher private SOL. The next Figure 3 shows  $n_{e,SOL}$  in the limiter sink (top figure) and at the RCP location (bottom figure) as a function of the limiter boundary location. Gas puffing and heating is the same as in Fig.2.

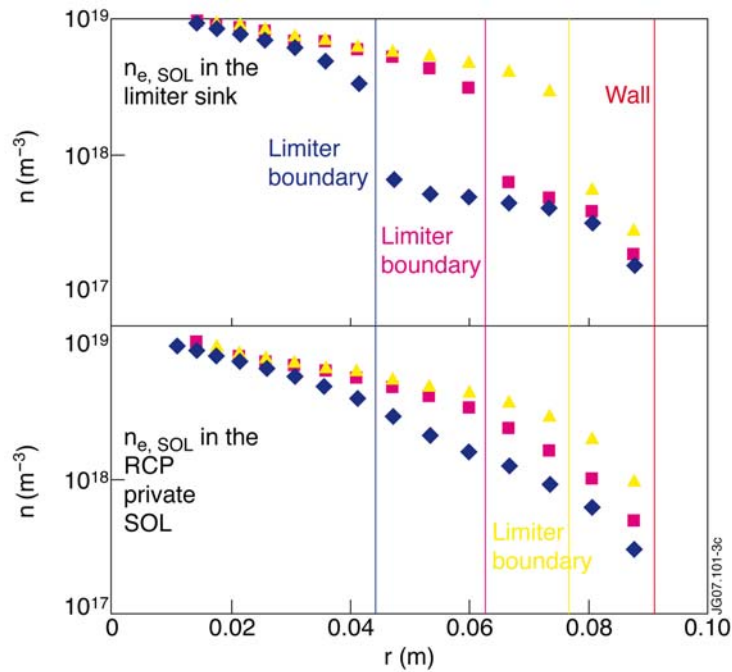


Fig. 3. Profiles of  $n_{e,SOL}$  near limiters and in the RCP private SOL.

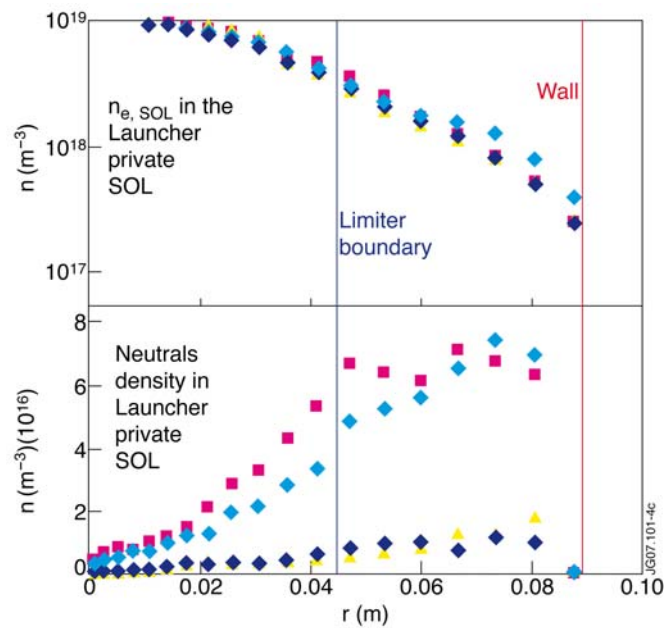


Fig. 4. Upper figure:  $n_{e,SOL}$  as a function of the heating and puff rates, at the bottom figure there are corresponding neutrals profiles in the OMP. Blue diamonds: 0 heating, 0 puff, magenta rectangulars: 0 heating, puff = 1e22 el/s, yellow triangles: heating = 150 kW, 0 puff, Cyan diamonds: heating = 150 kW, puff = 1e22 el/s.

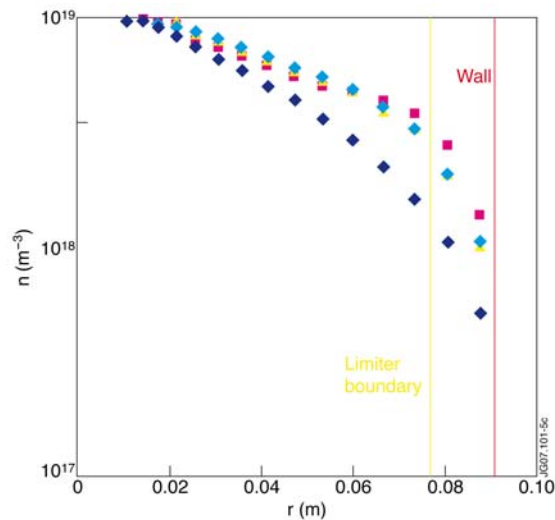


Fig. 5. Profile of  $n_{e,SOL}$  in the OMP in grill private SOL, as a function of the gas puff location. Blue diamonds: 0 heating, 0 puff, magenta rectangles: gas puff  $1e22$  el/s near OMP, yellow triangles: gas puff near RCP, cyan diamonds: gas puff at the top.

Figure 4 shows  $n_{e,SOL}$  in the OMP (upper figure) as a function of the heating and puff rates, with  $d_{LW} = 4.75$  cm; on the bottom figure there are neutrals profiles in the OMP. Let us note that joined heating and gas puff tend to flatten the  $n_{e,SOL}$  profile, cf. the cyan curve. It can be demonstrated that the flatness of the  $n_{e,SOL}$  profile depends also on the assumed profile of the LH wave dissipation. The more near to the grill the LH power is dissipated, the more flat is the  $n_{e,SOL}$  profile. Figure 5 shows  $n_{e,SOL}$  in the OMP in grill private SOL, as a function of the gas puff location,  $d_{LW} = 1.25$  cm, with heating in front of the grill = 150 kW.

**Main results:** The modeling shows that both puff and heating/ionization are important in raising the density in the far SOL, what is important for LH wave coupling in ITER like discharges. Although OMP seems to be the best location for gas puffing, the other two puff locations (near RCP, at the top) also give an increase in  $n_{e,SOL}$  with heating. This is again an important information for ITER, where top gas puffing is assumed. The modeling shows the flattening of the far  $n_{e,SOL}$  profile, which is observed in experiments [2].

All results mentioned above were obtained in a team effort.

#### References:

- [1] V. Petrzilka et al., 34th EPS07 Conference, Warsaw, July 2-6th, 2007, paper P4.100, preprint EFDA-JET-CP(07)03/60, to be submitted to Nuclear Fusion.
- [2] M.Goniche et al., 34th EPS07 Conference, Warsaw, July 2-6th, 2007 paper P1. 152, preprint EFDA-JET-CP(07)03/40.

## Cherenkov detectors for fast electron measurements

*V. Weinzettl, J. Stöckel, M. Vácha, M. Peterka*

In collaboration with:

*L. Jakubowski, M.J. Sadowski, J. Stanislawski, K. Malinowski, J. Zebrowski, M. Jakubowski,*  
Association EURATOM IPPLM, The Andrzej Soltan Institute for Nuclear Studies, Otwock-Swierk, Poland

*Fast electrons generated by the ohmic heating in the CASTOR tokamak plasma were recorded by means of the Cherenkov detection system described in [1]. The experimental data were collected in about 500 discharges. The shots were 25 ms long and performed at the toroidal magnetic field  $B_T$  ranging from 0.8 T to 1.4 T, the plasma current  $I_p$  varied from 5 kA to 15 kA. The measurements were limited to relatively low plasma densities  $n_e$  reaching  $0.5-1.5 \times 10^{19} \text{ m}^{-3}$  and a relatively high acceleration voltage  $V_{LOOP}$ , typically higher than 2 V.*

Measurements indicate that introduced modifications of the Cherenkov detection system enabled an electromagnetic interference to be reduced and a direct hard radiation to be eliminated completely. Using a radiation attenuation in lead shielding, an energy of the direct radiation was estimated as  $E = (3,9 \pm 1,0) \text{ MeV}$  that gives the same energy as for a test water shielding,  $E = (3,8 \pm 0,1) \text{ MeV}$ . A question on an unclear origin of this hard radiation reaching the detection system only during the tokamak discharges stays still unanswered.

The entrance window of the detector, by default oriented in the direction opposite to the plasma current allowing fast electron measurements, was turned around its axis by 180 degrees in agreement with the plasma current in some shots of the campaign. The recorded signals were in this case very low, see Fig.1, what confirmed that the recorded Cherenkov signals were induced just by fast electrons ( $>50 \text{ keV}$ ).

On the CASTOR tokamak, the dependences of the fast electron signals on the radial position of the Cherenkov detector, as well as on the plasma density, see Fig.1-2, plasma current and toroidal magnetic field were investigated [2,3]. A character of the signals depended very strongly on the radial position of the detector as well as on the plasma density. With an increase of the observation radius, the Cherenkov signal decreased and it appeared later. It was found that after 25 ms, when the transformer primary winding (inducing the ohmic heating) was short-circuited and the stabilization

system was turned off, a strong increase in the signal intensity appeared as a result of the destruction of the plasma column. A considerable influence of the plasma density was also observed. In the high-density discharges, the initial increase in the Cherenkov signal was followed by a stationary phase. It can be directly interpreted as a constant loss rate of the fast electrons. On the contrary, the low-density discharges showed almost an exponential growth of

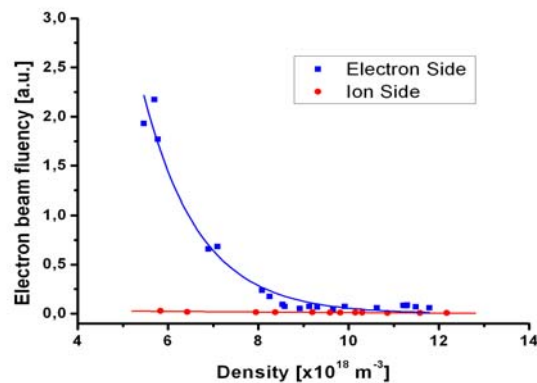


*Fig. 1. Integrated Cherenkov emission as a function of the plasma density. The blue curve corresponds to the orientation of the detector allowing fast electron measurements, the red curve shows electron signal at the opposite detector orientation.*

the Cherenkov signals lasting until the end of the discharge. The described effect might be connected with a magnitude of the acceleration electric field reaching a critical value in the low-density discharges.

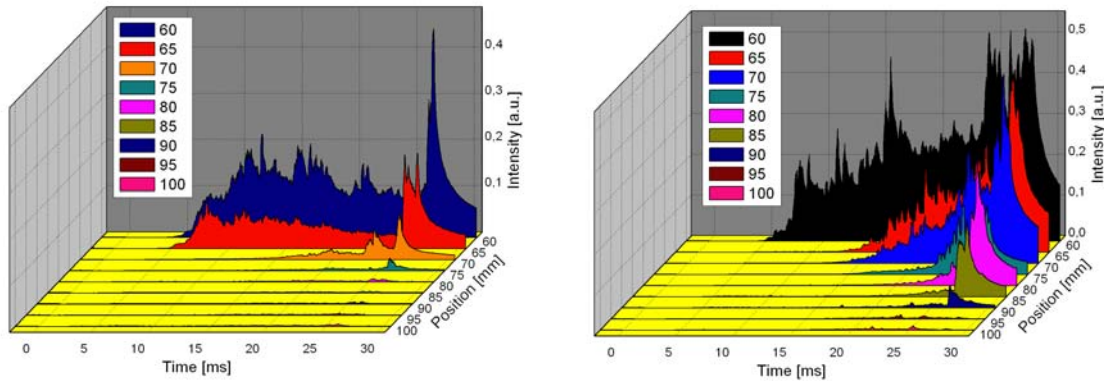


Fig. 2. Evolution of the Cherenkov signals as a function of the position of the detector head for high-density (left) and low-density (right) discharges.

A connection between the Cherenkov emission and hard X-rays (HXR), which were measured at a close vicinity of the Cherenkov detector, was also studied, see Fig.3. As it can be clearly seen, a global behaviour of the hard X-ray radiation differs from the Cherenkov emission; however, there are some common peaks at certain moments confirming an interaction of fast electrons with the Cherenkov detector head. But a correlation of the Cherenkov and local HXR signals can reach up to 70 % and its magnitude practically does not depend on the detector position, plasma density or toroidal magnetic field. A correlation peak FWHM varies from 6 to 11  $\mu$ s and slowly increases towards the plasma center. It should be noticed that a position of the correlation peak indicates a small but non-zero delay between the Cherenkov and hard X-ray emission in the range of 1-3  $\mu$ s (the hard X-rays outruns the Cherenkov emission).

The results of the statistical approach using a single-count analysis of the time-resolved Cherenkov data indicates possible transport mechanisms of fast electrons – the fast burst losses in combination with a slow diffusion.

#### References:

- [1] L. Jakubowski, et al., *34<sup>th</sup> EPS Conference on Plasma Physics, Warsaw, Poland, July 2-6, 2007*, ECA Vol.31F, P-5.097 (2007)
- [2] J. Zebrowski, et al., *PLASMA 2007 – International Conference on Research and Applications of Plasmas, Greifswald, Germany, October 16-19, 2007*, WeP3
- [3] L. Jakubowski, et al., *17<sup>th</sup> IAEA Technical Meeting on Research Using Small Fusion Devices, Lisbon, Portugal, October 22-24, 2007*, P17

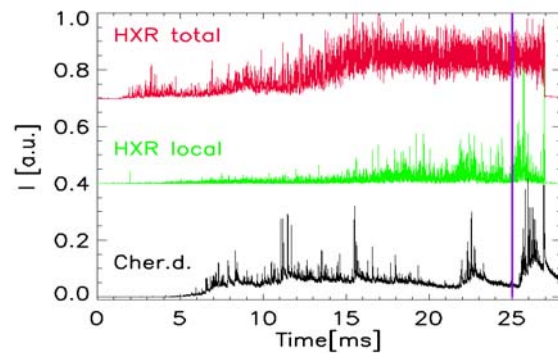


Fig. 3. Example of the temporal evolution of the Cherenkov emission measured at  $r = 60$  mm, the local hard X-ray, and the total hard X-ray intensity.

## JET neutron data analyses via inversion algorithms based on Minimum Fisher Regularisation

*J. Mlynář, V. Svoboda*

In collaboration with:

*G. Bonheure*, Association EURATOM-Etat Belge, ERM/KMS, Brussels, Belgium

*A. Murari*, Association EURATOM-ENEA, Consorzio RFX, Padova, Italy

*M. Tsalas*, Association EURATOM-Hellenic Republic, N.C.S.R. "Demokritos", Greece

*S. Popovichev*, Association EURATOM-UKAEA, Culham Science Centre, Abingdon, UK

*S. Conroy*, Association EURATOM-VR, Uppsala University, SE-751 05 Uppsala, Sweden

and JET EFDA contributors

*Minimum Fisher Information principle proved to provide robust analyses of sparse data in plasma diagnostics. At JET, in collaboration with the Association Euratom-IPP.CR, the inversion methods based on Minimum Fisher Regularisation (MFR) have been successfully validated both in spatial analyses of plasma neutron emissivities measured by the JET profile monitor (MFR tomography) and in spectral analyses of neutrons detected by the NE213 compact spectrometer (MFR unfolding). In 2007 the MFR tomography algorithm was extended by abelisation and by unisotropic smoothing constrained to magnetic flux surfaces.*

**MFR tomography of the JET neutron emissivity.** Neutron profile monitor at JET (see e.g. [1]) provides data for spatial analyses of plasma neutron emissivities, with separate measurements of D-D fusion products (2.5 MeV) and D-T fusion products (14 MeV). Although spatial resolution of the neutron profile monitor is rather sparse, it proved sufficient for tomography reconstruction by adapted algorithm of the Tikhonov kind with 2D mesh of rectangular pixels and the inverse regularisation optimised by Minimum Fisher Information principle [2].

Results in previous years clearly indicated potential of the neutron tomography in studies of fuel transport via ratio method [1], however the systematic errors (tomography artefacts) due to the sparse resolution seriously hampered reliability of the 2D reconstructions of neutron emissivities [2]. Therefore it was concluded that a further constraint on the MFR algorithm is required.

Magnetic flux surfaces provide a natural constraint, for it is expected that neutron emissivities do not change rapidly along flux surfaces. First, a full poloidal symmetry (abelisation) was implemented into the MFR [3], later a more sophisticated 2D reconstruction with unisotropic smoothing along flux surfaces was introduced [4].

In the poloidally symmetric case, known as the Abel inversion, the neutron emissivity is constrained to be constant on magnetic flux surfaces so that the tomography task is reduced to one-dimensional problem. The MFR abelisation was tested and then applied for studies of both the fuel transport in the TTE (see Fig. 1) and D-D data studies in

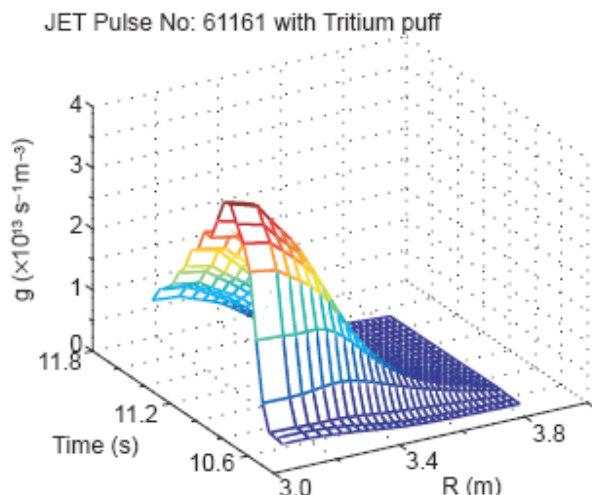


*Fig. 1. Evolution of the neutron emissivity profile during Tritium puff in the JET pulse #61161 as reconstructed by the MFR Abelisation [4]*

the recent ripple experiments [3]. The corresponding magnetic flux surfaces were uploaded from JET database of EFIT magnetic field reconstructions. These studies confirmed that the constraint is too restrictive for typical JET neutron emissivities which feature stronger radiation in the low field side. However, the Abel inversion can be used as a very sensitive indicator of asymmetries and/or as a tool for studies of symmetric neutron emissivities (e.g. in low plasma density discharges).

A considerably more complicated but more fruitful constraint consists in introduction of an unisotropic smoothing into the standard 2D MFR algorithm. In this method, amplitude of reconstruction smoothing is set stronger in the direction tangent to the flux surface and weaker in the perpendicular direction. This new constraint was successfully implemented and preliminary results in transport analyses from the TTE campaign provide - for the first time - distinct quantitative values [4], see Fig. 2. In these analyses, both D-D and D-T emissivities were reconstructed with the newly implemented unisotropic smoothing, and the ratio of the two emissivities - which reflects the fuel transport properties - was integrated in the poloidal direction in order to attenuate noise (statistical errors).

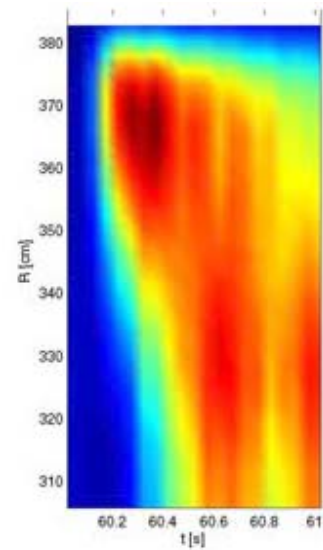
The MFR code is now ready for systematic studies of performance on simulated data, which will benchmark its features. Further minor improvements are foreseen, e.g. implementation of final width of viewing lines and of the up-down symmetry constraint.

**MFR unfolding of the JET neutron spectra.** The organic liquid scintillators known as NE213 provide relatively simple and robust neutron detection. Its pulse height spectrum carries also information on the energy of impacting neutrons, however, a proper detector calibration and unfolding technique is required. The MFR algorithm was successfully adapted to run the inversion process of the NE213 spectra unfolding with L-curve principle implementation [5] and semi-automated application at JET.

In the last year, progress in the MFR unfolding was modest due to priorities given to the MFR tomography. The planned extension of the unfolding to the Stilbene scintillator detector was postponed, because the diagnostic was not ready for the spectral analyses: The n-gamma pulse separation was under development, and the detector response matrix was not known to the required precision. Instead, limited effort went to further extension of the MFR unfolding algorithm for the NE213 neutron detector, in particular the dependence of the photomultiplier gain factor on the neutron intensity was implemented.

#### References:

- [1] G. Bonheure, et al., *Nucl. Fus.* 46 (2006) 725
- [2] J. Mlynar, et al., *48th Annual Meeting of the DPP, Bull. Am. Phys. Soc.* (2006) 196
- [3] J. Mlynar, et al., *34<sup>th</sup> EPS Conference on Plasma Physics, Europhysics Conference Abstracts* 31F (2007) P-2.129
- [4] G. Bonheure, et al., *to be presented at 35<sup>th</sup> EPS Conference on Plasma Physics (2008)*
- [5] J. Mlynar, et al., *FNDA 2006, Proceedings of Science PoS(FNDA2006)063*



*JET pulse 61372 (profile evolution of the ratio of reconstructed D-T/D-D emissivities) shortly after a tritium gas puff [4]*

## 2 Development of Plasma Auxiliary Systems

### Neutral beam injection system for COMPASS

*J. Urban, J. Mlynář, V. Fuchs, J. Stöckel, M. Stránský*

*Neutral beam injection system at COMPASS will present a new key element in the foreseen scientific programme, in particular with respect to the H-mode operation. Predictive simulations of the beam performance were focussed on the finalisation of the technical specifications for the system. Later in 2007, the specifications were agreed upon and implemented into detailed Call for tender for two neutral beam injectors for the COMPASS tokamak.*

Predictive simulations of the planned neutral beam injection (NBI) system have been performed to support the final NBI design and other COMPASS modelling. ACCOME [1] is presently applied for predictive equilibrium calculations. The ACCOME Fokker-Planck NBI module was conceived for computational speed within ACCOME, which iteratively calculates a self-consistent state between the tokamak MHD equilibrium and the inductive and non-inductively-driven currents: bootstrap, lower hybrid, and neutral beam. The ACCOME MHD equilibrium module SELENE [2] solves the free-boundary Shafranov equation problem under very general boundary conditions. One specifies the dimensions, positions and turns of the poloidal field coils, and then selects a particular type of boundary problem. Either one can specify coil currents and find the resulting plasma shape, separatrix and possible X-points, or else one specifies a desired plasma shape, and calculates the resulting required coil currents. At the moment, we work with single X-point equilibria: SND and SNT (high triangularity) [3, 4]. These equilibria, determined by SELENE with or without NBI, are then also used for other COMPASS simulations (see the report of M. Stránský and V. Fuchs) and will be used for future, more detailed NBI simulations with FAFNER [5] or NUBEAM [6]. In turn, Astra [7] simulations provide temperature profiles for ACCOME and the stand-alone NB module FAFNER, and eventually also for NUBEAM.

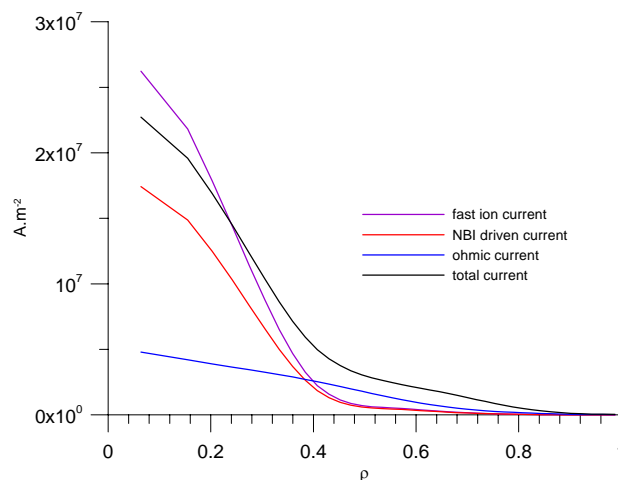


*Fig. 1. Current density profiles from ACCOME. SND equilibrium,  $I_p=170$  kA,  $B_0=1.2$  T.*

Toroidal current densities, computed by ACCOME for SND configuration with total plasma current  $I_p=170$  kA, central toroidal magnetic field  $B_0=1.2$  T and co-injected NBI with total power 500 kW, are plotted in Fig. 1. It follows that NBI can drive a substantial portion of the total plasma current. However, ACCOME does not account for important loss channels – orbit losses, charge exchange losses. Moreover, the current drive calculation is considerably simplified. As a result, the NBI driven current can be significantly overestimated. This had been shown by calculations with the Monte Carlo code FAFNER [5], although for a slightly different equilibria, in [8]. Installation of an advanced Monte Carlo NBI code, e.g. FAFNER or NUBEAM, is envisaged to enable more detailed and realistic NBI simulations at IPP Prague.

Following the above modelling work, detailed technical specification of the NBI system for the COMPASS tokamak was finalised and agreed upon at the end of 2007. The 40 keV deuterium neutral beam with total power of up to 600 kW will be launched to plasma by two NBI systems. The basic configuration – tangential injection in co-direction with respect to plasma current – is optimized for plasma heating. The aiming of both injectors can be shifted outside to achieve off-axis heating and current drive. For balanced injection both injectors will be located at the same port, aiming in co- and counter-current directions. Normal injection will be also possible, mainly for diagnostic purposes. Each injector must be able to operate at lower voltages (down to 20 keV), although at lower performance, and with hydrogen gas. Both units must be able to on/off modulate the beam with a minimum on-time of 20 ms and a minimum off-time of 20 ms using an external reference signal, with rise/fall time (from 10% to 90% beam power and vice-versa) max. 2 ms. The longest time of continuous beam operation will be 300 ms. In order to minimise hydrogen leakage to the plasma the pressure at the beam duct to the COMPASS chamber must be kept below  $10^{-2}$  Pa when the beam is operated,  $2 \cdot 10^{-4}$  Pa otherwise. Contents of heavy impurities must be kept below 1%, the beam energy and current accuracy has been specified to +/- 1% and 2%, respectively. The narrow vertical span of the COMPASS port in the tangential injection (70 mm) was pointed out as a major challenge so that performance tests with the port are required at the manufacturer's site. Magnetic field parameters, available power supplies, cooling systems, vacuum connections and control system including the interlocks have been specified as well.

### References:

- [1] Laqua, H.P., et al., *Bulletin of the American Physical Society*, vol. 52, no. 16 (2007) 280
- [2] Tani, K., Azumi, M., Devoto, R.S., *Journal of Computational Physics* 98 (1992) 332-341
- [3] Bilykova, O., et al., *Czechoslovak Journal of Physics* 56 (2006) B24-B30
- [4] Fuchs, V., et al., *33rd Annual European Physical Society Conference on Controlled Fusion and Plasma Physics* (2006) P-1.103
- [5] Lister, G.G., *IPP Report 4/222* (1985)
- [6] Pankin, A., et al., *Computer Physics Communications* 159 (2004) 157-184
- [7] Pereverzev, G.V. and Yushmanov, P.N., *IPP Report 5/98* (2002)
- [8] Urban, J., et al., *Czechoslovak Journal of Physics* 56 (2006) B176-B181

## Spectroscopic diagnostics for COMPASS

*V. Weinzettl, E. Dufková*

In collaboration with:

*V. Igochine*, Association EURATOM IPP, IPP Garching, Germany

*M. Berta, A. Szappanos*, Association EURATOM HAS, KFKI-RMKI Budapest, Hungary

*Spectroscopic diagnostics on the COMPASS tokamak will cover a wide spectral range of the core and edge plasma emission aiming to realize a fast tomography at microsecond time scales.*

A poloidal section of the diagnostic ports of the COMPASS tokamak suitable for fast spectroscopic detectors such as fast AXUV-based bolometers, semiconductor SXR detectors and visible radiation monitors was chosen with respect to a presence of the two NBI heating systems in the vacuum vessel and a possibility to realize tomographic reconstructions of the selected radiation ranges. The small size of the allocated ports, a large number of the detectors inside them and requirements for cooling during a vessel baking led to an optimization in a choice of the detectors and to an integrated port design. A high temporal resolution in a combination with a good spatial resolution, namely in the pedestal region, will be reached by the AXUV20-ELM (IRD Inc.) based arrays of bolometers and LD35-5T-JET-Windowless (Centronic) arrays of the SXR detectors located inside the diagnostic ports, see Fig.1. Visible light observations will be realized using a pinhole camera connected to optical fibers and a spectrometer/photomultipliers located in a diagnostic room.



*Fig.1: On the left, there are the six AXUV20-ELM (IRD Inc.) based 20-channel arrays of fast bolometers equipped with the ceramic sockets. On the right, there are the four LD35-5T-JET-Windowless (Centronic) 35-channel arrays of the soft X-ray detectors.*

A cooperation with HAS Association on the implementation of the fast visible camera on COMPASS has been started and the first model of the EDICAM camera with an exposition up to 20 microseconds was tested on the CASTOR tokamak in 2007, see Fig.2.

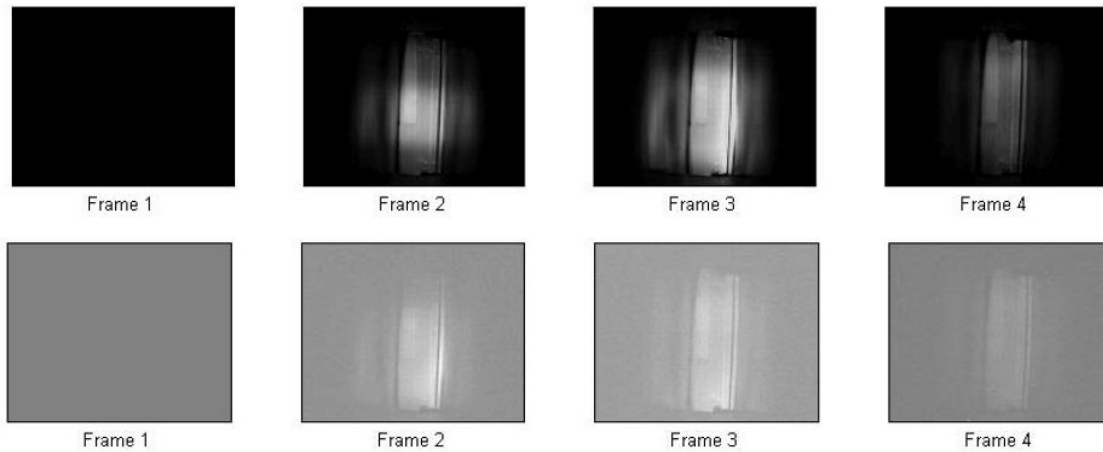


*Fig.2: Sequences of the 1280x1024 pixel frames taken by the EDICAM camera during CASTOR tokamak shots with 500  $\mu$ s (upper frames, original colors) and 20  $\mu$ s (lower frames, rescaled colormap) exposition time. Dynamically rescaled colormaps are used to visualize details, namely for exposition time shorter than 100  $\mu$ s.*

## Performance analysis of ITER candidate Hall sensors in tokamak environment

*I. Ďuran, J. Sentkerestiová, K. Kovařík, O. Bilyková, J. Havlíček, J. Stöckel*

In collaboration with:

*I. Bolshakova, R. Holyaka, V. Erashok*, MSL, Lviv Polytechnic National University, Ukraine

*A. Quercia*, Association EURATOM-ENEA CREATE

*P. Moreau*, Association EURATOM-CEA

*Use of various configurations of flux loops for measurement of magnetic field in fusion devices is inherently limited by the pulsed operation of these machines. A principally new diagnostic method must be developed to complement the magnetic measurements in true steady state regime of operation of fusion reactor. One of the options is the use of diagnostics based on Hall sensors. This technique is well established for many applications in experimental physics as well as industry, although it is rarely implemented in the fusion plasma physics. Therefore, besides the tests of radiation hardness of the ITER candidate Hall sensors, the experience with their use in tokamak environment must be gathered. Although, principally aimed for steady state applications, Hall sensors offer some advantages over magnetic coils also for present pulsed fusion devices. It is mainly their smaller size and direct relation of the measured signal to the magnetic field. The frequency response is typically limited to few tens of kilohertz. Several experiments dedicated to testing of various types of Hall probes were done and are being prepared on CASTOR, JET, and Tore Supra.*

### Poloidal ring of integrated Hall sensors on CASTOR

Advancements in semiconductor technology hand in hand with a broad spectrum of industrial applications have driven development of new types of Hall sensors for magnetic measurements in recent years. A particular advancement is the availability of 'integrated' Hall transducers, where the sensing element together with the complex electronic circuitry is integrated on a single small chip with characteristic dimension of a few millimeters. The on-chip integrated circuits provide



*Fig. 1. The ring of up to 16 Hall sensors, 16 coils and 96 Langmuir probes before its installation on CASTOR tokamak (left panel). Detailed view of the Hall sensors attachment system with a single Hall sensor shown before its installation on the ring (left panel).*

stabilization of the supply voltage, output voltage amplification, signal conditioning in order to suppress the high frequency noise, and elimination of temperature dependence of the sensor's output. Because of the widespread industrial use of such sensors, their cost is rather low (of the

order of 1 Euro/piece). We have performed the first tests of this type of Hall sensors in a tokamak in-vessel environment on CASTOR tokamak ( $R/a=0.4\text{m}/0.085\text{m}$ ,  $I_p=10\text{kA}$ ,  $B_T=1\text{T}$ ,  $n_e=10^{19}\text{m}^{-3}$ ). The 8 Hall sensors of A1322LUA type produced by Allegro MicroSystems, Inc. were mounted on a stainless steel ring symmetrically encircling the CASTOR plasma in poloidal direction 10 mm outside the limiter radius. The Hall sensors were oriented such that they measure the horizontal and vertical magnetic fields at four locations (top, bottom, high field side, and low field side). The special adjustable holders were used in order to ensure proper alignment and consequently to minimize the cross-talk from the toroidal magnetic field. The sensors have a nominal sensitivity of 31.25 mV/mT and dynamic range  $\pm 80$  mT. The peak-to-peak noise level is below 1mT. The reasonably flat frequency response was achieved in the range DC-10 kHz. The operating temperature range is from  $-40^\circ\text{C}$  to  $150^\circ\text{C}$ . A supply voltage of 5V is needed to drive each Hall sensor. More details on operational aspects of these Hall sensors can be found in [1]. We exploited the above described system of 8 Hall sensors to get further insight into vertical plasma position measurement on CASTOR. In previous years there was observed a systematic disagreement between CASTOR vertical plasma position measurements using the standard

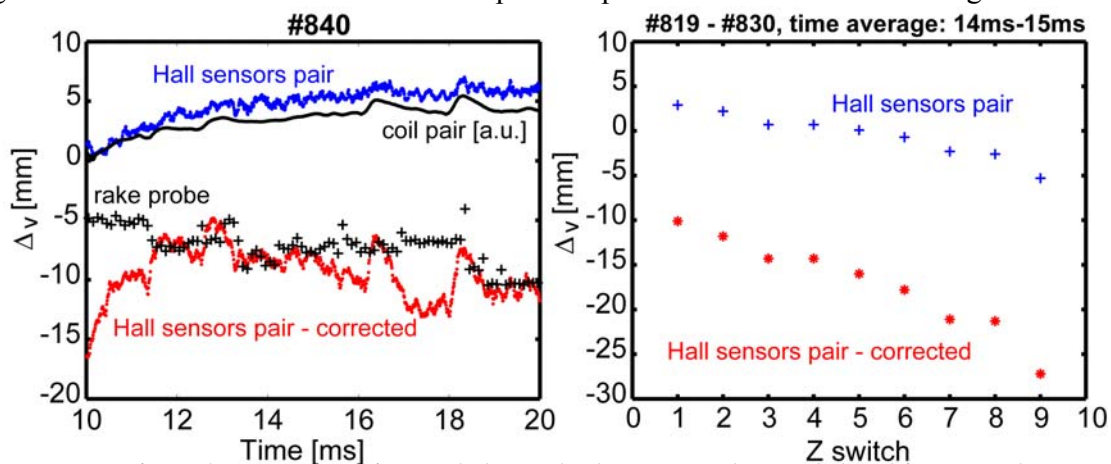


Fig. 2. Left panel: comparison of vertical plasma displacement evolutions deduced from: a coil pair (black line), Hall sensors pair (blue), Hall sensors pair corrected for presence of stray magnetic fields  $B_{ext}$  (red), and rake of Langmuir probes (black +). Right panel: vertical plasma displacement as a function of hardware CASTOR feedback system switch Z obtained as the simple differential signal of a pair of Hall sensors (blue) versus the same differential signal but corrected for presence of  $B_{ext}$ .

approach of a pair of magnetic coils placed at the top and at the bottom, inside the vacuum vessel and other available diagnostics (rakes of Langmuir probes, bolometers) [2]. The differential signal of the coils pair is used to drive the CASTOR vertical plasma position feed-back system [3]. The vertical plasma position deduced by this method is rather centred for most of the CASTOR operating regimes. In the contrary, measurement of separatrix position performed by a radial rake of Langmuir probes suggests significant downward shift of the plasma column. In these experiments the radial rake of Langmuir probes is introduced into the CASTOR edge plasmas from the top and the separatrix position is identified with the measured location of maximum in floating potential profile.

Explanation of this discrepancy was proposed, suggesting that the magnetic measurements have to be corrected for pick-up of stray magnetic fields induced by external tokamak windings. The present set-up of Hall sensors on the full poloidal ring allows measuring of these stray magnetic fields separately during plasma discharge. Consequently, it was possible to correct the evaluated signal of the vertical plasma position (see fig. 2). It is clearly seen in figure 2 (left panel) that a

rather good agreement was achieved in determination of plasma vertical displacement between magnetic diagnostic (Hall sensors) and rake of Langmuir probes after elimination of signal proportional to stray magnetic fields. Figure 2 (right panel) presents example, how the dependence of the vertical plasma displacement on setting of the Z switch changes after application of above described correction. The Z switch (positions 0 - 12) is a knob on the CASTOR vertical plasma position control system used to pre-define the desired vertical plasma position before each CASTOR shot.

### Installation of ex-vessel Hall probes on JET within JET EP2 enhancement project

The project aims for enhancement of the existing JET ex-vessel magnetic diagnostics system, by installing new sensors, capable of measuring the magnetic field both directly via sets of 3D Hall sensors and also by integrating voltages of coils which are attached to all the Hall sensors. The main rationale behind this project from the JET point of view is to provide additional data to enhance the database for iron core modelling and to improve equilibrium reconstruction. From ITER point of view, it is extremely important to test performance of these ITER candidate sensors under fusion neutron spectrum and also to gather experience from operating them at the large tokamak facility like JET. The project is led by Ass. ENEA, the probes and electronics are provided by MSL, Lviv Polytechnic National University, Ukraine. The Association IPP.CR participates on testing, installation, and the high level commissioning of the system on JET including analysis and assessment of the measured signals.

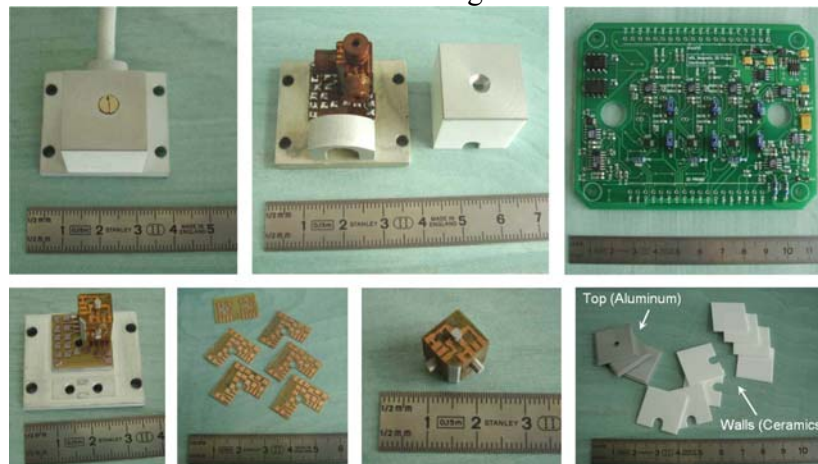


Fig. 3. One of the JET EP2 ex-vessel Hall probes, developed by MSL Lviv Ukraine, in various stages of manufacturing process.

### Hall probes on Tore Supra

High temperature resistant ( $<200^{\circ}\text{C}$ ) Hall probe developed by MSL Lviv, Ukraine in collaboration with IPP Prague, was installed in-vessel on Tore Supra tokamak behind the poloidal antennas protecting limiter. Special electronics driving this probe allows precise measurement of magnetic fields in the frequency band 0-250 kHz.

### References:

- [1] G. Van Oost et al., *Nuclear Fusion*, 47 (2007), 378-386
- [2] J. Sentkerestiová et al., *Czechoslovak Journal of Physics*, 56, D2 (2006)
- [3] M. Valovič, *Czechoslovak Journal of Physics*, B38 (1988)

## Development of advanced probe for edge tokamak plasmas - Emissive probes

A. Marek, P. Kudrna, M. Tichý

In collaboration with:

R. Schrittwieser, C. Ionita, P. Balan, Innsbruck University, Association EURATOM-ÖAW

*Emissive probe was in focus of the investigations in 2007. Two subjects were investigated: a) applicability of strongly emitting probe technique in the low temperature plasma; b) variations of the electron saturation current collected by probe at varying probe heating. Applicability of the strongly emitting probe technique depends on ratio of temperature of the emitted electrons and plasma electrons in case of low temperature plasma. Experimental data were compared with theoretical model.*

Construction of the emissive probe used in experiments is depicted in Fig. 1. The probe wire was made from tungsten or thoriated tungsten with diameter typically  $d = 150 \mu\text{m}$  in present experiments. Electrical contact between the probe wire and feeding line was realised by fine copper wires that were tightly bounded around the probe wire. This construction ensured excellent electrical contact and relatively easy probe preparation. Probe was placed into the double bored Degusit tube. Experiments were performed on the cylindrical magnetron system described e.g. in [1,2].

We have found that applicability of the strongly emitting probe technique for the estimation of the space potential depends on ratio  $T_e/T_{eW}$  and  $n$ , where  $T_e$  is temperature of plasma electrons,  $T_{eW}$  is temperature of emitted electrons and  $n$  is plasma density. This is illustrated in Fig. 2 for case of tungsten probe and different  $T_e$  at fixed plasma density. Data in Fig. 2 were computed by applying floating probe condition in 1D model of strongly emitting plane developed by Takamura et al. [3]. It is visible that if the  $T_e$  and  $T_{eW}$  are comparable the plasma potential determined by the strongly emitting probe can be markedly overestimated. If  $T_{eW}$  can be neglected with respect to  $T_e$  (hot plasma), the plasma potential determined by the strongly emitting probe is underestimated by approximately one  $kT_e/e$  as it was shown e.g. in [4].

Measurements with strongly emitting probe were performed in low temperature plasma of the shorter cylindrical magnetron at several radial positions and at two different pressures ensuring different  $T_e$ . Plasma potential determined by the strongly emitting probe technique  $U_{pIEM}$  was compared with plasma potential determined by Langmuir probe  $U_{pl}$ . Results of experiment are summarised in tables 1 and 2. According to model [3] and Fig. 2, the plasma potential determined by the strongly emitting probe at  $p = 1.5 \text{ Pa}$  should be more markedly underestimated than in case

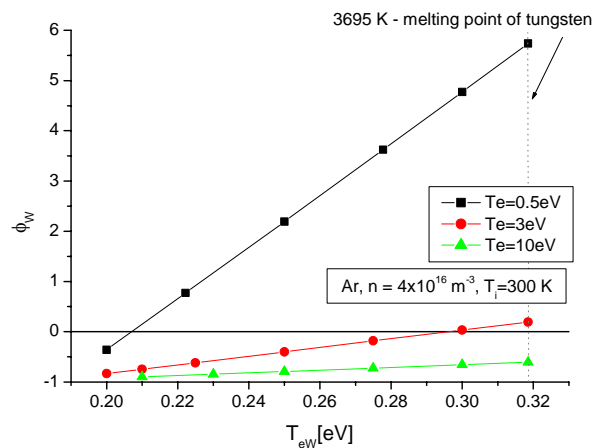


Fig. 2: Results of 1D model [3] – difference of normalized potential ( $\phi = e\phi/kT_e$ ) determined at the strongly emitting tungsten wall and plasma potential at increasing  $T_{eW}$  for three values of  $T_e$ .

of  $p = 6$  Pa since the electron temperature was higher in that case and the plasma density is comparable. However, this trend is not visible in our data. It is probably because the  $T_{eW}$  and difference in  $T_e$  were not sufficient. In both cases (Tables 1 and 2), the plasma potential determined by strongly emitting probe technique was underestimated by approximately  $0.3 kT_e/e$ .

In addition, a relatively thorough study of the electron saturation current variations at varying probe heating was performed in the cylindrical magnetron (Prague) and DP-machine (Innsbruck) plasma [5,6]. Magnitude of electron saturation current variations were characterized – variations were more pronounced in case of shorter probes. In [6] various possible processes leading to electron saturation current variations were discussed. New experimental data were recently obtained that give better understanding of studied phenomena. Profiles of variations given in [5,6] were obtained from the analysis of emissive probe current at chosen fixed voltage. In this study there were not obtained the whole current voltage characteristics but only the fixed probe bias was chosen and probe heating was varied. This approach enabled to assess better temperature induced processes.

We concluded that strongly emitting probe technique is applicable in low temperature plasma with  $T_e \sim 2-3$  eV and plasma density  $n \sim 10^{16} \text{ m}^{-3}$ . Observed variations of the electron saturation current at varying probe heating can be ascribed from the most part to the probe surface cleaning and contamination in laboratory argon discharge plasma. Preliminary results were published in SAPP 2007 and ICPIG 2007 Conference proceedings [7,8], final paper has been accepted for publication in Contributions to Plasma Physics (appears in 2008).

### References:

- [1] E. Passoth et al., *J. Phys. D* 30 (1997) 1763.
- [2] M. Holík et al., *Czech. Jour. Phys, Suppl D*, 52 (2002) D673.
- [3] S. Takamura et al., *Contrib. Plasma Phys.* 44 (2004) 126.
- [4] G.D. Hobbs and J.A. Wesson, *Plasma Phys.* 9 (1967) 85.
- [5] A. Marek et al., *Czech. Jour. Phys., Suppl B* 56 (2006) 932.
- [6] A. Marek, Doctoral thesis, Charles University in Prague (2007).
- [7] A. Marek, R. Apetrei, I. Picková et al., "Can a Strongly Emitting Probe Be Used in a Low Temperature Plasma?", In: Proceedings of SAPP XVI, 2007, Podbanske, January 20-25, (2007), (ed. J. Matuska, S. Matejčík, J. D. Skalný), pp. 225-226. ISBN 978-80-89186-13-6.
- [8] A. Marek, M. Jílek, I. Picková, P. Kudrna, M. Tichý, R. Schrittwieser, C. Ionita, P.C. Balan, Emissive probe diagnostic in low temperature plasma – effect of the space charge and variations of the electron saturation current, In: Proceedings of 28th ICPIG, 15-20 July 2007, Praha, ISBN 978-80-87026-01-4, pp. 1606-1609.

Tab 1: Normalized difference between plasma potential determined by strongly emitting probe and Langmuir probe in cylindrical magnetron.

Ar, 1.5 Pa, 20 m T, 50 m A			
r [mm]	$T_e$ [eV]	$n_e$ [ $\text{m}^{-3}$ ]	$(U_{pIEM} - U_{pl})/kT_e$
21	4.7	7.00E+15	-0.26
18	4.0	1.20E+16	-0.23
15	4.3	1.80E+16	-0.33
12	4.5	2.30E+16	-0.29
9	4.6	2.30E+16	-0.30

Tab 2: Normalized difference between plasma potential determined by strongly emitting probe and Langmuir probe in cylindrical magnetron.

Ar, 6 Pa, 20 m T, 50 m A			
r [mm]	$T_e$ [eV]	$n_e$ [ $\text{m}^{-3}$ ]	$(U_{pIEM} - U_{pl})/kT_e$
21	2.1	8.00E+15	-0.19
18	2.2	1.20E+16	-0.32
15	2.3	1.60E+16	-0.43
12	2.2	2.40E+16	-0.50
9	2.6	2.80E+16	-0.23

## **Development of millimeter-wave reflectometry system for the measurement of edge pedestal plasma in tokamak COMPASS**

*J. Zajac, F. Žáček, J. Vlček*

In collaboration with:

*M. Manso, A. Silva, P. Varela, L. Cupido*, Association EURATOM- Instituto Superior Technico / Centro de Fusão Nuclear, Lisbon

*This is for the Activity Report 2007, part of the construction of the microwave reflectometry system for Compass tokamak. IST/CFN Lisbon was agreed in 2006 to be the main supplier of the reflectometry system with the technical support of IPP Prague [1]. The reflectometry system for Compass will be mainly designed to perform relevant plasma density profile measurements in the pedestal region. Five individual reflectometers are supposed to measure the density profile. The advanced reflectometers allow an arbitrary frequency sweeping modes and therefore the reflectometers can be used as well as an experimental diagnostics for studies of plasma turbulence [2].*

The realization of the reflectometry system was supposed in a close collaboration with IST/CFN during 2006 – 2009 [1]. In the new timetable it is supposed that all parts of the reflectometry system will be constructed, assembled and tested by IST/CFN in Lisboa in 2008 - 2010, with the support of microwave engineers from IPP.CR.

In November 2007 the detailed design of the reflectometry system was agreed in Lisbon including the new timetable and cost estimation. The horizontal 8/9 Compass vessel port will be dedicated for the reflectometry system. The port has the inner diameter 150 mm and length of about 200 mm. The port is too small for the placing of a set of horn antennas into the vacuum vessel. Moreover one of NBI beam is crossing this port. Therefore the external antenna system for the reflectometry is more suitable. Then antennas are placed in front of the port. The port is equipped with a proper vacuum window transparent for microwaves (e.g. quartz window). The frequency combiners and quasi-optical antennas are necessary to transmit and receive all channels (O-mode K, Ka, U and E frequency bands and one X-mode Ka frequency band) in a tokamak port. A band-combiner combines the four O-mode beams and on X-mode beam into the one transmitting beam. The same combiner splits them from the receiving beam. Similar system has been developed for JET [4]. Due to the complexity of such a device, a suitable provider will be sought.

Transmitters and receivers for the all bands are individual. Only the Ka-band the O-mode and X-mode signal will be splitted from a common source. The block scheme of the electronics for the K band is in Fig. 1. Other bands have the same scheme in principle, only different voltage-controlled oscillators and frequency multiplication.

The original workplan of the collaboration agreed for 2006 was delayed. Therefore, the workplan for IPP was reformulated and the construction of the Ka-band (26.5 – 40 GHz) reflectometer was started at the beginning of 2007 in IPP. The design was made in a similar way to the reflectometers developed recently in IST [2,3]. Most of microwave electronics of this reflectometer was constructed and tested in parts in 2007. Development of control unit and

control SW is in progress. This reflectometer will be able to work with the suggested quasi-optical band-combiners and antennas. The control unit and control SW is developed by our own way.

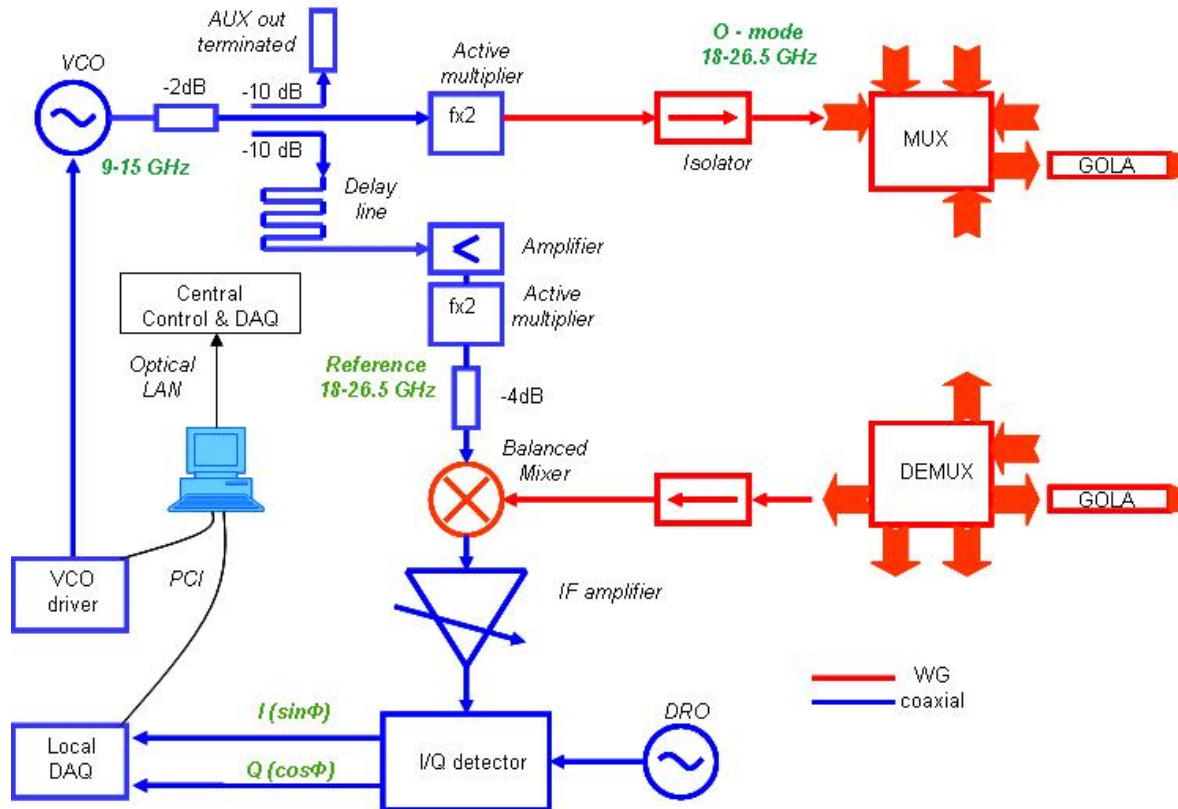


Fig. 1. Block scheme of O-mode 18-26.5 GHz transmitter and receiver

**References:**

- [1] Framework Agreement for Scientific Collaboration between Institute of Plasma Physics - Association Euratom/IPP.CR and Centro de Fusão Nuclear, Instituto Superior Técnico - Association Euratom/IST
- [2] L.Cupido et al., Frequency hopping millimeter wave reflectometer, *Review of Sci. Instr.*, 75 (10), 2004
- [3] A.Silva et al., Ultrafast broadband FM-CW reflectometry system to measure density profiles on Asdex-U, *Review of Sci. Instr.*, 67 (12), 1996
- [4] L.Cupido et al., New millimeter-wave access for JET reflectometry and ECE, *Fusion Engineering and Design* 74 (2005) 707–713

## Neutral particle analyzer for tokamak COMPASS

*J. Stockel. D. Naydenkova*

In collaboration with:

*M Petrov, Atomic Physics Department A.F.Ioffe Physical-Technical Institute, St Petersburg*

*Fast neutral atoms escaping from the COMPASS plasma will be analyzed by means of the neutral particle analyzer, which allows simultaneous analysis of hydrogen and deuterium atoms in the energy range 0.25-100 keV. Current status of this diagnostics is reported.*

The energy spectra of fast atoms will be measured by the neutral particle analyzer (NPA) ACORD 12. This analyzer was constructed by the Atomic Physics Department of the A.F.Ioffe Physical-Technical Institute in St. Petersburg, Russia and exploited for measurement of the ion temperature on COMPASS in Culham. The principal scheme of the analyzer is shown in Fig. 1 together with main elements. The picture of the NPA taken in Culham is shown in Fig. 2.

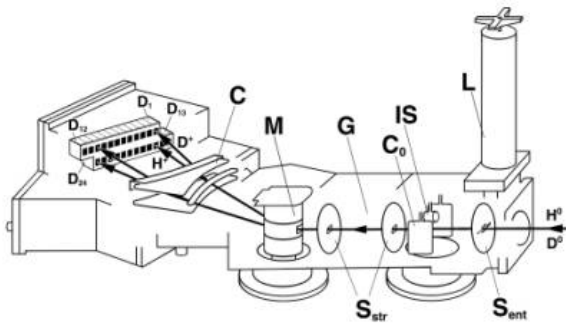


*Fig. 1 Major components Of the NPA: (L) vacuum shatter; (S<sub>ent</sub>) "step like" entrance slit; (C<sub>0</sub>) "cleaning" electrostatic condenser, removing charge particles from the flux; (G) stripping cell chamber; (S<sub>str</sub>) stripping chamber slits; (M) electromagnet; (C) analysing electrostatic condenser; (D<sub>1</sub> - D<sub>24</sub>) two rows of detectors; (IS) auxiliary ion source for NPA testing; (H<sup>0</sup>, D<sup>0</sup>) atoms emitted by plasma; (H<sup>+</sup>, D<sup>+</sup>) secondary ions.*

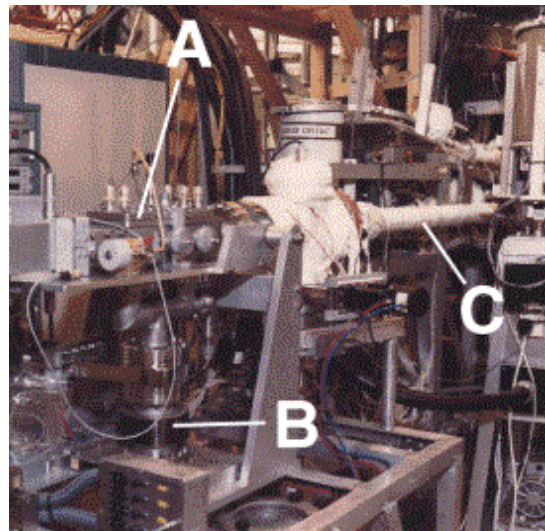


*Fig. 2. Some of the major elements labeled are: (A) NPA; (B) vacuum pump; (C) flight line connecting NPA with tokamak vacuum vessel*

Some characteristics of the NPA are shown in Tab 1.

Detection row	H row	D row
Overall dimensions	705 x 510 x 360 mm	
Number of energy channels	6	6
Minimal/maximal particle	0,25-100	0.3-50 keV

Tab. 1

energy	keV	
Energy dynamic range $E_{max}/E_{min}$ ,	7	7
Maximum allowed D-D neutron flux	$1 \times 10^7$ neutrons/cm <sup>2</sup> /s	
Maximum allowed stray magnetic field	2 mT	

The apparatus shown in Fig. 2 (the NPA and the vacuum system) was disconnected from the COMPASS tokamak in Culham and transported to IPP Prague. In May 2007, the major elements of the NPA were dismantled (stripping cell, analyzing elements, and the detector part) and their status was checked during the visit of M. Petrov from Ioffe Institute in Prague. Some key elements are depicted in Fig. 3.



Fig. 3. Pictures of some elements of the NPE (from left to right): Detector unit, view of the electrostatic analyzer, the analyzing magnet.

It was concluded that the status is satisfactory and ready for measurements soon after having a stable and well defined plasma. Just small refurbishment and connection to the central CODAC is required. It was decided that the NPA will be exploited for analyses of fast neutral atoms after installation of the neutral beam injection (NBI) for ion heating, which is scheduled for the first half of the year 2010. Therefore, installation of the NPA is planned on beginning of 2010.

Future collaboration with the A.F.Ioffe Physical-Technical Institute in the re-installation of the NPA on COMPASS is envisaged. Our colleagues will assist in the calibration of the NPA by means of the beam of potassium ions. Furthermore, the numerical code MC-DOUBLE, developed at Ioffe Institute St. Petersburg, will be purchased and modified to COMPASS geometry. This code is required for detail interpretation of experimental data.

## HRTS diagnostic development

*P. Böhm, M. Aftanas, J. Brotánková, V.r Weinzettl, P. Bilková*

In collaboration with:

*team of the Department of Optical Diagnostics, IPP AS CR, Turnov.*

*The use of the Nd:YAG laser at the second harmonic frequency was investigated and corresponding calculations of the scattered and detected photons were performed for this particular case. Calculations of the parameters of the detection system are being performed.*

## Calculations of photon number

A key parameter for the design of the TS detection system is the number of scattered photons. For the edge TS diagnostic this parameter is essential. Software for estimation of this value for arbitrary radial profiles of  $T_e$  and  $n_e$  was developed. As an input parameter for current calculations, the radial profiles of  $T_e$  and  $n_e$  measured on the COMPASS tokamak in the Culham laboratory (edge TS) are used. Number of collected photons in each spatial and wavelength channel for the edge TS is shown in figure 1.

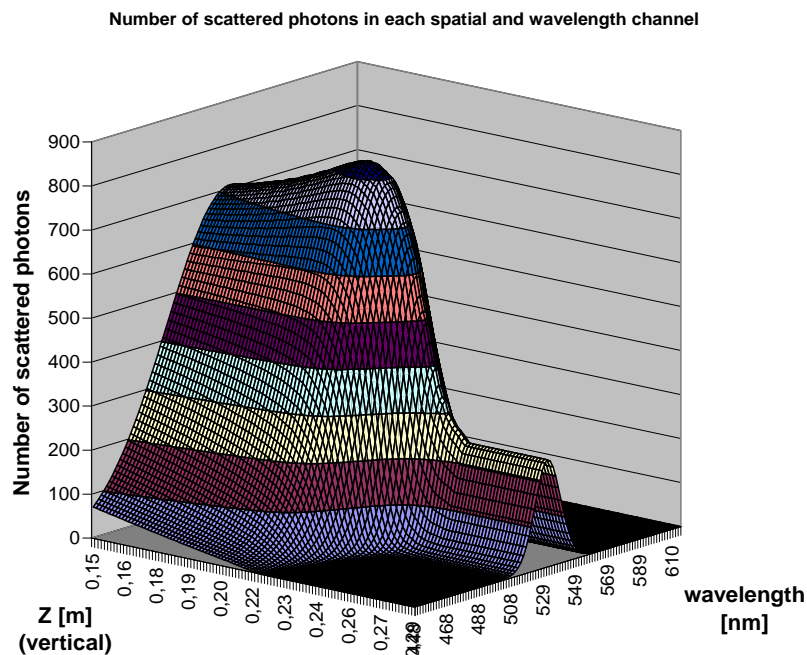


*Fig. 1. Number of collected photons in each wavelength and spatial channel of the detection camera. Energy of laser is 2.5 J on 532 nm, spectral channel width is 1 nm.*

The calculations were performed first and foremost for the plasma edge, since this is the critical part of the measured region. High density in the centre will ensure sufficient number of detected photons. Background radiation by Bremsstrahlung was estimated too.

## **Laser system**

Following demands on the laser system were set from the analysis of the scattering efficiency: Nd:YAG laser system running in pulse regime and generating second harmonic, i.e. wavelength 532 nm, energy of 2.5 J on the second harmonic for each pulse, and repetition rate of 30 Hz, which is closed to technological limit for high-power lasers.

Output beam must be polarized, because of polarization dependence of TS. Divergence of the beam should be less than 1 mrad to achieve good focus and beam diameter close to the tokamak vessel. Laser will be placed outside the tokamak hall; the optical path from the laser to the tokamak will be therefore about 15 m. Beam diameter on the laser output should be about 1 cm, thus on the focusing lens close to the tokamak, the diameter will be up to 3 cm. The lens ( $f = 1$  m) will focus the beam into the plasma, having sufficient focus depth to have 1 mm waist and having diameter less than 1 cm all-over the 40 cm long region of the core TS measurements. Beam pointing stability must be good enough to guarantee movements of the beam in the tokamak vessel about 1 mm.

In the future, an upgrade to multi-pass TS system will be possibly done, exploiting the experience of Petra Bilkova and Petr Bohm with the upgrade from mobility-stay on TEXTOR tokamak in the autumn 2007.

## **Detection system**

Highly sensitive back thinned intensified CCD or CMOS camera will be used for detection of the scattered light. Required range of detectable electron temperature, number of spatial points and spatial resolution determines requirements for the camera system for fast events and very low light level imaging. Optical design and simulation of the best parameters of imaging optics in the collected light path is being done by the ZEMAX software, as well as the layout of the spectrometer in the Littrow arrangement sense.

## **Magnetic diagnostics and development of the feedback system for the COMPASS tokamak**

*O. Bilyková, J. Havlíček, F. Janky, J. Horáček, M. Stránský, M. Hron, I. Ďuran, J. Vlček, J. Stöckel*

In collaboration with:

*H. Fernandes, J. Sousa, T. Pereira, I. Carvalho, A. Neto*, Association EURATOM-IST, Lisbon, Portugal

*M. Cavinato*, Associazione EURATOM - ENEA sulla Fusione, Padova, Italy

### **Magnetic diagnostics:**

The magnetic diagnostic of COMPASS is a complex set of many magnetic sensors distributed around the plasma column and mounted mostly on the vacuum vessel. The overview of the COMPASS magnetic diagnostic sub-systems including the number of sensors and the target quantity to be measured is given in [1]. The dismantling of the magnetic diagnostics on COMPASS was carried out during two missions of IPP staff in the Culham Science Centre in November 2006 and March 2007. The existing documentation of magnetic diagnostics was checked and completed. The magnetic sensor positions were identified and documented. Cables from magnetic sensors to corresponding cubicles were disconnected. All equipment was prepared and transported to IPP Prague. The magnetic sensors will be checked and calibrated in early 2008.

### **Feed-back system:**

The most important step in the re-installation of the COMPASS tokamak is to put into operation the feedback system for maintenance of a defined plasma position. The task of the vertical and radial feedback controls is to process the signals from magnetic sensors, which detect the plasma location, and to apply a correction signal to the power supplies to maintain the plasma in the required position.

To build the feedback system for COMPASS, we considered two options: refurbish and use the original COMPASS analogue system, or design and built a new system based on digital approach. Finally, we decided to pursue the later option because it is significantly more transparent, flexible, and up-to-date.

Digital system is developed under contract of collaboration with the IST Lisbon, which is experienced in building similar systems for other Associations [2].

- a) *Algorithms.* Algorithms for feedback control will be generated by the finite elements MAXFEA code, which is solving the free boundary equilibrium based on the 2D Grad Shafranov equation, developed by P. Barabaschi [3]. Geometry and mesh files were done for COMPASS. They include the exact position of the poloidal field coils, vacuum vessel and limiters. The material properties, resistivity and inductance are described in a material file. The connections of magnetising, equilibrium, shaping and feedback coils are stated in a circuits file with corresponding number of windings and with the currents to the shaping and equilibrium circuits.

- b) *Hardware and control.* The digital system will be based on the ATCA technology standard: multiple - input - multiple - output (MIMO) controllers, developed in IST, will be used. The output of the modelling will be converted to algorithms, which will be programmed to CODAC nodes. These nodes include ATCA modules, each one with 32 analogue input channels, 4 analogue output channels, and 8 digital input/output channels connected to a processor. Such set-up allows the implementation of the MIMO controllers.

Before the signals from the magnetic sensors (Internal Partial Rogowskis, Flux loops and saddle coils) will go to the digital feedback system, firstly they are integrated by original COMPASS analogue integrators, which were used in Culham. In 2007, we have performed basic test of several original COMPASS integrators connected to CASTOR magnetics. The results of these tests were rather mixed. The integrators showed a significant drift despite their embedded drift correction feature. Some integrators were even found to be not operational. In 2008, these initial tests will be completed systematically for all old COMPASS integrators and the final conclusions about their usability for the new COMPASS magnetic system will be drawn.

- c) *Power supplies.* Three identical fast amplifiers are being built in the IPP for the feedback stabilization of the horizontal (1 piece) and vertical (2 pieces in a bridge) plasma positions. The amplifiers are based on MOS transistors, each amplifier has maximum current of 5kA, voltage  $\pm 50V$ , frequency range DC-5kHz, output impedance of 5 m $\Omega$ , and inductance of 274  $\mu H$ . A passive cooling of the transistors is adopted through heat absorption in attached mass of aluminium blocks. The circuit safety is designed for overcurrent, overvoltage and optical isolation protection inside the energizer that determines the amplifiers inputs. There were designed three energizers (containing pre-amplifier, optical decoupling and protection circuits for the fast amplifiers) and digital PID controller (for the fast amplifiers control). In addition, amplifier zero-output-voltage pre-shot check and another delayed overcurrent protection is included.

### References:

- [1] Application for Preferential Support for enabling a programme of ITER relevant plasma studies by transferring and installing COMPASS-D to the Institute of Plasma Physics AS CR, Association EURATOM-IPP.CR. Phase II (2006)
- [2] A.J.N. Batista, *Rev. Sci. Instrum.* 77 (2006) 10F527
- [3] P.Barabaschi, *Plasma Control Technical meeting, ITER JHT*, Naka, Japan (1993)

## **COMPASS Control, Data Acquisition, and Communication system**

*M. Hron, J. Písačka, F. Žáček, J. Strnad, J. Vlček, J. Stöckel, R. Pánek*

In collaboration with:

*H. Fernandes, J. Sousa, B. Carvalho, T. Pereira, I. Carvalho, A. Batista*

Associação Euratom-IST, Lisbon, Portugal

*M. Cavinato*

Associazione Euratom-ENEA sulla Fusione, Consorzio RFX, Padova, Italy

*An efficient operation of COMPASS in Prague requires a new CODAC (Control, Data Acquisition, and Communication) system, which is being developed jointly by the Associations IPP.CR and IST. The tokamak control involves several areas, each of different levels: 24 hours a day control of building infrastructure, interlock, central experiment control, and real time control during the experiment run. Each of the systems has different purposes and diverse features.*

### **Control of slow processes**

The slow control of the overall plant during the 24 hours a day 7 days a week cycle includes the building infrastructure (cooling, heating, air conditioning) as well as the machine infrastructure running in the instantaneous service (experimental area access control, deionized water treatment, energetics systems, etc.).

All these systems are, in general, parts of the building, communications installations, and energetics deliveries, respectively. Specifications for these systems were derived by the IPP.CR staff during the design phase, then the construction and delivery was/is a responsibility of the contractors.

The control of these systems will be managed by their own controllers, while the communication links will secure the necessary exchange of information.

### **Personnel and machine protection**

Safe operation of COMPASS will be guaranteed by an interlock system. The personnel and machine protection will be separated in independent loops.

States of the experimental area will be based on the operational diagram, shown on right, and they will be set by an Area access control system. The personnel protection will be based on a restriction of the access in certain states of the experimental area, during operation of danger systems.

Next, the status of the machine systems will be checked by a safety loop during the preparation phase before each discharge. This will be done in parallel with the CODAC control checking.

Finally, during the discharge, the operation of the tokamak can be interrupted and/or operation of particular systems can be inhibited, depending on the evolution of the status of the individual systems.

### **Central control of the experiment**

The central controller with an operator interface, called “FireSignal“, will allow us to manage individual subsystems and will be used for the control of the experiment [1]. Data access will be managed by a Java based “SDAS layer” [2].

During 2007, the CODAC design was evaluated and the HW platform for CODAC nodes was selected. We will use the Advanced Telecommunications Computing Architecture (ATCA) and a real time linux, running on a PC. Such a system has been developed at IST Lisbon for the vertical stabilization for JET [3] and will be adopted for COMPASS. This set-up builds then a compact CODAC node, where the data acquisition is secured by A/D converters and FPGA arrays on the ATCA boards. The PC running the RealTime Application Interface (RTAI) for Linux gives us the necessary computation power. The available digital and analog outputs of the system are used for communication and control of the subsystems.

We specified the communication link to be used between the CODAC and the power supplies, which are delivered together with the Energetics (toroidal field, equilibrium field, magnetizing field, and shaping field power supplies). Basic features communication protocol were defined.

Next, several particular systems were defined: e.g. a communication module between the CODAC and fast amplifiers for feedback was designed; vacuum system control was designed, incl. a vessel baking module; NBI control requirements (see figure) were specified for the Call for Tender.

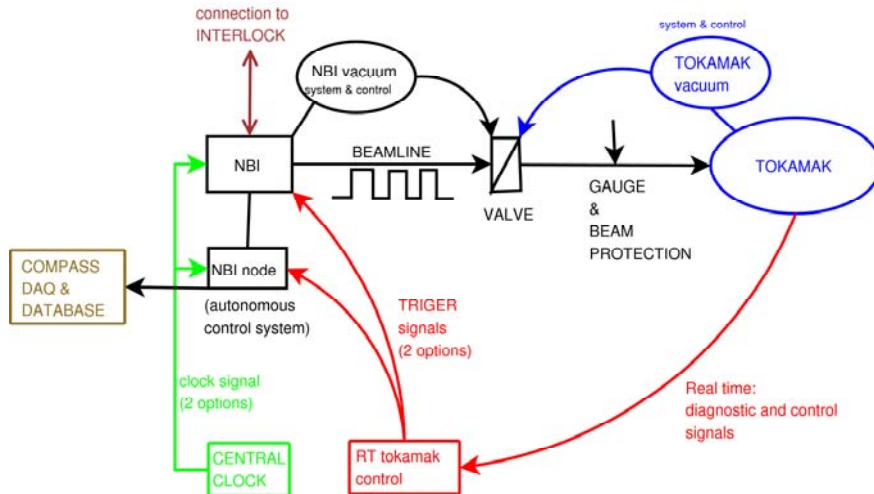


Fig. 1. NBI control requirements

### Real time control during the experiment run

The CODAC nodes described in the previous section will be capable of a real time processing of the acquired signals in a loop well below 50  $\mu$ s. The data acquired by the A/D converters will be pre-processed by the FPGA on board. Then, during the test and start-up phases, the output signals will be calculated in the CPU of the PC. Later, when the algorithms will be fixed, they may be transformed to the FPGA itself to speed-up the response of the feedback loop.

### References

- [1] A.Neto et al., Fusion Engineering and Design 82 (2007) 1359–1364
- [2] A.Neto: Fusion Engineering and Design 82 (2007) 1315–1320]
- [3] A.J.N.Batista et al., Rev. Sci. Instrum 77(2006) 10F52

---

## 3 Development of Concept Improvements and Advances in Fundamental Understanding of Fusion Plasmas

---

### EEDF Measurements in the CASTOR Tokamak Using the First Derivative Langmuir Probe Method

*R. Dejarnac, J. Stockel*

In collaboration with:

*Tsv. K. Popov, P. Ivanova, Association EURATOM-INRNE/Faculty of Physics, Sofia, Bulgaria.*

*F. M. Dias, Association EURATOM-IST/CFP, Lisbon, Portugal.*

*Langmuir probes (LP) allow local measurements of the plasma potential, the charged particles density and the electron energy distribution functions (EEDF) usually using the second derivative of the I-V characteristic. The recently developed kinetic theory [1, 2] may be used for the calculation of those plasma parameters from the first derivative of the electron saturation current measured by the probe. In this work we report the first results of the EEDFs measurements in the CASTOR tokamak edge plasma using this method.*

The I-V characteristics measurements in the CASTOR tokamak edge plasma were carried out by using an array of 16 single, small Langmuir probes oriented perpendicular to the magnetic field, covering a range of 35 mm in the radial direction.

The procedure for evaluating the EEDF from the I-V characteristics using the first derivative method is described in [3]. The connection between the first derivative of the probe current,  $dI(U)/dU$ , and the EEDF for probes oriented perpendicular to the magnetic field is:

$$\frac{dI(U)}{dU} = -const \frac{eU}{\psi(\varepsilon)} f(\varepsilon) \quad (1)$$

where  $e$  is the electron charge,  $U$  is probe potential with respect to the plasma potential and  $\psi(\varepsilon)$  is the diffusion parameter [3]. To calculate the diffusion parameter, we take into account the fact that, although the local diffusion near the probe is classical, the global transport is anomalous (Bohm diffusion) due to the turbulence [2,4]. The EEDF is thus described by:

$$f(\varepsilon) = - \frac{3\sqrt{2m}R \ln\left(\frac{\pi L'}{4R}\right) dI(U)}{32e^3 S R_L U} \quad (2)$$

where  $m$  is the electron mass,  $S$  is the probe area and  $R_L$  is the Larmor radius.

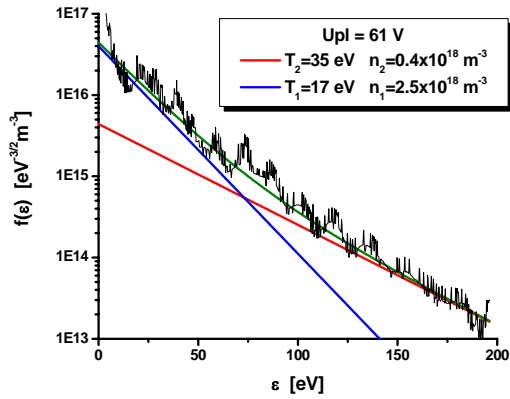


Figure 1

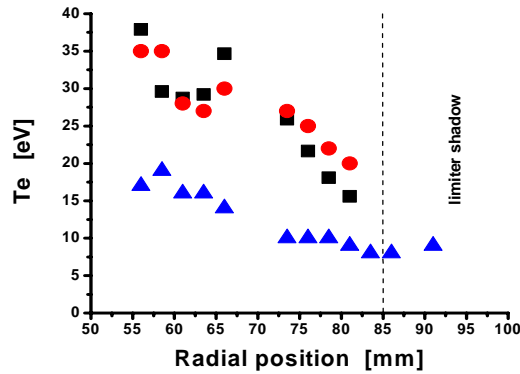


Figure 2

We normalize the EEDF by the electron density,  $n$ :  $\int_0^{\infty} f(\epsilon) \sqrt{\epsilon} d\epsilon = n$ .

An example of the EEDF for the radial position  $r = 56$  mm in stationary phase of the plasma current for the shot #26402 is shown in Figure 1. The green line is a sum of the red one and the blue one. It is clearly seen that the EEDF is bi-Maxwellian. In Figure 2 the radial profiles of the two electron temperatures are presented. The fit with the experimental EEDF was obtained with an accuracy of 5%. It has to be noted that in the limiter shadow,  $r > 85$  mm, the EEDF is Maxwellian with a temperature of about 8 eV. In the same figure the results obtained by Stangeby method [5] (**squares**) are also presented. We must point out that the Stangeby method assumes a Maxwellian EDF of the electrons. Only the temperature of the high energetic fraction of electrons dominates [6,7] and can be evaluated. We estimate the density of the hot population of electrons at about 10% of the bulk electron density. Figure 3 shows the total electron densities at different radial positions. We compare the first derivative method results (**dots**) with the Stangeby method (**squares**) using the cold electron temperature only. The uncertainty in the first derivative method values evaluated does not exceed  $\pm 30\%$ . We see that the two methods show good agreement. Moreover, the first derivative method allows one to obtain in addition the “real” EEDF and the plasma potential values as well (Figure 4).

We have to note that, for those results, the raw data are not filtered. By using an advanced method based on an adaptive choice of the filtering and differentiating instrument functions, the

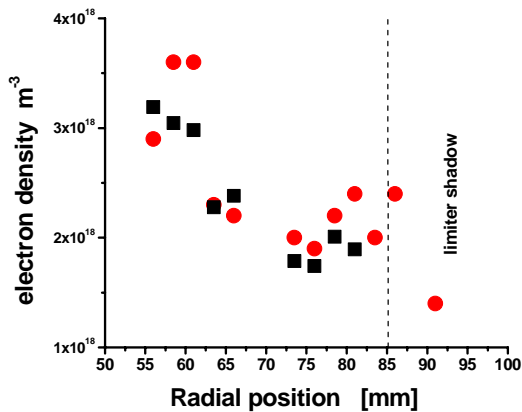


Figure 3

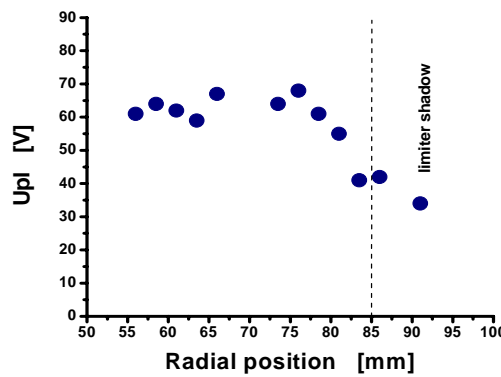


Figure 4

plasma parameters thus calculated are similar and we foresee that the advanced method will be useful for identifying the main modes of plasma turbulence.

**References:**

- [1] Arslanbekov R. R. et al., *Plasma Sources Sci Technol.* **3** (1994) 528 –538.
- [2] Demidov V. I. et al., *Phys Plasma* **6** (1999) 350-358.
- [3] Popov Tsv. K. et al., *Journal of Physics: Conference Series* **63** (2007) 012002.
- [4] Martines E. et al., *Plasma Phys. Control. Fusion* **44** (2002) 351.
- [5] Stangeby P. C., McCracken G. M., *Nuclear Fusion* **30** (1990) 1225-1379.
- [6] Shoucri et al., *Contrib. Plasma Phys.* **38** (1998) 225.
- [7] Batishchev O. V. et al., *Phys. Plasma* **4** (1997) 1672.

## Modelling of ITER Plasma Facing Component Damage and Consequences for Plasma Evolution Following ELMs and Disruptions

R.Dejarnac, M. Komm, R. Panek

We present in this study the power loads in the ITER castellated PFCs by means of kinetic calculations during ELMs. The code used for this purpose has been developed at the IPP Prague and is adapted to such a tile gap geometry [1] by taking into account the specific geometry of the components, the inclination of the magnetic field lines and the gyration of the incoming particles.

We simulate two types of gaps according to their orientations with respect to the magnetic field lines. Poloidal Gap (PG) refers to a gap which is perpendicular to the magnetic field lines, and Toroidal Gap (TG) refers to a gap parallel to the magnetic field lines.

The power deposition in the 0.5 mm wide gaps during ELMs is totally asymmetric for both PGs and TGs. Indeed, only one side is wetted by the plasma in each geometrical orientation. In the case of PGs, the wetted side is the plasma facing side and in the case of TGs, the wetted side is the one favored by the  $ExB$  drift. This feature is due to strong gradients of the asymmetrical electric potential in the gap. The related physics is explained more in detail in [1]. Moreover, a positive 'bump' with respect to the negative potential forms between the tiles and can let in the gap more or less plasma according to its size. Figure 1 shows typical profiles of the deposited power ( $P_{gap}$ ) in the 0.5 mm gaps for both orientations, PG & TG. The non-perturbed, perpendicular flux falling to the tile surface far from the gap ( $P_{tile}$ ) is also indicated for reference.

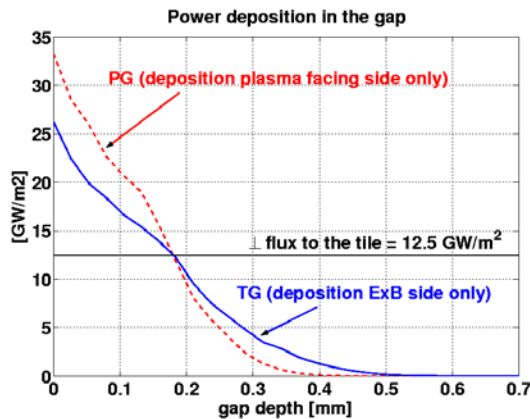


Figure 1: Power deposition in a 0.5 mm gap when parallel (TG) and perpendicular (PG) to B-field for  $2.1^\circ$  inclination and  $n_e = 10^{20} m^{-3}$ ,  $T_i = T_e = 5 keV$ .

perpendicular flux falling to the tile surface far from the gap ( $P_{tile}$ ) is also indicated for reference. At identical high plasma conditions, we observe that the power load at the entrance (peak value) is higher in the case of a PG (+27%) but then decays faster inside the gap than in a TG, hence, the plasma goes deeper in TGs. Moreover, we observe that the integrated power along the gap is almost identical ( $\pm 5\%$ ). It means that globally the same amount of plasma enters the gap in both orientations but is deposited differently. We observe here that the total particle flux inside the gap represents 85% of the unperturbed flux that falls onto the tile far away from the gap in the case of the TG orientation and 80% for the PG case. This result is not a fact related to the two geometry of the gap but it depends on the size of

the potential 'bump' and can vary quite strongly with the plasma conditions. Therefore, 15% and 20% of the incoming power, respectively, do not enter the gap and are deposited on the next tile according to the stream flow.

We also observe in Figure 1 that the decay is not exponential and seems to be divided into two phases. In order to quantify the power deposition inside the gap, we have defined a deposition length,  $L_{dep}$ , as the distance from the gap entrance where the power is 1/1000 the peak value. Figure 1 ( $P_{tile} = 12.5 GW/m^2$ ) corresponds to a two times large uncontrolled ELM ( $E_{tile} = 4.7 MJ/m^2$  with  $\Delta t = 375 \mu s$ ) which is a maximum limit, still acceptable for the thermo-mechanical properties of the PFCs. In this case, the power is deposited over  $L_{dep} = 0.6 mm$  for the

TG and  $L_{dep} = 0.45 \text{ mm}$  (-22%) for the PG, which is much greater than the geometric projection ( $L_{geo} = 0.018 \text{ mm}$  for  $\alpha = 2.1^\circ$ ).

For high plasma conditions, the effects of  $T_e$  and  $T_i$  on the plasma deposition length inside the gap are not significant and the density plays a little role by increasing  $L_{dep}$  marginally (+15% when we double the density).

An important parameter is the inclination angle of the magnetic field lines with respect to the gap. Figure 2 shows the normalized power loads profiles in a TG for two angles,  $\alpha = 2.1^\circ$  (dotted line) &  $\alpha = 1.2^\circ$  (full line), and for the same plasma conditions ( $n_e = 5.10^{19} \text{ m}^{-3}$ ,  $T_i = T_e = 2.5 \text{ keV}$ ,  $B_t = 5.9 \text{ T}$ ). The fluxes falling to the tile surface are in a ratio of a factor of 2 due to the different angles. However, the decrease of the wetted area inside the gap is only by 30%. We have a deposition of the power in the gap  $L_{dep} = 0.50 \text{ mm}$  for  $\alpha = 2.1^\circ$  whereas the deposition is  $L_{dep} = 0.35 \text{ mm}$  for  $\alpha = 1.2^\circ$ . It has to be noted that the peak value increases relatively to the incoming power to the tile with the smaller angle, but remains nevertheless lower in absolute value. We can note that the integrals of the curves shown in Figure 2 are identical due to this feature. This means that the total power inside the gaps is only dependant on the incoming power to the tiles. However, thanks to the change of the slope, by reducing  $\alpha$ , the power loads inside the gap are spread differently and the wetted area reduced.

The same conclusions concerning this effect of the incident angle apply to the PGs. The curves are similar, the only difference between the types of gaps coming from the geometric effect described previously in Figure 1.

This work was performed in the frame of the EFDA Task: TW6-TPP-DAMTRAN "Report(ing) on the expected power deposition profiles onto ITER PFCs during steady-state and transient loads with realistic PFC geometry by PIC modeling".

## References:

- [1] R. Dejarnac and J.P. Gunn, J. of Nucl. Mater. **363-365** (2007) 560-564.

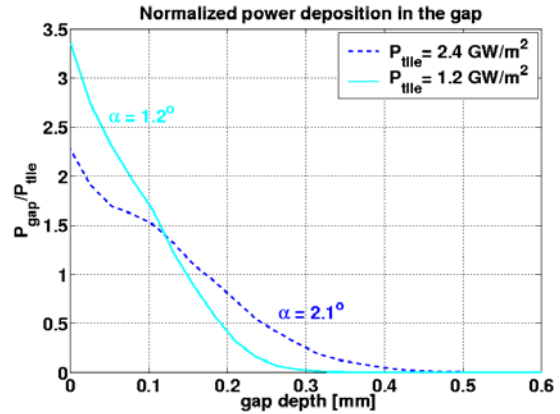


Figure 2: Normalized power deposition in a 0.5 mm TG for an inclination angle of  $2.1^\circ$  (dotted line) and  $1.2^\circ$  (full line) at identical plasma conditions.

## Measurement of plasma flows into tile gaps

R.Dejarnac, M. Komm, J. Stöckel, R. Panek

Particle and power loads in tile gaps are of high interest since ITER plasma facing components will be castellated [1]. Previous experimental studies all show shot- or campaign-averaged results of deuterium and impurities deposition inside the gaps [2,3], but giving no information on how the plasma flows between the tiles. In order to investigate more deeply the physics of the plasma deposition, we have developed a special probe that can measure the ion saturation current profile along the gap (see Figure 1). The experimental data are compared to the results of self-consistent kinetic simulations performed by a 2D particle-in-cell code developed here at the IPP Prague and described in [4].



Figure 1: Picture of the 2 components of the dismantled "sandwich probe" for measuring the plasma deposition into a gap between tiles.

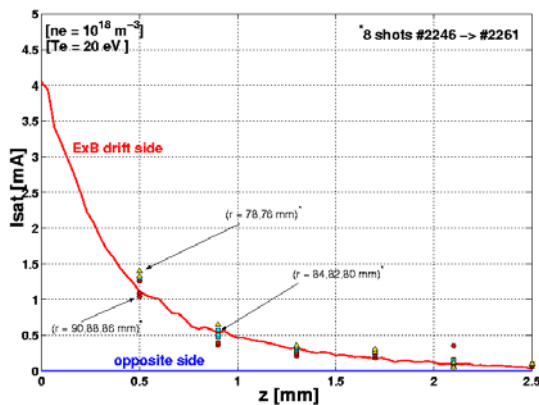


Figure 2: Ion saturation profile along a toroidal gap measured by the probe (points) and calculated by the 2D self-consistent PIC code (red full-line curve). It has to be noted that only one side of the probe shows signal.

are compared with the result of our kinetic calculations (the red/blue full-line curves). We detect here 2 important features that characterize the plasma deposition in toroidal gaps. First of all, we observe that the plasma deposition decreases exponentially along the gap with a decay length of 0.5 mm, which is well reproduced by the PIC simulations. The second important result is that the plasma is deposited only on one side of the probe. Indeed, the probe measures a signal only on the side favored by the ExB drift and nothing on the other side (noise). This physical

The 11 insulated segments of the probe are biased with a negative voltage ( $V_{\text{bias}} = -100\text{V}$ ) in order to collect the ions. The two components A & B are mounted face-to-face in order to create a gap of 1.1 mm width and the probe is inserted in the tokamak CASTOR SOL from the top. Two configurations are investigated experimentally. The first one corresponds to the gap parallel to the magnetic field lines (noted as "toroidal gap") and the second one is when the gap is perpendicular to the magnetic field lines (noted as "poloidal gap").

### 1-Toroidal gaps

Figure 2 shows the ion saturation current distribution along a toroidal gap measured by the probe for 8 reproducible shots, the 6 first segments being represented (points). These points

phenomenon is due to an asymmetry of the electric potential inside the gap as explained in [4] and is in good agreement with the numerical predictions.

## 2-Poloidal gaps

Figure 3-a shows the ion saturation current distribution along a poloidal gap measured for different inclinations of the probe with the magnetic field lines. We observe exponential decays only for low angles ( $\alpha \leq 32.8^\circ$ ) whereas the plasma seems to penetrate deeper and linearly for angles greater than  $32.8^\circ$ . The deposition shown here corresponds to the plasma facing side of the probe. The profiles calculated by our kinetic code are shown in Figure 3-b and we can observe that a similar behavior is well reproduced, with a non-exponential decay for high inclinations. The absolute values are in the same range as in the experiment, however we notice that the deposition is in reality deeper, especially for the larger angles. More investigations must be undertaken to understand this result which is reproducible over all the angle scans we performed.

On the other side of the probe (plasma shadowed side), we do observe some signals but with an intensity 10 times lower. We explain this deposit by a "bump" on the potential profile inside

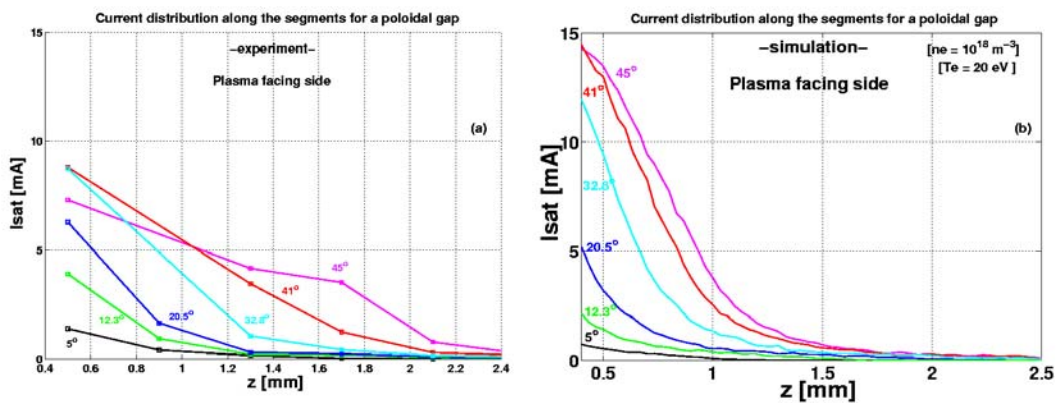


Figure 3: Ion saturation profile along a poloidal gap measured by the probe (a) and calculated by the 2D self-consistent PIC code (b) for different inclinations with respect to the magnetic field lines (from  $5^\circ$  to  $45^\circ$ ) and for the plasma facing side.

the gap, strong enough to repel the incoming ions towards the surface that is not directly wetted by the plasma [4]. Our simulations also reproduce the same asymmetry, plasma facing side/shadowed side. The absolute values at the entrance of the probe tend to be lower than the predicted ones but the radial deposition is in good agreement for all angles.

## Conclusion

We have developed a unique tool to measure the plasma deposition into a gap between tiles. The experimental data confirm the numerical predictions we made with our 2D self-consistent numerical code. In the case of toroidal gaps, we have a quantitative and qualitative agreement. However, in the case of poloidal gaps, it is only qualitatively acceptable. The 2-sided deposition is confirmed, with the good order of magnitude. This set of experiments confirms nevertheless the understanding of the plasma deposition in tile gaps presented in [4].

## References:

- [1] W. Daener et al., Fusion Eng. Des. **61&62** (2002) 61.
- [2] K. Krieger et al., J. of Nucl. Mater. **363-365** (2007) 870-876.
- [3] A. Litnovsky et al., Phys. Scr. **T128** (2007) 45-49.
- [4] R. Dejarnac, J.P. Gunn, J. of Nucl. Mater. **363-365** (2007) 560-564.

## Electron Bernstein waves simulations for WEGA

*J. Preinhaelter, J. Urban*

In collaboration with:

*H.P. Laqua*, Association EURATOM – Max-Planck-Institute für Plasmaphysik, Greifswald

*We have adapted our EBW code to obtain a crude estimate of the profile of the current driven by 2.45 GHz wave. We investigated the dependence of the current profile on the central magnetic field and the temperature of the hot component.*

WEGA plasmas are sustained by electron Bernstein wave heating. This produces a considerable suprathermal electron population. The fraction of this populations ranges up to  $\sim 20\%$  and the temperature reaches 200 – 300 eV (compared to  $\sim 50$  eV of the bulk electron population). These data are estimated from probe measurements and are only approximate. We have extended our EBW code to include the effects of the suprathermal electrons. Significantly different behaviour of the EBWs, compared to single component plasma, has been demonstrated by the simulations. Even a modes fraction of suprathermal electrons enables very efficient absorption.

Current density profile was, for the first time, measured by a small Rogowski coil during our visit [1]. Therefore, we have concentrated on current drive studies. We have simulated the absorbed power corresponding to individual resonances (and components) and determined the corresponding direction of the driven current, supposing Fish-Boozer current drive mechanism. The parallel wave vector direction of the EBWs can be reversed during the propagation through the plasma. The driven current direction has to be reversed analogously. Such behaviour has been observed experimentally [1]. We have investigated the effects of the central magnetic field and of the hot component on the EBW current drive.

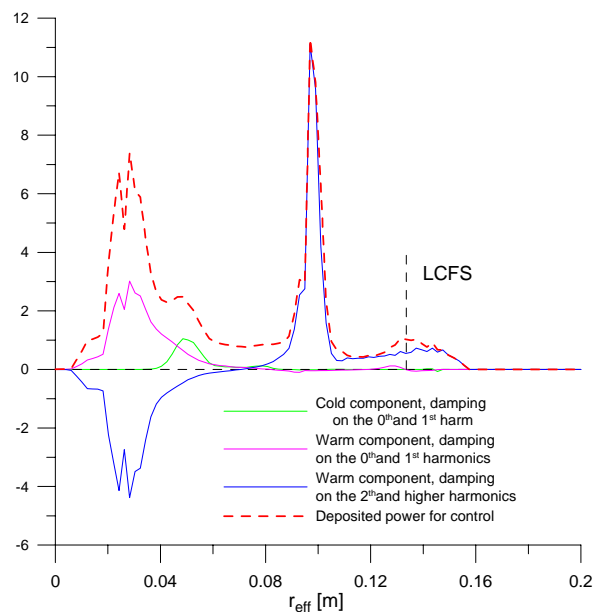


*Fig. 1. Distribution of the absorbed power between components and harmonics. Individual contributions are multiplied by the sign of  $v_{res} = (\omega - n\omega_{ce})/k_{\parallel}$ .  $B(R_0) = 0.65B_{ce}$ ,  $T_i = 300\text{eV}$ .*

Profiles of the power absorbed on the hot and the warm plasma components, corresponding to both the 0<sup>th</sup> and the 1<sup>st</sup> harmonics and the 2<sup>nd</sup> and higher harmonics, are shown in Fig. 1. We see that the resonant velocity of the absorbed power contribution of the 2<sup>nd</sup> harmonics has different sign at the plasma boundary and at the plasma centre. This behaviour is caused by the change of the sign of the corresponding  $k_{||}$  along the ray. This effect is probably responsible for the experimentally observed current reversal at the plasma centre. As an estimate of the current profile, we have summed individual components of the absorbed power, multiplied by the sign of the resonant velocity. We also scan this quantity with respect to the central magnetic field and the temperature of the hot component. Final results of the simulation are seen in Fig. 2 and 3. Current profile measurements were performed only for single antenna position and with constant vertical magnetic field. Therefore, we have investigated the effects of the central magnetic field magnitude (expressed as a multiple of the resonant magnetic field  $B_{ce}=2.45/28=0.0875$  T) and the temperature  $T_1$  of the hot component.

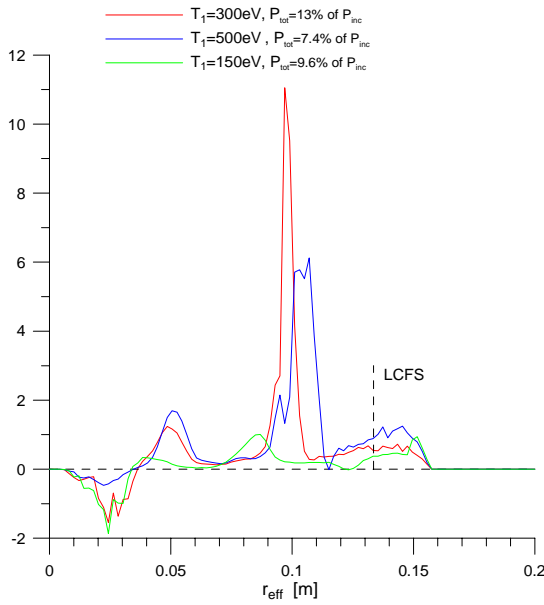


Fig. 2. Hot component temperature scans. Summed components of the absorbed power. Individual contributions are multiplied by the sign of  $v_{res}=(\omega-n\omega_{ce})/k_{||}$ .  $B(R_0)=0.65B_{ce}$ .

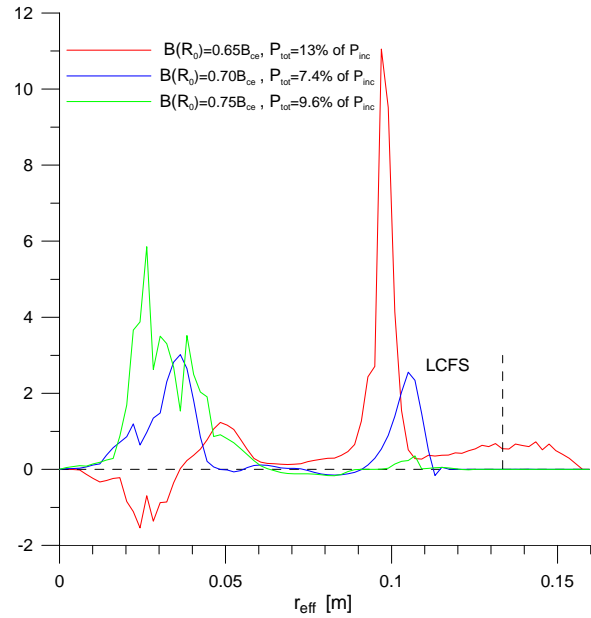


Fig. 3. Central magnetic field scans. Summed components of the absorbed power. Individual contributions are multiplied by the sign of  $v_{res}=(\omega-n\omega_{ce})/k_{||}$ .  $T_1=300eV$

## References:

- [1] Laqua, H.P., et al., *Bulletin of the American Physical Society*, vol. 52, no. 16 (2007) 280

## EFIT2006 Parallelization

*J. Urban, J. Havlíček*

In collaboration with:

*L.C. Appel*, Association EURATOM-UKAEA Culham

*EFIT2006 is a modern version of the magnetic equilibrium reconstruction code EFIT, developed at UKAEA Culham. A parallel version of the code was desirable to accelerate the calculations. EFIT2006 will be also used at IPP Prague for the COMPASS tokamak.*

Parallelization of EFIT2006 [1] has started from scratch. It has been decided to implement a coarse grained parallel version of EFIT2006 [2], i.e. to parallelize the high level interface, so that a master process will serve other processes with input data for individual time slices. These processes (slaves) will perform the computation and send the results back to the master, where all the outputs will be written to a file or sent to a database. The parallel version should run on computer grids or clusters using the MPI interface.

EFIT2006 is an object oriented code in C++, which is very beneficial for understanding and enhancements, but parallelization using MPI requires rather complicated transmission of C++ objects. Fortunately, the Boost C++ libraries have recently been extended by an MPI library, which allows transmitting complex C++ objects very conveniently. A functional version of parallel EFIT2006 has been implemented and its performance has been tested. The results are shown in Fig. 1. A linear growth can be clearly seen, even though the benchmarks have been run on serial computers interconnected by rather slow Ethernet network.

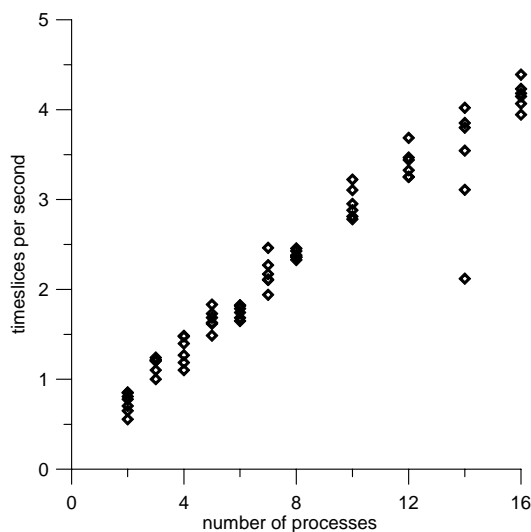


*Fig. 1. Benchmarking results of the parallel EFIT2006. heating and current drive systems.*

EFIT2006 and all the necessary libraries have already been installed at IPP Prague. Benchmarking results for the same inputs shows that the two installations are equivalent. IDAM, a general library for data access, is successfully working at IPP Prague, including the ability to remotely read data from UKAEA Culham server.

We have been able to reproduce equilibria with input from COMPASS experimental data provided by UKAEA. We have also succeeded to run EFIT2006 with predictions obtained with the ACCOME code [3]. The ACCOME code solves the Grad-Shafranov equation and allows prediction of plasma equilibrium for given poloidal field coils currents and external

### References :

- [1] Appel, L.C., et al., *33rd EPS Conference on Plasma Physics, Rome* (2006)
- [2] Havlíček, J. and Urban, J., *WDS'07 Proceedings of Contributed Papers: Part II - Physics of Plasmas and Ionized Media* (2007) 234-239
- [3] K. Tani, M. Azumi and R. S. Devoto, *J. Comput. Phys.* 98 (1992) 332

## QPIC study of secondary electron emission in response to fast electron flow to tokamak edge target plates, including the effect of electron emission on sheath potentials

*V. Fuchs, IPP Prague and J. P. Gunn, CEA Cadarache*

*We consider the the quasi-neutral self-consistent particle-in-cell (QPIC) simulation of a tokamak plasma scrape-off layer (SOL) bounded by two material walls – possibly divertor plates, limiters, probes, or a combination of these. At every time step of the simulation some ions and electrons reach the material walls, but suffer very different fates. The ions are absorbed by the walls and are lost from the simulation. A QPIC simulation satisfies local plasma quasineutrality so that during the simulation the plasma must also be globally neutral. It follows that not all electrons travelling to a wall are allowed to reach it: the total number of electrons lost to the walls must equal the total wall ion charge. If there is global charge balance at each wall, i.e if the ion and electron fluxes to a wall are equal, then the wall potential equals the floating potential. By definition, this floating potential is actually the energy of the most energetic electron which is reflected back into the plasma from it.*

Introducing secondary electron emission changes the wall potentials and the wall charge balance. We thus address here a persistent problem in the interpretation of probe data, which is the inconsistency between theoretical calculations of fast electron distributions that should give extremely large sheath potentials (~kV) and measurements, which only give 0-100 V. The reason might be due to secondary emission - the s.e.e. coefficient is of the order of 1 for energies in the 400 eV and higher range. That means that fast electrons do not contribute to the net electrical current, while only the thermal ones do. So instead of a very large potential drop with a very energetic electron flux reflected from the sheath back towards the SOL (what we get now), we would expect to have a reasonable potential drop with cold electrons sent back into the SOL.

As a basis for our kinetic treatment of secondary electron emission we adopt the semi-empirical form for the secondary electron emission – the s.e.e. - coefficient  $\delta$  [1,2]

$$\frac{\delta}{\delta_{\max}} = (2.72)^2 \frac{E}{E_{\max}} \exp \left[ -2 \left( \frac{E}{E_{\max}} \right)^{\frac{1}{2}} \right] ; \quad E = E_{\text{kin}} + V_w + E_{\perp} \quad (1)$$

where  $\delta_{\max}$  and  $E_{\max}$  are respectively the maximum value of  $\delta$  and the energy value where this maximum occurs. Further,  $E_{\text{kin}}$  is the electron kinetic energy,  $V_w < 0$  is its potential energy, and  $E_{\perp}$  its energy of gyromotion. The s.e.e coefficient thus normalized is shown in Fig.1. and selected values of  $\delta_{\max}$  and  $E_{\max}$  are shown in Table 1, both taken from Ref. [1].

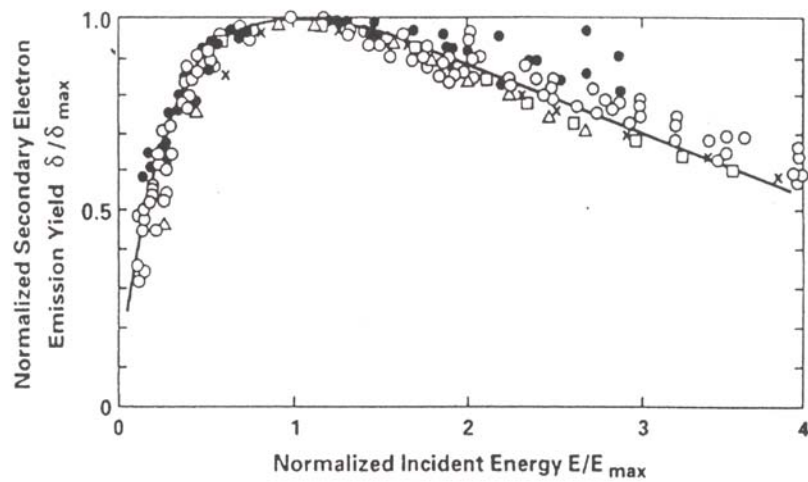


FIG. 1. Normalized secondary electron emission coefficient  $\delta/\delta_{\max}$  as a function of normalized energy  $E/E_{\max}$ . The circles are data for Li, Mg, Al, Si, Ti, Fe, Cu, Ni, Ga, Ge, Rb, Nb reproduced from the review of Kollath [ 2]. The other data points are for TaC ( $\times$ ), TiC ( $\Delta$ ) and ZrC ( $\square$ ) drawn from the work of Thomas and Pattison [ 3 ]. The line is the semi-empirical curve of Eq. (1).

TABLE I. MAXIMUM OF THE SECONDARY ELECTRON EMISSION YIELD,  $\delta_{\max}$ , AND PROJECTILE ENERGY AT WHICH IT OCCURS,  $E_{\max}$ , FOR SELECTED ELEMENTAL METALS AND CERTAIN OTHER MATERIALS

Target	Z	$\delta_{\max}$	$E_{\max}$
Be	4	0.5	200
C (graphite)	6	1.0	300
C (pocographite)	6	0.55	500
Al	13	1.0	300
Ti	22	0.9	280
Fe	26	1.3	400
Ni	28	1.35	550
Mo	42	1.25	375
W	74	1.4	650
TiC		1.0	460
TaC		0.84	270
ZrC		1.25	340
TiN		0.95	350
Stainless steel		1.22	400

The  $\delta$ -curve decreases for  $E > E_{\max}$  owing to deeper penetration of the incident electron into the target. It can be seen that for most tokamak edge electron energies (i.e. thermals and LH-generated fast electrons) and edge component materials of interest, the s.e.e coefficient  $\delta$  lies between 0.5 and 2. In the context of a particle-in-cell (PIC or QPIC) code this is to be interpreted as follows. Suppose that during a particular time step  $\Delta t$ , which in a QPIC code is limited in magnitude by the Courant condition  $\Delta t < \Delta z / v_{\text{thermal}}$ , there are  $N$  electrons incident upon a material target. Clearly, we would like the number  $N$  to be very large with a well-defined energy distribution so that we could interpret  $\delta \Delta N$  as the number of secondary electrons generated per time step by the  $\Delta N$  electrons falling into the energy range  $(E, E + \Delta E)$ . However,  $\Delta t$  is typically small and so is the corresponding number  $N$  of incident electrons per time step. Thus we cannot obtain significant ensemble statistics in a time step. On the other hand, in a typical QPIC simulation proceeding on the ion thermal transit time scale, the number of time steps is very large, typically around  $10^5$ .

The probabilistic meaning of the  $\delta$ -coefficient can be therefore retained by working with time – rather than ensemble – averages, adopting an electron-by-electron Monte-Carlo technique. This is done as follows. Take a particular electron which has reached the material target. (i.e. we assume that its energy exceeds in magnitude the self-consistent wall potential). This electron is characterized by its energy  $E$  and the corresponding  $\delta$  in Eq. (1) or Fig. 1. We furthermore assign the electron a uniformly distributed random number  $\text{RAND}$  from the interval  $(0, 1)$ . For the sake of illustration, let us consider the following simple emission algorithm: if the s.e.e probability is high enough, i.e. if  $\delta > 1$  or  $\text{RAND} < \delta < 1$ , then a secondary electron is emitted and the wall global charge is unchanged. If, however,  $\delta < \text{RAND}$ , then secondary emission does not occur and the wall charge state changes as the incident electron neutralizes one of the incident ions. In the long run, for  $N$  primary electrons in the energy range  $(E, E + \Delta E)$ , this algorithm clearly generates  $N\delta(E)$  secondary electrons.

We limit ourselves here to intermediate values of  $\delta$  such that no more than one secondary electron can be emitted. This has far-reaching consequences for the QPIC code and simulation, which thereby remains relatively simple to modify and execute. The essential simplification, as was already mentioned, is that a single electron emission event does not change the wall charge state. Hence the ion wall charge throughout the simulation only depends on ions reaching the walls. The only complication which can arise (and occasionally it does) is that with many secondary events we might in a particular time step run out of electrons capable of maintaining global wall charge balance since the corresponding primary electrons do not contribute to neutralizing the wall ion charge. Now imagine the much more severe consequences of a multiple secondary event. First, with multiple secondary events the wall positive charge increases and many more electrons than in single events are required for wall neutralization. In addition, the positive electron „holes“ arising in multiple secondary events must be included in global wall charge balance.

In the present work we therefore only deal with single secondary events and discontinue secondary electron production when in a time step the number of secondary events plus wall ion charge exceeds the number of electrons incoming to the target..

We now turn to the question of global charge conservation and the determination of self-consistent wall potentials in the presence of single secondary electrons ( i.e. the global positive wall charge per time step  $q$  comes only from incident ions). Even without secondaries this is a complicated non-linear problem involving global charge conservation together with Kirchoff's second law for the tokamak circuit with the discharge. We thus need to solve the system of two equations

$$q_{eL} + q_{eR} = q_{iL} + q_{iR} \equiv q \quad (2)$$

$$\oint \mathbf{E} \cdot d\boldsymbol{\lambda} = V_L - V_R + \Phi_{pL} - \Phi_{pR} + V_{bias} = 0 \quad (3)$$

where the elements of the potential arrays  $V_{L,R}(1:q)$  are the kinetic energies of the highest-energy incoming electrons. A solution of these two equations exists if the maximum  $V$  on one side is not smaller than the minimum  $V$  on the other, and at best it is only approximate, since the charges  $q$  are integers and the potentials  $V_{L,R}$  take on discrete values. The solutions are the wall potentials  $V_{wL,R}$ , functions of the appropriate wall electron charges  $q_{eL,R}$ . In practice we arrange the first  $q$  most energetic electrons on each side in descending order of kinetic energy, so that the first elements correspond to the electrons least likely to be reflected from, i.e. most likely to be "passing", the potential barrier. On each side we need  $q$  such electrons since we do not know beforehand which will be the combination of wall electron charges that will satisfy (2) and (3).

Let us now consider what happens when a secondary electron is emitted. As already mentioned, an electron which gives rise to a single secondary does not contribute to neutralizing the wall ion charge. Therefore another electron, less energetic than the ones already in the list, must be admitted. Thus for every secondary event, less energetic electrons take the place of the originally most energetic ones travelling to the target. It follows that the solutions of Eq. (3), the wall potentials  $V_{wL,R}$ , decrease in magnitude in the presence of secondary electron emission. This tendency is naturally stronger with multiple secondary events.

The solution itself of Eqs (2,3) is quite complicated. Without secondaries, the algorithm is fairly straightforward, but with secondaries an additional major complication arises owing to the dependence of energy  $E$  in Eq. (1) on the unknown value  $V_w$  of the wall potential. With secondaries, the resulting non-linear transcendental equations are resolved by a bisection method, which will be presented elsewhere. Convergence of the method is fast, typically in less than 100 iterations.

Results for thermal electrons are obtained mostly without problems, but we have been experiencing difficulties resulting from too many secondaries associated with fast primaries generated when lower-hybrid power is switched on. As mentioned above, we dealt with this problem by disabling secondary electron production when a certain critical number of secondaries is exceeded. Selected results are presented for illustration below.

In conclusion, we introduced secondary electron production in the QPIC code, carried out necessary code modifications and debugging, and obtained some first exploratory results. The main difficulties with introducing secondary electrons have been identified, some of which (e.g.

multiple secondary events) will be dealt with in the continuation of this project. We consider the milestones set out for this part (B) of the mission to have been met.

**Selected results**

Table II Some results of selected 6 QPIC simulations at the following conditions: "natural" Tore Supra SOL,  $T_{e0}=T_{i0}=50$  eV,  $n=5 \times 10^{17}$   $1/m^3$ ; initial number of particles per cell = 5000 ions, 5000 electrons; zero background drift velocity;  $E_{max}=300$  eV. Further,  $E_0$  is the LH grill electric field strength, and we imposed a symmetric LH grill spectrum in order to test the expected symmetry of the simulation. The subscript "L" refers to the left wall, "R" to the right wall.

$d_{max}$	$E_0$ [kV/cm]	spectrum	$V_{wL}$	$V_{wR}$	$T_{ewL}$	$T_{ewR}$	$T_{emax}$
0			-0.180	-0.187	0.09	0.09	0.163
1.0			-0.141	-0.139	0.09	0.09	0.167
1.6			-0.126	-0.127	0.09	0.09	0.174
0	1	symmetric	-13.20	-13.22	8.56	8.58	22.65
1.0	1	symmetric	-6.64	-7.12	7.20	7.60	19.06
1.6	1	symmetric	-4.58	-4.31	6.31	6.07	18.71

The wall potentials  $V_{wL,R}$  given in Table II are time-averages taken over the period when the simulation has reached equilibrium, as indicated below in Fig. 2 :

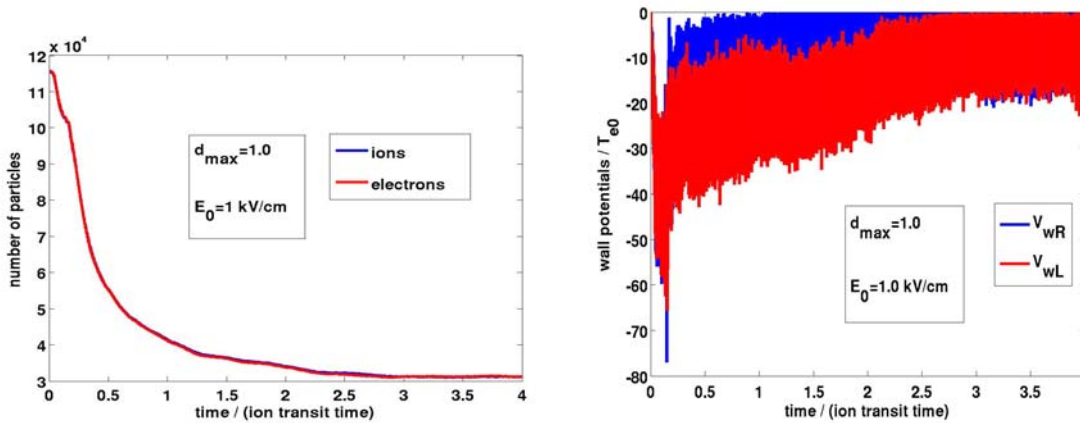


Fig 2. a) The number of ions and electrons in the simulation region as a function of time. The simulation is seen to reach equilibrium in about 3 ion transit times. b) The evolution of wall potentials  $V_{wL,R}$  at the left and right targets, respectively. Results are obtained at simulation conditions of Table II.

We note a small effect of secondary electrons on  $V_{\text{wall}}$  as  $d_{\text{max}}$  increases in the three simulations at thermal conditions of Table II , but a relatively much larger effect at LH conditions . This indicates that the effect of secondary electrons should be taken into account in the interpretation of probe diagnostics.

### References

- [1] E. W. Thomas, Supp. Nucl. Fusion 1 (1991) 79.
- [2] R. Kollath, Handbuch der Physik, Vol. 21, Springer Verlag, Berlin (1956) 232.
- [3] S. Thomas and E. B. Pattison, J. Phys. D3 (1971) 349.

## Simulation of processes in high-temperature plasma toward better interpretation of experimental data

R. Hrach, Z. Pekárek, E. Havlíčková, Š. Roučka

In collaboration with:

R. Pánek, Association EURATOM-IPP.CR

*The Faculty of Mathematics and Physics continued the work on development of hybrid code. The program under development presents a self-consistent model of central and border regions of this tokamak for different experimental conditions. The goal is to determine the anticipated range of plasma parameters in this system and to forecast the conditions for superior plasma confinement. Confinement like that is characterized by a low-temperature and low power load of the divertor. In addition the doctoral student Josef Havlíček participated in improving the EFIT 2006 program. This program enables calculating the current density, plasma shape and pressure and further plasma parameters. Our diploma, now PhD, student Michael Komm improved the SPICE code in such a manner that the program runs approximately 20 times faster.*

The work in 2007 covered two main areas: (i) Numerical investigations of plasma parameters in COMPASS tokamak and (ii) Preparation of 3D particle code of magnetized plasmas. In frame of the first part numerical investigation of plasma parameters in COMPASS tokamak was performed and presented in the 34th EPS Plasma Conference on Plasma Physics in Warsaw, Poland [1]. The plasma parameters in the device were analyzed in the frame of the self-consistent model of central plasma and edge region. The possibility of achieving high recycling and detached regimes in COMPASS divertor was discussed (see Fig. 1).

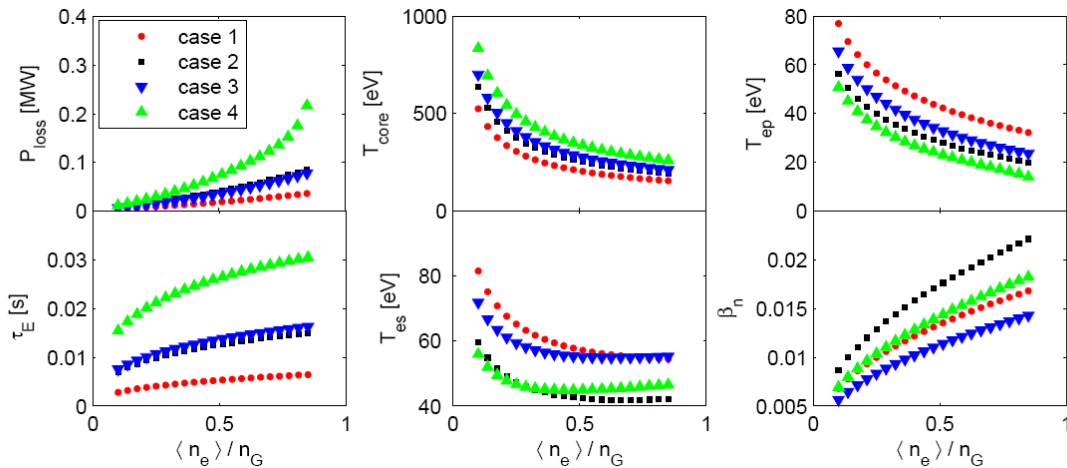


Figure 1. Total energy losses  $P_{loss}$ , energy confinement time  $\tau_E$ , average plasma temperature  $T_{core}$ , plasma temperature at the LCMS  $T_{es}$ , plasma temperature at the plate  $T_{ep}$  and normalized parameter  $\beta_n$  as functions of normalized volume average density  $\langle n_e \rangle / n_G$  for different configurations. Scaling (B).

In frame of the task preparation of 3D particle code of magnetized plasmas there was developed during 2007 the self-consistent fully 3D Particle-In Cell code for modeling of plasma-solid interaction with new Poisson solver based on direct LU decomposition combined with multigrid approach. The model was tested on a cylindrical cavity geometry, i.e. on a hollow cylindrical

chamber opened to the plasma, in both collisionless and collisional plasmas (see Fig. 2). The basic studied feature was the influence of non-axial orientation of magnetic field – this parameter is important for the analysis of experimental data from the Katsumata probe. Earlier version of the model was published in [2], the improved model developed in 2007 in [3,4].

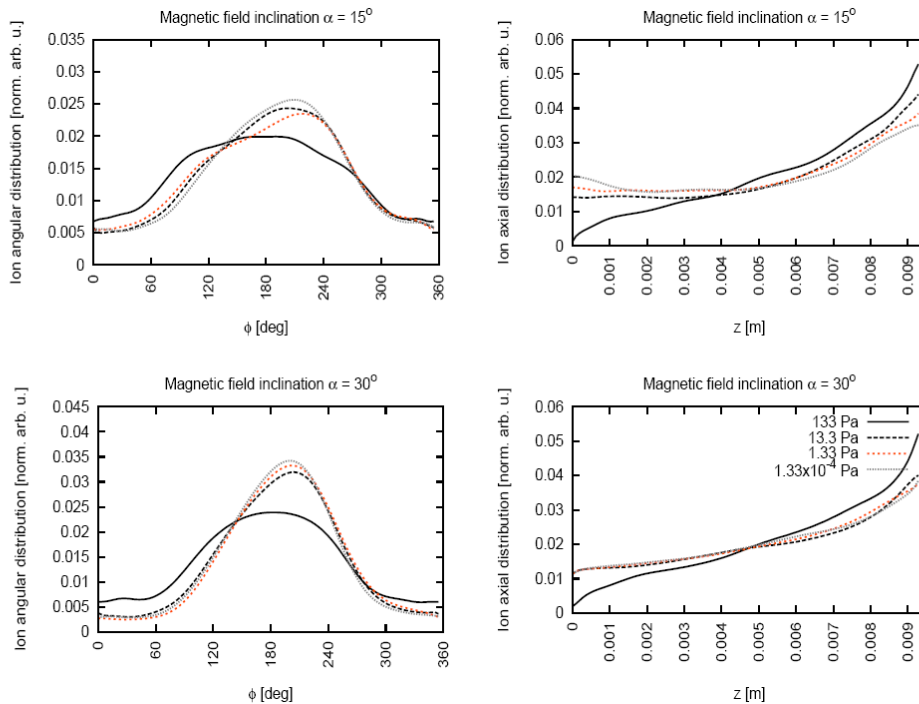


Figure 2. The angular (left) and axial (right) distributions of ions on the inner cylindrical wall, with the magnetic field inclination  $\alpha$  and ambient gas pressure as parameters.

### References:

- [1] E. Havlíčková, R. Zagórski, R. Pánek, Numerical Investigations of Plasma Parameters in COMPASS Tokamak, 34 EPS Conference on Plasma Physics, 2-6 July 2007, Warsaw, Poland, proceedings reference ECA Vol. 31F, P4-117 (2007).
- [2] Z. Pekárek, R. Hrach, Influence of Non-Axial Magnetic Field in a 3D3V Paraticle-In-Cell Plasma Model, Vacuum **82** (2008), 244-247.
- [3] Z. Pekárek, Š. Roučka, R. Hrach, 3D particle simulations of plasma-solid interaction: Magnetized plasma and a cylindrical cavity, 17th Interational Vacuum Congress IVC-17, 2-6 July 2007, Stockholm, Sweden.
- [4] Z. Pekárek, R. Hrach: Multigrid methods as a Poisson equation solver for 3D PIC models of plasma-solid interaction, Conference on Computational Physics CCP2007, 5-8 September 2007, Brussels, Belgium.

## Results of PIC modeling of the ball-pen probe

*J. Adánek, R. Pánek, J. Stöckel, M. Komm*

*This contribution presents the Particle-in-Cell (PIC) modeling of the Ball-pen probe using the 2D XOOPIC code developed in Berkeley University. The ball-pen probe has been designed for the direct measurements of the plasma potential. The probe head consists of a movable conducting collector, which is partially shielded by the isolator. This construction allows modification of the ratio of the electron and ion saturation currents with respect to the collector position.*

The basic idea of the direct plasma potential measurement by the ball-pen probe [1,2] is to adjust the ratio  $R = |I_{sat}^- / I_{sat}^+|$  in Eq. (1) to be equal to one. When this is achieved, the floating potential of the probe  $V_{fl}$  is equal to the plasma potential  $\Phi$  as follows from

$$V_{fl} = \Phi - T_e \ln(R) \quad (1)$$

Figure 1 shows the results of the PIC simulations ( $T_e=T_i=20$  eV,  $\Phi=0$ ,  $B_i=1$ T) of  $I$ - $V$  characteristics of the ball-pen probe using 2D XOOPIC (developed in Berkeley University) [3]. The  $I$ - $V$  characteristics are plotted for different collector positions, when the collector is partially exposed to plasma ( $h>0$ ). The probe current is normalized to the ion saturation current. It is evident that the value of the ratio  $R$  and the floating potential  $V_{fl}$  depend on the collector position. This is in a good agreement with the experiment and the theoretical predictions.

The relation between  $\ln(R)$  and  $V_{fl}$  can be approximately described by the linear function as seen in Fig. 2. The value of the plasma potential is according to the Eq. 1 estimated as  $\Phi = -24$ V, which is below the value of the plasma potential given in the PIC simulation ( $\Phi = 0$ V).

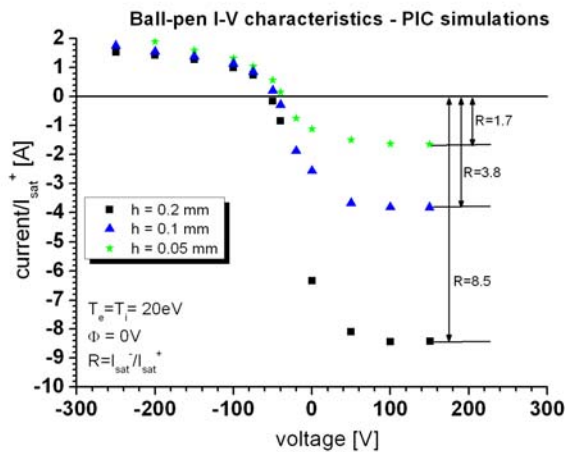


Fig.1.  $I$ - $V$  characteristics of the ball-pen probe for several collector positions calculated by the PIC simulations ( $T_e=T_i=20$  eV,  $\Phi=0$ ).

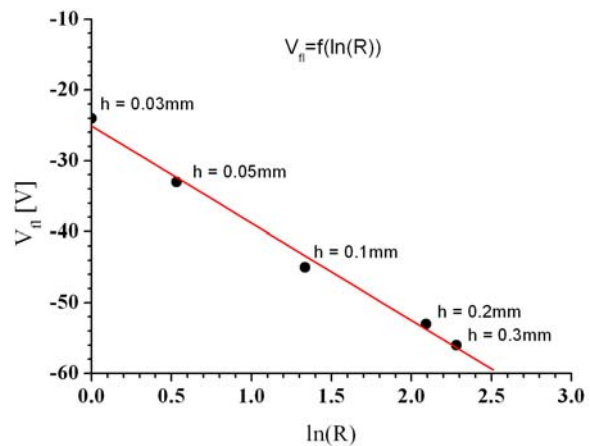


Fig.2. The dependence of the ball-pen probe potential  $V_{fl}$  on the logarithm of the ratio  $R$ , for several position of the ball-pen collector.

The discrepancy can be explained by detailed analysis of the potential around the ball-pen probe head. The 2D profile of the potential around the probe is plotted in Fig. 3. The plasma is injected

from the left and right side of the simulated area. The probe collector is exposed 0.2 mm to plasma and negatively biased by  $U = -150$  V. In spite of the fact, that plasma potential is equal to 0 V at the left and right boundary of the simulated area the potential inside area is below that value. It means that the plasma potential provided by the ball-pen probe (see Fig. 2) should be equal to the potential given by PIC modeling a few ion Larmor radii far from the probe head along  $y$  coordinate. The potential above the probe orifice at coordinates  $y = 3.0$  mm (dash line in Fig. 3) is approximately equal to -5 V and it might be assumed as the unperturbed plasma potential.

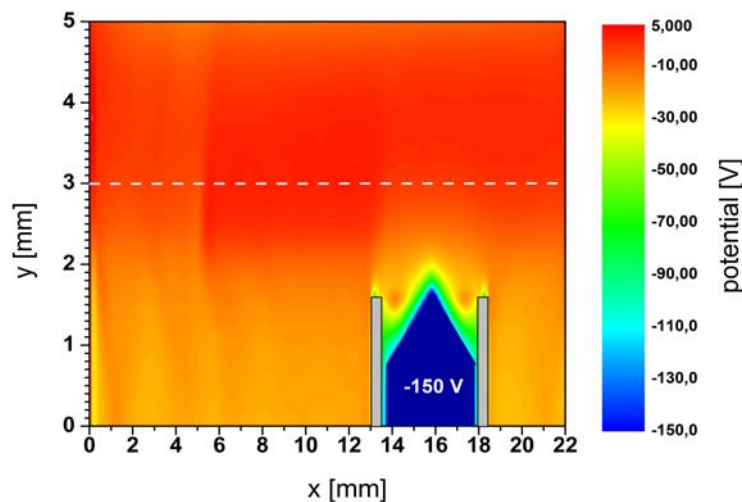


Fig.3. The 2D profile of the potential around the ball-pen probe. The probe collector is exposed 0.2 mm in plasma and negatively biased by  $U = -150$  V. The plasma is injected from left and right side of the simulated area. The magnetic field is parallel with  $x$  coordinate,  $B_x = 1$  and  $B_y = 0$  T.

It can be summarized that the results of the PIC simulations of the ball-pen probe confirmed that the relation between the difference of the plasma and floating potential and  $\ln(R)$  is linear as predicted the Langmuir probe theory (Eq. 1). However, the plasma potential provided by the ball-pen probe in Fig. 2 is approximately  $1 \cdot T_e$  ( $T_i = T_e = 20$  eV) less than the plasma potential estimated by using 2D profile of the potential in Fig. 3. The discrepancy can point out that the basic idea of the direct measurements of the plasma potential based on the simple Langmuir probe theory above mentioned is not suitable for this kind of magnetized plasma. However, it can be also explained by the fact that the model results in zero electron density inside the shielding tube, which was not observed in the experimental observation [1,2].

#### References:

- [1] J. Adamek et al., *Czech. J. Phys.*, **54** (2004), C95.
- [2] J. Adámek et al., *Czech. J. Phys.*, **55** (2005), 235-242.
- [3] J.P. Verboncoeur, A.B. Langdon and N.T. Gladd, "An Object-Oriented Electromagnetic PIC Code", *Comp. Phys. Comm.*, 87, May11, 1995, pp. 199-211.

## Adaptation of ASTRA and CRONOS for COMPASS simulations

*M. Stránský, V. Fuchs*

In collaboration with:

*V. Basiuk, Y. Peysson*, Association EURATOM-CEA Cadarache, France

*I. Voitsekhovitch*, Association EURATOM-UKAEA Abingdon, United Kingdom..

*Transport codes solve coupled diffusion equations for heat, matter, and magnetic field (current). These partial differential equations are coupled to a magnetic field equilibrium code and modules for LH and NB injection. Such codes thus allow fully self-consistent calculations of tokamak operation, and are highly desirable for the study of COMPASS operation with the planned LH and NB systems.*

Currently, the transport modeling of the tokamak COMPASS is performed using the ASTRA [1] and CRONOS [2] codes. The ASTRA code had been in use at IPP for some time and it has limited internal capabilities as far as external heating and current drive is concerned. It was therefore decided that a more advanced code, CRONOS, is necessary for the prediction and analysis of COMPASS operating scenarios. During the mobility stay of M. Stránský at CEA Cadarache in April 2007, the CRONOS transport code was acquired and adapted for the COMPASS tokamak, and installed in Prague by the CEA staff in November 2007. Currently both codes are capable of simulating ohmic heating schemes of various equilibrium settings.

During the visit of Irina Voitsekhovitch last September (2007) a robust transport model for COMPASS was developed for the ASTRA code, including the possibility of external heating. Simulations with externally calculated (ACCOMME, FAFNER) NBI heating and current drive were also successfully performed using both of these codes [3,4]. Even though such calculations are not automatically self-consistent, the transport models show reasonable behavior, and it can be foreseen that once the modules for NBI heating currently being developed at CEA for CRONOS are satisfactorily finished, self-consistent predictive simulations of NBI heating on COMPASS with CRONOS will be possible on a routine basis.

Fig. 1 shows an example calculation of the ion and electron temperature profiles calculated by the ASTRA code using the transport model developed with I.Voitsekhovitch for the SND equilibrium with  $I_p = 200$  kA,  $B_T = 1.2$  T and central electron concentration of  $3.5 \cdot 10^{19} \text{ m}^{-3}$  for co-NBI and counter-NBI each delivering 300 kW. The NB power deposition profiles were calculated using the FAFNER code [5-7].

In December 2007, Yves Peysson of the CEA staff has also made available to us the “Starwars” suite of lower hybrid (LH) toroidal ray-tracing (C3PO) and 3-D Fokker-Planck (LUKE) codes [8], which can simulate LH heating and current drive in a stationary state. This LH current drive module takes as an input an externally provided equilibrium, provided presently by the ACCOME code [9]. One of the results of the “Starwars” calculation are the LH power deposition and driven current density profiles.

Results from the “Starwars” module were compared with ACCOME LH results, and several conclusions about the COMPASS LH heating scheme became evident. The particularly unfavorable lower hybrid slow wave accessibility conditions at the foreseen Phase I level operating conditions ( $I_p=170$  kA,  $B_0=1.2$  T) indicate that rays travel around the plasma edge for a

long time before penetrating into the central plasma region with significant absorption near the edge, and the rays also show very stochastic behavior in COMPASS.

Presently there is an ongoing effort to incorporate the non-inductive current drive modules into CRONOS for the COMPASS configuration with promised help from CEA staff.

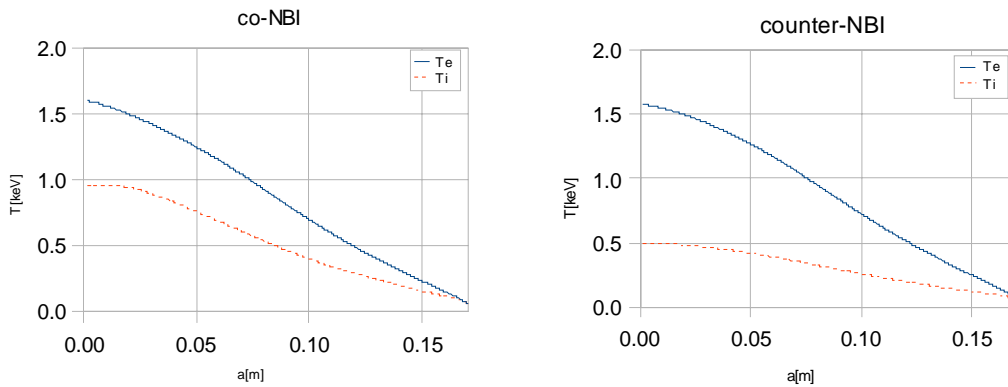


Fig. 1. Ion and electron temperature profiles calculated by the ASTRA code for the SND equilibrium with  $I_p=200$  kA,  $B_1=1.2$  T and central electron concentration of  $3.5 \cdot 10^{19} \text{ m}^{-3}$  for the co-NBI and counter-NBI each at 300 kW.

## References:

- [1] G. V. Pereverzev and P. N. Yushmanov: *ASTRA - Automated System for Transport Analysis*, IPP Garching report IPP 5/98, February 2002.
- [2] V. Basiuk, J. F. Artaud, F. Imbeaux et al.: *Nucl. Fusion* **43** (2003) 822.
- [3] V. Fuchs, I. Voitsekhovitch, O. Bilyková et al.: *33rd EPS Conf. Proceedings, ECA*, **30I** (2006) 1.103.
- [4] O. Bilyková, V. Fuchs, R. Pánek et al.: *Czech. J. Phys.* **56B** (2006) B24-B30.
- [5] G. G. Lister: *A fully 3D neutral beam injection code using Monte Carlo methods*, Max-Planck-Institut für Plasmaphysik Technical Report IPP 4/222, 1985.
- [6] A. Teubel and F. P. Penningsfeld: *Plasma Phys. Control. Fusion* **36** (1994) 143.
- [7] J. Urban, V. Fuchs, R. Pánek et al.: *Czech. J. Phys.* **56B** (2006) B176-B181.
- [8] J. Decker and Y. Peysson: *On Self-consistent Simulation of Lower-Hybrid Current Drive*, 33rd EPS Conference on Plasma Physics, Roma, Italy, June 19-23, **30I** (2006).
- [9] K. Tani and M. Azumi: *J. Comput. Phys.* **98** (1992) 312.

# III TECHNOLOGY

## OVERVIEW OF TECHNOLOGY TASKS

In the Association EURATOM-IPP.CR, research for the technology tasks is focussed on properties of various diagnostic and structural elements and materials of future thermonuclear reactors, both before and under neutron irradiation. Two irradiation sites are available for this purpose: the light water experimental fission reactor LVR-15 (operated by NRI plc), and the isochronous cyclotron U-120M with the maximum proton energy of 37 MeV (operated by NPI ASCR). Both institutes are members of the Association EURATOM-IPP.CR and their facilities are located in Řež research site about 20 km north of Prague.

The technology research in the Association EURATOM/IPP.CR covered the following areas in 2007:

- **Tritium Breeding and Materials**
  - **Breeding Blanket**
  - **Materials Development**
- **Physics Integration**
  - **TPDC Diagnostics - Ceramics**
- **Vessel/In Vessel**
  - **Blanket**

All the technology tasks are listed below; followed by a more detailed report on the progress in individual deliverables.

### **UT7\_IFMIF\_IPPCR\_NPI**

#### **Measurement of activation cross sections at neutron energies below 35 MeV. Data for Nickel.**

Field/Area: Tritium Breeding and Materials / Materials Development

Principal Investigator: P. Bém, Nuclear Physics Institute Řež

Co-authors: V. Burjan, M. Götz, M. Honusek, V. Kroha, J. Novák and E. Šimečková

In collaboration with: U. Fischer and S.P. Simakov, Association FZK-Euratom, Forschungszentrum Karlsruhe, Germany

Due date, 30.11.2007, status: completed

### **UT7-WELD-IPPCR-IAM**

#### **Development of new numerical macroelements method for distortion prediction of the big welded construction**

Principal Investigator: M. Slováček, IAM Brno

Field: Vessel/In-Vessel

Collaborative staff: L.Vlček, PhD.

**UT 2007 PFW\_IPPCR\_NRI****Establishing of a specialized laboratory for handling, manipulations and analysis of Beryllium specimens (e.g. Be coated PFW mock-ups)**

Principal Investigator: Vl. Masařík, NRI, Řež

Field: Vessel /In Vessel, Area: Blanket, Materials

Coordinated by NRI staff: Vl. Masařík, T Klabík, J. Hájek

**UT7\_SURF\_IPPCR\_IPM1****Structure and phase composition of surfaces of materials modified by plasma treatment**

Field/Area: Tritium Breeding and Materials/ Materials Development

Principal Investigator: Oldřich SCHNEEWEISS, Institute of Physics of Materials, Brno

Co-authors: Jiří BURŠÍK, Jiří ČERMÁK, Petr KRÁL, Pavla ROUPCOVÁ

Due date, status: 2007, completed

**IPP-CR\_UT7\_DEGR\_IPM2****The Eurofer steel: microstructural degradation and embrittlement**

Field/Area: Tritium Breeding and Materials / Materials Development

Principal Investigator: I. Dlouhý, Institute of Physics of Materials AS CR, Brno

Co-authors: H. Hadraba, V. Kozák, P. Čupera, Z. Chlup

Due date, status: 2007, completed

**TW6-TVV-SYSEG****Assessment of PSM Welding Distortions and Field Welding**

Principal Investigator: M. Slováček, IAM Brno

Field: Vessel/In-Vessel

Collaborative staff: L.Vlček PhD.,V. Diviš, M. Slováček,PhD.

**TW3-TVB-FWPAMT****Mechanical Testing of PFW panel attachment system**

Contract: FU06-CT 2004 – 00061, EFDA/04-1137

Field/Area: Vessel / Mechanical Structures

Principal Investigator: Vladislav Oliva, CTU in Prague - FNSPE Prague

Co-authors: Aleš Materna (FNSPE Prague), Jaroslav Václavík (ŠKODA Výzkum Ltd., Pilsen)

In collaboration with: P. Lorenzetto, A. Furmanek, EFDA- CSU, Garching

Revised due date: 31. 12. 2007

Status: completed

**IPP-CR\_TW4-TVB-TFTEST2, 1****Thermal fatigue testing of PFW mock-ups at high heat flux conditions.**

Principal Investigator: T. Klabík, NRI, Řež

Field: TV – Vessel in Vessel, Area: TVB Blanket

Collaborative staff: Vl. Masarik, P. Hájek, O. Zlámal

In collaboration with: P.Lorenzetto, F4E, Barcelona, Spain

**IPP-CR\_TW6-TTMS-003, D5****Study of fatigue and crack propagation issues of EUROFER in liquid Pb-Li.**

Development and testing cold traps, high temperature flanges and circulation pump for the liquid metal Pb-Li loop

Principal Investigator: Vl. Masarik, NRI, Řež

Field: Tritium Breeding and Materials, Area: Breeding Blanket

Collaborative staff: L. Kosek, J. Berka, M. Ruzickova, M. Zmitko, K. Splichal

#### **IPP-CR\_ TW6-TTMS-003, D5**

##### **Development of design of Pb-Li auxiliary system for HCLL TBM.**

Evaluation Pb-Li compatibility of EUROFER samples coated by Al and Er<sub>2</sub>O<sub>3</sub> layers under higher temperature conditions

Principal Investigator: K. Šplíchal, NRI, Řež

Field: Tritium Breeding and Materials, Area: Materials Development

Collaborative staff: L. Kosek, J. Berka, M. Zmitko

#### **IPP-CR\_ TW2-TTMS-003b, D4**

##### **Hydrogen compatibility and embrittlement issues of EUROFER weldments.**

EUROFER and Pb-Li melts testing under higher temperature irradiation conditions

Principal Investigator: K. Šplíchal, NRI, Řež

Field: Tritium Breeding and Materials, Area: Materials Development

Collaborative staff: J. Berka, M. Zmitko, V. Masarik, Z. Lahodová, L. Viererbl

#### **IPP-CR\_ TW2-TTMS-001, D3**

##### **Behaviour of EUROFER weldments in Pb-Li.**

Static and dynamic fracture toughness of plates and weldments at the transition irradiated up to 2.5 dpa at 200°C – 250°C

Principal Investigator: P. Novosad, NRI, Řež

Field: Tritium Breeding and Materials, Area: Materials Development

Collaborative staff: M. Falcnik, M. Kytka, K. Splichal

#### **TW7-8\_TTMN\_002B\_D6**

##### **Development of activation foils dosimeters for determination of IFMIF-relevant flux spectra: validation experiments.**

Experiments for the validation of Bi cross-sections up to 35 MeV in a quasi-monoenergetic neutron spectrum

Field/Area: Tritium Breeding and Materials / Materials Development

Principal Investigator: P. Bém, Nuclear Physics Institute Řež

Co-authors: V. Burjan, M. Götz, M. Honusek, V. Kroha, J. Novák and E. Šimečková

In collaboration with: U. Fischer and S.P. Simakov, Association FZK-Euratom,

Forschungszentrum Karlsruhe, Germany

Due date, 30.06.2008, status: in progress

## Measurement of Activation Cross Sections at Neutron Energies below 35 MeV, Data for Nickel

Principal Investigator: P. Bém, NPI AS CR, Řež

[bem@ujf.cas.cz](mailto:bem@ujf.cas.cz), tel. +420 266 172 105 (3506)

### Task: UT7\_IFMIF\_IPPCR\_NPI

Field: Vessel/In-Vessel

Collaborative staff: V. Burjan, M. Götz, M. Honusek, V. Kroha, J. Novák and E. Šimečková

In collaboration with: U. Fischer and S.P. Simakov, Association EURATOM-FZK, Karlsruhe, Germany

The neutron cross-section data of reactions at incident energies  $E_n > 20$  MeV are needed to improve the accuracy of neutronic calculations incorporated with various advanced nuclear-energy technologies. There are almost no experimental cross-sections data on Ni for neutron energies  $> 20$  MeV and only limited data exist for neutron energies  $< 20$  MeV [1]. In the following sections the quasi-monoenergetic  $p$ - ${}^7\text{Li}$  neutron source, the activation experiment on CrNi foils and the method of data evaluation are described. The resulting radioactive isotopes were studied by means of gamma spectroscopy methods. The preliminary analysis of measured activities was carried out by comparison of measured and predicted reaction rates. In the analysis, the neutron cross sections for different neutron reactions on Ni nucleus were taken from EAF 2007 library [1].

The target station of quasi-monoenergetic neutron source based on  ${}^7\text{Li}(p,n)$  reaction is described elsewhere [2] together with preliminary results of present work. The proton beam from isochronous cyclotron U-120M strikes the  ${}^7\text{Li}$  foil at four energies between 20 and 37 MeV. The carbon backing of the cooled Li foil serves as a beam stopper. The irradiated foils were placed at and above distance of 46 mm from the Li foil.

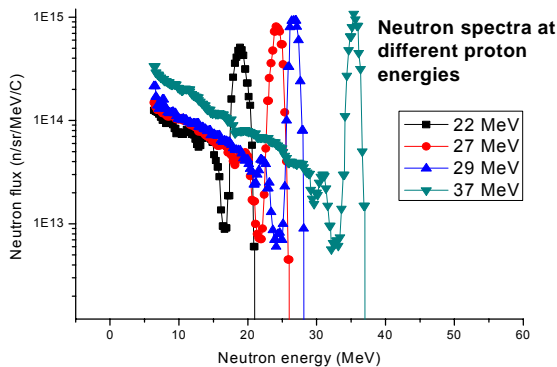


Fig. 1. Neutron spectra of the  $p$ - ${}^7\text{Li}$  source

To evaluate the neutron flux at sample positions, the spectral yield of source reaction  $p+{}^7\text{Li}(\text{C backing})$  were calculated using data from Ref. 3. The spectrum consists of quasi-monoenergetic part corresponding to the reactions to g.s. and 0.429 MeV states in  ${}^7\text{Be}$ , and of the low-energy tail generated a) by reactions on  ${}^7\text{Li}$  leading to further excited states in  ${}^7\text{Be}$  and b) reactions of protons on carbon stopper. Experimental data were taken at incident proton energies of 22.0, 27.2, 29.5

Tab. 1. Neutron reaction products, observed in present experiment

Reaction	Reaction product	$T_{1/2}$	Threshold (MeV)
$\text{Ni}58(n,3n)$	$\text{Ni}56$	6.077 d	22.857
$\text{Ni}58(n,2n)$	$\text{Ni}57$	35.60 h	12.432
$\text{Ni}58(n,nt+)$	$\text{Co}55$	17.53 h	21.517
$\text{Ni}58(n,t+)$	$\text{Co}56$	77.27 d	11.259
$\text{Ni}58(n,d+)$	$\text{Co}57$	271.97 d	6.051
$\text{Ni}58(n,p)$	$\text{Co}58$	70.86 d	0
$\text{Ni}60(n,t+)$			11.699
$\text{Ni}58(n,p)$	$\text{Co}58m$	9.04 h	0
$\text{Ni}60(n,t+)$			11.674
$\text{Ni}61(n,p)$	$\text{Co}61$	1.650 h	0.548
$\text{Ni}62(n,d+)$			9.057
$\text{Ni}60(n,2p)$	$\text{Fe}59$	44.503 d	10.490
$\text{Ni}62(n,\alpha+)$			0.450
$\text{Ni}58(n,p\alpha+)$	$\text{Mn}54$	312.3 d	6.424

and 37.5 MeV (neutron spectra peaking at 19.0, 24.3 26.6 and 35.6 MeV, respectively – see Fig. 1). The stacks of irradiated foils (NiCr and Au) were activated at two distances (46 and 86 mm) from the source target to test the effect of the flux-density gradient in the vicinity of neutron source. The Au foil was used as a "reference monitor" [3].

The time profile of the neutron source strength during the irradiation was monitored by the proton beam current, recorded by a calibrated current-to-frequency converter on PC. The typical beam current was about 3  $\mu$ A. The irradiation was carried separately with Li+C and C targets to investigate the contribution of neutrons from carbon stopper. The density of neutron flux at foil positions was approximately evaluated using the data of Ref. 3.

Irradiated samples were investigated by means of gamma-spectroscopy method. Two calibrated HPGe detectors of 23 and 50 % efficiency and FWHM of 1.8 keV at 1.3 MeV were used. Reaction products were identified on the basis of  $T_{1/2}$ ,  $\gamma$ -ray energies and intensities. Cooling times of gamma measurement ranged from minutes to approx. 100 day. (Each foil was measured at approx. 5 cooling times).

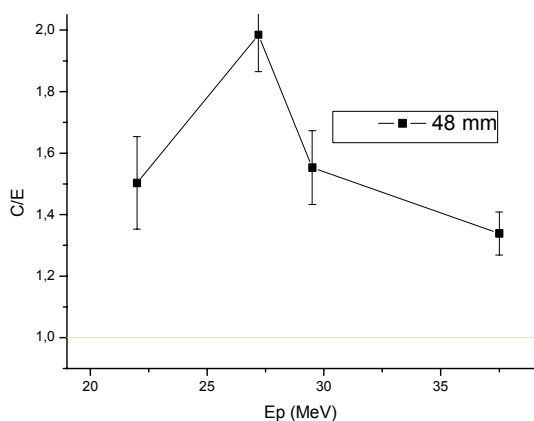


Fig3. C/E ratio for the reaction  $Ni58(n,p\alpha+)Mn54$

Up to 14 isotopes (see Tab. 1) were determined from measured activities. Experimental cross sections (derived from observed reaction rates) were compared with theoretical predictions based on the usual C/E ratio (C and E correspond to the calculated and experimental cross sections, respectively). In these calculations, theoretical cross sections were taken from EAF-2007 library [1]. In most cases, the deviation of C/E from unity clearly indicates the difference between experimental and predicted (EAF-2007 library) values of relevant neutron cross section.

As an example, the C/E ratios for the reaction  $Ni58(n,p\alpha+)Mn54$  ( $E_{th}=6.424$  MeV) are given in Fig. 1. As the preliminary conclusion, an upgrade of EAF-2007 library is needed [4,5].

This work was performed within the partial support of EFDA Technology Program and of the Ministry of Trade and Industry of CR.

### References:

- [1] R. A. Forrest, J. Kopecky, M. Pillon, K. Seidel, S. P. Simakov, P. Bém, M. Honusek and E. Šimečková, UKAEA Report, UKAEA FUS 526, 2005
- [2] P. Bém, V. Burjan, U. Fischer, M. Götz, M. Honusek, V. Kroha, J. Novák, S.P.Simakov, E. Šimečková, Neutron activation experiments on chromium and tantalum in the NPI p- $^7$ Li quasi-monoenergetic neutron field, Proc. on the Int. Conf. on Nuclear Data for Science and Technology 2007, Nice, April 2007, in print
- [3] Y.Uwamino et al., NIM A389 (1997) 463.
- [4] E. Šimečková, P. Bém, V. Burjan, U. Fischer, M. Götz, M. Honusek, V. Kroha, J. Novák and S.P.Simakov, Activation experiment on Cr in the NPI p-D2O white-spectrum neutron field, EUR 23235EN, pp. 35-39, [http://www.irmm.jrc.be/html/publications/technical\\_reports/index.htm](http://www.irmm.jrc.be/html/publications/technical_reports/index.htm),
- [5] M. Honusek, E. Šimečková, P. Bém, V. Burjan, U. Fischer, M. Götz, V. Kroha, J. Novák and S.P.Simakov, Benchmark tests of activation cross sections for Cr and Ni using the quasimonoenergetic neutrons below 35 MeV, *ibid*, pp. 39-43

## **Development of new numerical macro elements method for distortion prediction of the big welded construction**

*Principal Investigator: L.Junek, PhD. NPI AS CR, Řež*

[junekl@uam.cz](mailto:junekl@uam.cz), tel: +420-606 717 655

### **Task : UT7-WELD-IPPCR-IAM**

Field: Vessel/In-Vessel

Collaborative staff: L.Vlček, PhD.

*The manufacturing process of the Vacuum Vessel requires a lot of the welding operations. The weld joints are very long and contain a lot of welding passes. The local global approach is a new methodology for prediction of distortion of the large structure during welding assembly process. Each welding operations and weld joints generate residual distortions. The final distortion has to comply with the very strict manufacturing tolerances and requirements for final size and shape of the construction parts.*

The numerical computation of distortion by using local/global approach can be described by four following stages:

1. Typical welding joints on the structure are chosen and simulated by numerical analysis of local models. Total elastic-plastic deformations are computed as the results of local model computations
2. The global model which represents the whole welding structure is created
3. Only plastic deformations obtained on local models are transferred onto the global model as the load of global model
4. The structural elastic analysis of the global model including each welding joints is computed. The results of this part are distortion during and on the end of assembly process

Local models are usually computed by so-called transient method. This well known method describes the real moving heat source very sharply, but generally the solution is very time consuming. Now, improvement of local model solution is proposed and the whole idea is based on so-called macroelements or macro bead deposition (MBD). Due to the fact mentioned above the several experimental mock-ups have been done and also these experiments were numerically analyzed. These mock-ups represent one of the main types of welding joints using in real welding assembly process. The aim of this work is to compare between classical transient method and new method of macroelements.

Numerical method of welding solution by macroelements or macro bead deposit (MBD) consists of the same steps as in the case of classical or transient method. It covers thermal calculation followed by mechanical analyses. The main difference of MBD is in temperature analyses. In the case of transient analyses the heat flux into the material is defined by mathematical model of heat source, which is depended on location of its space coordinates and time. To the contrary MBD inserts the whole fictive temperature, which is needed for welding one bead, into the material volume representing the whole bead. Next, inserted heat is distributed by heat conductivity between melting metal and base material in user defined time steps. Number of time steps depends on welding velocity and the length of bead. Finally, time step (or steps) has to be chosen in order to melt through the real thickness of material. The MBD does not require very fine mesh in melt area and that is why the computational time is reduced in comparison with classical transient method. The MBD has been used in order to verify the process of “right” fictive temperature input in to the bead volume. In parallel different time steps and numbers of macroelements have been tested.

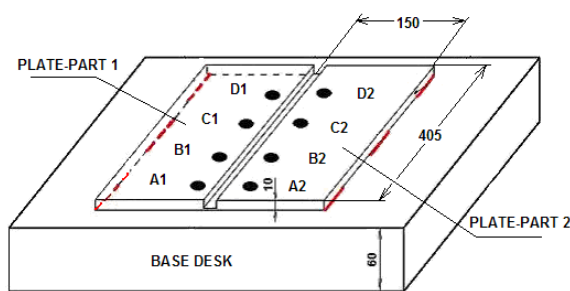


Fig.1 Experimental model of plate

At first, the variant of plate welding with totally fixed edges has been solved. On the base of our results it can be said that there are no significant difference when the different numbers of macroelements have been used. This fact results from the short length of each bead (approximately 400 mm). Finally, the whole deposit of weld

material corresponded to one bead has been described by one MBD in the same time.

Inserting of temperature into the whole beat is the fastest computational variant. It can be seen very good agreement between measured and computed values of shrinkage. Size and shape of plastic deformation spread in the material is nearly the same as in transient analysis. This fact is very important mainly because of real residual stress distribution after welding and releasing.

No. bead	shrinkage [mm]							
	Section A1-A2		Section B1-B2		Section C1-C2		Section D1-D2	
	M	C	M	C	M	C	M	C
1	0,32	0,43	0,50	0,49	0,59	0,49	0,40	0,44
2	0,82	0,90	1,08	1,00	1,17	1,00	0,94	0,92
3	1,52	1,43	1,62	1,55	1,74	1,55	1,52	1,46
after releasing	1,57	1,44	1,62	1,56	1,74	1,56	1,53	1,46

Tab.1: Measured (M) and computed(C) shrinkage

As results from performed analyses very good agreement was observed between experiments and numerical calculations. Moreover, the new MBD method is very promising and power tool for numerical analyses of large welded structures, which consider many beads. The total fictive temperature is defined on the base of temperature measurement by thermocouples and melting zone size. On the base of performed mock-ups and their numerical analyses it can be said, that MBD method reduces computer time very significantly, while numerical outputs has the same quality as in the case of classical transient method. MBD method should be used for numerical simulations of complicated structures.

### References:

- [1] Diviš V., Slováček M., Evaluation of welding distortion of VV poloidal segment, stage 1: Validation of method, experiments, October 2004, IAM Brno 3616/04
- [2] Collective of authors, Material characteristic of AISI 316 LN steel, Material database in electronic form
- [3] Labanti M., Martignani G., Minoccaro G.L., Ricci A., High temperature tensile tests on AISI 316 LN cast and forged stainless steel, ENEA report, IMAP-14011-R-001, Bologna, Italy, 2002

## Establishing of a specialized laboratory for handling, manipulations and analysis of beryllium coated PFW mock-ups

Principal Investigator: Vl. Masařík, NRI, Řež

[mas@ujv.cz](mailto:mas@ujv.cz), tel: +420-26617-2453

**Task:** UT 2007 PFW\_IPPCR\_NRI

**Field:** Vessel /In Vessel, Area: Blanket, Materials

**Collaborative staff:** Vl. Masařík, T Klabík, J. Hájek

*The main objective is commissioning and operation of a dedicated workplace for handling and manipulations with beryllium coated Primary First Wall (PFW) mock-up specimens. This workplace needs to be operated to fulfill requirements for safe handling beryllium to minimize health hazard of the involved personnel. This workplace will be used for preparation and realization of the thermal fatigue tests under the framework of the EFDA technology programmes (EFDA tasks TW3-TVB-INPILE, TW4-TVB-TFTEST2 and TW6-TVM-TFTEST).*

The Beryllium laboratory for handling and manipulations with Be coated PFW mock-up specimens needs to be commissioning and operating in accordance with the requirements of the health and safety authorities.

In the last period the following activities have been performed:

- Establishing of the certified Beryllium workplace approved by the state health and safety authorities; for this reason necessary documentation has been prepared, including the elaboration of the Safety Report, Limits and Conditions of the Laboratory Safe Operation, the Emergency Plan, the Personnel Monitoring Plan, etc.
- Application of the Quality Assurance and Quality Control system at operation of the Be workplace. These include the elaboration of the Working Procedures, personnel training, personnel entrance/exit checking, utilization of personnel protection tools, etc.



Fig 1. Laboratory for handling and manipulation with beryllium coated specimens

- Installation and testing of the beryllium workplace air-conditioning system, including setting of underpressure in the room, HEPA filters performance, checking, replacing and monitoring.

- Necessary adaptation of the PFW mock-up specimens to be used for testing by drilling, grinding, polishing.
- Assembly of the preliminary PFW dummy specimens for qualification test.
- Realization of the qualification test consisting of thermal cycling of dummy specimens.
- Dismantling of the PFW dummy specimens from the test rig after completion of the qualification test.

**References:**

- [1] Technical documentation for beryllium workplace: air-conditioning, cooling, and electrical system, 2007
- [2] Working Manual for Beryllium Workplace, NRI Internal Report (in Czech), 2006

## Structure and phase composition of surfaces of Eurofer 97-2 modified by plasma treatment

Principal Investigator: O. Schneeweiss, IPM AS CR, Brno

[schneew@ipm.cz](mailto:schneew@ipm.cz), tel: +420 532290434

### **Task:** IPP-CR\_UT7\_SURF\_IPM1

**Field:** Tritium Breeding and Materials, **Area:** Materials Development

**Collaborative staff:** Jiří Buršík, Jiří Čermák, P. Král, P. Roupcová

*The motivation of this study was investigation behaviour of the Cr<sub>2</sub>O<sub>3</sub> coating prepared by plasma spraying and its interface with the EUROFER substrate in the dependence on the conditions of heat treatments. Possible effect of tritium penetration was modelled by comparison of effect of surrounding atmospheres by annealing. The detailed structure investigations were focused on stability of both the EUROFER substrate and the Cr<sub>2</sub>O<sub>3</sub> coating during the annealing in range 550-750 °C in argon and hydrogen. No gradients of chemical composition of metallic elements were found in the substrate near the coating by means of EDX analyses. The concentration curves of the main elements at interface Cr<sub>2</sub>O<sub>3</sub> layer/EUROFER measured by WDS show redistribution of manganese only. For samples annealed in argon, diffusion coefficients of manganese were calculated. The results showed that negative influence of the hydrogen as the surrounding atmosphere by the annealing at 750°C/100h occurred. It can be important drawback for an application of the Cr<sub>2</sub>O<sub>3</sub> coating due to expected tritium penetration.*

EUROFER steel is taken as possible structural materials in the programme of European Breeding Blanket Programme for the DEMO design. Its properties were already described, e.g., in [1]. Further research has been focused on corrosion and optimising tritium recovery cycle. Coatings which would form barriers protecting EUROFER from a direct lithium lead contact were taken into account [2]. The problem is still open because increase of the steel temperature in contact with the lithium lead increases the tritium penetration towards He-coolant.

Research on Al based permeation barriers from the side of lithium lead exhibited some problems with applications of these coatings [2,3]. Therefore other kinds of barriers can be important. Cr<sub>2</sub>O<sub>3</sub> can be taken into account as good candidate from the point of view of reduced-activation characteristics of the irradiated EUROFER structures. Another point of view is operation of removing of the coating layer from the supporting steel structures at dismounting of the blanket.

The motivation of this study was investigation behaviour of the Cr<sub>2</sub>O<sub>3</sub> coating prepared by plasma spraying and its interface with the EUROFER substrate in the dependence on the conditions of heat treatments. Possible effect of tritium penetration was modelled by comparison of effect of surrounding atmospheres - argon and hydrogen – by the annealing. The material used for preparation of the substrate is the European reference steel EUROFER 97 produced by Böhler Edelstahl company. Its chemical composition is given in table 1. The surfaces of the samples were ground by mechanical grinding. Before the plasma spraying the surface was cleaned once more by standard industrial procedure using sand jet. Subsequently thermally sprayed Cr<sub>2</sub>O<sub>3</sub> coating was deposited by Ar+H<sub>2</sub> gas stabilized plasma torch.

The structure of the original state of the ingot was characterized in details by x-ray diffraction (XRD), Mössbauer spectroscopy, optical and electron microscopy. The specimens

were cut using spark erosion and the surfaces were ground and subsequently coated by chromium oxide using plasma spraying using a standard industrial technology procedure. The phase composition of the as-deposited coating was checked by XRD and characterized by means of analytical scanning electron microscopy. That includes overall microstructure characterization and EDX analyses of existing phases in various regions of coating/substrate system.

In the next step, heat treatment modelling exploitation conditions were performed with the aim to study influence of temperature and the surrounding atmosphere. For this purpose the coated samples were annealed in various regimes (at three temperatures - 550, 650, and 750 °C for 100 hours - and in two types of surrounding atmosphere - either argon or hydrogen).

For conclusions we can summarize following results:

1. Structure of both the substrate and the coating are stable during the annealing in range 550-750 °C in argon and hydrogen.
2. The microstructure of plasma sprayed layers shows a variety of layering and stacking of the coatings. From the plan view of the inner surface of peeled off coating it is seen that some powder particles did not completely melt during spraying. Analysis of the microstructure shows that the bonding between the EUROFER substrate and coating is very good especially at lower applied annealing temperatures. Annealing at 750 °C in hydrogen deteriorates the quality of bonding between substrate and sprayed layer. Chemical composition of the coating is inhomogeneous and this is not smeared out by applied thermal treatment. Large Al-rich particles were found frequently at the interface in annealed samples. No gradients of chemical composition of metallic elements were found in the substrate near the coating by means of EDX analyses.
3. The concentration curves of the main elements at interface Cr<sub>2</sub>O<sub>3</sub> layer/EUROFER measured by WDS show redistribution of manganese only. Concentration changes of other elements (Cr, O, V, W, Ta) are insignificant. This result is not valid for sample annealed at 750°C/100h in hydrogen where de-cohesion between L and E along large areas of L/E interface was found. We suppose that hydrogen promotes both a creation of C- and Mn-rich interlayer at L/E interface and the L – E de-cohesion.
4. Diffusion coefficients  $\tilde{D}_{Mn}$  were calculated for samples annealed in argon only. Obtained value of  $\tilde{D}_{Mn}$  at 750 °C agrees very well with known diffusion coefficient  $D_{Mn}^{aFe}$ . Other diffusion coefficients  $\tilde{D}_{Mn}$  (at 650 and 550°C) are higher than  $D_{Mn}^{aFe}$ . This phenomenon is probably a consequence of Mn redistribution during plasma deposition of Cr<sub>2</sub>O<sub>3</sub> layer. Reliable values of  $\tilde{D}_{Mn}$  at 650 and 550°C should be obtained from redistribution curves that would be measured after much longer anneals.
5. Negative influence of the hydrogen as the surrounding atmosphere by the annealing at 750°C/100h was observed. It can be important drawback for an application of the Cr<sub>2</sub>O<sub>3</sub> coating due to expected tritium penetration.

#### References:

- [1] Tavassoli AAF, Alamo A, Bedel L, Forest L, Gentzmittel JM, Rensman JW, Diegele E, Lindau R, Schirra M, Schmitt R, Schneider HC, Petersen C, Lancha AM, Fernandez P, Filacchioni G, Maday MF, Mergia K, Boukos N, Baluc, Spatig P, Alves E, Lucon E, J. Nuclear Mater. 329 (2004) 257.
- [2] Boccaccini LV, Giancarli L, Janeschitz G, Hermsmeyer S, Poitevin Y, Cardella A, Diegele E, J. Nuclear Mater. 329–333 (2004) 148.
- [3] Smith DL, Konys J, Muroga T, Evitkhin V, J. Nucl. Mater. 307–311 (2002) 1314.

## The Eurofer steel: microstructural degradation and embrittlement

Principal investigator: Ivo Dlouhy, IPM AS CR, Brno, Czech Republic

e-mail: [idlouhy@ipm.cz](mailto:idlouhy@ipm.cz), tel.: +420 532 290 342, fax.: + 420 541 218 657

### Task: IPP-CR\_UT7\_DEGR\_IPM2

Field: Tritium Breeding and Materials, Area: Materials Development

Collaborative staff: Hynek Hadraba, Vladislav Kozak, Pavel Cupera, Zdenek Chlup

The utilization of the ferritic-martensitic reduced activation steel Eurofer'97 steels for in-vessel components of proposed fusion reactors is limited up to a temperature about 550°C. The long term exploitation of the steel at high temperatures leads to microstructural changes (see Fig. 1). The aim of the work has been to investigate the influence of thermal ageing on fracture properties of Eurofer'97 steel. The short time thermal ageing of two sheets with different thickness (14 and 25 mm) was simulated by step cooling treatment. For description of thermal ageing static and dynamic tensile tests and Charpy impact tests were performed.

The thermal ageing of Eurofer'97 steel was simulated by means of step cooling treatment: 650°C/1 h, 590°C/15 h, 575°C/24 h, 550°C/48 h and 520°C/72 h. The microstructural observations (light optical and scanning electron microscopy) before (as-received - AR) and after thermal ageing (step-cooled - SC) revealed no substantial differences in microstructural parameters. The microstructure of Eurofer'97 steel sheets was fully martensitic with equiaxed prior austenitic grains of diameter from 5 µm to 10 µm. The prior austenite grains were decorated by Cr-rich  $M_{23}C_6$  carbides.

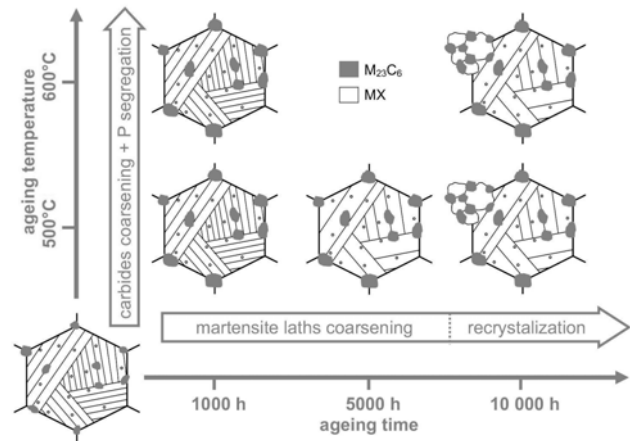


Fig. 1. Microstructural changes of Eurofer'97 steel after long term thermal ageing.

Basic mechanical properties of the

Eurofer'97 steel were investigated by means of static and dynamic tensile tests (see Table 1). Static tests were performed at room temperature and dynamic tensile tests were performed at room temperature and temperature near the  $t_{gy}$  transition temperature (-55°C and -75°C in the case of 25 mm and 14 mm sheet respectively) identified by means of impact tests. There was

difference in static and dynamic tensile properties between 14 mm and 25 mm sheets. The 14 mm sheet kept higher value of ultimate tensile strength ( $\sigma_{UTS}$ ), fracture stress ( $\sigma_{FR}$ ) and total elongation ( $\epsilon_T$ ) in comparison with 25 mm sheet. Also the small difference in dynamic tensile properties between 25 mm sheets in as-received and in step-cooled state was observed: the steel in as-received state kept higher value of ultimate tensile strength comparing to SC steel.

Sheet	temp.	$\sigma_Y$	$\sigma_{UTS}$	$\sigma_{FR}$	$\epsilon_T$
	[°C]	[MPa]	[MPa]	[MPa]	[%]
<i>static tensile properties (strain rate of 2 mm.min<sup>-1</sup>)</i>					
14 mm	RT	550	693	344	25
25 mm	RT	555	678	317	24
<i>dynamic tensile properties (strain rate of 1 m.s<sup>-1</sup>)</i>					
14 mm	RT	1219	1566	695	29.8
	-75	1783	1959	875	13
25 mm	RT	1199	1524	608	27.8
	-55	1600	1779	720	22.8
25 mm	RT	1172	1505	610	31.2
	-55	1548	1790	747	23.3

Table 1: Static and dynamic tensile properties of the sheets used.

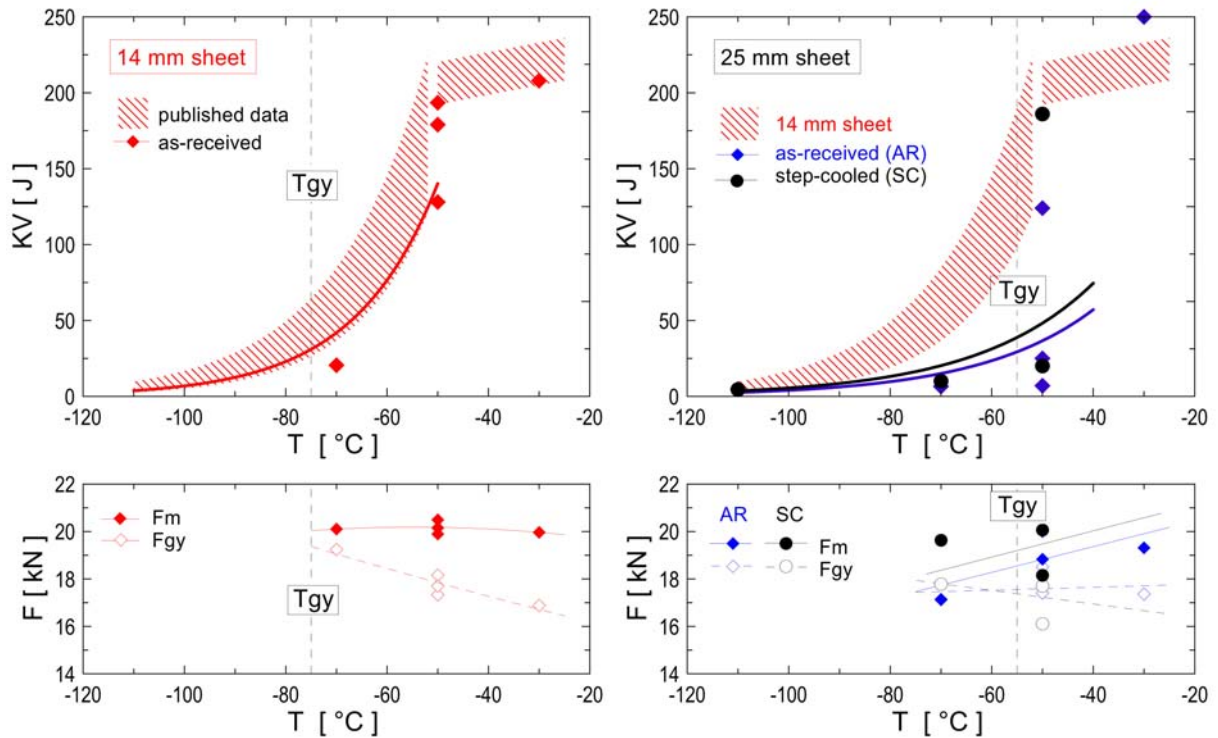


Fig. 2. Temperature dependencies of Charpy impact energy of Eurofer'97 steel (left 14 mm sheet, right 25 mm sheet, upper figures – temperature dependence of impact energy, bottom – temperature dependence of  $F_{gy}$  and  $F_m$ ).

The temperature dependence of impact energy for 14 mm and 25 mm sheet compared with values collected from literature is given in Fig. 2. It is evident that the fracture behaviour of 14 mm Eurofer'97 steel was comparable with published results. The  $t_{gy}$  transition temperature of 14 mm sheet was about  $-75^{\circ}\text{C}$ . The comparably different fracture behaviour of 25 mm sheet compared with 14 mm sheet was observed: the transition temperature  $t_{DBTT}$  and transition temperature  $t_{gy}$  were shifted for about  $+20^{\circ}\text{C}$ . No difference between temperature dependence of impact energy of 25 mm sheet in as-received state and in state after step-cooling was observed.

The cleavage mechanism of crack initiation and propagation in Eurofer'97 steel in as-received state and in step-cooled state under the conditions of brittle fracture (near  $t_{gy}$  transition temperature) was identified.

The results obtained by solving this project were published in the proceedings of workshop Fracture and Design of Materials (ISBN 978-80-254-0725-7, in Czech) held in Brno, Czech Republic, in October 31<sup>th</sup> – November 1<sup>th</sup> 2007 [1] and in the proceedings of 13<sup>th</sup> International Conference on Fusion Reactor Materials held in Nice, France, in 10<sup>th</sup> to 14<sup>th</sup> December 2007 [2].

The work will be followed by analysis of fracture behaviour of long isothermally aged (up to 5000 h) specimens. The results from this analysis were not available during preparation the report because of continuing thermal ageing exposition.

### References:

- [1] Hadraba, H., Dlouhy, I.: Thermal ageing of Eurofer'97 steel. Proceedings of workshop Fracture and Design of Materials, Brno (2007) 85-96, ISBN 978-80-254-0725-7.
- [2] Hadraba, H., Dlouhy, I.: Effect of Thermal Ageing on the Fracture Behaviour of EUROFER'97 Steel. Proceedings of 13<sup>th</sup> International Conference on Fusion Reactor Materials, Nice, France (2007) 659-671.

## Assessment of PSM welding distortions and field welding

Principal Investigator: L.Junek, PhD. NPI AS CR, Řež

[junekl@uam.cz](mailto:junekl@uam.cz), tel: +420-606 717 655

### **Task : TW6-TVV-SYSEG**

Field: Vessel/In-Vessel

Collaborative staff: L.Vlček PhD., V. Diviš, M. Slováček, PhD.

*The manufacturing of the vacuum vessel requires a lot of the welding operations. The weld joints are very long and contain a lot of welding passes. Each welding operations (weld joints) generate residual stresses (deformation) and distortions. The final distortion has to comply with the very strict manufacturing tolerances and requirements for final size and shape of the construction parts. Due to stated facts the three experimental mock-ups (VMO, LMVMO and VVPSM) have been done and also manufacturing process was numerically analyzed. The final welding technology can be proposed based on the obtained experimental and calculated experiences.*

The project was divided into three tasks. In the first task “Modification of VMO and LMVMO models” the VMO (Validation MOCk-up) and LMVMO (Local Model Validation Mock-up) final manufacturing processes were numerically simulated. VMO and LMVMO represented typical weld joints they are contained on VVPSM. The VMO mock up was done for narrow TIG gap welding technology qualification for 60 mm thick plate.

Weld joints on LMVMO	Measured [mm]	Calculated [mm]
Weld no.1	2,74	2,77
Weld no.2	10,82	9,74

The numerical parameters (size and shape of molten zone, input welding parameters, heat input), which were found out on VMO and LMVMO, were used for all narrow TIG automat weld joint and T-joint on VVPSM.

Tab.1 Comparison of results on LMVMP

The VVPSM full-scale mock-up has been

prepared and done in cooperation between Companies ANSALDO (Genoa, Italy) and SIMIC (Camerana, Italy). VVPSM is the full-scale model of the PS1 and PS2 parts of the vacuum vessel from austenitic steel AISI 316 LN ITER GRADE. The very good agreement between calculated and measured final shrinkage after welding were observed (Tab.1).

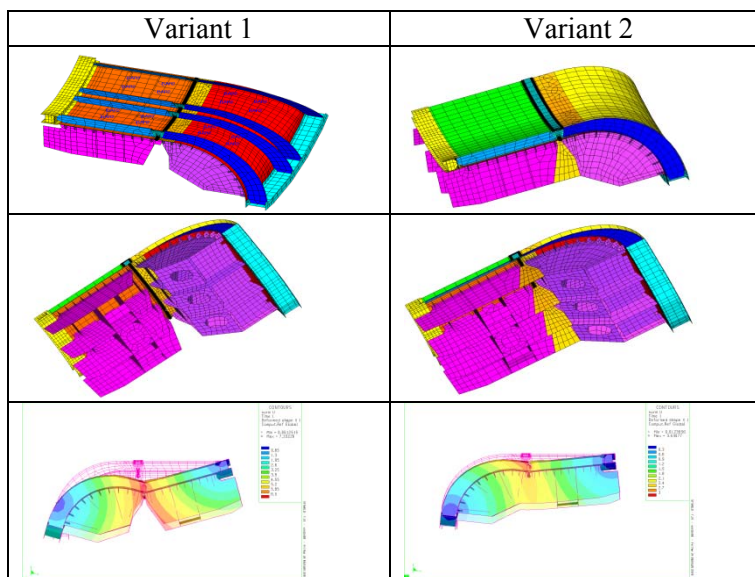


Fig.1 Variants of PS1 and PS2 weld connection

In the second task 2 “Weld joints optimization” the connection between PS1 and PS2 of VVPSM were numerically simulated. These welding joints are done as last assembly step and have got the big influence on the final distortion. The numerical optimization of the PS1 and PS2 weld joints was done and several modifications of the technology and construction stiffness were proposed (Fig.1). Based on the calculated results and internal discussion with

EFDA, IAM Brno, ANSALDO and SIMIC the modification of the welding technology and stiffness of the bracing tools were proposed. Based on the calculated results the welding technologies were modified.

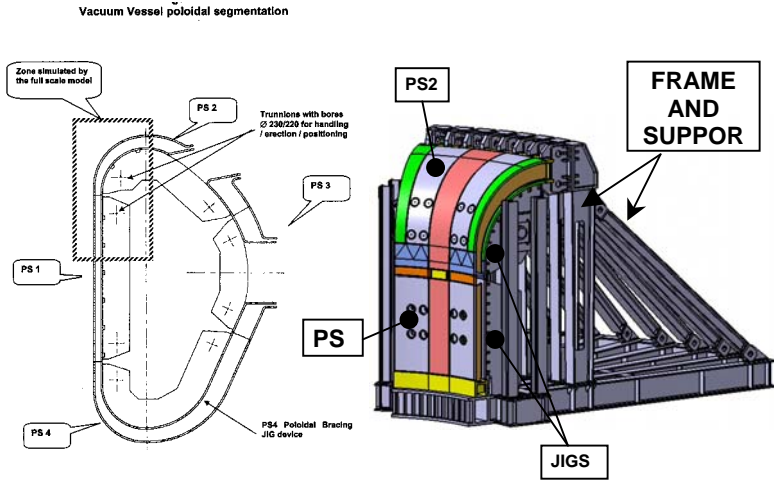


Fig.2 VV PSM mock-up

Continuing on the previous task 1 and 2 the third task “PS1 and PS2 of VVPSM, numerical analyses and results comparison” was done. VV PSM consists from two parts – PS1 and PS2. The numerical analyses of PS1 and PS2 manufacturing process and comparison between measured and calculated results were done. In this task PS1 and PS2 according to real welding fabrication process were numerically simulated. Macro

bead deposit method (MBD) and local-global method (LGA) for manufacturing distortion prediction were applied. Welding parameters from the task 1 for the numerical simulation of PS1 and PS2 were used. Results of numerical predictions (distortions and shrinkages) with distortion measurement on PS1 and PS2 were compared. On the basis of these comparisons, conclusions were done.

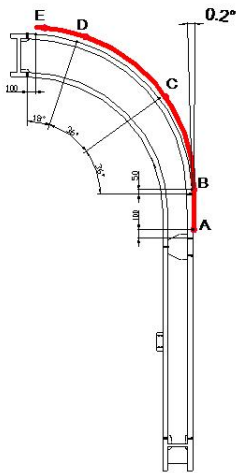


Fig.3 Comparison points

	$\Delta X$ [mm]		$\Delta Z$ [mm]	
	M	C	M	C
A	1	0,8	0	-0,8
B	3	3,0	0	-0,8
C	7	7,8	2	1,1
D	10	10,5	6	5,3
E	10	10,7	7	7,8

Fig.2 Comparison of measured (M) and calculated (C) results

**References:**

- [1] Slováček M., Diviš V.: Assessment of PSM Welding Distortions and Field Welding, *Task 1: Modification of VMO and LM VMO Models*, report IAM Brno, archive No. 4038 / 07, Brno, February 2007
- [2] Slováček M., Diviš V.: Assessment of PSM Welding Distortions and Field Welding, *Task 2: Weld joints optimization*, report IAM Brno, archive No. 4031 / 07, Brno, February 2007
- [3] Diviš V.: Assessment of PSM Welding Distortions and Field Welding, *Task 3: PS1 and PS2 of VVPSM, numerical analyses and results comparison*, report IAM Brno, archive No. 4082 / 07, Brno, June 2007

## Mechanical testing of a primary first wall panel attachment system (ITER)

Principal Investigator: V. Oliva, CTU in Prague – FNSPE, Prague  
[vladislav.oliva@fffi.cvut.cz](mailto:vladislav.oliva@fffi.cvut.cz)

### **Task: TW3-TVB-FWPAMT**

Field/Area: Vessel / Mechanical Structures

Collaborative staff: A. Materna (FNSPE Prague), J. Václavík (ŠKODA Research Ltd., Pilsen)

In collaboration with: P. Lorenzetto, A. Furmanek, EFDA- CSU, Garching

The delayed project from the year 2004 was completed. Following experiments were performed in Škoda Research Ltd. with the PFW panel to shield block attachment system of the key and key-way type: measurements of the preload relaxation in special connecting studs during prescribed long-term thermal cycling, fatigue tests under prescribed cyclic radial moment, cyclic poloidal force and cyclic poloidal moment. Finite element method was used for modeling of all fatigue experiments as well as for theoretical simulations of combined loads effects at CTU-FNSPE. The results have shown that the attachment system shows only small loss of the assembling studs preload, no loss of the desirable contact between the panel and shield block and no plastic deformation of contact surfaces. The simultaneous effect of poloidal moment and radial force during VDE represents the most dangerous case under study.

At the beginning of 2007, the massive panel (1100 x 250 x 50 mm) and shield block mock-ups from 316L SS steel were already made and also organization of the experiments was essentially proposed, verified by FEM simulations and provided from the technical and device point of view. After the obtaining of the special connecting studs (Ph 13-08 Mo martensitic steel) from EFDA, the following experiments were performed in Škoda Research Ltd, Pilsen according the Technical specification of the project [1]:

- Test on panel blind hole thread relaxation under thermal cycling (30 000 cycles from 100°C to 200°C). The drop of initial stud preload 111 kN with the number of cycles was measured,
- Mechanical test of the assembly panel-shield block under cyclic radial moment ( $\pm 24.5$  kNm), poloidal force ( $\pm 108$  kN) and poloidal moment ( $\pm 53$  kN, see Fig.1). The drop of the initial connecting stud preload (111 kN or 54 kN), plastic deformation of the key in panel or the key-way in shield block and the loss of the contact between both test objects were studied. All these tests were also simulated using finite element method at CTU in Prague - FNSPE.

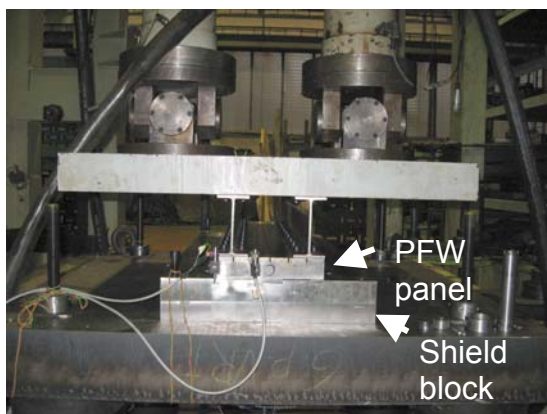


Fig. 1 Mechanical test of the panel to shield attachment system under poloidal moment

In addition to real experiments, the simulations of hypothetical experiments with off-normal events (Halo currents and VDNs) leading to the combined loads were performed in Feasibility study.

The major results of experimental and theoretical works can be summarized as follows [2]:

Thermal cycling between operation and room temperature leads to the drop of the studs preload. However, the residual preload 63 kN is still higher than the lower prescribed value for mechanical tests.

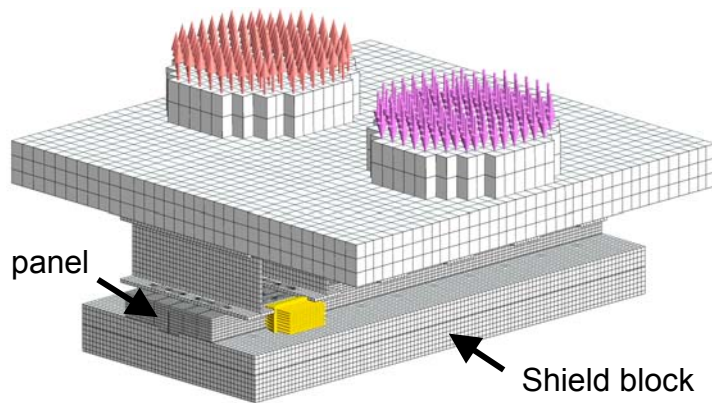


Fig.2 FE model simulating VDEs (poloidal moment + radial force + radial moment)

Load capacity in tension of the Spirallock thread in panel blind hole is higher than tensile force for the brittle fracture of the high-strength assembling stud. Formation of the gap already during the stud preloading process was observed below the panel lateral strips in two fatigue tests. The cyclic loading of the panel opens these gaps.

Both real and FEM experiments have shown that the panel to shield attachment system shows

no loss of the assembling studs preload, no loss of a vertical contact between the panel and shield block in the key way and no macro plastic deformation of contact surfaces under individual prescribed mechanical cycling even with the preload of only 54 kN. A small vertical gap in the key way was observed only under cyclic poloidal moment with the stud preload decreased to the very low value of 45 kN.

Hypothetical combination of the poloidal moment and radial force (Fig. 2) during VDE represented the most dangerous case under study. A comparison of these FEM results with the experimental results of individual performed fatigue tests predicts that VDE loads could lead to the loss of the contact between the panel and shield block in a key-way. The real extent of this phenomenon can be found out only experimentally. The additional experimental test on VDE loads is therefore recommended.

### **References:**

- [1] Lorenzetto P., Furnmanek A.: Mechanical Testing of a Primary First Wall Panel Attachment System, Technical Specification. Rep. No. EFDA/04-1137, EFDA-VP-SP-4.4. CSU EFDA Garching, 2007, 13 p.
- [3] Oliva V., Materna A., Václavík J.: Mechanical Testing of a PFW Panel Attachment System for ITER, Final Report. Rep. No. V-KMAT-706/07, Dept. of Materials, CTU in Prague - FNSPE, 2007, 152 p.

*This research has been supported by MŠMT grant No. OK 483 and MŠMT grant MSM 6840770021*

## Thermal fatigue test of beryllium coated primary first wall mock-ups

Principal Investigator: T. Klabík, NRI, Řež

[kla@ujv.cz](mailto:kla@ujv.cz), tel: +420 266 172 460

### **Task:** IPP-CR\_TW4-TVB-TFTEST2, 1

**Field:** TV – Vessel in Vessel, **Area:** TVB Blanket

**Collaborative staff:** Vl. Masarik, P. Hájek, O. Zlámal

**In collaboration with:** P.Lorenzetto, F4E, Barcelona, Spain

*The objective of this task deliverable is to perform thermal fatigue testing of actively cooled Primary First Wall (PFW) mock-ups. This involves designing the facility ensuring thermal fatigue tests of beryllium coated primary first wall mock-ups to compare the fatigue performance of different beryllium/CuCrZr alloy joints simulating Be coated PFW mock-up specimens. The main effort has been devoted to the development and testing of the suitable heat flux generation system. A long-term qualification test of graphite heating panel material has been performed. Qualification test has to prove the feasibility of equipment to achieved 20,000 thermal cycles with heat flux of approx.  $0.7 \text{ MW/cm}^2$  and resistivity of mock up specimens to thermal fatigue loading.*

The investigations have been focused on the development and testing of the suitable heat flux generation system. This activity has been performed both for this task and for the task TW3-TVB-INPILE, D3. The thermal fatigue tests of beryllium coated primary first wall mock-ups of dimensions 250 mm x 110 mm x 70 mm were used to compare the fatigue performance of different beryllium/CuCrZr alloy joints. The task shall consist of two test campaigns of 4 mock-ups, each tested in parallel. The tests shall be performed at  $0.8 \text{ MW/m}^2$  surface heat flux for a total number of 30,000 cycles each of about 300 s duration. The inlet water temperature shall be about  $120 \text{ }^\circ\text{C}$  with a water velocity of about 5 m/s. Ultrasonic testing should be performed on each mock-up to check the integrity of the Be/CuCrZr joints before starting the thermal fatigue testing, after 15,000 cycles and at the end of each test campaign of 30,000 cycles.



Fig. 1. Thermal fatigue loading equipment.

Several qualification experiments were suggested and tested. A long-term qualification test of graphite heating panel material has been performed using Be coated PFW mock-up specimens. A design of graphite heating panels has been introduced aiming at uniform heat distribution. The equipment will contain four PFW mock-ups situated in vertical position and will be filled with He gas (Fig. 1.). Electrically heated panels situated at a small distance parallel to beryllium surface are used to evoke required heat flux.

Heat flux on the PFW surface consists of heat radiation, helium gap convection and conductivity. Inductive method is used to heat-up the heating panels. The PFW mock-ups are

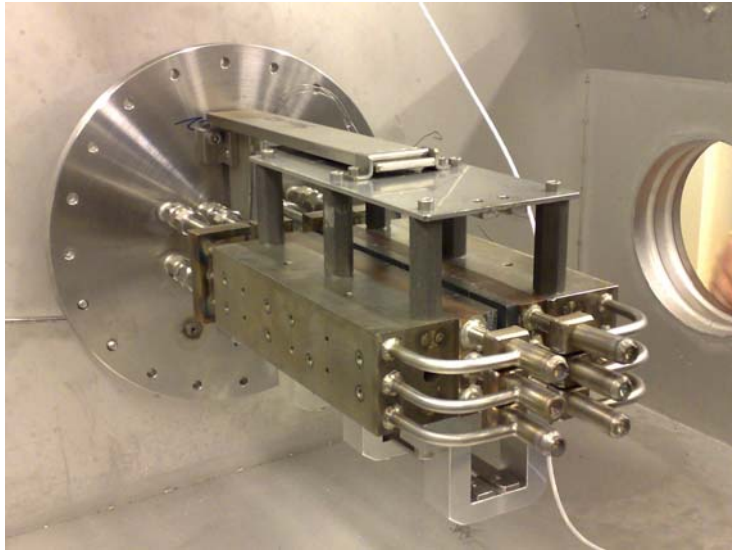


Fig. 2. Mock up specimens with cooling systems

connected in parallel (Fig. 2) and actively cooled using coolant water. Flow rate of the cooling water is controlled to specified Be/CuCrZr joint temperature range and is adjusted during a mock-up test using a special regulation valves and flow rate measurement. The rig include: one thermocouple located in the Be tile of each PFW mock-up, one thermocouple in Cu-alloy, monitoring of inlet and outlet cooling water temperature as well as electric power of each heating panel. A PC collects measured data. Contact detachment of one beryllium tile from a PFW mock-

up during thermal cycling is detected by control system to minimize the spread of contamination and to exclude conductive contact between the beryllium tile and any hot graphite surface. Ultrasonic testing should be performed on each mock-up to check the homogeneity of the Be/CuCrZr joints before starting the testing, after 12,000 cycles and at the end of loading.

Pre - test thermal fatigue experiments were performed with beryllium specimen and cooper specimen and 12 000 cycles was achieved. Homogeneity and output thermal on Be tile surface were evaluated and results correspond to required testing parameters and required lifetime conditions.

#### **References:**

- [1] T. Klabík, Vl. Masařík, J. Hájek, Kahle: Beryllium Laboratory Operating Safety Instructions, NRI Řež, April 2007
- [2] I. Buldra: Results of Mechanized Ultrasound Examinations of Beryllium Tiles – Copper Plate Interface of the PFW specimens, NRI Řež, November 2007
- [3] O. Zlámal, J. Hájek, J. Kysela: Calorimetry Report, NRI Řež, February 2008
- [4] Qualification Testing of ITER PFW mock-ups at the NRI BESTH Facility, NRI Řež – EFDA Garching, February 2008

## Static and dynamic fracture toughness of plates and weldments at the transition irradiated up to 2.5 dpa at 200°C – 250°C

Principal Investigator: P. Novosad, NRI, Řež

[nov@ujv.cz](mailto:nov@ujv.cz), tel: +420-26617-2456

### Task: IPP-CR\_TW2-TTMS-001, D3

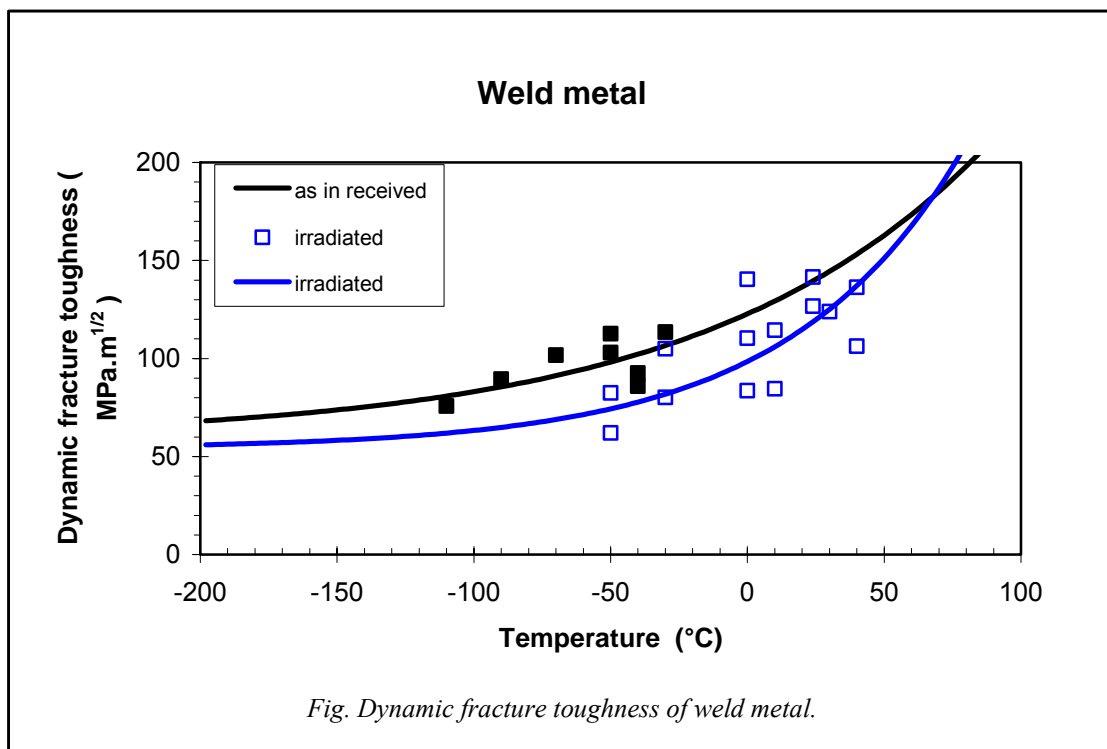
Field: Tritium Breeding and Materials, Area: Materials Development

Collaborative staff.: M. Falcnik M. Kytka, K. Splichal

Reduced activation ferritic and martensitic (RAFM) steels are considered as structural materials for the fusion reactor applications. At the present time experimental studies are focused on effects of neutron irradiation at lower temperatures 230° C on fractural properties of martensitic steel EUROFER 97 which was developed as a structural material for the first wall TBM (Test Blanket Module). Fracture toughness testing at the transition temperature should be performed and static and dynamic fracture toughness should be evaluated in as received state and after irradiation.

Static and dynamic toughness at the transition temperature of plates and weldments are measured at room temperature and the temperature of about 250°C with KLST sub size specimens 4 x 3 x 27 mm. Neutron irradiation was performed at the temperature of 235° C up to neutron dose of 2.5 dpa. Böhler Bleche GMBH manufactured plate IMF I-E 14 of EUROFER 97 steel from Heat E 83698. EUROFER segment No 4/15 was cut and steel sample plate 330 x 300 x 14 mm was delivered to NRI by Forschungszentrum Karlsruhe.

For dynamic fracture toughness testing, the cells have been equipped with a Tinius Olsen Model 74, Zwick RKP450 and RKP50 impact test machines, instrumented with data acquisition and analysis system. The equipment has been fitted with a resistance furnace and a cooling box working with liquid nitrogen for test temperatures from -170° C to +310° C. For fatigue pre-cracking of the specimens, Alfred J. Amsler model 421 machine of 20 kN



capacity is used. Static fracture toughness samples are measured using INSTRON tensile testing machine, PC control stations using Instron's software control their function. This standard equipment was tailored for hot-cell operation by adding stainless steel pull rods and opening furnaces and cooling boxes (operated by manipulators) of NRI's own design. The heating and cooling system covers test temperatures from -170 °C to +310 °C. During the tests, the load point displacement is measured by LVDT transducer gauges mounted on pull rods outside the furnace or cooling box.

Irradiation experiment was performed in Chouca rig at the temperature of 235°C with fast neutron flux  $4.4 \cdot 10^{13} \text{ cm}^{-2} \text{ s}^{-1}$  under He atmosphere of 100 kPa. The temperature and He pressure are online monitored. Total irradiation time from the beginning of the experiment was 11,246 hours, total reactor work about 96,924 MWh and total radiation level about 2.51 dpa.

Testing of dynamic fracture toughness was finished and the transition temperature curves of base and weld metals in as received state and after irradiation at the temperature of 235°C were evaluated (Fig. 1).

**References:**

- [1] M. Falcnik, Kytka M., Laboratory Report 2007/ 37, NRI, 2007
- [2] E. Lucon, M. Decreton, E.van Walle, Mechanical characterization of EUROFER 97 irradiated (0.32 dpa, 300°C), J, Nucl. Mat., 2004

## Development and testing cold traps, high temperature flanges and circulation pump for the liquid metal Pb-Li loop

Principal Investigator: Vl. Masarik, NRI, Řež

[mas@ujv.cz](mailto:mas@ujv.cz) , tel: +420-26617-2456

**Task:** IPP-CR\_TW6-TTMS-003, D5

**Field:** Tritium Breeding and Materials, **Area:** Breeding Blanket

**Collaborative staff:** L. Kosek, J. Berka, M. Ruzickova, M. Zmitko, K. Splichal

*This task will be focused on development and testing of key components for the Pb-Li liquid metal loop of the design of Helium Cooled Lithium Lead (HCLL) Test Blanket Module (TBM). Based on the previous design studies of Pb-Li auxiliary system the following components are to be developed, in particular cold traps, high temperature flanges and a circulation pump. Development of these components has to be performed by their testing in Pb-Li liquid metals. The aim is to verify their feasibility and operation performance in terms of cold traps purification efficiency, flanges reliability and manipulation and mechanical pump feasibility.*

During the TBM operation corrosion products of structure materials and different impurities will be formed and accumulated in the Pb-Li auxiliary circuit, and the necessity of their removal will arise. For this reason, an appropriate Pb-Li purification system needs to be proposed and designed. Also, special high temperature flanges for liquid metal pipelines allowing connection and disconnection in an inert gas need to be developed and their operational performance tested in relevant Pb-Li auxiliary system conditions. In addition, a suitable liquid metal circulation pump needs to be developed and its performance tested.

Testing of the developed components is to be performed in Pb-Li liquid metal with flow rate of 5-30 mm/s at the temperature of 260-500°C.

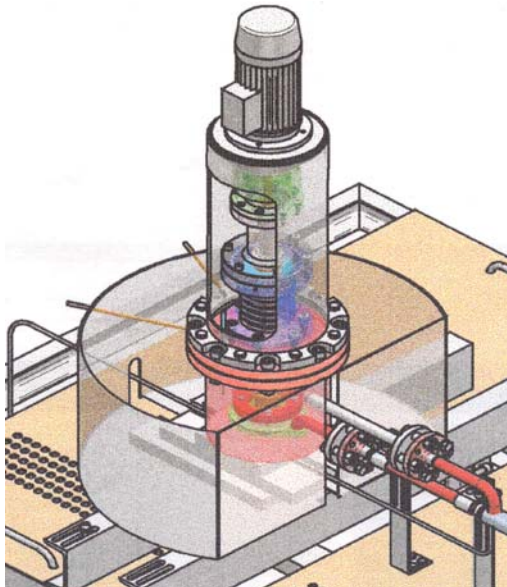
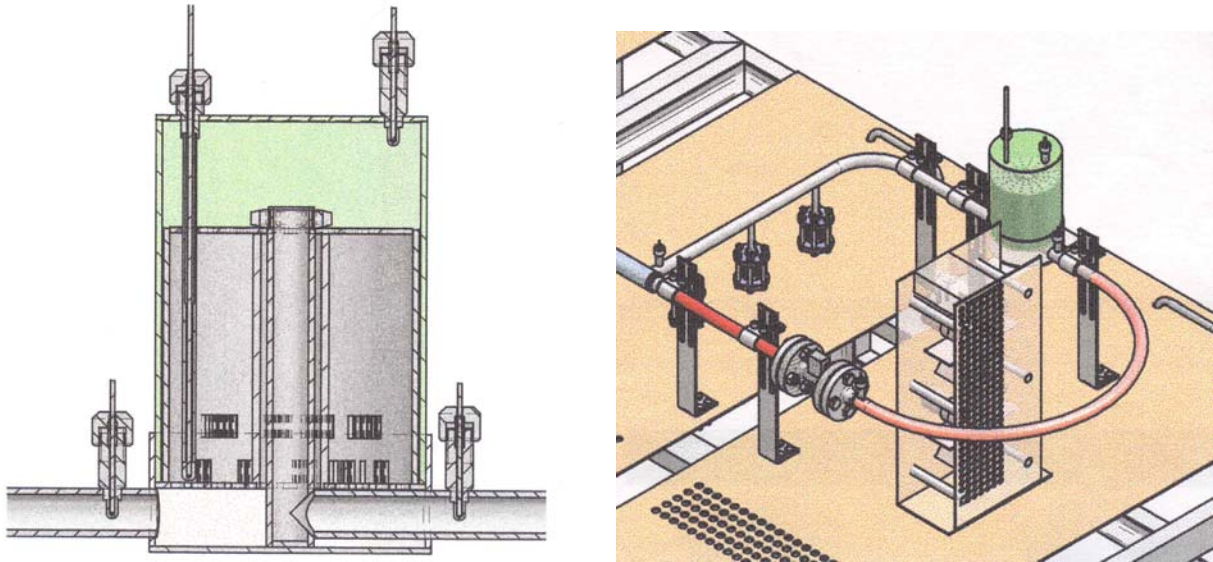


Fig. 1 Pb-Li loop circulation pump.

Cold trap purification procedures are to be investigated to remove typical corrosion products (CPs) and impurities from Pb-Li liquid metal. For this reason model experiments will be carried out with two eutectic heats, which will simulate liquid metal mixture: The first one with higher content of CPs Fe, Cr, Mn, the second one with certain content of Bi as the main element of impurities. Purification experiment with Bi has to be assessed in terms of thermodynamic data and melt temperature of intermetallic compounds and eutectic systems.

Implementation of the suggested testing is to be revised. Two cold traps for CP removing will be tested: one with wire mesh corresponding to the higher specific area of cooling surface and the other one with rigs corresponding to the lower specific area. The cold trap will be tested with lower and higher melt flow rates. The high temperature flanges will be investigated.

Manipulation involves assessments of disassembly, dismantling of bellows systems, testing of displacement mechanisms, evaluation of sealing surface conditions and handling. A mechanical type circulation pump will be designed and verified under testing conditions. The characteristic parameters will be evaluated.



*Fig. 2. Pb-Li cold trap and loop cold part.*



*Fig. 3. Pb-Li loop Meliloo.*

Two testing cycles were performed in the last year. During the first cycle a leak in the weld joint of the cold trap vessel was proved. In the second cycle a small defect in the area of lower part of the mechanical pump was indicated. The corrective actions were performed and tightness of metal loop was proved. Verifications of operational parameters continue after assembling of the Pb-Li loop.

**References:**

- [1] J. Hájek, V Richter, M Zmitko, Pb-17Li Auxiliary and purification systems: Design of the auxiliary Pb-Li loop for Helium, NRI 12096, 2004

## Evaluation Pb-Li compatibility of EUROFER samples coated by Al and Er<sub>2</sub>O<sub>3</sub> layers under higher temperature conditions

Principal Investigator: K. Šplíchal, NRI, Řež

[spl@ujv.cz](mailto:spl@ujv.cz), tel: +420-26617-2456

**Task:** IPP-CR\_TW6-TTMS-003, D5

**Field:** Tritium Breeding and Materials, **Area:** Materials Development

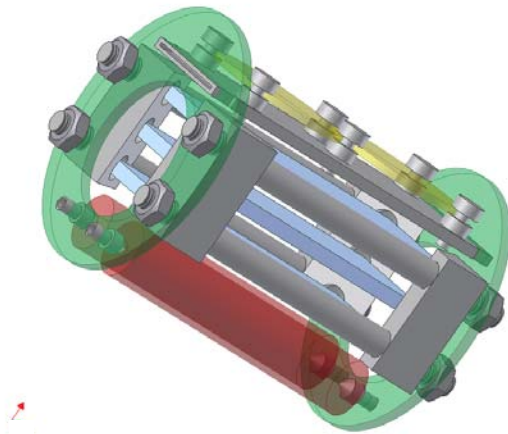
**Collaborative staff:** L. Kosek, J. Berka, M. Zmitko

*Under Test Blanket Module operation conditions sufficient corrosion resistance and limitation of tritium penetration through EUROFER steel are required. Several types of anti-corrosion and/or tritium anti-permeation coatings on EUROFER steel were selected. The main objective of experimental works is investigation of the coatings compatibility with Pb-Li liquid metal and their corrosion resistance. The investigation will evaluate kinetics of the coating thickness, mechanism of interaction of eutectic melt with coating layers, microstructure and chemical composition of layers and characterization coating - base metal bonding.*

The liquid metal loop available in NRI Rež will be used as a facility for corrosion and compatibility testing in real Test Blanket Module (TBM) conditions. Different types of coating layers should be investigated. They include erbium oxide, Al coating (electrochemical deposition process), W plasma spraying technique. The coatings have to ensure required properties of protective barriers under long-time exposure at higher temperatures.

The corrosion and compatibility test will be performed at 550°C in flowing Pb-15.7Li eutectic with anti-corrosion and tritium anti-permeation coatings at 550°C in flowing velocity

in the range of 1-10 cm/s in long-term exposure up to 5,000 hours. Cold trap in the loop circuit should enable to remove impurities in particular corrosion products release, from Pb-15.7 Li melts. Rectangular samples will be used and coating layers of various thicknesses will be investigated. The experimental investigations are discussed with Forschungszentrum Karlsruhe and IPP Garching. Two types of specimens with Al coating should be prepared in FZK. The cylindrical Ø of 8 mm, length of 40 mm and flat 20 x 40 mm x 1.5 mm were



suggested. The specimens of Ø 20 mm and thickness 2 mm with erbium oxide will be prepared in IPP. A new holder of specimens (Fig.) was designed to improve the manipulation of specimens during the experiments in Pb-Li loops.

According to TBM task changes it is foreseen that two types of coating layers will be only prepared and subsequently tested in the liquid metal loop: a) specimens with erbium oxide (IPP Garching), b) specimens with Al coating (Forschungs-zentrum Karlsruhe). The start up of Pb-Li operation is delayed due to defects that were indicated in weld joints of the pump and the cold trap. Damaged components were replaced. Coating investigation will start after verifications of operational parameters of the Pb-Li loop and the specimen holder.

## EUROFER and Pb-Li melts testing under higher temperature irradiation conditions

Principal Investigator: K. Šplíchal, NRI, Řež

[spl@ujv.cz](mailto:spl@ujv.cz) , tel: +420-26617-2456

**Task:** IPP-CR\_TW2-TTMS-003b, D4

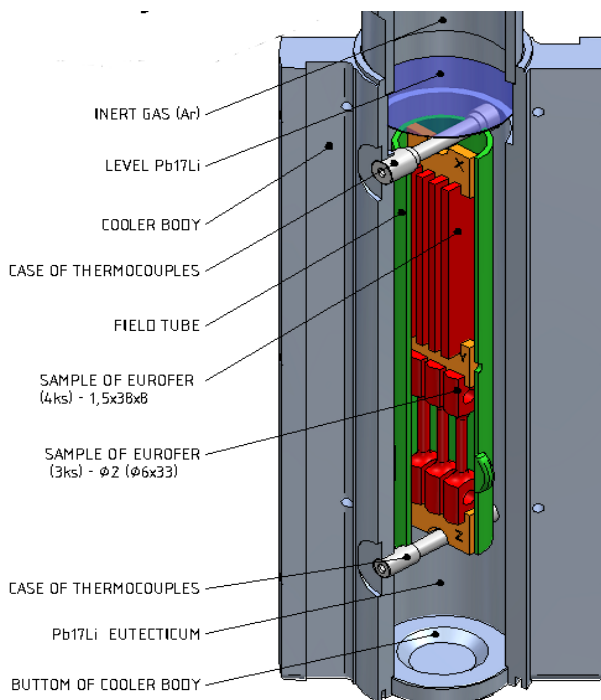
**Field:** Tritium Breeding and Materials, **Area:** Materials Development

**Collaborative staff:** J. Berka, M. Zmitko, Vl. Masarik, Z. Lahodová, L. Viererbl

*Compatibility of martensitic steel EUROFER 97 was investigated with Pb-Li eutectic melt under at temperature 500°C under irradiation condition. Effect of irradiation on Pb-Li melts properties was investigated regarding microstructure, chemical composition and radioactivity. The irradiation of eutectic melts results in the production of tritium and polonium owing to transmutation reaction and bismuth from induced reaction. The post irradiation examinations did not show any noticeable attack of martensitic steel.*

The aim of the task was to perform compatibility tests of EUROFER weld material with Pb-17Li liquid metal under neutron irradiation at 500°C. In-pile corrosion testing of TBM weld metal was situated in molten Pb-Li and located in the active channel of a reactor LVR 15. The weld specimens were irradiated for 6,630 hr up to the level of 1.45 dpa. After dismantling the irradiation rig post-irradiation examinations of the specimens are continuing in the hot cell at the present time.

The Pb-Li in pile rig was designed (Fig.). Three mock up experiments were performed and operational parameters were measured. Computer programme COSMOS FloWorks was used for drawing the design and input data were corrected according to the results of Pb-Li in pile rig mock-ups. The rig consists of an inner part with Pb-17Li liquid, specimens and helium atmosphere and outer part also with helium atmosphere, which separates hot part from outer rig tube. Different pressures of two gas systems are monitored. It enables checking the tightness of the systems. The inner part consists of the field tube enabling liquid metal circulation. Temperatures of the inner part are measured. Different pressures of two gas systems are monitored. It enables checking the tightness of the systems.



Generated nuclear heating was used for in pile rig, an external electrical heating was not used. Nuclear heating and dedicated cooler of the rig ensured required test temperature of about 500-550°C in the hot part and about 350-400°C in the cold part.

Corresponding temperature gradient is in the range of 100-150° C. Flow of the molten Pb-17Li eutectic was driven by natural convention.

Overflowing generated heat is dissipated by reactor basin water and can be controlled in a certain range. The irradiation rig was dismantled in hot cells and the internals were prepared for specimen holder disassembly.

Element	$\gamma$ -analyses [g/g Pb-Li alloy]	Calculated value [g/g Pb-Li alloy]
Tritium	$2.2 \cdot 10^{-9}$	$9.1 \cdot 10^{-6}$
Polonium 210	$7.3 \cdot 10^{-11}$	$4.5 \cdot 10^{-11}$
Bismuth 210	-	$1.5 \cdot 10^{-12}$

Dedicated equipment was prepared and verified for post-irradiation investigation. Sampling of Pb Li melt was performed after melting of Pb-Li metals at 500°C in the laboratory furnace and simultaneously the specimens were pulled out from the holder. Pb-Li residue was removed by washing the specimens in sodium at higher

temperatures and inert atmosphere of argon. Post irradiation examination of Pb-Li specimens has been carried out by metallo-graphic investigations. Microstructure of Pb-Li melt did not show any eutectic structure and corresponded to one of lead without alloy elements. The rest of eutectoid microstructure was not indicated with specimens taken from different positions of rig axial axis. Lithium content was not indicated because removing of Pb-Li metals from rig inner part was not suitable. This enabled segregation of lithium during the re-melting of eutectic alloy. Segregation was also the reason of higher heterogeneous distribution of elements Fe, Mn and Cr.

Gamma-spectrometric analyses of eutectic specimens proved tritium (H3) and polonium Po as a result of transmutation reaction, bismuth Bi as a result of induced reaction. The comparison of gamma analyses and calculation results (Tab.) show that the measured H3 content is about two orders lower than the calculated one and the content of Po is similar for both values. Structure of Pb-17Li melt did not show eutectic structure as results of Li segregation. No increase of Cr, Fe, Mn, Ni contents in Pb-17Li melt was observed as a results of interaction of EUROFER weld metal with in pile environments.

### **References:**

- [1] M. Zmitko, Y. Poitevin, R.Lässer: The European Concepts of the Blanket Module Development, EFDA, Garching, 2005
- [2] H. Moryyma at all: Tritium recovery from liquid metals, Fus. Engin. And Design 28 (1995), 226

## Experiments for the Validation of Bi Cross-Sections up to 35 MeV in a Quasi-monoenergetic Neutron Spectrum

Principal Investigator: P. Bém, NPI AS CR, Řež

[bem@ujf.cas.cz](mailto:bem@ujf.cas.cz), tel. +420 266 172 105 (3506)

### Task: TW7-8\_TTMN\_002B\_D6

Collaborative staff: V. Burjan, M. Götz, M. Honusek, V. Kroha, J. Novák and E. Šimečková

In collaboration with: U. Fischer and S.P. Simakov, Association EURATOM-FZK, Karlsruhe, Germany

The task is a part of a program for developing an off-line method for the neutron spectrum determination in the IFMIF Test Cell Modules. In previous investigations (TW6-TTMI-003, Deliverables 3 and 4) the multiple foil activation method was discussed in details and the selected set of dosimetry reactions were tested at the U-120M cyclotron facility of the Nuclear Physics Institute. The  $D_2O(p,xn)$  neutron source reaction at 37 MeV proton energy was utilized leading to the white neutron spectrum with IFMIF-relevant energies (except its end above 35 MeV).

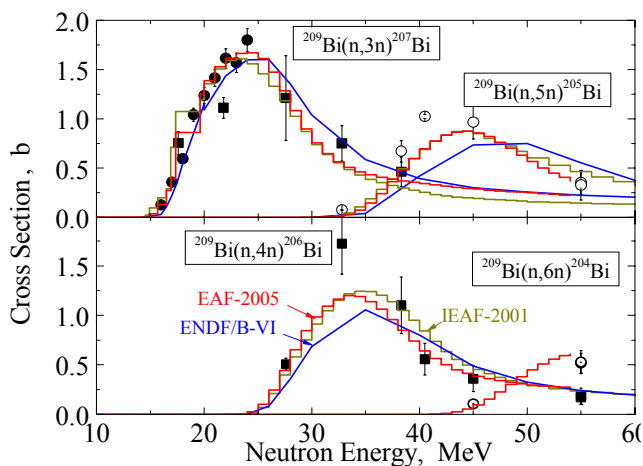


Fig. 1. The activation cross sections of  $^{209}\text{Bi}(n,xn)$  reactions

from measured ones) [1]. For the further suitable reactions in the high-energy region -  $^{209}\text{Bi}(n,3-6n)^{207-204}\text{Bi}$  - only two independent measurements of cross sections above 20 MeV neutron energies were reported up to now with data uncertainties of about 30% - see Fig. 1. No preference could be done for evaluated  $^{209}\text{Bi}(n,xn)$  reactions cross sections for the libraries EAF-2005, ENDF-VI.8 or IAEA-2001 within such uncertainties. New cross section measurements are therefore needed (TW6-TTMN-002B, D6).

The experimental investigation of  $^{209}\text{Bi}(n,3-6n)^{207-204}\text{Bi}$  cross-sections was carried out utilizing the quasi-monoenergetic neutrons from the NPI p-7Li source [2] in neutron energy range from 20 to 35 MeV (peak neutron energy). Neutrons were produced from irradiation of self supporting  $^7\text{Li}$  (carbon stopper)-target by protons at incident energies of 22.1, 27.1, 32.1 and 36.5 MeV. At present, the data on measured specific activities are processed. In particular, the cross sections of the (n,3n) and (n,4n) reactions on  $^{209}\text{Bi}$  are studied in details. Measured data will be analyzed in terms of EASY-2007/ ENDF-VI.8 under close collaboration with the team of FZ Karlsruhe (TW7-TTMN-002B, D5, S. Simakov).

For the determination of the neutron spectra from the  $\gamma$ -activities induced on Al, Ti, Fe, Co, Nb, Rh, In, Tm and Au set of DF foils, the modified code SAND-II was used. In the neutron energy range 10 to 25 MeV (21 dosimetry reactions included), the uncertainties of the spectrum assessed as a mean square deviation of  $A_{\text{cal}}/A_{\text{exp}}$  ratios from unity amount of 3%. Above 25 MeV, only  $^{59}\text{Co}(n,3n)^{57}\text{Co}$  and  $^{197}\text{Au}(n,4n)^{194}\text{Au}$  reactions were used in adjustment procedure, for which the cross section uncertainty could be estimated at level of 20 - 30% (mean deviations of EAF-2005 cross sections

**References:**

- [1] S.P. Simakov , P. Bém , V. Burjan , U. Fischer, M. Götz , M. Honusek , V. Kroha , J. Novák and E. Šimečková, Development of activation foils method for the IFMIF neutron flux characterization, *Fus. Eng. and Design*, **82**(15-24) 2007. pp.2510-2517
- [2] P. Bém , V. Burjan , M. Götz , M. Honusek , U. Fischer, V. Kroha , J. Novák, S.P. Simakov and E. Šimečková, The NPI Cyclotron-based Fast neutron Facility ND-2007, *Proceedings of the International Conference on Nuclear Data for Science and technology*, Nice, April 2007

# IV Keep-in-Touch Activities on Inertial Confinement Fusion

Activities of the Prague Asterix Laser System (PALS) in the field of inertial confinement fusion have been carried out in close collaboration with Institute of Plasma Physics and Laser Micro-fusion, Warsaw, Poland, with participation of scientists from France. In 2007 the experimental work was focused on investigation of production of plasma jets.

## Interaction of laser-produced plasma jets with ambient gas

*J. Ullschmied, Eduard Krouský, Karel Mašek, Jiří Skála*

In collaboration with:

*A. Kasperczuk, T. Pisarczyk, D. Baran, Association EURATOM-IPPPM, Warsaw, Poland  
Ph. Nicolai, V. T. Tikhonchuk, C. Stenz, CELIA, Université Bordeaux 1, Talence, France  
J. Kravárik, D. Klír, FEE Czech Technical University in Prague, Prague, CR*

*The origin, propagation, and stability of plasma jets are fundamental issues in both laboratory astrophysics and inertial confinement fusion (ICF) research. In the ICF context, the material mixing and jet formation could perturb the performance of high-yield laser targets. For that reason the formation of plasma jets and their interaction with ambient media are important issues for the ICF community. The jet production by laser beams depends strongly on the target irradiation geometry and on the properties of materials composing the target. Recent experiments carried out at the Prague Asterix Laser System (PALS) iodine laser facility have demonstrated that well-formed plasma jets can be produced in a simple way by using a single laser beam and a planar target.*

When choosing properly the laser intensity, focal spot radius, and target atomic number a radiative plasma jet can be launched from a metallic planar target. Remarkably stable dense plasma jets were created by focusing the PALS third-harmonic beam on the massive targets made of high-Z metals, like copper, tantalum or lead. Our experiments have shown that well-formed plasma jets can be created at a modest laser energy not exceeding 100 J. Thus, laser experiments of that type ceased to be a privilege of multi-beam super lasers like NOVA or

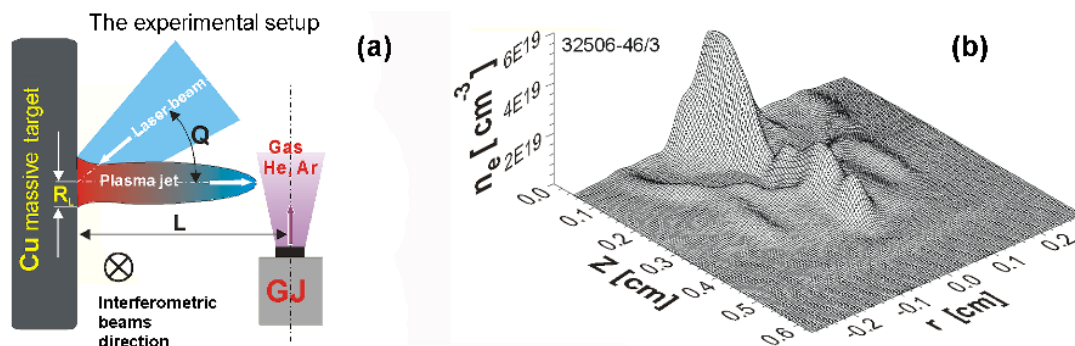


*Fig. 1. Scheme of the experiment on interaction of plasma jet with a gas target (a) and the electron density profile of the interacting jet obtained by laser interferometry (b). A shock wave generated in the gas is well seen at the penetrating jet tip.*

GEKKO XII. The jets produced at PALS have a diameter of typically just a fraction of millimeter, they are several millimeters long, and last longer than 15 ns. The jet velocity exceeds 500 km/s, its Mach number is greater than 10, and the density higher than  $10^{18}$  cm<sup>-3</sup>. For measurements of the development of the jet density, temperature and velocity in the time interval 0-18 ns a three-frame laser interferometer/shadowgraph, a framing x-ray pinhole camera, and an x-ray streak camera were used. The optimum conditions for jet formation (in dependence on the laser energy, colour, and focused intensity) have been found for several target materials (Cu, Ag, Ta, Pb), for both the perpendicular and oblique incidences of the laser beam. The optimised Cu plasma jets produced at the oblique incidence of laser beam were used in experiments on jet interaction with ambient gas (Fig.1).

The interaction of laser-produced plasma jets with a gas target was systematically studied during the IPPLM mission to PALS in April 2007. A high-pressure (2-20 bars) supersonic gas nozzle created a cylindrical column of argon ( $Z=18$ ) or helium ( $Z=2$ ). Variations of the gas atomic number and pressure made it possible to control the jet to ambient gas density ratio in

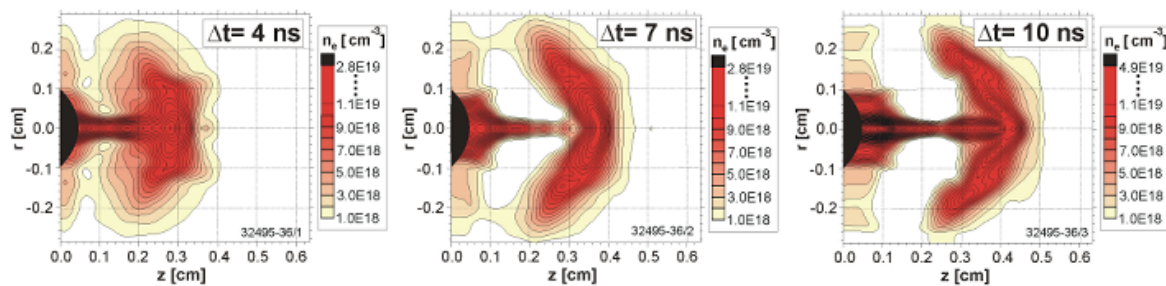


Fig. 2. Development of the transverse plasma density profiles of Cu-jet penetrating He-gas target. Pressure at the gas nozzle 20 bar (pictures by T. Pisarczyk, IPPLM Warsaw).

the range of 0.1 – 10. The oblique incidence of the laser beam of 30° with respect to the target normal avoids gas preionisation in the jet formation area. The time development of transverse electron density profiles of the Cu-plasma jet interacting with a He-target is shown in Fig. 2.

The shock waves created in ambient gas by the penetrating plasma jet are well seen in several series of unique pictures obtained by a 4-frame pinhole x-ray CCD camera, an example of which is shown in Fig. 3. The camera detected soft x-rays in the energy range 10 - 1000 eV.

The following three stages can be distinguished in the interaction process: (i) ablative plasma generation and preliminary ionization of the ambient gas, (ii) creation of the primary shock wave in, (iii) plasma jet forming and generation of a secondary shock wave. Processing of the experimental results and their theoretical interpretation is in progress now. The experiments with plasma jet will continue also in 2008.

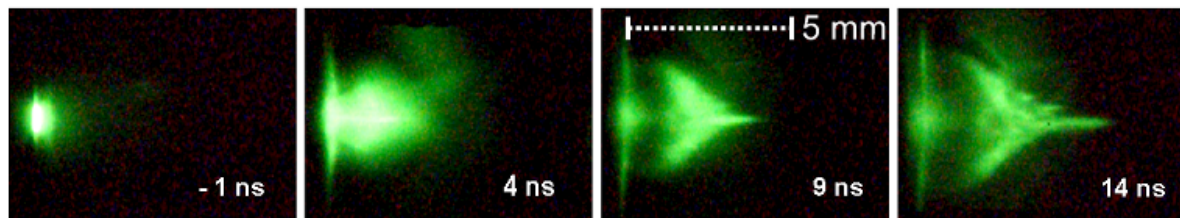


Fig. 3. Plasma jet and shock wave hot regions originating at the jet penetration in argon gas cloud. Pressure at the gas nozzle 5 bar. Exposure time of each frame is 4 ns. (pictures by D. Klir, FEE CTU in Prague).

**References:**

- [1] Kasperczuk, et al., Physics of Plasmas 14 (2007) Art. No. 102706
- [2] Kasperczuk, et al., Physics of Plasmas 14 (2007) Art. No. 032701
- [3] Kasperczuk, et al., Laser and Particle Beams 25 (2007) 425-433
- [4] Kasperczuk, et al., Optica Applicata 37 (2007) 73-82
- [5] T. Pisarczyk, et al. Plasma Phys. Control. Fusion 49 (2007) B611-B619
- [6] P. Nicolai, et al., Astrophysics and Space Science 307 (2007) 87-91
- [7] T. Pisarczyk et al, PLASMA 2007, October 16-19, 2007 Greifswald, Germany, paper WeP44.

# V

## Training, Education, Outreach and Public Information Activities

### Training and education

*J. Stöckel, J Mlynář, M. Hron, R. Dejarnac, M. Řípa, V. Svoboda*

*In collaboration with:*

*G. Veres, M. Berta, A. Bencze, Association EURATOM-HAS, Hungary*

*R Miklaszewski, A. Szydłowski, J. Rządkiwicz, I. Książek, L. Ryc, Association EURATOM/IPPLM, Poland*

*G. van Oost, Association EURATOM/Etat Belge, Belgium*

*Training and education effort was focused on-co organization of the **Summer Training Course (SUMTRAIC)** together with the Association EURATOM/HAS, the organization of semester course **Physics and Technology of Thermonuclear Fusion** for master and PhD students of the Faculty of Nuclear Science and Physical Engineering (FNSPE) of the Czech Technical University. In addition, a new full BSc and MSc Curriculum with the same title continued for the second year at FNSPE.*

The **SUMTRAIC 2007** was organized by the KFKI-Research Institute for Particle and Nuclear Physics in Budapest in the period 10-18 July 2007. Such arrangement was agreed because of shut-down of the CASTOR tokamak. The Association EURATOM IPP.CR was represented by three supervisors of experiments (J. Stockel, M. Hron and R. Dejarnac). The summer school was attended by nine students from four countries. The eleven lectures was presented to students during first three days of the school. Two of them were given by our Association:

R. Dejarnac: Langmuir probe theory and applications

J. Stockel: Langmuir probe measurements on CASTOR and other tokamaks

The remaining time was devoted to laboratory experiments: There were three types of measurements performed with equipment provided by HAS with some contribution from IPP Prague:

- 1) Langmuir probe measurements to determine the electron density and temperature in a glow discharge tube at atmospheric pressure
- 2) Electron density fluctuation measurements
- 3) Spectroscopy measurements to determine plasma composition
- 4) Processing of probe data from the CASTOR tokamak

The IPP supervisors assist in the items 1,2, and 4. We also provided some equipment for these experiments (power supplies and circuits for probe measurements).

The course, **Physics and Technology of Thermonuclear Fusion**, actually takes place at the Faculty of Nuclear Science and Physical Engineering (FNSPE) but is open also for the students from the Charles University. It is organized for students in the last year of their Master studies, at the Department of Nuclear Reactors, and the lecturers are mostly, though not exclusively, from the IPP. In the winter semester 2007, twelve lectures were presented. They were devoted to energy problems in general, basics of plasma physics, principle of fusion reactor, plasma diagnostics, principle of tokamaks, inertial confinement, status of

magnetic confinement, pulsed plasma systems and to material problems of fusion. Two excursions to Prague Asterix Laser and the CASTOR tokamak were organized as well.

From the school year 2006/2007, a new Curriculum **Physics and Technology of Thermonuclear Fusion** was started at FNSPE (for the students in the third year of their studies), and this course is gradually converged to the corresponding regular Master Programme. Within this curriculum, several new courses were launched in 2007, including Introduction to thermonuclear fusion, Physics of tokamaks, Physics of ICF, Introduction to Power Production, Theory of Plasmas. Other new or modified courses (Plasma diagnostics, Technology of thermonuclear devices, Atomic and molecular physics and Topics from MCF) were under preparation for the MSc summer term with the first run in 2008. Considerable ratio of the courses are read by fusion experts from IPP Prague.

On the 3 September 2007, the first bachelor degree of the curriculum was awarded to Mr Michal Kubič. On 21st September 2007 FNSPE hosted the international meeting of European universities, participants in joint call for EURATOM CSA in education. Association IPP.CR actively participates in several proposed workpackages of this call and heads the workpackage „multimedia“. On 18th December 2007, FNSPE transferred the hardware of the decommissioned tokamak CASTOR to the faculty premises in the Břehová street, with a strong determination to find a new educational role for the historical device.



*A fusion lecture at FNSPE during the Fusion Expo exhibition*

## Outreach and Public Information Activities

*M. Řípa, J. Mlynář*

The year began by very successful launching ceremonial of book translation G. McCracken, P. Stott “Fusion – the Energy of the Universe” (godfathers: prof. V. Pačes – chairman of Academy of Science, prof. P. Chráska – director of Institute of Plasma Physics AS CR, v. v. i., Ing. V. Remek – first non Russian and US astronaut and Member of European Parliament), Jan Mlynar said Good bye! to long time stay in EFDA JET CSU at Culham by an overview book for high-school students “Focus On: JET”.

During the year 2007 Association EURATOM-IPP.CR has published 14 articles in different mainstream newspapers and magazines. The members of Association were interviewed six times in radio broadcast and six times in TV broadcast. Very interesting were one hour radio interview with MEP Vladimir Remek “Talking about Fusion Expo”, “Twenty minutes with Martin Veselovsky” about fusion, 20-minutes tv reportage “The way to artificial Sun” about Castor and Compass tokamaks, fusion education and Fusion Expo Prague 2007. Another example was interview with the IPP director in the TV series "Eurofondue" focussed on successful applicants to the EU funds. The internet newspaper [www.aktualne.cz](http://www.aktualne.cz) is covering the construction of Compass tokamak in a continuous reportage "Hledá se energie zítřka. Buďte u toho" („Future power sources are being searched for. Get involved!“). Several high school excursions visited the fusion departments of our Association.

The Fusion Expo exhibition has been presented in Prague from 11th to 23rd June, 2007. It was hosted by the Czech Association Euratom-IPP.CR in the building of Faculty of Nuclear Sciences and Physical Engineering of the Czech Technical University, located in Prague Old City. Because this faculty opened a new fusion-oriented Masters curriculum in the last academic year 2006/2007, posters and exhibits detailing role of the Czech Association in the European fusion research, in particular focussed on the imminent installation of the Compass tokamak in the Institute of Plasma Physics in Prague, enhanced Fusion Expo. Twenty-one of public lectures, that accompanied the exhibition, proved to be popular with the audience. Moreover, special fusion-promoting souvenirs had good sales: T-shirts, teacups, the Czech translation of the book “Fusion: The Energy of the Universe” - or just a postcard with the Fusion Expo stamp. A large publicity of the Fusion Expo has been organized in media and a special website (in Czech language) <http://fusionexpo.fjfi.cvut.cz> has been arranged to see more Expo details, images and all posters presented.



More than 2000 visitors – that is the final score of the Fusion Expo presentation in Prague in 2007. The visitors often asked surprisingly detailed questions and had many enriching comments to the topics. Compared to 1998, when Fusion Expo visited Prague for the first time, the public seemed to be much better informed about the problem and much more concerned with the global energy challenge.

Very extraordinary is a number “twenty” of the members of Association’s lectures for wide public and high school students.

Two members of Association were awarded for meaningful act in physics popularization by Association of Czech Mathematicians and Physicists’ Czech Physical Society.

Two 9<sup>th</sup> events – Open Days and Tour de Plasma bike trip finished successful Association public activity year.

## LIST OF PUBLIC ACTIVITIES

### **Book:**

**Jan Mlynář et al:** „Focus on JET: The European Centre of Fusion Research“, EFDA JET Close Support Unit, Culham Science Centre, Abingdon, Oxfordshire, OX14 3EA, United Kingdom, 2007

### **Book translation: G. McCracken, P. Stott: Fusion – the Energy of the Universe**

Launching ceremonial, eight recensions in newspapers and magazines, two in television, one in broadcast

Launching ceremonial: (godfathers: prof. V. Pačes – chairman of Academy of Science, prof. P. Chráska – director of Institute of Plasma Physics AS CR, v. v. i., Ing. V. Remek – first non Russian and US astronaut and Member of European Parliament), 22. února 2007, 14:00 hod., Akademie věd, Národní 3, Praha 1, posluchárna 206

### **Appreciations:**

Association of Czech Mathematicians and Physicists’ Czech Physical Society awarded **Milan Milan Řípa** for meaningful act in physics popularization – longtime and comprehensive popularization of thermonuclear fusion

Association of Czech Mathematicians and Physicists’ Czech Physical Society awarded **Jan Jan Mlynář** for meaningful act in physics popularization – book „Focus On: JET“

**Milan Řípa:** Nomination in the competition Czech Head for media category

### **Exhibitions:**

#### ***František Žáček et al, Fusion Expo, Praha, June 11 to June 23, 2007***

2000 visitors, press conference, invitation cards, folders, booklets, posters, books, fusion promoting merchandisers (T-shirts, teacups, postcard with the Fusion Expo stamp), 21 lectures, special websites, 13 servers, info broadcasting three times per day from June 8 to June 16, ten newspaper and magazines papers, included into the projects of „The Science on the Streets“ and „Physical Week 2007“

**Jan Mlynář, Milan Řípa:** Poster „Participation in projects of JET and ITER“, Reopening of Conference Centrum of the Academy of Science of the Czech Republic, Liblice, September 6 to September 20, 2007

**Milan Řípa:** Fragments of Fusion Expo, Week of Science nad Technology, Praha, November 1 to November 11 2008

### **Author’s papers:**

**Dagmar Jáňová, Milan Řípa:** Fúze – Energie vesmíru (Fusion – the Energy of the Universe), Zpravodaj České energetické agentury, No 1, March 2007, cover p. 4

**Milan Řípa:** Kutil vyrobil termojaderný reaktor (The handyman has made the thermonuclear reactor), Lidové noviny, March 17 2007, p. 11

**Milan Řípa:** ITER současnosti: od fyziky k technologii (Today ITER: from physics to technology), Technický týdeník, 55 (2007), p. 18

**Milan Řípa:** Patent, který si dává na čas (Patent with long time delay), Lidové noviny, April 27, 2007, p. 17

**Milan Řípa:** Fúze dnes a zítra (Fusion Today and Tomorrow), Mladá Fronta Dnes, attachment Věda, 18, číslo 140, p. C/8, June 16, 2007

**Milan Řípa:** Budeme rozlišovat jaderné štěpné a jaderné fúzní elektrárny (We shall differentiate between fission nuclear plant and fusion one), Halo noviny, 17, No 139, p. 8, June 15, 2007

**Milan Řípa:** Fusion Expo – putovní evropská výstava v Praze! (Fusion Expo – the Traveling European Exhibition in Prague), Technický týdeník, 55, No 11, May 29, 2007, p. 13

**Milan Řípa:** Přítomný stav energie pro budoucnost (Today Status of the Energy for the Future), Energetika, 57(2007), No 7, pp. 234 – 235

**Milan Řípa:** Ohlédnutí za výstavou Fusion Expo (Hindsight the Fusion Expo exhibition), Akademický bulletin, No 9, 2007, p. 12

**Milan Řípa:** Jak tokamak a stellarátor soutěžily (How the tokamak and stellarator had competed), Vesmír, 86 (2007), No 9, pp. 583 – 585

**Milan Řípa:** Vesmírný tokamak na Zemi (The universe tokamak on the Earth), Inovační podnikání, 15 (2007), No 3, pp. 12 – 14

**Milan Řípa:** Výzkum termojaderné fúze u protinožců (The fusion research by antipodes); Technický týdeník, 55, No 21, October 9, 2007, p. 29

**Milan Řípa:** Rusko chce předběhnout svět (Russian wants to outrun the world), Lidové noviny, November 28, 2007, p.17

**Štěpán Plaček (interview with Jan Stöckel):** Paliva bude dost miliony let (The fuel will be enough for millions years), Nedělní svět, Svět vědy, p. 9, January 14, 2007

**Marek Telička (interview with Pavel Chráska):** Jak se staví slunce (How the sun is building), Svět, February 2007, pp.12 – 17

### Papers – tutition

**Matouš Lázňovský (Milan Řípa – tutor):** Podaří se spoutat Slunce? (Shall we be succensful in sun enchainment?), Lidové noviny, Byznys book, Věda attachment, p. 17, June 11, 2007

**Darina Boumová (Milan Řípa – tutor),** infoWIN: Jak snést energii hvězd na Zemi?(How star energy bring down on the earth?, No 6, 2007, p. 1

**Zdenka Petáková (Milan Řípa – tutor):** Jaderná fúze: vzdálená naděje (Nuclear Fusion – beautiful hope), Krásná paní, 2007, No 10, pp. 50 to 51

### Lectures

**Milan Řípa:** Hvězdy míří na Zem – střípky z fúzní historie (The stars head for the Eather – the crocks from fusion history), Fusion Expo, June 21, 2007

**Milan Řípa:** Hvězdy míří na Zem – střípky z fúzní historie (The stars head for the Eather – the crocks from fusion history), lecture for high school teachers in the frame of Expo Fascination by light, Veletržní palác, November 1, 2007

**Milan Řípa:** Iter je cesta (ITER is a way), Gymnasium Turnov, Decemebr 6, 2007

**Milan Řípa:** Iter je cesta (ITER is a way), Gymnasium Čáslav, December 19, 2007

**Vladimír Kopecký:** Plazma, budoucí zdroj energie z termojaderné fúze, Otevřená věda, Praktické kurzy z fyziky, 15. března 2007, Akademické a univerzitní centrum Nové Hrady

**Vladimír Kopecký:** „Plazma, budoucí zdroj energie z termojaderné fúze“ (Plasma – the source of the energy of the future), The multibranch seminary: The science opened to regions , Tréšř castle, April 28, 2007

**Jan Mlynář:** Světlo pozemských hvězd – jak vidíme termionukleární fúzi (i doslova) (The light of the earthly stars – how we see the thermonuclear fusion (even literally), The week of science and technology, Academy of Science of the Czech Republic, Praha , November 6, 2007

**Vladimír Weinzettl, Vladimír Kopecký, Jan Mlynář, Milan Řípa:** Zkrocení Prometheova ohně (Subjugation of Prometheus's fire), Fusion Expo, June 19, 2007

**Vladimír Kopecký:** Fúzní energie pro modrou planetu (The fusion energy for blue planet), Fusion Expo, Praha, June 11, 2007

**Pavel Pavlo:** Česko a fúzní Evropa (The Czech Republic and fusion Europe), Fusion Expo, Praha, June 12, 2007

**Jan Stöckel:** Fúzní minulost Česka – tokamak CASTOR (The fusion history of the Czech Republic – tokamak CASTOR), Fusion Expo, Praha, June 13, 2007

**Radek Pánek:** Fúzní budoucnost Česka – tokamak COMPASS, (The fusion future of the Czech Republic – tokamak COMPASS), Fusion Expo, Praha, June 18, 2007

**Vladimír Weinzettl:** Zkrocení Prometheova ohně (Subjugation of Prometheus's fire) Assembly of young physicists and mathematicians, Faculty of Mathematics and Physics of Charles University, Plasnice v Orlických horách, July 8, 2007

**Vladimír Weinzettl:** Zkrocení Prometheova ohně (Subjugation of Prometheus's fire), Open Science project, gymnasium Voderadska, Praha, October 11, 2007

**František Záček:** Tokamak ITER a kdo je víc? (Tokamak ITER and who is more?), Fusion Expo, Praha, June 19, 2007

**Jan Mlynář:** Evropský tokamak JET je největší na světě (European tokamak JET is the biggest all of the world), Fusion Expo, Praha, June 20, 2007

**Jan Mlynář:** Fúze – věc veřejná: informace & studium (The fusion – public item: information & studies), Fusion Expo, Praha, June 22, 2007

**Milan Řípa:** Soubor popularizačních činů na téma termojaderná fúze (The collection of popularization items on the theme of fusion), The competitive display of meaningful acts in physics disclosure for public, Charles University, Praha, December 4, 2007

**Jan Mlynář:** Kniha „Focus on JET: The European Centre of Fusion Research“, The competitive display of meaningful acts in physics disclosure for public, Charles University, Praha, December 4, 2007

**Pavel Šunka:** Termojaderná fúze – energie pro jednadvacáté století (Thermonuclear fusion – the energy for 21th century), Gymnázium v Jevíčku, Jevíčko, April 24, 2007

### **Television and broadcasting**

**Milan Řípa (Dagmar Jánová),** Termojaderná fúze (Thermonuclear fusion), Český rozhlas, Meteor, March 3, 2007

**Malina:** Tři minuty s Milanem Řípou – seznámení s překladem knížky Garry McCrackena, Peter Stotta: Fúze – Energie vesmíru (Three minutes with Milan Ripa – presentation of the Czech translation of the book Garry McCracken, Peter Stott: Fusion – the energy of the future)), UPC, December 5, 2006

**Luboš Veverka, Milan Řípa, Vladimír Remek:** Beseda o Fusion Expo (Talking about Fusion Expo), Třetí dimenze, ČRo Leonardo, June 11, 2007

**Vladimír Kunz (Milan Řípa – co-ordinator, starring Jan Mlynář, Jan Stöckel, František Záček):** Cesta k umělému Slunci (The way to artificial Sun), Port, Popularis, ČT2, June 13, 2007

**Martin Veselovský (interview with Milan Řípa about fusion):** Dvacet minut s Martinem Veselovským (Twenty minutes with Martin Veselovsky), Radiožurnál, July 23, 2007, 17:32

**Zdeněk Vališ (interview with Milan Řípa):** Čeští vědci studují termojadernou fúzi (Czech scientists are studying thermonuclear fusion), Radio Prague – broadcasting abroad, Kaledioskop – věda a technika, , October 13, 2007

**Jiří Adámek:** Kulový blesk (Fireball) Zprávy, Nova, June 22, 2007:

**Pavel Chráska:** Otevření výstavy Fusion Expo (Lauchnig of Fusion Expo), TV (ČT2), June 11., 2007

**Pavel Chráska:** Zahájení výstavy Fusion Expo (Lauchnig of Fusion Expo), Radiožurnal, June 11, 2007

**Pavel Chráska,** Fusion Expo: Eurofondue o Tokamaku (Eurofondue about tokamak), ČT 2, August 31, 2007; repetition two times

**Kořen (Pavel Chráska, Radek Pánek):** Na pražské sídliště Kobyličky dorazilo zařízení tokamak (The facility tokamak has arrived in Prague habitation) , ČT 1, Události, November 20, 2007

**Martina Mašková (Pavel Chráska):** Fúze – energie budoucnosti (The fusion – the energy of the future), Radio Leonardo, October 22, 2007 -

### Folders

**Milan Řípa:** Termojaderná fúze? Ano! (Thermonuclear fusion? – Yes!), ČEZ,

**Milan Řípa:** Fusion Expo

### Translations

**Milan Řípa, Jan Mlynář** (subtitles): ITER, the way to fusion power, DVD European Commission,

### Internet

**Josef Tuček:**Hledá se energie zítřka. Buďte u toho („Future power sources are being searched for. Get involved!“), <http://aktualne.centrum.cz/veda/clanek.phtml?id=391542>

### Others:

9th Open days: November 9 to 10, 2007

9th Tour de Plasma: September 21 to 23, 2007, bike trip from Prague to Mariánská (IPP ASCR, v.v.i., cottage) and back.

## APPENDIX

### **Overview of the tokamak COMPASS reinstallation in the Institute of Plasma Physics AS CR, v.v.i., Association EURATOM-IPP.CR in 2007**

#### **CONTENTS:**

Executive Summary of the Appendix	133
1. COMPASS-D Tokamak Dismantling and Transport	134
2. Tokamak Building	136
3. Tokamak Energetics	138
4. Vacuum System	142
5. Diagnostics	143
6. CODAC, Interlock, and IT Infrastructure	149
7. Feedback Control	151
8. Modelling	152
9. Neutral Beam Injection	154
10. Human Resources for the Reinstallation of the COMPASS Tokamak	156
11. Financial Report	159
12. Timetable	162

## **EXECUTIVE SUMMARY OF THE APPENDIX**

This appendix to the 2007 Activity report summarizes the status of the project „Enabling a programme of ITER relevant plasma studies by transferring and installing COMPASS to the Institute of Plasma Physics AS CR, Association EURATOM-IPP.CR”.

In all critical aspects the progress of the project is satisfactory. The tokamak COMPASS has been dismantled and transported to IPP Prague as soon as the building construction allowed. The construction of the new building is finished and COMPASS is fixed in its place. The tokamak energetics has been manufactured and is currently being installed. The vacuum system has been successfully tested and is ready for installation. Diagnostics, CODAC, Interlock, and IT Infrastructure are progressing essentially as scheduled. For feedback control the digital solution has been adopted and both, hardware and software, are in production. The tender for neutral beam injection is delayed. This should not affect the delivery at the end of 2009 and commissioning foreseen for 2010. Human resources for re-installation are available. Financial situation is manageable.

There are no indications that the next significant milestone – first plasma at the end of 2008 – would not be achieved.

## 1. COMPASS-D TOKAMAK DISMANTLING AND TRANSPORT

- Dismantling of COMPASS-D started on October 16, 2006 (Fig. 1.1) and finished by August 2007.
- IPP staff spent in UKAEA Culham a total 56 menweeks.
- 6 lorries of tokamak equipment has been transported to IPP Prague.
- Special transportation frame and box has been designed and manufactured in Prague for safe transport of the tokamak.
- After dismantling, the COMPASS-D tokamak was lifted through the dismantled roof of D1 building using a 500-ton crane and specially manufactured lifting cross on September 17, 2007 (Fig. 1.2 and 1.3).
- Consequently, the tokamak was placed on a frame, fixed to it and moved into the JET Assembly hall for temporary storage (Fig. 1.4).
- There, an iron frame covered by wooden panels was put around the tokamak to protect the tokamak during storage and, especially, for transport to IPP Prague.
- The COMPASS-D tokamak was loaded on a special oversized lorry; the transport left for IPP Prague on October 16, 2007 (Fig. 1.5) and arrived in Prague on October 20, 2007 (Fig. 1.6).
- In IPP Prague COMPASS was unloaded and put into temporary storage in the new assembly hall for six weeks.
- Finally, the COMPASS tokamak was placed to its final position on December 11, 2007 (Fig. 1.7)



*Fig. 1.1: COMPASS hall before start of dismantling*



*Fig. 1.2: The COMPASS-D tokamak lifting (inside the experimental hall).*



*Fig. 1.3: The COMPASS-D tokamak lifting (outside view on crane).*



*Fig. 1.4: Temporary storage of COMPASS-D in JET Assembly hall.*



*Fig. 1.5: The COMPASS-D tokamak leaves for Prague.*



*Fig. 1.6: The COMPASS tokamak arrives to IPP Prague. New tokamak building is behind the lorry.*



*Fig. 1.7: The COMPASS tokamak is placed on its final location in the new tokamak hall.*

## 2. TOKAMAK BUILDING

- The new building consists of the assembly hall, tokamak hall and administrative part with offices and control room.
- The tender for the new tokamak building was launched at the end of December 2006.
- Company Podzimek a synove, s.r.o. was chosen as a supplier.
- The contract was signed on March 9, 2007.
- The construction started in May 2007.
- The Assembly and tokamak hall were finished in December 2007.
- The administrative building has been finished in January 2008.
- The final building approval is planned for the end of March 2008 – after installation of most of the technology.



*Fig 2.1: Tokamak building - south view.*



*Fig 2.2: Tokamak building - north view.*



*Fig 2.3: Tokamak building - west view.*



*Fig 2.4: Tokamak hall –*



*Fig 2.5: Tokamak hall - first*



*Fig 2.6: Tokamak hall - second floor (tokamak level).*



*Fig 2.7: Cabel compartment – direction to flywheel generators .*



*Fig 2.8: Cabel compartment – direction to transformers and convertors.*



*Fig 2.9: Assembly hall and power supply area.*

### 3. TOKAMAK ENERGETICS

- The tender for COMPASS energetics was launched at the end of December 2006
- CKD Nove Energo was chosen as a supplier for the energetic system.
- The contract was signed on April 10, 2007.
- It has been decided to procure two flywheel generators in the frame of this project. This solution (performance upto  $B_t = 2.1$  T) was chosen for the following reasons (AHGs recommendations):
  - Better plasma performance – impact on scientific programme
  - In case of procurement of two generators the price of the generator is considerably reduced.
  - In case of malfunction of one generator, COMPASS can still operate at reduced performance.
- Presently, all parts of the energetic system have been delivered to IPP Prague (except for the flywheel generators) and are being installed in the new hall.
- The experts from IPP Prague were present at the tests of the individual systems at the supplier companies (convertors, OH system, transformers, etc).
- All tests were successful and required parameters were fulfilled and often also exceeded.
- The timetable for energetics is kept and no crucial delay is envisaged.

#### a) Flywheel generators

The two flywheel generators are presently being manufactured in the CKD Nove Energo (Figs. 3.1 and 3.2). The first one will be delivered in February 2008 and the second generator in March 2008 (the schedule is followed).

Detailed calculations were made to assess the impact of generator vibrations during the shot. The basement was sized (over 1 000 tons of reinforced concrete) according to these calculations to accumulate the energy of the impulse (Fig. 3.3-3.5).



*Fig. 3.1: Stator of the generator is assembled in CKD Nove Energo*



*Fig. 3.2: Rotor of the generator is assembled in CKD Nove Energo*



*Fig. 3.3: Basement (re-inforcement) of flywheel generator*



*Fig. 3.4: Two special frames for the flywheel generators are installed*



*Fig. 3.5: Finished flywheel generators basement.*

### **b) 6 kV switching station, transformers and convertors**

All the systems have been already manufactured (convertors – CKD Elektrotechnika a.s., 6kV switching station – ABB Brno, transformers – SGB Regensburg, etc ) and have been delivered into the COMPASS hall (Figs. 3.6-3.11). Most of the systems are already installed and work on cabelling has started (Fig. 3.12). The progress is according to the timetable and no delay is envisaged.



*Fig. 3.6: Low-voltage area.*



*Fig. 3.7: High-voltage area – part of the 6kV switching station.*



*Fig. 3.8: Convertors for toroidal and poloidal circuits including their control.*



*Fig. 3.9: Tokamak basement – deprecated chokes (back) and the crowbar system (front).*

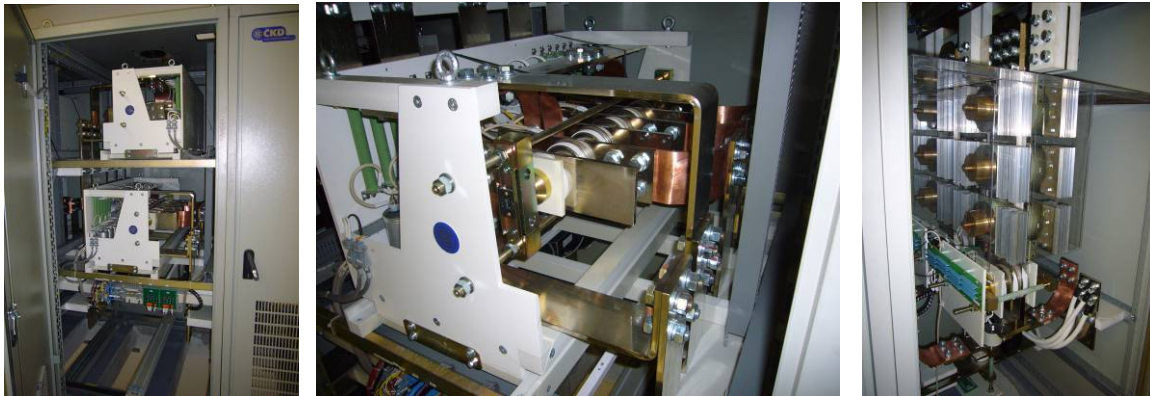


*Fig. 3.10: Detailed view inside the convertor cubicle (left), on the thyristors (middle) and the OH system (right).*



*Fig. 3.11: Transformers have been delivered and are being installed.*



*Fig. 3.12: Heavy current cabling is under work.*

## 4. VACUUM SYSTEM

### 4.1 Activities done:

1. The original pumping stand (maybe 5-6 years out of operation) was moved to IPP Prague from Culham. The system was revised and the necessary maintenance (oil replacement etc.) has been performed. The stand has operated several months for pumping of the CASTOR tokamak. The operation of the system was controlled manually. The pressure  $10^{-6}$  mbar was achieved without any baking of the stand.



*Fig. 4.1.1. The pumping system of COMPASS after testing on CASTOR*

2. All parts of the gas filling system (Mass flow controllers and valves) have been identified and their functionality was tested.
3. The scheme of computer control of both the pumping and the gas filling systems was designed in collaboration with IST Lisbon and some parts were already tested. Implementation of the control system in the central CODAS of COMPASS is under way. New vacuum gauges (with a digital output), which are necessary in the new control system were identified (Pfeiffer HPT 100, CPP and 100 PPT 100) and shall be purchased.

### 4.2 Present status:

1. The pumping system is functional and prepared for installation in the new tokamak hall. As the first step, manual operation (using existing vacuum gauges brought from Culham) is envisaged.
2. Hardware required for the computer control of the pumping system has been designed and it is already partially under construction.

### 4.3 Future activities:

1. Installation of both the pumping and gas filling systems in the new hall and their connection to the COMPASS tokamak.
2. Fabrication of missing flanges of the vacuum vessel (some ports have remained open after dismantling at Culham).
3. Immediate purchasing and installation of the digital gauges for communication with computer control system.
4. Manufacturing of all HW (and development of corresponding software) needed for the computer control of the pumping and the gas filling systems.
5. Installation of the heating systems of all evacuated parts together with a unit for temperature measurements and control.

## 5. DIAGNOSTICS

**5.1 Magnetic diagnostics** – the system of magnetic diagnostics was carefully dismantled and documented during the stays of IPP staff at Culham in 2007. The equipment (four cubicles + cables) have been transported to IPP Prague. Some parts, which will be re-used for the plasma control, in particular analogue integrators of signals from magnetic sensors were tested under realistic conditions on the CASTOR tokamak. Only a few of them are operational and compatible with original documentation. Remaining integrators, which were found to be non-operational, were modified already during COMPASS operation. Using the existing COMPASS database, the signals from magnetic sensors have been exploited for reconstruction of magnetic surface by means of the modified EFIT code.

**5.2 Microwave interferometer** – the existing equipment (the single channel interferometer at 2 mm) was transported from Culham. The system was tested successfully on the CASTOR tokamak using its 4-mm waveguides and antennae – see Fig. 5.2.1 and Fig. 5.2.2. The interferometer electronics was equipped by the conditioned cabinet for a better day-to-day operation. In 2007, IPP staff was trained for interferometer operation and signal processing by V.Shevchenko (UKAEA). In the first half of 2008, the interferometer will be installed on COMPASS.



Fig. 5.2.1 Test of 2-mm interferometer on CASTOR

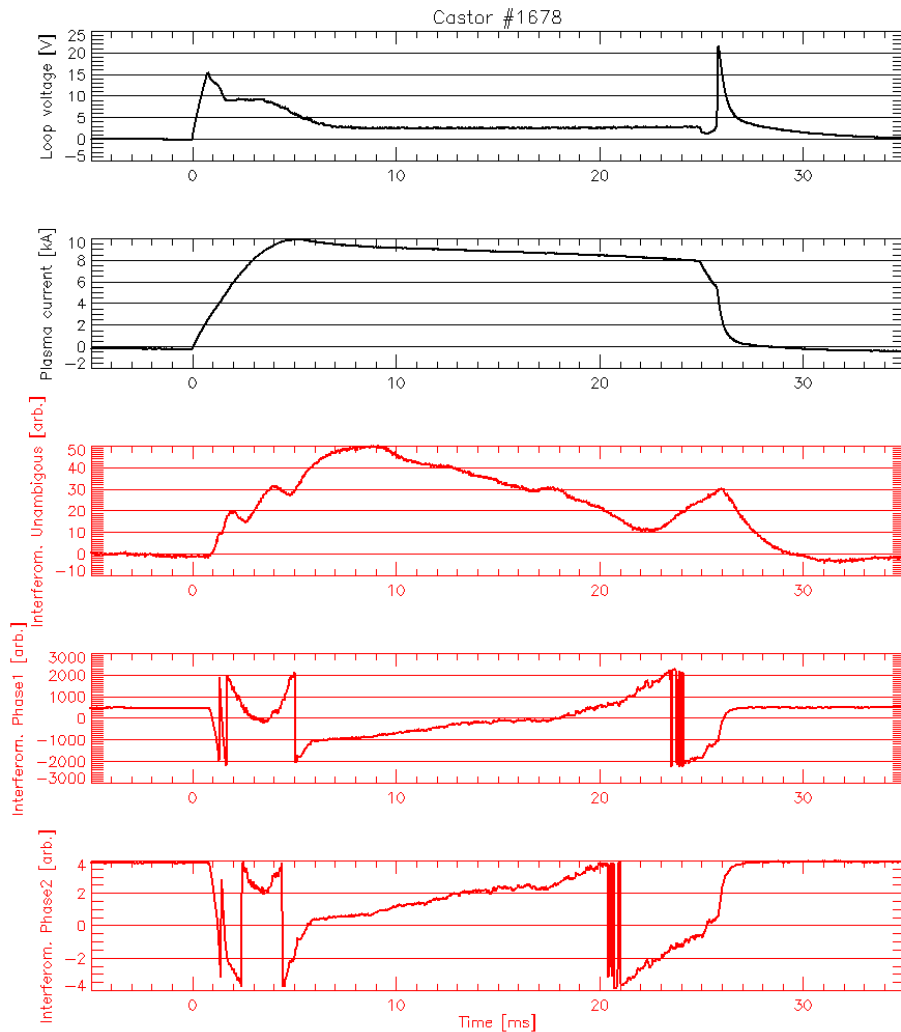


Fig. 5.2.2 Interferometric signals in a standard shot of the CASTOR tokamak(red).

**5.3 Spectroscopic diagnostics** – a poloidal section of the diagnostic ports of COMPASS suitable for fast spectroscopic detectors such as fast AXUV-based bolometers, semiconductor SXR detectors and visible radiation monitors was chosen with regard to the presence of the two NBI heating systems in the vacuum vessel and a possibility to realize tomographic reconstructions of the selected radiation ranges. The small size of the allocated ports, a large number of the detectors inside them and requirements for cooling during a vessel baking led to an optimization in a choice of the detectors and to an integrated port design. The design including a placement of necessary multi-pin feed-through will be finalized after an access to the COMPASS planned to spring 2008 will be reached and information on available space around the ports will be known. High temporal resolution in combination with good spatial resolution, namely in the pedestal region, will be attained by the recently purchased 6 AXUV20-ELM (IRD Inc.) based arrays of bolometers and 4 LD35-5T-JET-Windowless (Centronic) arrays of the SXR detectors (in a cooperation with V.Igochine, IPP Garching) located inside the diagnostic ports, see Fig. 5.3.1. Visible light will be observed using optical fibers and a spectrometer/photomultipliers located in a diagnostic room.



Fig. 5.3.1 On the left, there are the six AXUV20-ELM (IRD Inc.) based 20-channel arrays of fast bolometers equipped with the ceramic sockets. On the right, there are the four LD35-5T-JET-Windowless (Centronic) 35-channel arrays of the soft X-ray detectors.

**5.4 Fast visible camera** - a cooperation with HAS Association (M.Berta, A.Szappanos) on the implementation of the fast visible camera on COMPASS has been started and the first model of the EDICAM camera with an exposure time up to 20 microseconds was tested on the CASTOR tokamak, according to the contract between IPP Prague and KFKI-RMKI Budapest signed in July 2007. The final hardware design and implementation of the sensor module and the Image Processing and Control Unit (IPCU) together with final tests are planned on 2008.

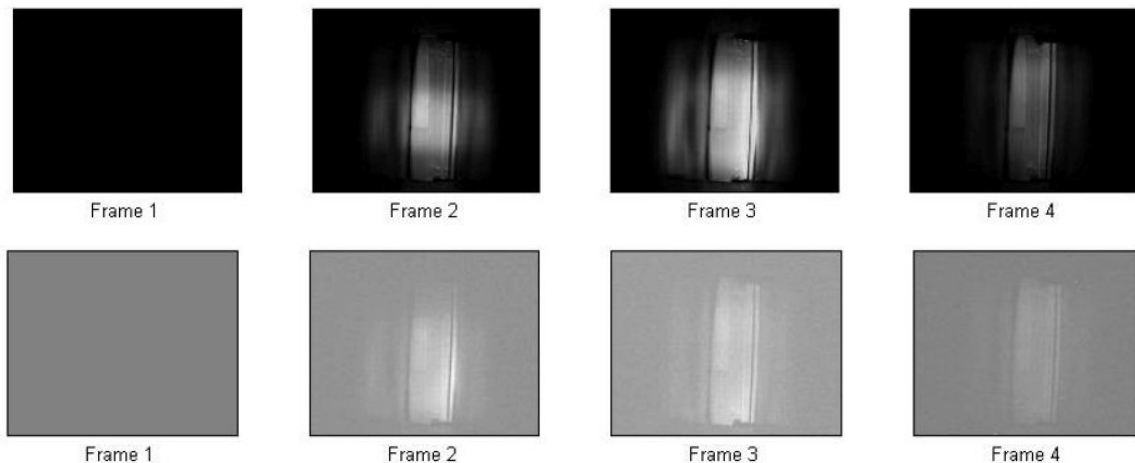


Fig. 5.4.1 Sequences of the 1280x1024 pixel frames taken by the EDICAM camera during CASTOR tokamak shots with 500  $\mu$ s (upper frames, original colors) and 20  $\mu$ s (lower frames, rescaled colormap) exposition time. Dynamically rescaled colormaps are used to visualize details, namely for exposition time shorter than 100  $\mu$ s.

**5.5 Thomson Scattering** – the High Resolution Thomson scattering for COMPASS is under design. Calculations of plasma background contribution to a scattered radiation signal were done and taken into account for selecting the laser parameters. In autumn 2007, an exchange of experts with the TEXTOR tokamak, Forschungszentrum Jülich, Germany was organized.

System parameters relevant to the TS layout on the reinstalled COMPASS tokamak were discussed in detail. Work on a design of the diagnostic set-up is in progress. Namely, the laser part of the system was specified after calculations and discussions as follows:

- Nd:YAG laser system used at the second harmonic frequency
- energy about 2.5 J per pulse on 532 nm
- pulse length in the range of 10-20 ns
- repetition rate at least 30 Hz

Contacts to possible suppliers of the laser system itself were arranged and negotiations will continue in spring 2008. The detection part of TS diagnostics will consist of focusing optics, optical fibers, a spectrometer in Littrow arrangement and ICCD camera, see Fig. 5.5.1. Detailed specifications are on the way in conjunction with experts from the optical workshop of IPP in Turnov.

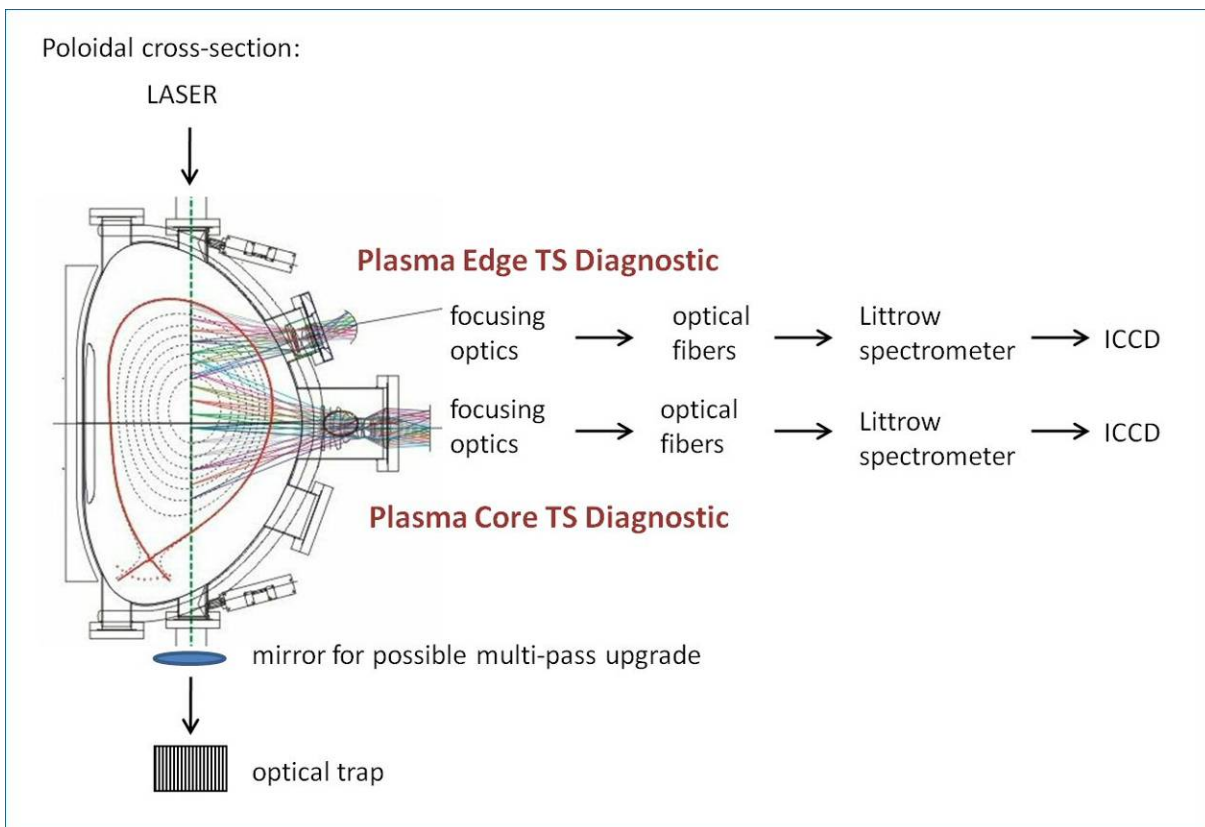


Fig. 5.5.1 The detection scheme of TS for the COMPASS tokamak.

**5.6 Microwave reflectometer** - the millimetre-wavelength reflectometer will be constructed for the pedestal electron density measurements on COMPASS in close collaboration with the Associação EURATOM / IST as specified by the contract between Institute of Plasma Physics AS CR, v.v.i. and CFN/IST on the design and construction of the system consisting of 5 reflectometers in 4 frequency bands. The total frequency range 18-90 GHz will allow measurements of the edge plasma density profile. The reflectometers will have O-mode polarization with the exception of the Ka-band (26.5 – 40 GHz), in which both O and X-mode polarizations will be used because of their complementary functions. The scientific exchange between IPP and CFN/IST to accelerate the design phase was realized in autumn 2007. The agreed design of the system includes the technical aspects of the block scheme of the reflectometry electronics, quasi-optical band-combiner and antenna including the positioning in front of the tokamak port – see Fig. 5.6.1 and Fig. 5.6.2. All parts of the reflectometric system will be constructed, assembled and tested by CFN/IST in Lisboa in 2008/09, with the support of microwave engineers from IPP.CR. The deadline for the work is pending on the reply of the manufactures, in particular concerning the development of special

components such as the band-combiners/decombiners. By the end of 2007, the offer to collaborate on the project was addressed to the Usikov’s Institute for Radiophysics and Electronics NAS of Ukraine (IRE NASU, Kharkov). At the the beginning of 2008, the decision regarding which parts of the system would be developed at IRE NASU, will be taken.

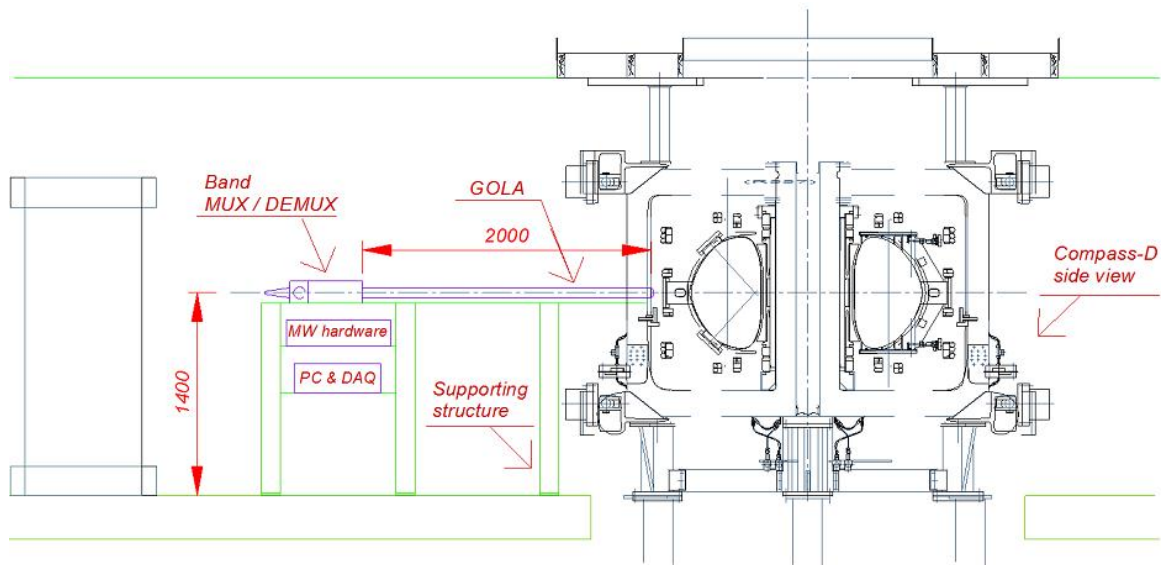


Fig. 5.6.1 Reflectometr system in the tokamak hall – side view

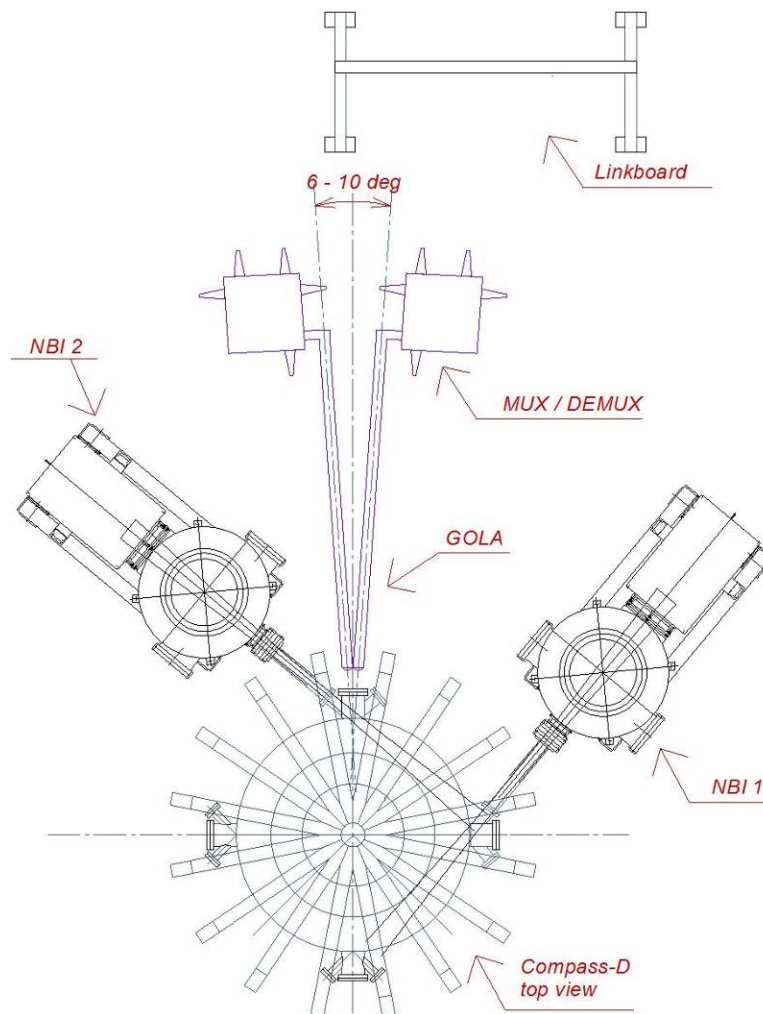


Fig. 5.6.2 Reflectometr system in a tokamak hall – top view

**5.7 Diagnostic neutral beam** – is developed by the Association EURATOM/HAS under the Contract on collaboration signed on July 2007. Modeling of beam-plasma interaction for edge plasma parameters of COMPASS was performed. A design of the atomic beam system - optical layout, detector type, vacuum and control system and the design of the detection system for beam emission spectroscopy is planned on 2008.

**5.8 Neutral particle analyser** – existing NPA was transported from Culham. The status of key elements (in particular detectors) was checked and found to be satisfactory. The NPA will be put in operation in collaboration with Ioffe Institute, St Petersburg at the end of 2009.

## **6. CODAC, INTERLOCK AND IT INFRASTRUCTURE**

### **6.1 CONTROL, DATA ACQUISITION, AND COMMUNICATION SYSTEM (CODAC)**

A completely new COMPASS CODAC system is being built in close collaboration with the Association Euratom/ IST. The CODAC tasks cover the experiment control, data acquisition and data handling, and operator / user communication environment.

The following CODAC interface will be used: “FireSignal“ [A. Neto et al.: Fusion Engineering and Design 82 (2007) 1359–1364]. Data access will be managed by the “SDAS“ layer [A. Neto: Fusion Engineering and Design 82 (2007) 1315–1320].

The control of slow and long-lasting processes („24 hours / day control“) is ensured by individual industrial systems:

- Control of energetics will be managed by its own control system, which was developed and will be provided by the supplier (ČKD). A communication link with CODAC will secure the exchange of requested and actual values of currents, respectively.
- Cooling water control will be a part of „Measurement and regulation system“, which controls the building systems operation – including the cooling water conditioning and also heating and cooling of the building.

#### **6.1.1 Tasks achieved:**

1. CODAC design was evaluated;
2. HW platform for the CODAC nodes was selected, namely the ATCA system [A.J.N. Batista et al.: Rev. Sci. Instrum. 77, 10F527 (2006)] developed at IST Lisbon.
3. We specified the communication protocol to be used between the CODAC and the power supplies, which are delivered together with the Energetics (toroidal field, equilibrium field, magnetizing field, and shaping field power supplies). A controller for the tests of Energetics was designed.
4. communication module between the CODAC and fast amplifiers (feedback) was designed;
5. vacuum system control was designed, incl. a vessel baking module;
6. NBI control requirements were specified for the Call for Tender.

#### **6.1.2 Present status:**

1. production of the CODAC node's HW is under way
2. production of the vacuum system controller is under way
3. production of the controller of the fast amplifiers is under way
4. preparation of a controller for tests of the CODAC – Energetics communication is under way

#### **6.1.3 Next activities:**

1. installation of the vacuum control system (March 2008)
2. tests of the Energetics system including the communication with CODAC (March 2008)
3. installation and tests of the CODAC nodes (April – June 2008)
4. programming of the control nodes (July – August 2008)

## **6.2 Interlock**

### **6.2.1 Activities done:**

1. control of the access of personnel to the experimental area has been designed;
2. principle design of the central interlock was prepared;
3. interfaces of local interlocks of individual systems were defined;

### 6.2.2 Present status:

1. the experimental area access system is installed in the building
2. design of the central interlock, connecting the individual systems, is being updated and finalized in details

### 6.2.3 Next activities:

1. tests of the experimental area access system and adjustment of the access control (February 2008)
2. installation of the central interlock system (April – May 2008)
3. test of the interlock (June 2008)

## 6.3 IT infrastructure

The COMPASS installation and its putting in operation in the new building requests a new IT infrastructure. This task covers the building's network installation, data storage, computational power, and client stations for individual users.

### 6.3.1 Activities done:

1. design of the IT networks in the new building;
2. specifications for servers for data storage and for user's computation and data evaluation were fixed; a supplier was selected and the HW was ordered.

### 6.3.2 Present status:

1. installation of the IT networks is close to completion;
2. specifications for the data storage media (hard drives) are fixed, ready for a call for offers of possible suppliers;
3. specifications for the client stations are fixed, request for offers was placed.

### 6.3.3 Next activities:

1. purchase of the remaining server HW (January 2008);
2. installation and configuration of the servers (January – March 2008);
3. purchase and tests of the client stations (February – April 2008);
4. tests (since March 2008) and full operation of the new IT infrastructure (since May 2008).

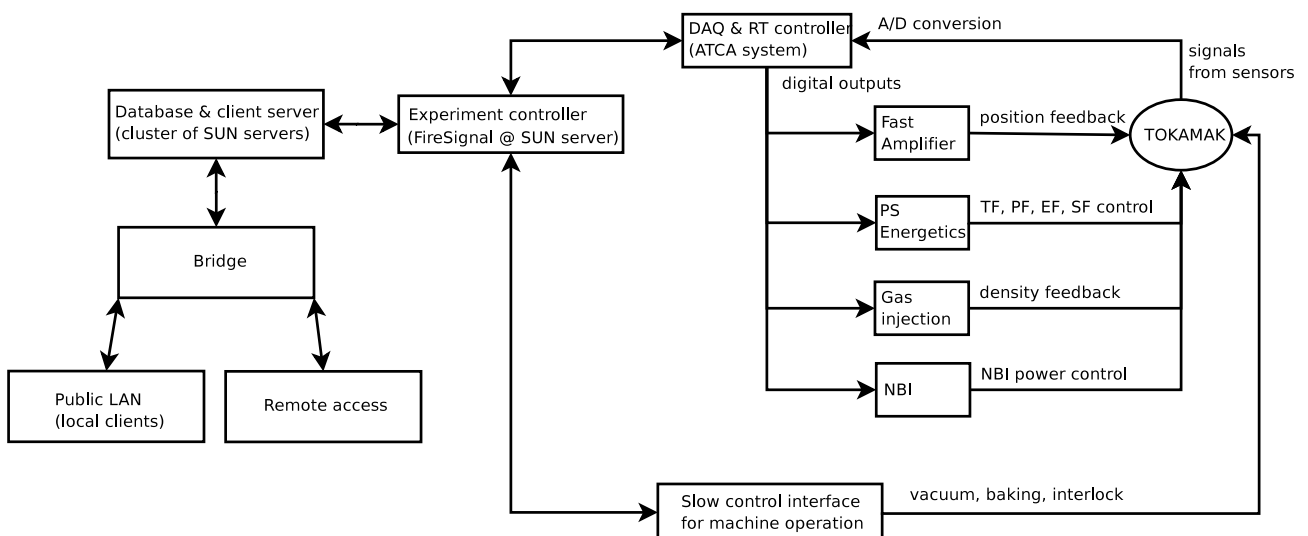


Fig. 6.1.1: Data flow in the CODAC and feedback schemes

## 7. FEEDBACK CONTROL

A new feedback system is under construction for the plasma control. From the original COMPASS-D systems from Culham, only the analog signal integrators will be used. The remaining part of the feedback is being built newly and it is based on a digital approach.

A modelling of the feedback is performed in order to create the algorithms for feedback system. A dynamic simulation of the evolution of the magnetic configuration during a discharge is performed using a non-linear FEM code MAXFEA.

The output of the modelling will be converted to algorithms, which will be programmed to the CODAC nodes. These nodes include ATCA modules, each one with 32 analog input channels, 4 analog output channels, and 8 digital input/output channels connected to a processor. Such set-up allows the implementation of MIMO controllers.

Three identical fast amplifiers are being built in the IPP for the feedback stabilization of the horizontal (1 piece) and vertical (2 pieces in a bridge) plasma positions. The amplifiers are based on MOS transistors, each amplifier has maximum current of 5kA,  $\pm 50V$  voltage, frequency range DC-5kHz and output impedance of 5 m $\Omega$  - 274 mH.

The circuit safety is designed for overcurrent, overvoltage and optical isolation protection inside the energizer that determines the amplifiers inputs. In addition, amplifier zero-output-voltage pre-shot check and another delayed overcurrent protection is put in.

### 7.1 Activities done:

1. analog integrators were tested (see also Diagnostics section)
2. COMPASS geometry was implemented to MAXFEA and mesh files were created in the feedback modelling;
3. fast amplifiers for the feedback control were designed;
4. cooling of the transistors is designed as passive cooling through heat absorption in attached mass of aluminium blocks;
5. digital PID controller was designed for the control of the fast amplifiers;
6. three energizers for the fast amplifiers (containing pre-amplifier, optical decoupling and protection circuits) were designed.

### 7.2 Present status:

1. in modelling of the feedback, material description files are being created currently;
2. 3 amplifiers are under construction in IPP: one for the horizontal plasma position stabilization and two (in a bridge) for the vertical stabilization;
3. the energizers are built and ready for testing.

### 7.3 Next activities:

1. compilation of the magnetising circuit current profile to the MAXFEA code (February 2008);
2. calculation of the feedback model using MAXFEA (February – March 2008);
3. creation of the algorithms from the results of the model (April – June 2008);
4. programming of the model to the control CODAC node (June – July 2008);
5. construction of the amplifiers (till May 2008);
6. tests of the fast amplifiers (May – June 2008);
7. tests debugging of the whole feedback system (July – September 2008).

## 8. MODELLING

This part of the monitoring report summarizes briefly main results achieved in modeling during the last year. The first part deals with plasma performance with additional heating (NBI+LH), the second one on progress in modeling of resonant magnetic perturbation technique, which is envisaged to be applied on COMPASS for ELM mitigation.

### 8.1 Modeling of plasma performance

Currently, transport modeling of the tokamak COMPASS is performed using the ASTRA and CRONOS codes. The CRONOS transport code was acquired last year from CEA Cadarache and adapted for the COMPASS tokamak. Currently both codes are capable of simulating ohmic heating schemes of various equilibrium settings. During I.Voitsekhovitch's visit last September (2007), a robust transport model for COMPASS was developed for the ASTRA code, including the possibility of external heating. Simulations with externally calculated (Accome, Fafner) NBI heating and current drive were also successfully performed using both of these codes. Even though such calculation isn't automatically self-consistent, the transport models show reasonable behavior, and it can be foreseen that once the modules for NBI heating currently being developed at CEA for CRONOS are satisfactorily finished, self-consistent predictive simulations of NBI heating on COMPASS with CRONOS will be possible on a routine basis. The following figures show the ion and electron temperature profiles calculated by the ASTRA code using the transport model developed with I.Voitsekhovitch for the SND equilibrium with  $I_p = 200$  kA,  $B_T = 1.2$  T and central electron concentration of  $3.5 \cdot 10^{19} \text{ m}^{-3}$  for co-NBI and counter-NBI each at 300 kW:

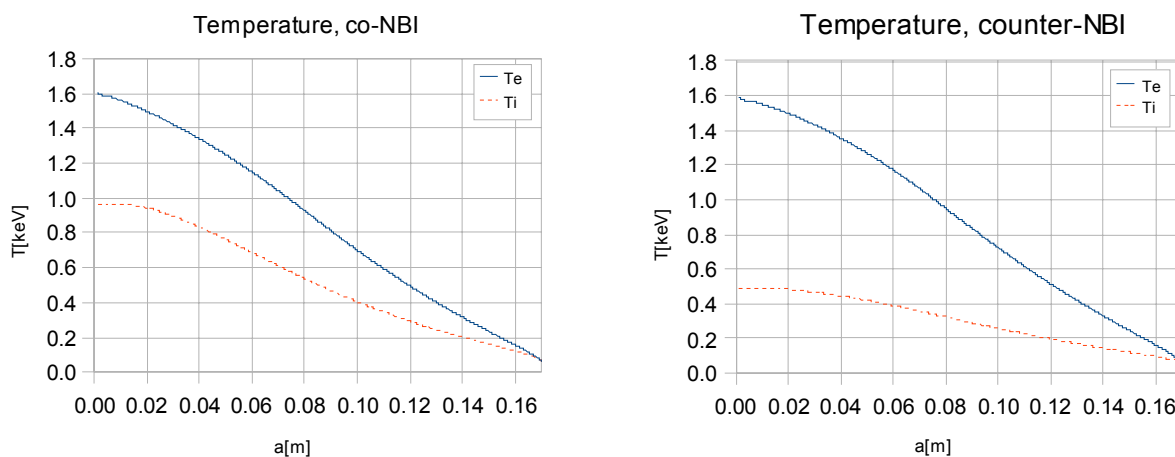


Fig. 8.1.1 The absorbed power in the co-NBI scheme is 190 kW while in the counter-NBI scheme it is 120 kW for the given equilibrium.

Our group has also recently acquired a LHCD simulations package from CEA Cadarache consisting of the ray-tracing code C3PO, and the 3-D relativistic bounce-averaged drift kinetic code LUKE. With the help of Y.Peysson, the code was adapted to the COMPASS LH configuration with a 1.3 GHz lower hybrid RF power source. Preliminary simulations were performed for the SND equilibrium and a launched  $n_{||}$  ranging from 1.95 to 3. The results were satisfactory giving full power absorption of 210 kW and a driven current of 67 kA for  $n_{||}=1.95$ ; the deposition being mostly at normalized toroidal  $\rho$  of 0.25 and 0.5; while for larger  $n_{||}$  the absorption place moves outwards. Compatible LHCD results were obtained with ACCOME. Currently we are in the process of learning and fine-tuning the code for the COMPASS tokamak, in view of eventually making self-consistent predictive transport simulations including both LHCD and NBI sources.

## 8.2 Modelling of resonant magnetic perturbations and edge ergodization

The COMPASS tokamak is equipped with a unique set of saddle coils for producing resonant magnetic perturbations (RMPs). During the operation of COMPASS at Culham these coils were used, for example, to investigate neoclassical tearing modes, mode penetration, and control of Type-III ELMs. It was then discovered on the DIII-D tokamak that RMPs can lead to complete suppression of Type-I ELMs [T. Evans et al.: Journal of Nuclear Materials, 337-339, (2005) 691]. As there is a possibility that the newly installed COMPASS will exhibit Type-I ELMs thanks to the planned NBI system, the availability of a flexible set of RMP coils opens a way to test this ELM mitigation technique.

As part of preparation for COMPASS operation in Prague, we performed calculations of spectra of RMPs caused by saddle coils. The emphasis was on edge ergodization, which is believed to be a key element of the ELM suppression mechanism. The calculations follow the same principle which was used for the calculations of RMP spectra for the ELM suppression experiments on DIII-D, JET and MAST and for the design work of RMP coils for ITER. The ERGOS codes, developed at CEA Cadarache, have been already used for those cases [E. Nardon et al.: J. Nucl. Mat. 363-365, (2007) 1071] and only required some modifications for the coil system of COMPASS, which is significantly more complicated than in other machines.

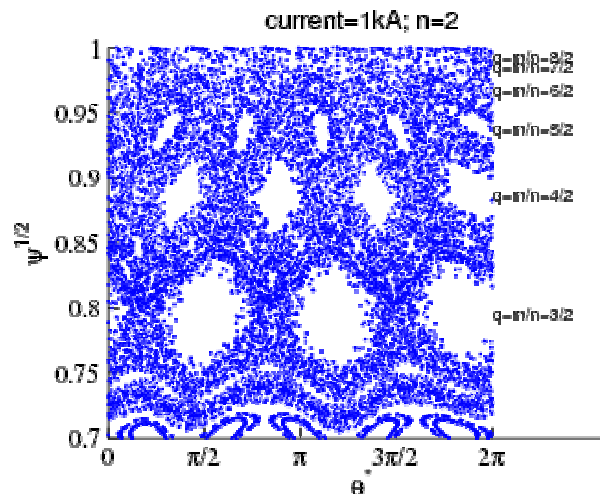


Fig. 8.2.1 Poincaré plot of field line tracing, showing the pedestal region. The x-axis is  $\theta^*$ – the straight field line poloidal angle, the y-axis is the radial position  $s=\psi^{1/2}$ , with  $\psi$  being the normalized poloidal flux. Every dot represents an intersection of a field line with the poloidal plane.

Spectra of the perturbations are calculated by computing the vacuum field of the coils and the field components are then projected on a mesh of intrinsic coordinates created as part of the equilibrium calculation by the MHD equilibrium code HELENA [G. Huysmans et al.: Proc. CP90 Europhysics Conf. on Comput. Phys., (1991) 371]. The perturbation spectra are thus coupled to a specific equilibrium. For our calculations we use equilibria predicted by the ACCOME code [K. Tani et al.: J. Comput. Phys. 39, (1992) 332]. The perturbation field creates magnetic islands whose sizes are determined by Fourier harmonics of the radial perturbation. The leading toroidal mode of the perturbation has  $n=2$  due to the symmetry of coils. Ergodization is then estimated by applying the criterion of island overlap and verified by field line tracing.

Results show that for the chosen configuration of RMP coils an ergodic layer appears in the pedestal region (Fig. 8.2.1). This is similar to the results for the ELM suppression experiment at DIII-D, thus a comparable effect on ELMs can be expected.



Third, following key decisions on design principles of the COMPASS control system and interlocks, final specifications of the NBIs control and safety could be released, see the Fig. 9.1. The NBIs will have their own control nodes, each of them running a state machine, whose parameters can be set from the central COMPASS control system. The systems will have an own XML description, which will allow their set-up from the central system. The interlocks will use a serial link of relays.

The Call for Tender for the two Neutral beam injectors for the COMPASS tokamak will be released in early 2008. The successful contender will be notified in summer 2008, and the complete system of the two NBIs is expected to be installed in the COMPASS experimental hall in the second half of 2009.

## 10. HUMAN RESOURCES FOR THE REINSTALLATION OF THE COMPASS TOKAMAK (*status as of January 2008*)

At the beginning of the year 2008, the total number of the IPP.CR staff involved in the re-installation of the COMPASS tokamak is 48 employees. Not all of them are involved full time – the total manpower is 39.9 ppy. The manpower is slightly above the number promised in the Phase II proposal (35+). This manpower is divided according categories as follows:

	Persons	ppy
Senior scientists and postdocs:	21	19.2
PhD students	12	12
Engineers and technicians:	9	8.5
Undergraduate students	6	1.2

The support of the project from IPP (management of IPP, financial matters and mechanical workshop) is very important, but not specified. The list of IPP staff is shown in Table 1. The involvement in particular topics is indicated.

In addition, a strong collaboration on COMPASS re-installation has been established between IPP and Association EURATOM HAS and IST. Our colleagues from Portugal and Hungary are involved in design and implementation of the CODAC and development of particular diagnostics. The number of collaborators changes in time, the total manpower is estimated as not less than 2 ppy for HAS and 2 ppy for IST. More detailed information on collaborating staff is shown in Table 10.2.

The distribution of duties of the staff according to topics is as follows:

- Management: J. Stockel (project leader), R. Pánek (deputy project leader), M. Hron (administr.)
- Supervision of building construction: R. Pánek, J. Kladrubský
- Supervision of power supplies: R. Pánek, J. Kladrubský, J. Zajac
- Control and Data Acquisition: M. Hron, J. Písačka, J. Adámek, J. Sova + IST staff
- Installation of IT: J. Písačka, K. Rieger, P. Cahyna, F. Janky
- Feedback system and PS control: M. Hron, J. Horáček, O. Bilyková, M. Stránský, J. Vlček, K. Rieger, F. Janky, R. Beňo, J. Seidl + IST
- Vacuum and gas handling system: J. Stránský, F. Žáček, M. Šatava, J. Stockel
- Additional heating: J. Stockel, J. Mlynář, V. Píffl (NBI), F. Žáček, J. Zajac (LHCD)
- Diagnostics development: V. Weinzettl
  - Magnetics: I. Ďuran, O. Bilyková, J. Havlíček (EFIT), K. Kovařík, J. Stockel
  - Optical diagnostics: V. Weinzettl, D. Naydenkova, V. Píffl, M. Vácha, + HAS
  - Thomson scattering: P. Bílková, J. Brotánková, P. Bohm, M. Aftanas, Z. Melich, D. Šesták
  - Edge plasma diagnostics: R. Dejarnac, J. Adámek, J. Horáček
  - Microwave diagnostics: J. Zajac, F. Žáček, J. Vlček, M. Vašulka, M. Kazda + IST
  - Beam diagnostics: HAS + V. Weinzettl, J. Stockel
- Theory and modeling: R. Pánek
  - LHCD+transport: V. Fuchs, V. Petržílka, P. Pavlo, M. Stránský
  - NBI: J. Urban, J. Preinhealter
  - RMP: P. Cahyna, L. Krlín
  - Edge plasma modeling: R. Dejarnac, E. Havlíčková, M. Komm
- General technical support: M. Šatava (drawings), F. Jiránek, K. Boušek, K. Rieger, V. Havlík

The composition of the groups may change according progress of individual topics and other duties, which may appear.

No.	Work description	Family	name	ranking	capacity
1	proj. leader	Stockel	Jan	senior scientist	1.0
2	IT/CODAS	Hron	Martin	senior scientist	1.0
3	deputy project leader	Pánek	Radomir	senior scientist	1.0
4	modelling	Krlín	Ladislav	senior scientist	0.6
5	modelling	Fuchs	Vladimír	senior scientist	0.5
6	modelling	Preinhaelter	Josef	senior scientist	0.8
7	modelling	Petržílka	Václav	senior scientist	1.0
8	modelling	Pavlo	Pavol	senior scientist	1.0
9	NBI heating	Mlynář	Jan	senior scientist	1.0
10	microwaves	Žáček	František	senior scientist	0.8
11	optical diag.	Weinzettl	Vladimír	senior scientist	1.0
12	magnetics	Đuran	Ivan	senior scientist	1.0
13	beam diag.	Piffl	Vojtěch	senior scientist	0.5
14	edge plasma diagnostics	Dejarnac	Renaud	senior scientist	1.0
15	microwave diagnostics	Zajac	Jaromír	senior scientist	1.0
16	IT/CODAS	Písačka	Jan	senior scientist	1.0
17	feedback system	Horáček	Jan	Postdoc	1.0
18	edge plasma diagnostics	Adámek	Jiří	Postdoc	1.0
19	magnetic diagnostics	Bilykova	Olena	Postdoc	1.0
20	Thomson scattering	Bilkova	Petra	Postdoc	1.0
21	simulations	Stránský	Michal	Postdoc	1.0
1	NBI	Urban	Jakub	PhD student	1.0
2	Thomson scattering	Aftanas	Milan	PhD student	1.0
3	magnetic diagnostics	Havlíček	Josef	PhD student	1.0
4	modelling	Havlíčková	Eva	PhD student	1.0
5	Thomson scattering	Brotánková	Jana	PhD student	1.0
6	Thomson scattering	Boehm	Petr	PhD student	1.0
7	magnetic diagnostics	Naydenkova	Diana	PhD student	1.0
8	feedback system	Janky	Filip	PhD student	1.0
9	feedback system	Seidl	Jakub	PhD student	1.0
10	edge plasma simulations	Komm	Michael	PhD student	1.0
11	resonant mag. perturbations	Cahyna	Pavel	PhD student	1.0
12	optical elements	Šesták	David	PhD student	1.0
1	vacuum	Šatava	Miloš	technician	1.0
2	general technician	Jiránek	František	technician	1.0
3	IT	Rieger	Karel	technician	1.0
4	general technician	Boušek	Michal	technician	1.0
5	power suppl.	Kladrubský	Jan	technician	1.0
6	vacuum	Strnad	Jiří	engineer	1.0
7	feedback system	Vlček	Jiří	engineer	1.0
8	optics for TS	Melich	Zbynek	engineer	1.0
9	gen. techn.	Havlík	Vladimír	technician	0.5
1	microwave diagnostics	Vašulka	Michal	student	0.2
2	feedback system	Beňo	Radek	student	0.2
3	interlock system	Sova	Jan	student	0.2
4	microwave diagnostics	Kazda	Michal	student	0.2
5	SXR detection	Vácha	Miroslav	student	0.2
6	magnetic diagnostics	Kovařík	Karel	student	0.2

Table 10.1: IPP.CR Staff involved in the re-installation of the COMPASS tokamak

1	beam diag	Berta	Miklos	HAS
2	beam diag	Dunai	Daniel	HAS
3	visible camera	Szapanos	András	HAS
4	CODAC – control+feedback	Neto	André	IST
5	CODAC – vacuum	Pereira	Tiago	IST
6	CODAC – power supplies	Carvalho	Ivo	IST
7	CODAC	Souza	Jorge	IST
8	CODAC	Fernandes	Horacio	IST
9	microwave diagnostics	Silva	Antonio	IST

*Table 10.2: International collaboration with HAS and IST*

### **Potential Risks**

Manpower foreseen and necessary for the success of the COMPASS project is currently fully available. However, a large part of it is represented by PhD students mostly funded by scholarships. Though they are all competent and intend to continue their work into employment by IPP, this will soon imply an increasing demand on salaries which may be difficult to meet.

We have originally counted upon EURATOM contribution (baseline support) of the order of 20%. However, the ceiling for baseline allocated to IPP.CR for 2008 (221.7 keuro) represents only 16% contribution, and that only due to the fact that COMPASS operational costs will start up growing gradually this year (depreciation, in particular); otherwise, it would be around 14% only. If the diagnostics (included in the original Phase 2 proposal as non-eligible for PS) were charged against the CoA under baseline support as investments in 2008, the EURATOM support would be even less (11% in 2008).

Lack of resources to provide adequate salaries to these young people upon their regular employment represents a potential risk of losing them for the work on COMPASS, or even for the Community. Encouraging people to increase their work under COMPASS-unrelated EFDA tasks, or seeking long-term secondments in other associations, CSUs etc. would have, at this moment, the same detrimental effect of reducing the manpower available.

## 11. FINANCIAL REPORT

The table 11.1 compares the current estimates for re-installation of COMPASS with numbers presented in the Phase II proposal.

Costs in kEuro	Phase II proposal		2008	difference
	B=1.2 T	B=2.1 T	2.1 T	B=2.1 T
Transport from Culham	30	30	74	44
Power supplies	2,750	4,160	4,867	707
CODAC	480	480	515	35
Diagnostics	794	794	835	41
NBI Heating	994	994	994	0
Refurbishment	0	0	93	93
<b>Total</b>	<b>5,048</b>	<b>6,458</b>	<b>7,378</b>	<b>920</b>

*Table 11.1: Estimate of COMPASS re-installation costs*

The first column is taken over from the Phase II proposal, where just a single flying-wheel generator was envisaged to operate the tokamak at 1.2 T. The original calculation of the cost increase for operation at maximum  $B_T$  is presented in the second column.

The third column represents the current estimate of the final cost for 2.1 T. The last column shows the difference between the Phase II proposal (based on 2005 costs) and the current status of the budget.

Before discussing the differences in individual items in detail, we have to note that:

- The estimates of the cost for the Phase II proposal were based on the 2005 costs in Czech crowns (CZK), using the exchange rate 29.70 CZK / EUR. Current estimates are based on the exchange rate 26.00 CZK / EUR, expected for 2008.
- Inflation rate was 2.5% in 2006 and 2.8% in 2007, 6% is expected in 2008.
- The increase of costs of raw materials (Cu, Fe, etc.) was disproportional and significantly above the inflation rate.

These factors are partially responsible for the increase of the current costs with respect to the Phase II proposal.

Let us discuss the individual items in more detail.

### Transport from Culham

Additional expenditures for transport (by 44 kEuro) have appeared after dismantling of the COMPASS tokamak in Culham. The main reasons for this were a/ the construction of a special transport frame for the facility and b/ the cost of the oversized transport.

### Power supplies

An increase of the power supplies cost is due to the decision to install both flying-wheel generators from the very beginning of the project. This arrangement will allow to operate the tokamak at maximum toroidal magnetic field up to  $B = 2.1$  T and provide some redundancy.

This decision follows the recommendation of the AHG.. Furthermore, during the specification of the contract with the manufacturer it turned out that the overall cost of two generators manufactured simultaneously is much lower than the total cost of step-by-step purchase. This solution also avoids the necessary shut-down for installation of the second generator at a later phase of the project.

The tendered price for the complete solution was higher by ~707 kEuro, namely due to the increase of the raw material costs, increase of technical requests, and more strict safety regulations.

## CODAC

Some increase of the budget appeared also in the CODAC. The status of the analogue feedback system for the plasma control has been found non-satisfactory after the dismantling (namely because some elements, like waveform generators were controlled by an old fashion and non-existing software. Therefore, a completely new, fully digital control system was designed, which had some impact on the budget (an increase by 35 kEuro).

## Diagnostics

The cost of diagnostic systems has also increased by 41 kEuro with respect to the Phase II proposal. This increase has appeared mainly after revision of the detail design of the key diagnostics – the high resolution Thomson scattering. A more precise estimate is now 700 kEuro, which is higher by 215 kEuro than the Phase II value. The increase is caused by an enhancement of the core detection, which is designed as multi-channel with spatial resolution (there was only a single central channel in the Phase II proposal). On the other hand, the estimates for re-installation of the magnetic diagnostics were overestimated by ~50 kEuro in the original proposal. After dismantling of the system in Culham and after the decision to exploit the digital control system it was found that only ~12 kEuro is required for refurbishment of the magnetic diagnostics. In addition, the planned expenditures for microwave reflectometry were also reduced significantly (by ~144 kEuro), because the full responsibility for this diagnostics was taken over by the Association IST. A more detail cost breakdown for plasma diagnostics is shown in the Table 11.2.

	Phase II (kEUR)	2008 (kEUR)	
Magnetic diagnostics	61	12	digital control
$D_a$ and $Z_{eff}$ arrays	10	13	
Visible camera	43	43	HAS
Fast bolometers	0	7	increased No of arrays
SXR – arrays	5	6	
Interferometry	0	6	refurbishment of existing equipment
TS-edge+core	485	700	improved design with more channes in the core
Microwave reflectometry	150	6	IST responsibility
Beam diagnostics	40	40	HAS
Langmuir probe divertor	0	2	refurbishment
<b>Total</b>	<b>794</b>	<b>835</b>	

Table 11.2: Estimation of diagnostics costs

However, an enhancement of the diagnostic capabilities would be required in the later phase of the project. Installation of the neutral particle analyzer (after NBI), VUV & XUV spectrometers, reciprocating Langmuir probe and radiometry is envisaged. These equipments already exist, but their refurbishment will require additional costs, which are estimated as ~84 kEuro.

## Refurbishment

Furthermore, it was found during the dismantling of COMPASS in Culham and preliminary tests at IPP Prague that some key elements for re-installation of COMPASS require a refurbishment. In particular, new gauges for vacuum and gas handling systems are required for their computer control, new oil for turbo-molecular pumps, etc. There are also some construction elements (supports for diagnostic cables, galleries around the machine, ...) that have to be replaced. These expenditures were not envisaged. Therefore, a new line is added to the Table 11.1 is added indicating the amount of 93 kEuro required for refurbishment of the above items.

### **Building construction**

The construction of the new tokamak building is not a subject of the preferential support. However, for information we note here that its cost has risen to 3 963 kEuro, which is significantly more than originally estimated in the year 2005, i.e. before starting the tendering process. In spite of the fact that the tenderer offered the lowest price, the tendered amount was much higher. Furthermore, during the realization of the project, the technology part of the building appeared to be more complex than expected (equipment for de-mineralized water, fire-protection systems, basement of the second fly-wheel generator, unexpected problems at excavation of the ground, ...). The extra costs for the building construction were provided by the Government of the Czech Republic and by the Academy of Sciences of the Czech Republic.

## 12. TIMETABLE

	2006		2007				2008				2009				2010		Present status
	Q3	Q4	Q1	Q2	Q3	Q4	Q1	Q2	Q3	Q4	Q1	Q2	Q3	Q4	Q1	Q2	
<b>Building construction</b>																	
project and licencing	■																ON TIME
tender		■															
construction			■	■	■	■											
<b>Tokamak transport</b>																	
dismantlement & documentation	■																ON TIME
transport		■															
installation					■	■	■										
<b>Central power supply</b>																	
tender		■															ON TIME
design			■														
manufacturing				■	■	■											
installation and commisioning							■										
<b>Convertors (toroidal and poloidal field)</b>																	
tender		■															AHEAD OF SCHEDULE
design			■	■													
manufacturing				■	■	■	■										
installation and tests								■	■	■							
<b>Plasma control - feedback systems</b>																	
algorithms design	■	■															ON TIME
control SW development				■	■	■	■										
power supplies - tender	■																
power supplies - design			■	■													
power supplies - manufacturing				■	■	■	■										
installation and tests								■	■	■							
<b>Vacuum and chamber conditioning</b>																	
vacuum systems installation								■	■								ON TIME
glow discharge system installation									■								
boronization system installation										■							
<b>Control and data acquisition</b>																	
system design	■	■															DELAY - 2 MONTHS - NO IMPACT ON FIRST PLASMA
algorithm development		■	■	■													
HW manufacturing			■	■	■	■											
SW development				■	■	■	■	■	■								
testing and commissioning								■	■	■							
<b>Security systems</b>																	
design	■	■															DELAY - 3 MONTHS - NO IMPACT ON FIRST PLASMA
implementation			■	■	■	■											
<b>Additional heating systems</b>																	
<b>NBI</b>																	
tender		■															DELAY - 9 MONTHS - NO IMPACT ON DELIVERY AND COMMISSIONING
design			■	■	■	■	■										
manufacturing								■	■	■	■						
commissioning												■					
<b>LH</b>																	
re-furbishment												■	■				
installation													■				

Appendix – Tokamak COMPASS reinstallation in IPP Prague

	2006		2007				2008				2009				2010		Present status
	Q3	Q4	Q1	Q2	Q3	Q4	Q1	Q2	Q3	Q4	Q1	Q2	Q3	Q4	Q1	Q2	
<b>Diagnostics</b>																	
<b>magnetics</b>																	
re-design																	
refurbishment																	
tests																	
<b>microwave interferometer</b>																	
installation																	
<b>D<sub>α</sub> and Z<sub>eff</sub> measurement</b>																	
design																	
installation																	
<b>Fast camera for visible range</b>																	
design																	
installation																	
<b>Thomson scattering</b>																	
design																	
purchase and assembly																	
installation and callibration																	
<b>Fast bolometers</b>																	
re-design																	
installation																	
<b>SXR – array of diodes</b>																	
re-design																	
installation																	
<b>Neutral particle analyzer</b>																	
re-design																	
installation																	
<b>VUV and XUV spectrometers</b>																	
design																	
installation																	
<b>Langmuir probes</b>																	
refurbishment																	
<b>Beam diagnostics</b>																	
design																	
manufacturing																	
installation																	
<b>Microwave reflectometry</b>																	
design																	
production																	
installation																	